



HAL
open science

Targeting CAIX with small molecules: design, synthesis and biological efficacy

Nanda Kumar Parvathaneni

► To cite this version:

Nanda Kumar Parvathaneni. Targeting CAIX with small molecules: design, synthesis and biological efficacy. Medicinal Chemistry. Université Montpellier; School for Oncology and Developmental Biology (Maastricht, Pays-Bas), 2017. English. NNT: 2017MONTT187. tel-01869836

HAL Id: tel-01869836

<https://theses.hal.science/tel-01869836>

Submitted on 6 Sep 2018

HAL is a multi-disciplinary open access archive for the deposit and dissemination of scientific research documents, whether they are published or not. The documents may come from teaching and research institutions in France or abroad, or from public or private research centers.

L'archive ouverte pluridisciplinaire **HAL**, est destinée au dépôt et à la diffusion de documents scientifiques de niveau recherche, publiés ou non, émanant des établissements d'enseignement et de recherche français ou étrangers, des laboratoires publics ou privés.

THESE POUR OBTENIR LE GRADE DE DOCTEUR DE L'UNIVERSITE DE MONTPELLIER

En Ingénierie Biomoléculaire

École doctorale Sciences Chimiques Balard

Unité de recherche UMR5247 - Institut des Biomolécules Max Mousseron

Targeting CAIX with small molecules: Design, Synthesis and Biological efficacy

Présentée par Nanda Kumar PARVATHANENI

Le 12 Décembre 2017

Sous la direction du Pr. Jean-Yves WINUM et du Pr. Philippe LAMBIN

Devant le jury composé de

Alberto MARRA, Professeur, Université de Montpellier

Ludwig DUBOIS, Professeur associé, Université de Maastricht (Pays-Bas)

Philippe LAMBIN, Professeur, Université de Maastricht (Pays-Bas)

Daumantas MATULIS, Professeur, Université de Vilnius (Lituanie)

Jean-Yves WINUM, Professeur, Université de Montpellier

Raivis ZALUBOVSKIS, Professeur assistant, Université de Riga (Lettonie)

Président du jury

Examineur

Co-directeur de thèse

Rapporteur

Directeur de thèse

Rapporteur

**Targeting CAIX using small molecules:
Design, Synthesis and Biological efficacy**

Cover:

Dual drug targeting approach towards hypoxic tumors

Cover design: Nanda Kumar Parvathaneni

ISBN:

Print:

© Nanda Kumar Parvathaneni, Maastricht, 2017

**Targeting CAIX with small molecules:
Design, Synthesis and Biological efficacy**

DISSERTATION

to obtain the degree of Doctor at Maastricht University
on the authority of the Rector Magnificus
Prof. Dr. Rianne M. Letschert
in accordance with the decision of the Board of Deans,
to be defended in public
on Tuesday 12th of December 2017 at 13:30 hours

by

Nanda Kumar Parvathaneni

Supervisors:

Prof. dr. Philippe Lambin

Prof. Jean-Yves Winum (Montpellier University, France)

Co-supervisor:

Dr. Ludwig Dubois

Assessment committee:

Prof. dr. F.C.S. Ramaekers (chairman)

Prof. dr. Guido R.M.M. Haenen

Prof. Daumantus Matulis (Vilnius University, Lithuania)

Dr. Kasper M.A. Rouschop

Dr. Raivis Žalubovskis (Riga Technical University, Latvia)

Contents

Chapter 1: Introduction and thesis outline	7
Chapter 2: Overview of Structure Activity Relationship studies on nitroimidazoles as antimicrobial and radiosensitizing agents	29
Chapter 3: Hypoxia-targeting carbonic anhydrase IX inhibitors by a new series of nitroimidazole -sulfonamides/sulfamides/sulfamates	59
Chapter 4: New approach of delivering cytotoxic drugs towards CAIX expressing cells: A new concept of dual-target drugs	87
Chapter 5: Design and synthesis of carbonic anhydrase IX inhibitors with different bio-reducible warheads	127
Chapter 6: Novel carbonic anhydrase IX targeting bio-reducible sulfonamides	160
Chapter 7: Discussion and future perspectives	185
Summary	199
Valorization addendum	203
Acknowledgements	209
Curriculum Vitae	213
List of Publications	214

Chapter 1

Introduction and thesis outline

Introduction

Cancer and metabolism

Cancer can be defined as the uncontrollable growth of a group of abnormal cells by disregarding the normal rules of cell division. Cancer cells develop a degree of autonomy from the signals that dictate whether a cell should divide, differentiate into another cell or die, resulting in uncontrolled growth and proliferation [1]. Initiation and progression of cancer depends on both external environmental factors (e.g. tobacco, chemicals, radiation and infectious organisms) and factors within the cell (e.g. inherited mutations, hormones, immunity and metabolism-induced mutations i.e. specific mutation in the tumor leading to accumulation of oncometabolites) [2]. These factors can act together or sequentially, resulting in abnormal cellular behavior and excessive proliferation [3].

Cancer is a multi-gene, multi-step disease originating from a single abnormal cell (clonal origin) with an altered deoxyribonucleic acid (DNA) sequence, also referred to as mutation. To enable the formation of a tumor, successive rounds of mutations and selective expansion are required. Individual cell behavior is not autonomous; it usually relies on external signals from surrounding cells. These signals are known as the hallmarks of cancer (i.e. sustained proliferation, desensitization to growth suppressors, apoptotic evasion, replicative immortality, angiogenesis promotion and invasion and metastasis) proposed by Douglas Hanahan and Robert Weinberg in 2000 [4]. Two additional hallmarks were postulated a decade later: reprogramming of energy metabolism and immune system evasion [5].

Cancer cells preferentially utilize glycolysis, instead of oxidative phosphorylation, for their metabolism and energy supply even in the presence of oxygen. This phenomenon of aerobic glycolysis, referred to as the “Warburg effect”, commonly exists in a variety of tumors [6]. Recent studies further demonstrate that both genetic factors, such as oncogenes and tumor suppressors, and microenvironmental factors, such as spatial hypoxia and acidosis, can regulate the glycolytic metabolism of cancer cells. Reciprocally, the altered cancer cell metabolism can modulate the tumor microenvironment, which plays important roles in cancer cell somatic evolution, metastasis formation and therapeutic responses [7].

Hypoxia and the acidic tumor microenvironment

Hypoxia literally means deprivation of adequate oxygen levels and occurs within solid tumors as a result of abnormal blood vessel formation, defective blood perfusion and unlimited cancer cell proliferation. As tumor growth outpaces that of adequate vasculature, oxygen and nutrient delivery become insufficient (Figure 1). This dynamic interplay between the normal stroma and the malignant parenchyma, coupled with inevitable hypoxia, is common in many solid tumors.

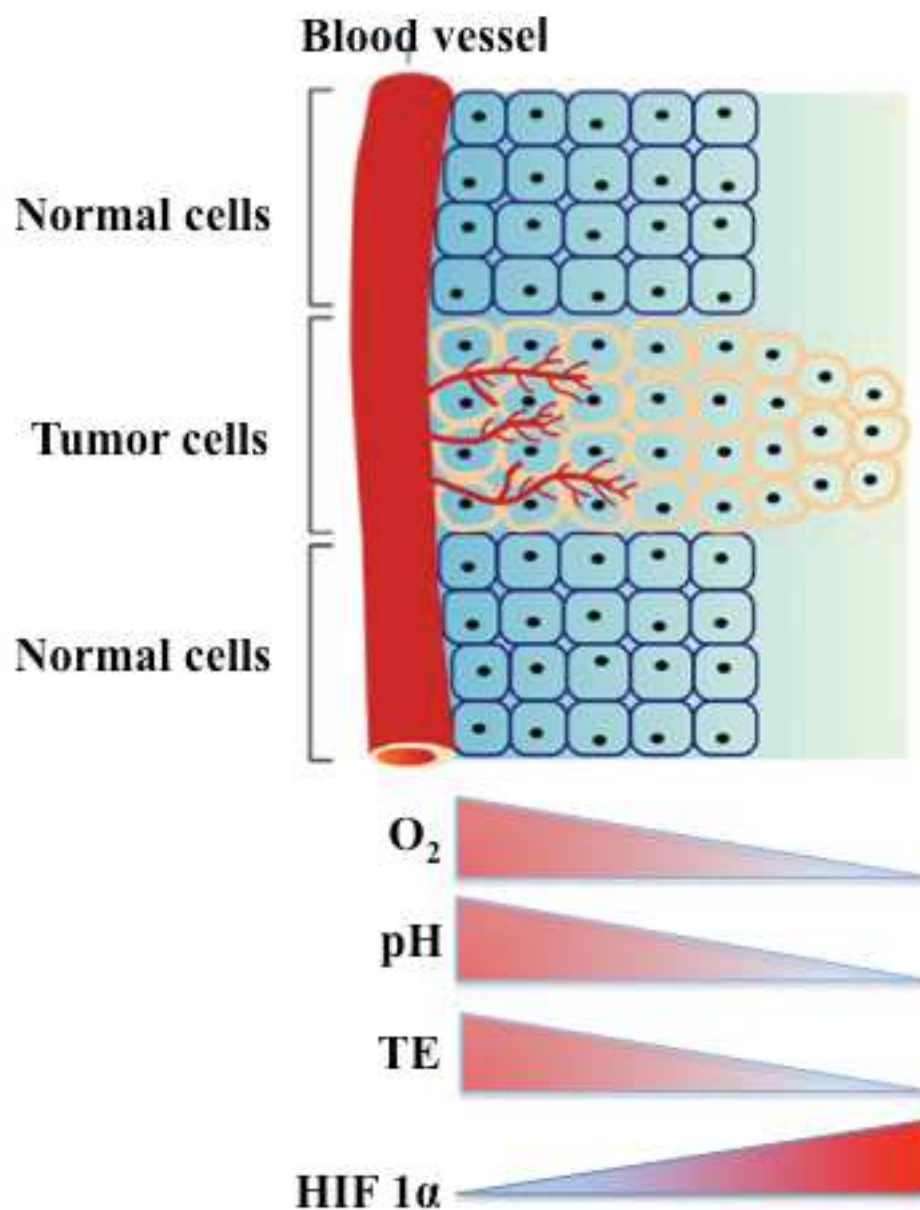


Figure 1. Schematic representation of the tumor microenvironment. The inadequate diffusion and supply of oxygen from blood vessels to tumor cells causes

deprivation of oxygen with increasing distance from blood vessels. Areas with low oxygen in tumor become hypoxic, which is closely associated with stabilization of HIF-1 α that leads to lower (acidic) extracellular pH and decreases in treatment efficacy (TE) of conventional chemo and radiotherapies (Adopted from Expert Reviews in Molecular Medicine 2005 Published by Cambridge University Press).

The progression of hypoxia over time is a consequence of increased oxygen consumption by abnormally proliferating cancer cells. In this sense unlimited tumor cell proliferation lowers pO₂ and drives tumors towards more hypoxic. Therefore hypoxia has been well-studied since it negatively affects radiotherapy and chemotherapy outcome [8-13]. In radiotherapy, when cancer cells are exposed to ionizing radiation, radiochemical damage can occur either by a direct or indirect action. Direct action occurs when alpha particles, beta particles or X-rays create ions, which physically break one or both of the sugar phosphate backbones or break the base pairs of the DNA. Indirect action occurs by radiolysis of water, which produces free radicals that induce DNA damage in cancer cells [12, 14]. Free radicals are molecules that are highly reactive due to the presence of unpaired electrons on the molecule. Free radicals may form molecules, such as hydrogen peroxide, which could initiate harmful chemical reactions within the cells. As a result of these chemical changes, cells may undergo a variety of structural transformations leading to altered functions or cell death [15]. Molecular oxygen reacts with damaged DNA forming peroxy radical (-OOH) adducts. This makes the DNA less accessible for DNA repair molecules resulting in sustained DNA damage. This reaction occurs less under hypoxia [10, 13]. Approximately a three-fold higher radiation dose is required to kill the same level of cells upon oxygen-deprived compared to well-oxygenated conditions, the so-called oxygen enhancement ratio [8]. Chemotherapeutic agents, designed to target cells with high proliferation rates, will fail even if they reach the hypoxic cells. Many viable tumor cells are not exposed to detectable concentrations of drug under hypoxic conditions, e.g. uptake of weak-basic drug like doxorubicin is hampered because of extracellular acidity, which prevents drug distribution [9, 16-18].

Upon hypoxia, cancer cells must adapt in order to sustain tumor growth or to survive and will therefore trigger several molecular mechanisms to facilitate metabolic

adaptations, such as upregulation of glycolytic enzymes, inhibition of oxidative phosphorylation and glucose-independent citrate production for fatty acid synthesis [19]. Hypoxia inducible factor (HIF) activation is the most understood and characterized molecular response governing many of these altered metabolic pathways upon hypoxia [20]. HIF-1 is a heterodimeric transcription factor composed of an α and β subunit. The α subunit is oxygen sensitive while the β subunit is constitutively expressed [20]. Under normoxia, the prolyl hydroxylase domain-containing (PHD) enzymes hydroxylate the proline residues 402 and 564 within the HIF oxygen dependent degradation domain (ODDD) of the α subunit. This reaction initiates the interaction between HIF-1 α and the ubiquitin E3 ligase domain of the von Hippel-Lindau protein (pVHL) tumor suppressor complex [21, 22] for subsequent ubiquitination of HIF-1 α followed by degradation via the proteasome. Conversely, under low oxygen concentration, the PHD enzymes cannot execute their hydroxylation function and HIF-1 α will therefore be stabilized, form a complex with HIF-1 β and translocate into the cell nucleus together with the co-factor P300. In the nucleus the complex binds to the hypoxia responsive element (HRE) regions in the promoter region of multiple genes, resulting in the transcription of e.g. Glucose Transporter 1 (GLUT1), Vascular Endothelial Growth Factor (VEGF) and Carbonic anhydrase IX (CAIX) to promote cellular survival during hypoxia [23, 24] (Figure 2).

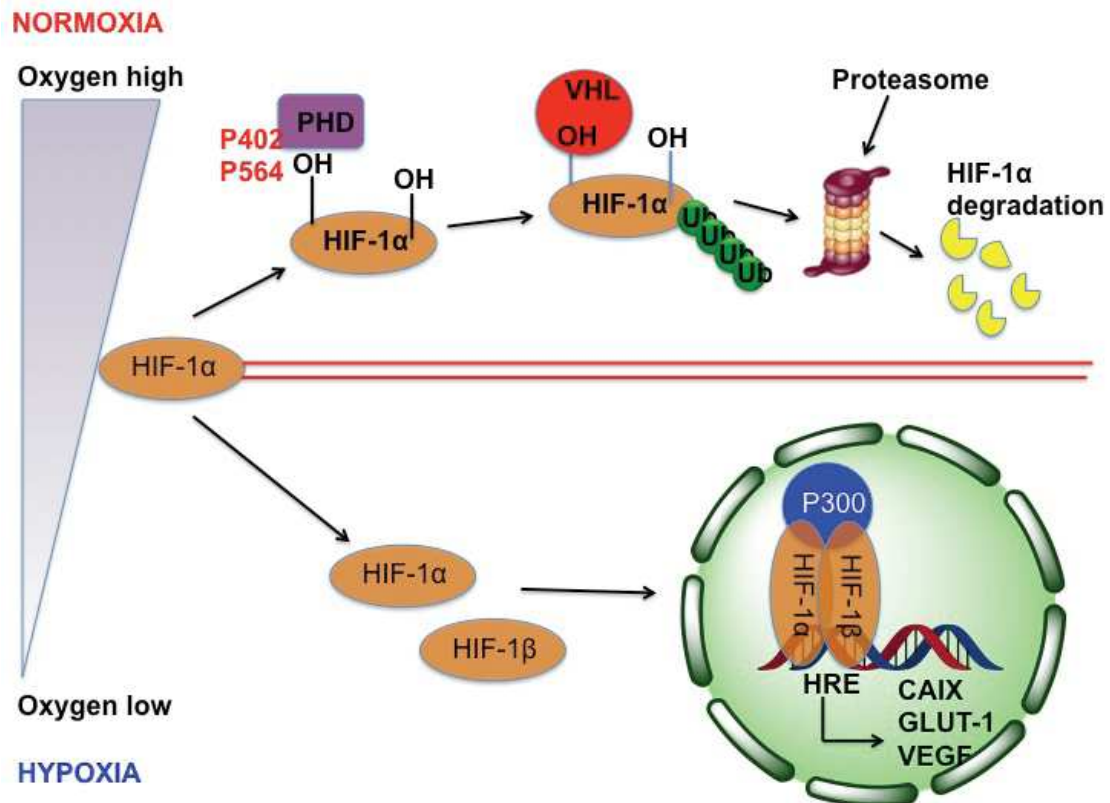


Figure 2. Schematic representation of HIF stabilization mechanism under Hypoxia. The HIF pathway is activated under hypoxic conditions and modulates several cellular functions via the transcription of multiple genes. Abbreviations: Hypoxia Inducible Factor (HIF); Hydroxyl group (OH); Prolyl hydroxylase (PHD); Von Hippel-Lindau protein (VHL); Transcriptional coactivator P300 (P300); Hypoxia responsive element (HRE); Carbonic anhydrase IX (CAIX); Glucose Transporter 1 (GLUT1); Vascular Endothelial Growth Factor (VEGF) [25].

Hypoxic tumors have long been known to depend even more on glycolytic energy production allowing the survival of cancer cells in the hostile hypoxic environment. This survival is promoted by upregulation of GLUT1, through transcriptional activation via HIF, to increase the availability of glucose for the cells' glycolytic metabolism. Glycolysis however produces lactate as a byproduct, which is secreted by several HIF-regulated ion transporters, e.g. monocarboxylate transporters (MCT), to prevent intracellular acidification [26, 27]. Additionally, glycolysis also results in the production of carbon dioxide, which can diffuse passively across the plasma membrane and requires the transmembrane protein CAIX to be scavenged away [28].

Carbonic anhydrase IX (CAIX) and acidosis

CAIX is a zinc metallo-enzyme, a member of 16 carbonic anhydrase family proteins and the most strongly upregulated protein in response to hypoxia and HIF-1 α [29, 30]. Initially termed MN-protein, CAIX was first identified by Pasterokova et al. in a HeLa human cervical carcinoma cell line [31, 32]. Of the different isoforms, the expression of CAIX is most strongly associated with cancer progression. In fact, CAIX mediates several physiological and pathological responses such as, respiration and transport of CO₂/bicarbonate between metabolizing tissues and lungs, pH and CO₂ homeostasis, electrolyte secretion in a variety of tissues/organs, biosynthetic reactions (gluconeogenesis, lipogenesis and ureagenesis), bone resorption and tumorigenicity [30, 33]. Furthermore, CAIX expression was found to be highly tumor specific with only marginal expression in the gastrointestinal tract [34]. The predominant tumor-specific expression combined with its hypoxia-regulated transcription potentiated the use of CAIX as an endogenous hypoxia biomarker. Several meta-analysis studies showed clearly that high CAIX expression is an adverse prognostic marker in solid tumors [35-42].

Moreover, the glycolytic switch produces acidic metabolites that lower the intracellular pH (pHi). Disruption of the pHi negatively impacts biological processes including membrane stability, proliferation and metabolism. CAIX is part of the cellular machinery to maintain pHi homeostasis [27, 43-45]. Most CAs are efficient catalysts for the reversible hydration of carbon dioxide to bicarbonate (CO₂ + H₂O \rightarrow HCO₃⁻ + H⁺) [27], the important physiological reaction in which they are involved (Figure 3). CAIX promotes tumor cell survival [46] by maintaining a pHi within the physiological constraints (pH = 7.2 - 7.4) at the expense of a normal, balanced extracellular pH (pHe = 6.5 - 7.0). The HCO₃⁻, produced extracellularly by CAIX, is transported into the cytosol by sodium bicarbonate transporters (NBC) and anion exchangers (AE) (Figure 3). The intracellularly transported bicarbonate can be used as a buffer via CAII, which forms a metabolon with CAIX [47], and converts the intracellular bicarbonate back to water and carbon dioxide. The H⁺ ions that arise after hydration of carbon dioxide by CAIX remain at the cell surface where they potentiate the extracellular acidity [48], affecting the interaction of the cell with its extracellular matrix. The importance of this mechanism is demonstrated by the fact that

bicarbonate concentrations cause slightly alkaline intracellular pH, which promotes tumor cell survival and growth in the hostile acidic microenvironment [45, 49, 50]. Therefore, CAIX is an important partner in the cellular pH regulation and acid-base balance of tumor microenvironment, resulting in a tightly regulated intracellular pH around 7.4 and a pH of the tumor microenvironment range from pH 5.5 to 7.4 [51-55].

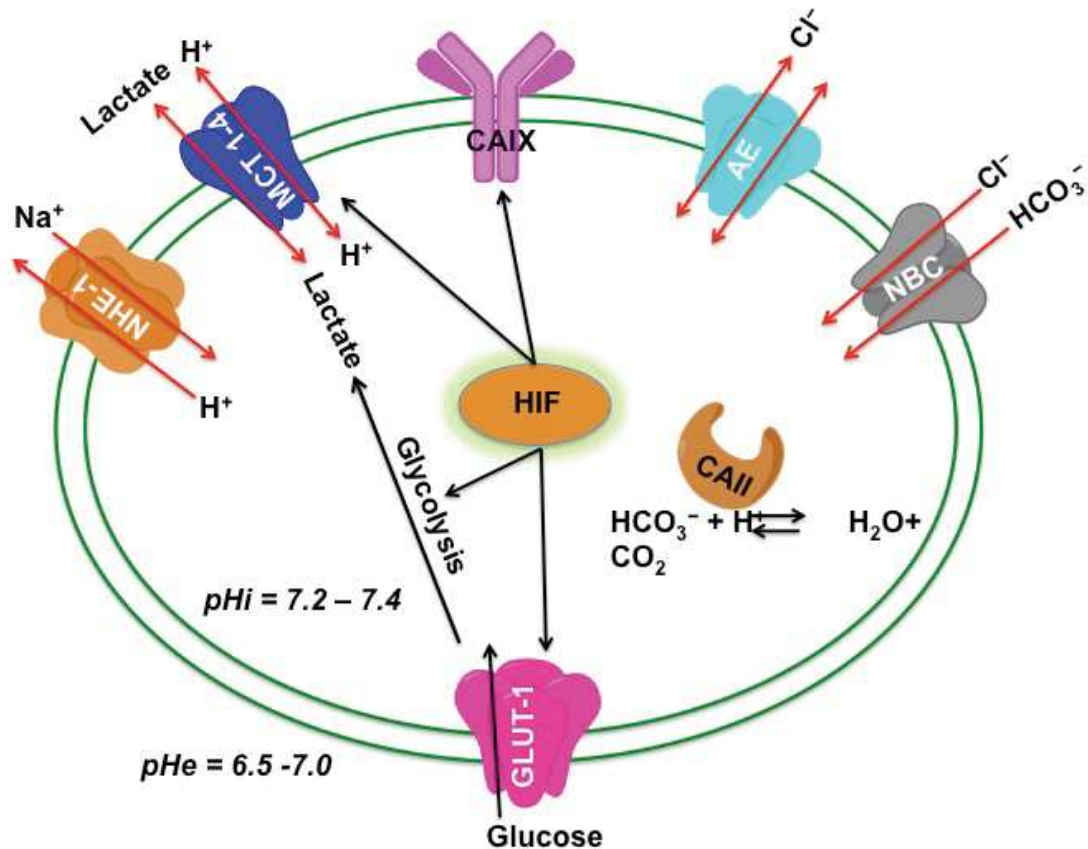


Figure 3. CAIX and other enzymes as pH balance mechanisms to maintain cellular pH. Many enzymes are involved in maintaining the cellular pH balance of hypoxic tumor cells to compensate for the increased production of acid during glycolysis. Abbreviations: Glucose Transporter 1 (GLUT1); Sodium-hydrogen antiporter 1 (NHE-1); Anion exchanger (AE); Carbonic anhydrase IX (CAIX); Carbonic anhydrase II (CAII); Monocarboxylate transporter (MCT); Sodium-bicarbonate cotransporter (NBC); Intracellular pH (pHi); Extracellular pH (pHe) [56].

Furthermore, CAIX is also involved in the process of cell adhesion and migration. It has been reported that CAIX binds competitively to β -catenin via its PG-like domain, to modulate E-cadherin-mediated adherent junctions between cells. By interfering with the E-cadherin/ β -catenin binding, CAIX destabilizes cell-cell adhesions and promotes cell motility [57]. Additionally, CAIX expression is shown to be involved in the selection of a more aggressive phenotype. Firstly, CAIX expression is associated with several stem cell markers, such as CD 133, CD 24⁺/CD 24^{-/low} and may therefore be involved in the maintenance of cancer stem cells, which are more resistant to therapy [58, 59]. Secondly, CAIX further promotes metastasis formation by

acidifying the extracellular environment through degradation of extracellular matrix and activation of matrix metalloproteinase [60, 61].

Different approaches to target hypoxia-associated CAIX

The minimal expression of CAIX in normal tissues, its important role in maintaining the pH balance, and its location on the surface of tumor cells make it an attractive therapeutic target. Many transmembrane-specific carbonic anhydrase inhibitors have therefore been designed [62, 63], which are hypothesized to result in intracellular acid accumulation and tumor-specific cell death [46, 64, 65]. In addition, CAIX inhibitors bind to the zinc ion in the active site via a sulfonamide, sulfamide or sulfamate as the zinc-binding group (ZBG). This occurs when the compounds are in a deprotonated form displacing the zinc-bound water/hydroxide molecule while still maintaining the tetrahedral coordination about the zinc ion when exposed to hypoxic conditions [66, 67]. CAIX inhibitors can be exploited as direct anti-cancer agents, as prodrugs, as carrier for cytotoxic agents or antibody conjugated agents. Several classes of CAIX inhibitors have been shown to attenuate primary tumor growth in MDA-MB-231 human breast cancer xenografts, reduce tumor cell migration *in vitro* and decrease metastases formation *in vivo*, e.g. CAI 17 and U-104 [58, 64, 68, 69]. CAIX inhibitors that exhibit “prodrug-like” properties exist in the form of fluorescently-labeled sulfonamides, coumarin derivatives, glycoconjugates, and even photo-triggered compounds unmasking by hypoxic niche, e.g. disulfide linked sulfonamide drugs [70]. In addition to targeting CAIX directly for anti-cancer treatments, alternative routes utilize the antigenic properties of the enzyme as a means to deliver therapeutic payloads directly to the tumor site. This is possible due to both the cell-surface location of CAIX and its overexpression in various tumor types [71-73]. In addition, CAIX can be targeted for specific delivery of cytotoxic drugs to those CAIX expressing hypoxic tumors, by combining cytotoxic drugs with CAIX inhibitors, to minimize normal tissue toxicity [74]. Moreover, bio-reducible agents, which undergo reduction specifically at low oxygen concentrations, such as nitrogen mustards (alkylating agents) and nitroimidazoles (radiosensitizers or cytotoxins) combined with CAIX inhibiting sulfonamides to target CAIX, an isozyme abundantly overexpressed in hypoxic tumors.

Combination therapies of CAIX inhibitors with conventional treatment modalities, such as chemo- and radiotherapy, might be another effective approach, as CAIX inhibitors have the potential to increase the efficacy of those conventional treatments by complementary targeting of the hypoxic tumor microenvironment. CAIX inhibitors only bind to the zinc-containing active site when exposed to hypoxic conditions [48, 67], therefore allowing for the specific targeting of the hypoxic areas of tumors, while conventional treatments are effective against well-oxygenated cells. Therefore it is believed that the combination of both may increase the therapeutic outcome. CAIX inhibitors combined with nitroimidazoles (well-known radiosensitizers and tumor hypoxia imaging agents) [75, 76] have been shown to increase radiosensitivity of tumor xenograft and chemosensitivity when combined with doxorubicin *in vitro* [77]. Furthermore, specific CAIX inhibition was also reported to increase doxorubicin efficacy *in vivo* [78].

Thesis Outline

CAIX associates closely with hypoxic regions of tumors and plays an important role in the acid-base balance of tumor cells ensuring survival in hostile acidic conditions. CAIX is overexpressed in hypoxic tumor cells rather than in normal cells making it a potential therapeutic target for cancer. More specially, because CAIX inhibition can increase the treatment efficacy of chemo- and radiotherapy, it is very interesting to study the effect of CAIX inhibition in combination therapies.

To improve the selectivity of tumor cell killing by anti-cancer drugs, such as cytotoxic agents and bio-reducible pro-drugs that can be selectively delivered or activated in the tumor tissue, some unique aspects of tumor such as hypoxia and selective CAIX expression can be exploited. The general goal of this thesis (Figure 4) is to study the potential of targeting CAIX as an anti-cancer therapy, either by increasing the efficacy of conventional treatment options by combining them with CAIX inhibitors, or by exploiting CAIX overexpression under hypoxia as a target to cytotoxic or bio-reducible drug delivery.

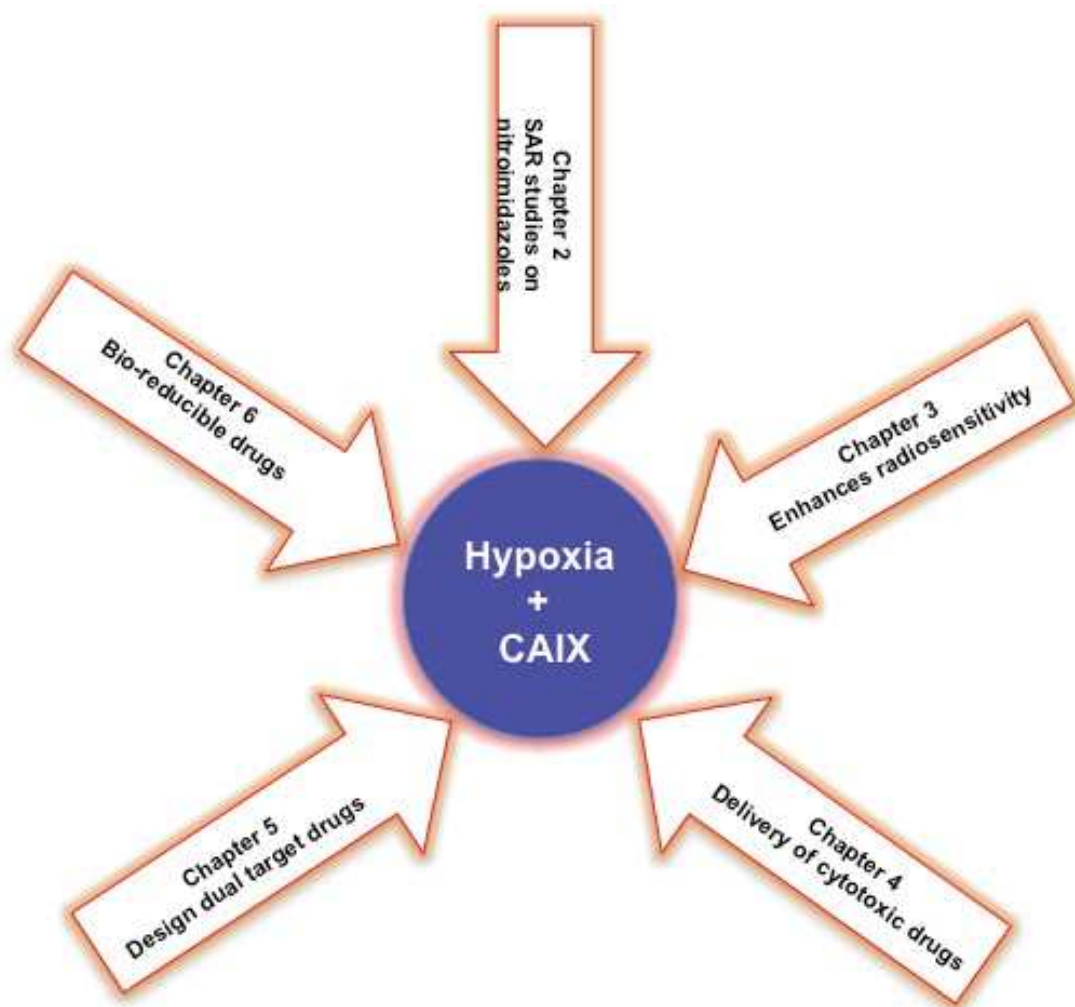


Figure 4. Schematic representation of thesis outline.

Carbonic anhydrase inhibitors have been used not only as anti-cancer agents, but also as anti-anaerobic bacterial agents and hypoxic cell sensitizers. **Chapter 2** gives a detailed discussion of the Structure Activity Relationships (SAR) of 2-, 4- and 5-nitroimidazole derivatives and future directions are provided to address resistance towards existing anti-bacterial agents and to develop good radiosensitizers with minimal cytotoxic adverse effects.

Resistance towards conventional modalities such as radio- and chemotherapies is not only caused by hypoxia, but also by extracellular acidity [79]. Combining nitroimidazole agents (see chapter 2) with CAIX inhibitors (CAIXi) might be an interesting dual-drug approach to sensitize hypoxic tumors to radio- and chemotherapy more specifically with reduced toxicity, since CAIX functions as a carrier of nitroimidazole specifically into the hypoxic tumor cells. **Chapter 3**

describes the synthesis of a series of 2- and 5- nitroimidazole CAIX inhibitor derivatives and its biological evaluation in context of sensitization towards the chemotherapeutic agent doxorubicin.

CAIX expression is closely associated with the hypoxic areas of a tumor. Therefore targeting CAIX might also facilitate the delivery of cytotoxic drugs to these hypoxic tumor regions. **Chapter 4** discusses the design and synthesis of several new classes of dual-target compounds. These compounds consists of different classes of well-established anti-cancer drugs, such as chlorambucil, temozolamide and tirapazamine, combined with CAIXi with the aim to deliver cytotoxic drugs specifically to hypoxic CAIX expressing cells. We envision that this approach will increase the tumor specific efficacy of these anti-cancer drugs and reduces the normal tissue toxicity.

Hypoxia-activated prodrugs are bio-reducible drugs targeting hypoxic tumors and release their DNA alkylating agent upon reduction of the nitro-group on imidazole or nitrogen mustards at low oxygen concentrations [80]. Combining these compounds with CAIX inhibitors might direct bio-reducible drugs more effectively to the site of hypoxic tumor by targeting CAIX. **Chapter 5** and **Chapter 6** discuss the design and synthesis of bio-reducible capable *N*-oxide tirapazamine, 2-, 5-nitroimidazoles and DNA alkylating agents, which undergo reduction especially under hypoxic conditions to target CAIX expressing cells. These derivatives are also evaluated for their therapeutic potential using several biological assays.

Finally, **Chapter 7** of this thesis provides a general discussion on the use of CAIX as a target to treat hypoxic cancers exploiting different strategies. Future directions and perspectives for the development of CAIX targeting drugs are also addressed.

References

1. Alison, M., *Cancer*. www.els.net (introductory article), 2001.
2. DeBerardinis, R.J. and N.S. Chandel, *Fundamentals of cancer metabolism*. *Sci Adv*, 2016. **2**(5): p. e1600200.
3. Leochler, E., *Environmental carcinogens and Mutagens*. www.els.net (standard article), 2003.
4. Hanahan, D. and R.A. Weinberg, *The hallmarks of cancer*. *Cell*, 2000. **100**(1): p. 57-70.
5. Hanahan, D. and R.A. Weinberg, *Hallmarks of cancer: the next generation*. *Cell*, 2011. **144**(5): p. 646-74.
6. Liberti, M.V. and J.W. Locasale, *The Warburg Effect: How Does it Benefit Cancer Cells?* *Trends Biochem Sci*, 2016. **41**(3): p. 211-8.
7. Justus, C.R., E.J. Sanderlin, and L.V. Yang, *Molecular Connections between Cancer Cell Metabolism and the Tumor Microenvironment*. *Int J Mol Sci*, 2015. **16**(5): p. 11055-86.
8. Bertout, J.A., S.A. Patel, and M.C. Simon, *The impact of O₂ availability on human cancer*. *Nat Rev Cancer*, 2008. **8**(12): p. 967-75.
9. Gray, L.H., et al., *The concentration of oxygen dissolved in tissues at the time of irradiation as a factor in radiotherapy*. *Br J Radiol*, 1953. **26**(312): p. 638-48.
10. Grimes, D.R. and M. Partridge, *A mechanistic investigation of the oxygen fixation hypothesis and oxygen enhancement ratio*. *Biomed Phys Eng Express*, 2015. **1**(4): p. 045209.
11. Minchinton, A.I. and I.F. Tannock, *Drug penetration in solid tumours*. *Nat Rev Cancer*, 2006. **6**(8): p. 583-92.
12. Rockwell, S., et al., *Hypoxia and radiation therapy: past history, ongoing research, and future promise*. *Curr Mol Med*, 2009. **9**(4): p. 442-58.

13. Yoshimura, M., et al., *Microenvironment and radiation therapy*. Biomed Res Int, 2013. **2013**: p. 685308.
14. Krall, N., F. Pretto, and D. Neri, *A bivalent small molecule-drug conjugate directed against carbonic anhydrase IX can elicit complete tumour regression in mice*. Chemical Science, 2014. **5**(9): p. 3640-3644.
15. Jackson, S.P., *Sensing and repairing DNA double-strand breaks*. Carcinogenesis, 2002. **23**(5): p. 687-96.
16. Alfarouk, K.O., et al., *Resistance to cancer chemotherapy: failure in drug response from ADME to P-gp*. Cancer Cell Int, 2015. **15**: p. 71.
17. Primeau, A.J., et al., *The distribution of the anticancer drug Doxorubicin in relation to blood vessels in solid tumors*. Clin Cancer Res, 2005. **11**(24 Pt 1): p. 8782-8.
18. Wojtkowiak, J.W., et al., *Drug resistance and cellular adaptation to tumor acidic pH microenvironment*. Mol Pharm, 2011. **8**(6): p. 2032-8.
19. Eales, K.L., K.E. Hollinshead, and D.A. Tennant, *Hypoxia and metabolic adaptation of cancer cells*. Oncogenesis, 2016. **5**: p. e190.
20. Schofield, C.J. and P.J. Ratcliffe, *Oxygen sensing by HIF hydroxylases*. Nat Rev Mol Cell Biol, 2004. **5**(5): p. 343-54.
21. Ivan, M., et al., *HIF α targeted for VHL-mediated destruction by proline hydroxylation: implications for O₂ sensing*. Science, 2001. **292**(5516): p. 464-8.
22. Kondo, K., et al., *Inhibition of HIF is necessary for tumor suppression by the von Hippel-Lindau protein*. Cancer Cell, 2002. **1**(3): p. 237-46.
23. Denko, N.C., *Hypoxia, HIF1 and glucose metabolism in the solid tumour*. Nat Rev Cancer, 2008. **8**(9): p. 705-13.
24. Wouters, B.G. and M. Koritzinsky, *Hypoxia signalling through mTOR and the unfolded protein response in cancer*. Nat Rev Cancer, 2008. **8**(11): p. 851-64.

25. Franke, K., M. Gassmann, and B. Wielockx, *Erythrocytosis: the HIF pathway in control*. *Blood*, 2013. **122**(7): p. 1122-8.
26. Neri, D. and C.T. Supuran, *Interfering with pH regulation in tumours as a therapeutic strategy*. *Nat Rev Drug Discov*, 2011. **10**(10): p. 767-77.
27. Parks, S.K., J. Chiche, and J. Pouyssegur, *pH control mechanisms of tumor survival and growth*. *J Cell Physiol*, 2011. **226**(2): p. 299-308.
28. Sedlakova, O., et al., *Carbonic anhydrase IX, a hypoxia-induced catalytic component of the pH regulating machinery in tumors*. *Front Physiol*, 2014. **4**: p. 400.
29. Potter, C. and A.L. Harris, *Hypoxia inducible carbonic anhydrase IX, marker of tumour hypoxia, survival pathway and therapy target*. *Cell Cycle*, 2004. **3**(2): p. 164-7.
30. Supuran, C.T. and A. Scozzafava, *Carbonic anhydrases as targets for medicinal chemistry*. *Bioorg Med Chem*, 2007. **15**(13): p. 4336-50.
31. Pastorek, J., et al., *Cloning and characterization of MN, a human tumor-associated protein with a domain homologous to carbonic anhydrase and a putative helix-loop-helix DNA binding segment*. *Oncogene*, 1994. **9**(10): p. 2877-88.
32. Pastorekova, S., et al., *A novel quasi-viral agent, MaTu, is a two-component system*. *Virology*, 1992. **187**(2): p. 620-6.
33. Supuran, C.T., *Carbonic anhydrases: novel therapeutic applications for inhibitors and activators*. *Nat Rev Drug Discov*, 2008. **7**(2): p. 168-81.
34. Pastorekova, S., et al., *Carbonic anhydrase IX, MN/CA IX: analysis of stomach complementary DNA sequence and expression in human and rat alimentary tracts*. *Gastroenterology*, 1997. **112**(2): p. 398-408.
35. Douglas, C.M., et al., *Lack of prognostic effect of carbonic anhydrase-9, hypoxia inducible factor-1alpha and bcl-2 in 286 patients with early squamous cell carcinoma of the glottic larynx treated with radiotherapy*. *Clin Oncol (R Coll Radiol)*, 2013. **25**(1): p. 59-65.

36. He, F., et al., *Noninvasive molecular imaging of hypoxia in human xenografts: comparing hypoxia-induced gene expression with endogenous and exogenous hypoxia markers*. *Cancer Res*, 2008. **68**(20): p. 8597-606.
37. Kim, S.J., et al., *Prognostic value of carbonic anhydrase IX and Ki-67 expression in squamous cell carcinoma of the tongue*. *Jpn J Clin Oncol*, 2007. **37**(11): p. 812-9.
38. Olive, P.L., et al., *Carbonic anhydrase 9 as an endogenous marker for hypoxic cells in cervical cancer*. *Cancer Res*, 2001. **61**(24): p. 8924-9.
39. Smeland, E., et al., *Prognostic impacts of hypoxic markers in soft tissue sarcoma*. *Sarcoma*, 2012. **2012**: p. 541650.
40. Stewart, D.J., et al., *Membrane carbonic anhydrase IX expression and relapse risk in resected stage I-II non-small-cell lung cancer*. *J Thorac Oncol*, 2014. **9**(5): p. 675-84.
41. Wykoff, C.C., et al., *Expression of the hypoxia-inducible and tumor-associated carbonic anhydrases in ductal carcinoma in situ of the breast*. *Am J Pathol*, 2001. **158**(3): p. 1011-9.
42. van Kuijk, S.J., et al., *Prognostic Significance of Carbonic Anhydrase IX Expression in Cancer Patients: A Meta-Analysis*. *Front Oncol*, 2016. **6**: p. 69.
43. Hilvo, M., et al., *Biochemical characterization of CA IX, one of the most active carbonic anhydrase isozymes*. *J Biol Chem*, 2008. **283**(41): p. 27799-809.
44. Bartosova, M., et al., *Expression of carbonic anhydrase IX in breast is associated with malignant tissues and is related to overexpression of c-erbB2*. *J Pathol*, 2002. **197**(3): p. 314-21.
45. Swietach, P., et al., *Tumor-associated carbonic anhydrase 9 spatially coordinates intracellular pH in three-dimensional multicellular growths*. *J Biol Chem*, 2008. **283**(29): p. 20473-83.

46. Chiche, J., et al., *Hypoxia-inducible carbonic anhydrase IX and XII promote tumor cell growth by counteracting acidosis through the regulation of the intracellular pH*. *Cancer Res*, 2009. **69**(1): p. 358-68.
47. Kurtz, I., *Molecular mechanisms and regulation of urinary acidification*. *Compr Physiol*, 2014. **4**(4): p. 1737-74.
48. Svastova, E., et al., *Hypoxia activates the capacity of tumor-associated carbonic anhydrase IX to acidify extracellular pH*. *FEBS Lett*, 2004. **577**(3): p. 439-45.
49. Swietach, P., et al., *The role of carbonic anhydrase 9 in regulating extracellular and intracellular pH in three-dimensional tumor cell growths*. *J Biol Chem*, 2009. **284**(30): p. 20299-310.
50. McIntyre, A., et al., *Disrupting Hypoxia-Induced Bicarbonate Transport Acidifies Tumor Cells and Suppresses Tumor Growth*. *Cancer Res*, 2016. **76**(13): p. 3744-55.
51. Bhujwala, Z.M., et al., *Combined vascular and extracellular pH imaging of solid tumors*. *NMR Biomed*, 2002. **15**(2): p. 114-9.
52. Gatenby, R.A. and R.J. Gillies, *Why do cancers have high aerobic glycolysis?* *Nat Rev Cancer*, 2004. **4**(11): p. 891-9.
53. Schornack, P.A. and R.J. Gillies, *Contributions of cell metabolism and H⁺ diffusion to the acidic pH of tumors*. *Neoplasia*, 2003. **5**(2): p. 135-45.
54. van Sluis, R., et al., *In vivo imaging of extracellular pH using 1H MRSI*. *Magn Reson Med*, 1999. **41**(4): p. 743-50.
55. Vaupel, P., F. Kallinowski, and P. Okunieff, *Blood flow, oxygen and nutrient supply, and metabolic microenvironment of human tumors: a review*. *Cancer Res*, 1989. **49**(23): p. 6449-65.
56. Damaghi, M., J.W. Wojtkowiak, and R.J. Gillies, *pH sensing and regulation in cancer*. *Front Physiol*, 2013. **4**: p. 370.

57. Svastova, E., et al., *Carbonic anhydrase IX reduces E-cadherin-mediated adhesion of MDCK cells via interaction with beta-catenin*. *Exp Cell Res*, 2003. **290**(2): p. 332-45.
58. Lock, F.E., et al., *Targeting carbonic anhydrase IX depletes breast cancer stem cells within the hypoxic niche*. *Oncogene*, 2013. **32**(44): p. 5210-9.
59. Currie, M.J., et al., *Immunohistochemical analysis of cancer stem cell markers in invasive breast carcinoma and associated ductal carcinoma in situ: relationships with markers of tumor hypoxia and microvasculature*. *Hum Pathol*, 2013. **44**(3): p. 402-11.
60. Overall, C.M. and O. Kleinfeld, *Tumour microenvironment - opinion: validating matrix metalloproteinases as drug targets and anti-targets for cancer therapy*. *Nat Rev Cancer*, 2006. **6**(3): p. 227-39.
61. Kessenbrock, K., V. Plaks, and Z. Werb, *Matrix metalloproteinases: regulators of the tumor microenvironment*. *Cell*, 2010. **141**(1): p. 52-67.
62. Monti, S.M., C.T. Supuran, and G. De Simone, *Anticancer carbonic anhydrase inhibitors: a patent review (2008 - 2013)*. *Expert Opin Ther Pat*, 2013. **23**(6): p. 737-49.
63. McKenna, R. and C.T. Supuran, *Carbonic anhydrase inhibitors drug design*. *Subcell Biochem*, 2014. **75**: p. 291-323.
64. Gieling, R.G., et al., *Antimetastatic effect of sulfamate carbonic anhydrase IX inhibitors in breast carcinoma xenografts*. *J Med Chem*, 2012. **55**(11): p. 5591-600.
65. Winum, J.Y., et al., *Ureido-substituted sulfamates show potent carbonic anhydrase IX inhibitory and antiproliferative activities against breast cancer cell lines*. *Bioorg Med Chem Lett*, 2012. **22**(14): p. 4681-5.
66. Dubois, L., et al., *Imaging of CA IX with fluorescent labelled sulfonamides distinguishes hypoxic and (re)-oxygenated cells in a xenograft tumour model*. *Radiother Oncol*, 2009. **92**(3): p. 423-8.

67. Dubois, L., et al., *Imaging the hypoxia surrogate marker CA IX requires expression and catalytic activity for binding fluorescent sulfonamide inhibitors*. *Radiother Oncol*, 2007. **83**(3): p. 367-73.
68. Ward, C., et al., *Evaluation of carbonic anhydrase IX as a therapeutic target for inhibition of breast cancer invasion and metastasis using a series of in vitro breast cancer models*. *Oncotarget*, 2015. **6**(28): p. 24856-70.
69. Lou, Y., et al., *Targeting tumor hypoxia: suppression of breast tumor growth and metastasis by novel carbonic anhydrase IX inhibitors*. *Cancer Res*, 2011. **71**(9): p. 3364-76.
70. Reich, R., et al., *Carbamoylphosphonates control tumor cell proliferation and dissemination by simultaneously inhibiting carbonic anhydrase IX and matrix metalloproteinase-2. Toward nontoxic chemotherapy targeting tumor microenvironment*. *J Med Chem*, 2012. **55**(17): p. 7875-82.
71. Shinkai, M., et al., *Targeting hyperthermia for renal cell carcinoma using human MN antigen-specific magnetoliposomes*. *Jpn J Cancer Res*, 2001. **92**(10): p. 1138-45.
72. Torchilin, V.P., *Recent advances with liposomes as pharmaceutical carriers*. *Nat Rev Drug Discov*, 2005. **4**(2): p. 145-60.
73. Dubois, L.J., et al., *New ways to image and target tumour hypoxia and its molecular responses*. *Radiother Oncol*, 2015. **116**(3): p. 352-7.
74. van Kuijk, S.J., et al., *New approach of delivering cytotoxic drugs towards CAIX expressing cells: A concept of dual-target drugs*. *Eur J Med Chem*, 2017. **127**: p. 691-702.
75. Hall, E.J., et al., *The nitroimidazoles as radiosensitizers and cytotoxic agents*. *Br J Cancer Suppl*, 1978. **3**: p. 120-3.
76. Konse-Nagasawa, S.K.-K.a.H., *Significance of nitroimidazole compounds and hypoxia-inducible factor-1 for imaging tumor hypoxia*. *Cancer Science*, 2009. **100**(8): p. 1366-1373.

77. Dubois, L., et al., *Targeting carbonic anhydrase IX by nitroimidazole based sulfamides enhances the therapeutic effect of tumor irradiation: a new concept of dual targeting drugs*. *Radiother Oncol*, 2013. **108**(3): p. 523-8.
78. Gieling, R.G., et al., *Inhibition of carbonic anhydrase activity modifies the toxicity of doxorubicin and melphalan in tumour cells in vitro*. *J Enzyme Inhib Med Chem*, 2013. **28**(2): p. 360-9.
79. Quennet, V., et al., *Tumor lactate content predicts for response to fractionated irradiation of human squamous cell carcinomas in nude mice*. *Radiother Oncol*, 2006. **81**(2): p. 130-5.
80. Konopleva, M., et al., *Phase I/II study of the hypoxia-activated prodrug PR104 in refractory/relapsed acute myeloid leukemia and acute lymphoblastic leukemia*. *Haematologica*, 2015. **100**(7): p. 927-34.

Chapter 2

Overview of Structure-Activity Relationship studies on nitroimidazoles as antimicrobial and radiosensitizing agents

Submitted to Curr. Pharm. Design.

Nanda Kumar Parvathaneni^{*}, Raymon Niemans, Ala Yaromina, Philippe Lambin,

Ludwig J. Dubois, Jean-Yves Winum

Abstract

Low oxygen regions or hypoxia is a common feature of solid tumors and a well-established factor of radio (chemo) resistance. Limited success of treatment modalities aiming at improving tumor oxygenation such as hyperbaric oxygen, hyperthermia, blood transfusions and erythropoietin stimulating agents, advanced the search for alternative treatment options like nitroimidazole-based radiosensitizers. Tissue environments with a low oxygen tension also facilitate the development of anaerobic bacterial infections, where surgery and hyperbaric oxygen treatment have been proposed as therapies, however without significant benefits. Antimicrobial therapies based on nitroimidazoles have been used since 1960.

The imidazole nucleus forms the main structure of most components of human organisms, for example histidine, Vitamine B12, DNA base structure, purines, histamine and biotin. Bioreductively-activated 2-, 4- and 5-nitroimidazoles have been proven as effective antimicrobial agents against different types of infections and have also been evaluated as hypoxic cytotoxins and radiosensitizers in the treatment of cancer. Nitroimidazoles undergo selective reduction through the transfer of electrons from reductase enzymes under hypoxic conditions to produce reactive intermediate species that cause irreversible cellular damage leading to cell death.

A thorough understanding of the mechanism(s) of existing antibacterial agents resistance should provide a foundation for the development of alternative chemotherapies for treatment for infections caused by these organisms. SAR studies and minimal resistance of nitroimidazole to a plethora of bacteria shows that this area of research is still thriving research interest for future antibiotic development. Oxygen mimicking small molecules has the potential to sensitize hypoxic tumors to radiation. Aqueous solubility, electron affinity and reduction potentials play a key role in nitroimidazoles as a good radiosensitizers. Altering one of these parameters and SAR studies would help to develop potent radiosensitizer with minimal side effects.

In this overview, we summarized the extensive studies of Structure Activity Relationship on 2-, 4- and 5-nitroimidazoles as antibacterial and radiosensitizing agents.

Introduction

Low oxygen regions or hypoxia is a common feature of solid tumors, most often due to a blood supply inadequate to meet the tumor's demands, and is associated with worse outcome after surgery, chemotherapy and radiotherapy [1]. Hypoxia modification strategies, such as hyperbaric oxygen, hyperthermia, blood transfusions and erythropoietin stimulating agents, have been investigated in clinical trials, however with limited success [2]. Alternatively, a class of compounds known to undergo different intracellular metabolism depending on the availability of oxygen in tissue, the nitroimidazoles, have been advocated as radiosensitizers [3] and imaging agents of hypoxia in tumors [4, 5]. When a nitroimidazole enters a viable cell the molecule undergoes a single electron reduction, to form a potentially reactive intermediate. In the presence of normal oxygen levels, the molecule is immediately reoxidized (**Fig.1**). Most nitroimidazole-based hypoxic imaging agents developed are 2-nitroimidazole derivatives. No Structure Activity Relationship (SAR) studies related to hypoxic imaging agents have been done, as was extensively reviewed before [6-8]. These imaging agents are therefore out of the scope of this review.

Hypoxia is also present in the gastro-intestinal tract and favors growth of anaerobic bacteria. Although surgery and hyperbaric oxygen treatment have been proposed as therapies against infections, no significant benefits have yet been observed [2]. Antimicrobial therapies based on nitroimidazoles have been available since 1960 and has recently gained a lot of interest because of the increased resistance of anaerobes against penicilline, quinolones, clindamycin and cephalosporins [9]. The slow growth of these organisms, their polymicrobial nature and the growing resistance of anaerobes to antimicrobials complicate the treatment of anaerobic infection [10]. Resistance of anaerobic Gram-positive cocci against nitroimidazoles is rare [11], and over 90% of obligate anaerobes are susceptible to less than 2 µg/ml metronidazole (Mtz) [12]. This shows that SAR studies on nitroimidazoles might be useful to address resistance of existing antibiotics.

The 2-, 4- and 5-nitroimidazoles and their derivatives show versatile applications in treatment of different diseases. This versatility can be explained by the fact that the imidazole nucleus forms the main structure of most components of human organisms, e.g. histidine, Vit-B12, DNA base structure, purines, histamine and biotin [9]. The versatility of the nitroheterocyclic drugs is due to the nitro group attached to the

imidazole ring. The bio-reducible capacity of the nitro group on the imidazole ring explains the ability of nitroimidazoles to act as antibacterial and radiosensitizing agents [13]. Depending on the nature of substituents and the position of the nitro group, the nitroimidazole derivatives demonstrate various pharmacological activities, but generally they inhibit DNA replication, protein synthesis and cellular respiration [2, 9].

Within this review, we will highlight the role of nitroimidazoles as effective antibacterial and anticancer agents by evaluating the SAR on different derivatives.

Nitroimidazoles as antibacterial agents

The discovery of nitroimidazoles as antibacterial drugs in the late 1960's heralded a new era in the treatment of gram-negative and positive bacterial infections. The 2-nitroimidazole antibiotic azomycin **1**, isolated from the Streptomyces [14], was the first discovered active nitroimidazole acting as the main impetus for a systematic search for drugs with activity against bacteria. The highly selective effect of these drugs is dependent on specific nitroreductase enzymes, such as ferredoxin or flavodoxin-like electron transport pathway components, characteristic for anaerobic bacteria [15]. These enzymes form short-lived cytotoxic free radical intermediates, which finally decompose into nontoxic end products. These intermediates cause toxicity due to their interaction with deoxyribonucleic acid (DNA) and possibly with other macromolecules. Even if nitro group reduction were to occur in presence of oxygen, damage would be very limited or almost absent because oxygen is the best biological electron acceptor for reforming the original drug [16]. Reduction of the nitro group is a prerequisite for all biological activity. Complete reduction involves the stepwise addition of 6 electrons to form the amine ($6e^-$) via the nitroso ($2e^-$) and hydroxylamine ($4e^-$) intermediates, although many drugs do not proceed beyond the hydroxylamine derivative (**Fig. 1**). Drug reduction in the presence of DNA suggests that the short-lived intermediates are the primary cause of DNA damage [17].

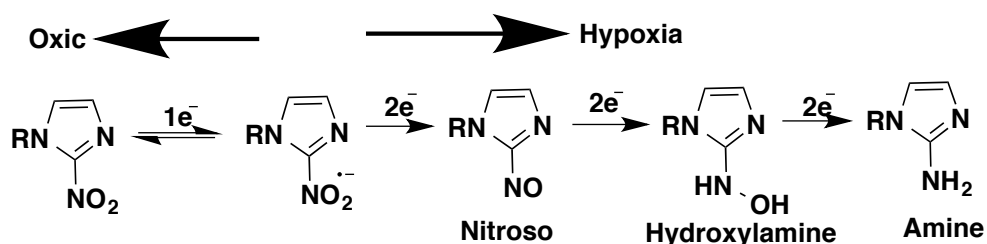


Figure. 1: Nitroimidazole reduction sequence.

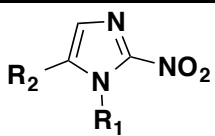
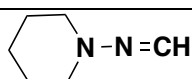
Depending on the nature of the substituents and the position of the nitro group, the imidazole derivatives show various pharmacological activities [18, 19]. Electron affinity decreases from 2, 5 to 4-nitroimidazole derivatives. The redox potential $E(1)$ is much more negative (lower) in anaerobes providing selective reduction of the nitro group. Any redox reaction in the cell possessing a reduction potential more negative, or lower, than that of the nitroimidazole will donate its electrons preferentially to the drug, i.e. a redox active compound of higher potential is a more efficient electron acceptor, it is more 'electron affinic'. Thus, all anaerobes possess redox mechanisms between -430 to -460 mV, the value typical of ferredoxin, whereas Mtz has a reduction potential of -415 mV. Consequently, the drug is a more efficient electron acceptor [16]. The compounds with nitro group at position 4 are usually less active than the corresponding 5-nitro derivatives. For example, the 4-nitroimidazole PA-824 is less active against anaerobic *Mycobacterium tuberculosis* (Mtb) as compared to the 5-nitroimidazole. Tuberculosis lesions are usually [20], do not actively replicate and are therefore significantly less sensitive to the standard antituberculosis drugs that interfere with processes essential for rapid aerobic growth [21]. New agents active against these metabolically altered bacteria are therefore urgently needed.

Furthermore, bacteria that are difficult or impossible to treat are becoming increasingly common due to resistance and are causing a global health crisis. Understanding the mechanisms by which bacteria are either intrinsically resistant or acquire resistance to antibiotics becomes increasingly important. The mechanisms of resistance include the prevention of access to drug targets, changes in the structure of antibiotic targets and the direct modification or inactivation of antibiotics [22]. Several synthetic programs have been developed to address resistance of existing drugs and development of new antibiotics and are based on SAR studies.

SAR studies on 2-nitroimidazoles

The 2-nitroimidazole azomycin **1** (**Fig. 2**), purified from the streptomycete, was found to have potent activity against *Trichomonas vaginalis* in 1960 [23]. 2-nitroimidazoles were the first class of nitroimidazoles with reported antitubercular activity. A large array of compounds belonging to this class substituted at 1- and 5-positions was screened against Gram-positive and Gram-negative bacteria. SAR studies on a selected set of antituberculosis active 2-nitroimidazole derivatives are presented in **Table 1** [24]. The majority of compounds with alkyl, amide, or alcohol substituents were found to be inactive against all organisms tested [25]. Alkyl **2–5**, halide **6–8** and amide **9 & 10** substitution at the 1- as well as the 5-position showed poor activity, whereas vinyl **13 & 14** substituents at the 5-position showed increased potency. The most active compound in the initial series [21] with a minimum inhibitory concentration (MIC) of 29.93 μM had an ethyl at N1- and an unsubstituted vinyl at the 5-position [24]. Subsequently, vinyl-substituted 2-nitroimidazoles (e.g. **19**) were made with only marginal improvement in antimycobacterial activity [26]. Substitution at the 5-position with large groups (e.g. **21**) provided only marginal improvement in antitubercular activity. In general, increasing the lipophilicity at the 5-position of the 2-nitroimidazoles enhanced the antimicrobial activity of Gram-positive bacteria, including *Mtb* [27]. Etanidazole **23** substitution at 1-position did not show potent activity against actively replicating *Mtb*, but did demonstrate some selective activity against the hypoxia-induced non-replicating *Mtb*. This trend mimics the activity observed in mammalian cells that 2-nitroimidazoles are selectively reduced in hypoxic, but not in normoxic conditions [28].

Table 1: Minimum inhibitory concentrations (MIC) of 2-nitroimidazoles against Mtb H37Rv†

			
Compound	R ₁	R ₂	MIC (μM)
2	H	<i>n</i> -C ₃ H ₇	>128.97
3	CH ₃	CH ₃	>1417.94
4	CH ₃	C ₂ H ₅	>1289.74
5	CH ₃	CH ₂ CH ₂ OH	>1169.18
6	CH ₃	CH ₂ CH ₂ Cl	>1058.03
7	C ₂ H ₅	CH ₂ CH ₂ Cl	98.50
8	CH ₂ CH ₂ Cl	CH ₃	>1058.03
9	CH ₂ CONH ₂	CH ₃	>543.30
10	CH ₂ CONHCH ₃	CH ₃	>1009.69
11	CH ₃	CHO	64.50
12	CH ₃	COCH ₃	295.77
13	CH ₃	CH ₂ =CH	130.68
14	C ₂ H ₅	CH ₂ =CH	29.93
15	CH ₃	C ₆ H ₅ CH=CH	>87.30
16	C ₂ H ₅	C ₆ H ₅ CH=CH	41.14
17	CH ₃	HC(NO ₂)=CH	25.25
18	CH ₃	CH ₃ C(NO ₂)=CH	23.58
19	CH ₃	<i>n</i> C ₄ H ₉ C(NO ₂)=CH	19.68
20	CH ₃	<i>n</i> -C ₅ H ₁₁ N(O)=CH	208.23
21	CH ₃	<i>n</i> -C ₁₀ H ₂₁ N(O)=CH	16.12
22	CH ₃		210.86

†Data from [24, 26, 27, 29, 30].

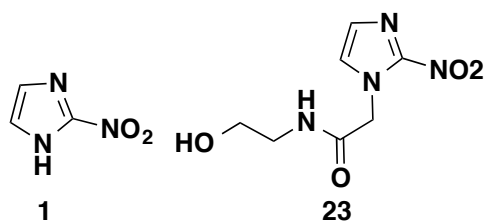


Figure 2: Structures of 2-nitroimidazoles

SAR studies on 4-nitroimidazoles

The 4-nitroimidazole based derivative **24** (PA-824, **Fig. 3**), is part of a promising new class of compounds that have shown antitubercular activity under hypoxic conditions and are evaluated clinically [31]. Fundamental SAR studies of nitroimidazoles as antitubercular compounds have been performed, with special emphasis on the structural requirements for aerobic versus anaerobic activities [32]. In order to understand the influence of the trifluoromethoxybenzyl ether side chain on the activity of 4-nitroimidazoles, the importance of a side chain was studied in compounds **25** and **26**. Removal of the side chain leading to the 4-nitro alcohol **25** derivative resulted in a dramatic and complete loss of both aerobic and anaerobic activities. Similarly, the methyl ether **26** derivative showed a similar loss of activity, ruling out a potential effect of different lipophilicities between **25** and **26**. The opening analogue of **27** retained some aerobic activity compared to the parent compound, but anaerobic activity was significantly decreased. Furthermore, the 2-oxy substituent, e.g. **28**, is a critical determinant of both aerobic and anaerobic activities. Compound **29** resembling Mtz, did not display any activity thus showing the importance of the nitro group position explaining Mtz's anaerobic activity. Replacing the oxazine oxygen with a methylene unit resulting in compound **31** restores the rotational constraints of the compound **24** and reduces the aerobic activity of compound **31** more than 30-fold compared to **24**. Interestingly olefinic precursor to **31**, compound **30** showed negligible aerobic and anaerobic activity [31].

Furthermore, different compounds with bicyclic nitroheterocycles varying heteroatoms in the 4/8-position of the adjacent six-membered ring of the nitroimidazooxazine tuberculosis drug **24** have been designed [33]. These compounds span a wide range (-570 to -338 mV) of one-electron reduction potentials $E(1)$, as compared with -534 mV for the S-form of **24**, which are closely correlated with the substituent constant (σ_m) values of the adjacent heteroatom. Although many of the different nitroheterocyclic compounds have $E(1)$ values close to that of **24**, only the nitroimidazothiazines (having sulfur at 4/8 positions) showed significant in vitro antitubercular activity. This study [33] with different nitroheterocyclic compounds suggests that $E(1)$ values are not major determinant of their antitubercular activity, instead which may depend on their fit to the reducing enzyme and/or nature of reactive species formed and its subsequent reactions. The results are consistent with the nitroimidazooxazine chromophore having particular utility in tuberculosis chemotherapy, with specific

substitution at the 2-position of the 4-nitroimidazole ring determining it's the major activity [32], whereas compound **34** exhibits no antibacterial activity. SAR studies suggest that a nitro group should possibly be present on C-5 position and that a partial charge on carbonyl oxygen in benzofuran is necessary for antibacterial action, such as in **54** [25].

Nitroimidazoles exhibit high microbicidal activity, where mutagenic, genotoxic and cytotoxic properties have been attributed to the presence of the nitro group. Recently, the antibactericidal compound **32** has been designed based on the 1, 2-disubstituted-4-nitroimidazole compounds with structure **33** (**Fig. 3**). It shows the unique and surprising property of being totally non-mutagenic [34, 35]. Furthermore, nitroimidazoles bearing different substituents for their potential reduction of genotoxicity and mutagenicity have been investigated. Compounds **35** and **36**, which contain a nitro group at C-4 and a CH₃ group at C-2, respectively, were not genotoxic compared to **39**, **40** and **41**, which possess a nitro group at C-5 exhibiting moderate to high genotoxicity. Nitroimidazole **39** (**Fig. 4**) also demonstrated moderate mutagenic effect [34]. Comparable results have been observed for the non-genotoxic **35** (2-CH₃ and 4-NO₂) and its analogue **45** (2-CH₃ and 5-NO₂), which is known to be a mutagenic agent [33]. However, when the nitroimidazole had no CH₃ group at C-2, the position of the NO₂ group had no influence on genotoxic activity. This is the case for **37** (4-NO₂) and **42** (5-NO₂), which behaved similar to **35** and **36** (no genotoxicity). When comparing pairs of similar compounds, for instance, **37** (4-NO₂ and N-CH₂OAcCH₂Cl) with **38** (4-NO₂ and N-CH₂OAcCH₂F) and **40** (2-CH₃, 5-NO₂ and N-CH₂ OHCH₂F) with **41** (2-CH₃, 5-NO₂ and N-CH₂OHCH₂OH), the presence of fluorine induced genotoxicity. The fluorinated compound **40** and **38** showed higher genotoxicity regardless of the presence of CH₃ at C-2 or NO₂ at C-4 or C-5. However, in compounds **35** (2-CH₃, 4-NO₂ and N-CH₂OHCH₂Cl) and **12** (2-CH₃, 4-NO₂ and N-CH₂ OHCH₂F), the fluorine atom had no influence on genotoxicity [33].

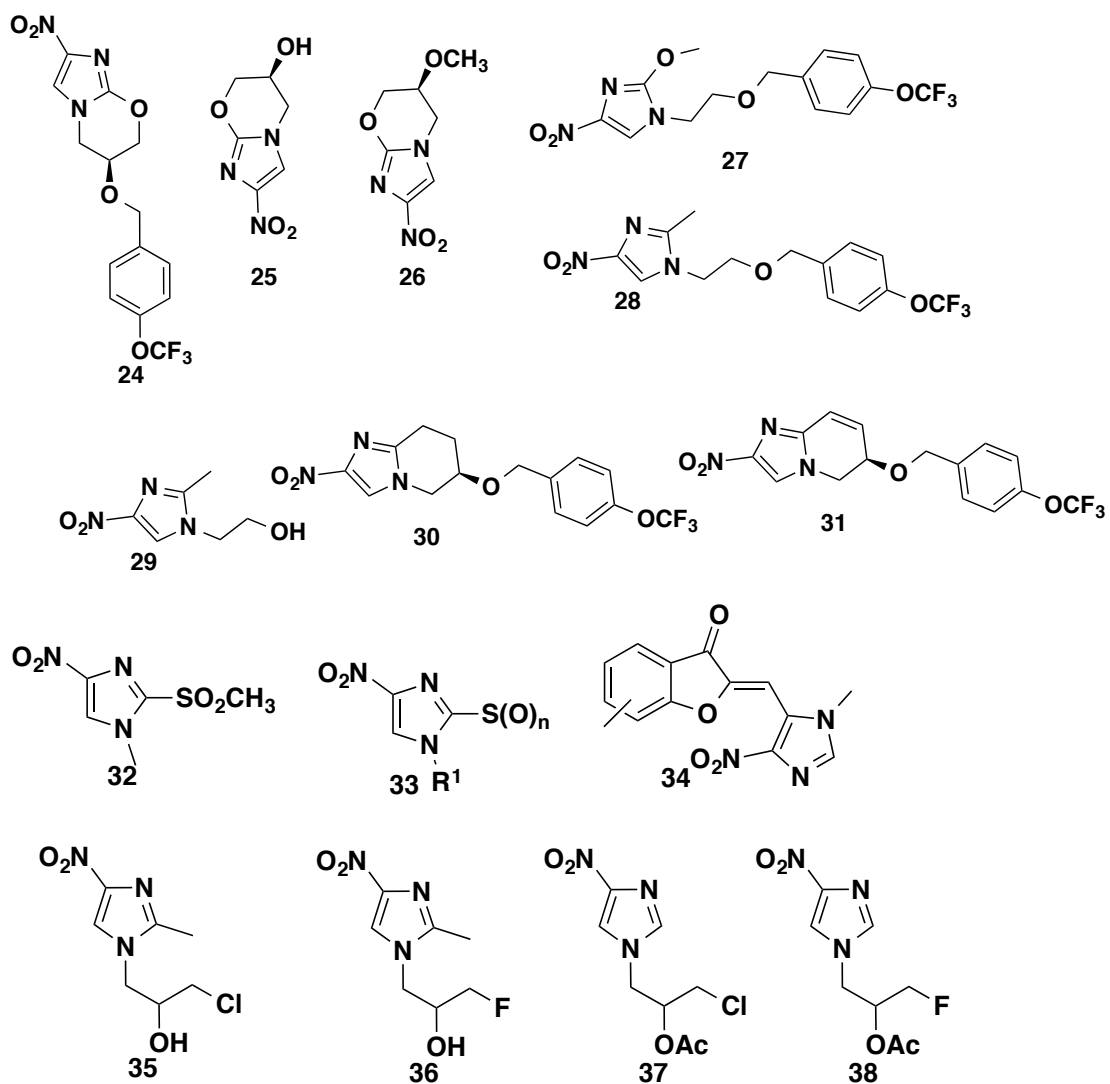


Figure 3: Structures of 4-nitroimidazoles

SAR studies on 5-nitroimidazole

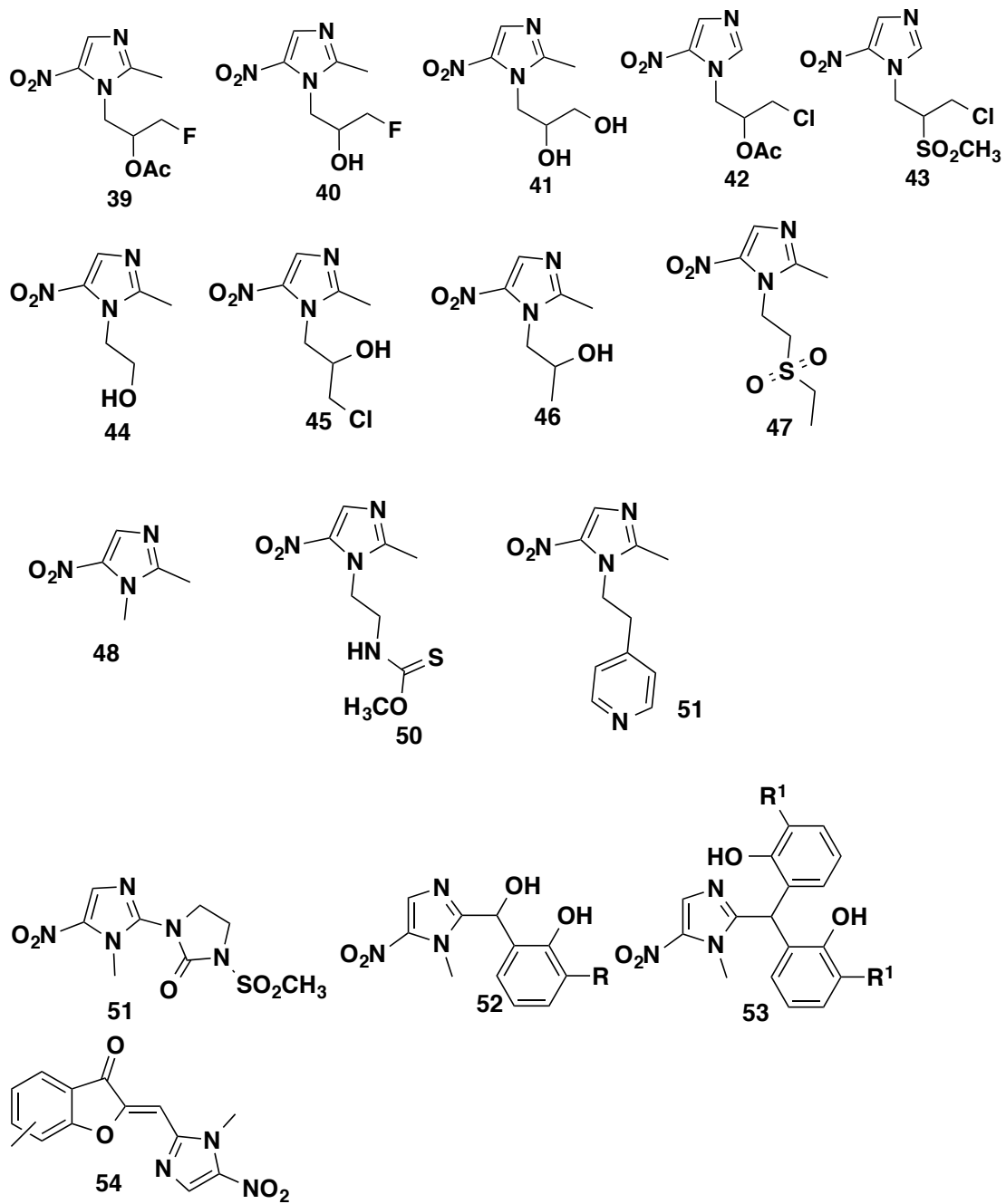
Mtz **44** (**Fig. 4**) belongs to the first class of nitroimidazoles listed by WHO as essential medicines [36] and was discovered in the mid-1950s at Rhône-Poulenc while searching for a cure for the sexually transmitted disease trichomoniasis [23], caused by *Trichomonas vaginalis*. Since its discovery, many Mtz derivatives have been used successfully for the treatment of diseases caused by anaerobic bacteria, amongst others secnidazole **46**, tinidazole **47**, ornidazole **45**, dimetridazole **48**, carnidazole **49** and panidazole **50** (**Fig. 4**). In the mid-1990s, it was discovered that Mtz showed only activity against the hypoxic, and not against aerobic and active replicating Mtb [37] raising the prospect of SAR studies for future drugs [38, 39]. An important consideration during nitroimidazole drug development is the selective microbial reduction as opposed to their mammalian hosts. 5-nitroimidazoles have a lower reduction potential compared to 2-nitroimidazoles, making them more selective for anaerobic microorganisms. Therefore, more SAR studies have been conducted on 5-nitroimidazoles [40].

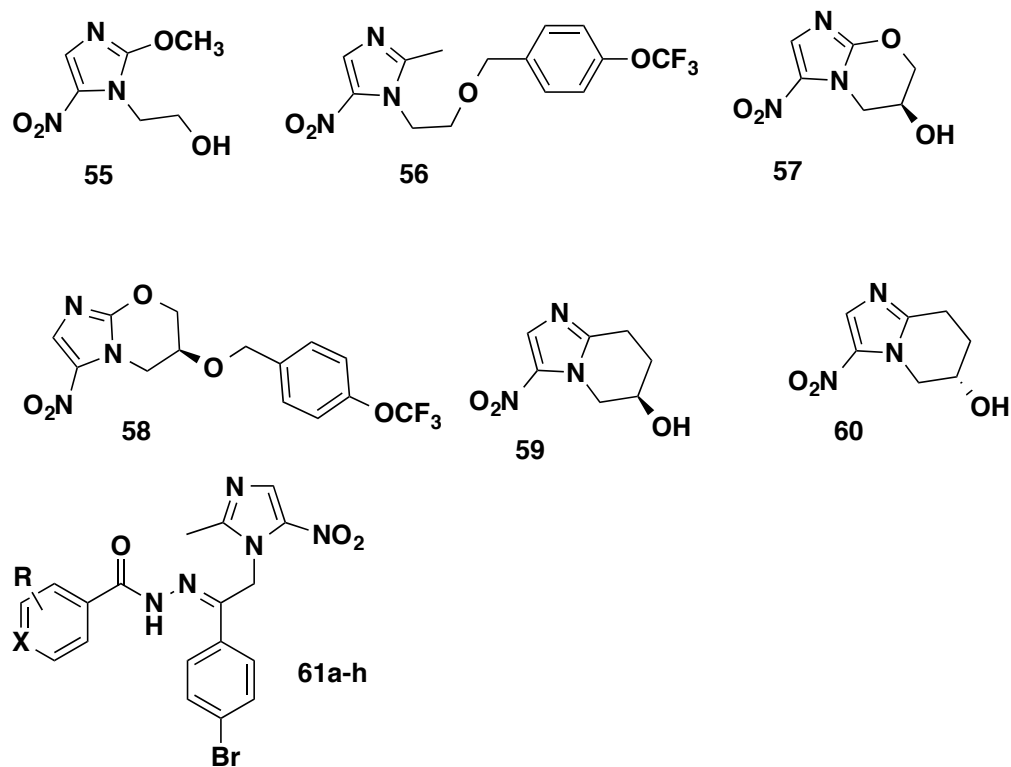
N1-substituted 5-nitroimidazoles were evaluated for activity against *Bacteroides* spp. and ranked (**Table 2**) according to their activity: tinidazole **47** > panidazole **50** > ornidazole **45** > Mtz **44** ≥ secnidazole **46** > carnidazole **49** > dimetridazole **48** [41]. GO-10213 **51** was found to be more active than Mtz against aerobes, microaerophilic organisms and anaerobes but its development halted due to the mutagenicity of the imidazolidinone ring [42]. 2-hydroxyaryl-(1-methyl-5-nitro-1H-imidazol-2-yl)methanols **52**, **53** with substituted phenolic rings in the ortho and/or para positions, containing bulky and strong lipophilic groups such as a t-butyl group in the carbocyclic ring have been reported for their antimicrobial activity and lack of mutagenicity [43].

SAR studies on 5-nitroimidazoles have been performed in order to understand their antitubercular activity (**Fig. 4**) [34]. Starting with lipophilic side chain, compound **56** containing benzyl ether of **24** appended to the Mtz **44** core structure, failed to display activity against Mtb and showed a significant decrease in anaerobic activity. This observation marks the distinction between 4- and 5-nitroimidazoles, since the presence of the lipophilic side chain did not confer aerobic activity and decreased anaerobic activity in the 5-nitro series. Incorporation of a 2-position oxygen atom, a structural element of **24**, into Mtz leading to compound **55** did not convey aerobic and anaerobic activities in the 5-nitro series, in contrast to the 4-nitro series. Indeed, **55**

lost anaerobic activity relative to Mtz. The bicyclic analogue of Mtz, compound **57**, unexpectedly showed aerobic and weak anaerobic activity. The rigid bicyclic structure imparts both aerobic and anaerobic activity compared with compound **55**. This result is also in contrast to compound **25**, which was inactive. Addition of trifluoromethoxy benzyl side chain from **24** yields compound **58** and improves both the aerobic and anaerobic activity of **59**. Compound **58** can also be viewed as the 5-nitro isomer of **24** and is only slightly less active compared to that parent. To understand the influence of the 2-position oxygen atom alone, the conformationally rigid, bicyclic forms of Mtz, compounds **59** and **60**, have been designed. Comparing compounds **57**, **59** and **60** show that replacing the 2-position oxygen atom from **57** finds that replacing only the 2-position oxygen with a methylene results in the loss of both aerobic and anaerobic activities. This result indicates that for 5-nitroimidazooxazines the 2-position oxygen atom is an essential requirement for both activities, but not for 4-nitroimidazooxazines, as discussed above. Compound **30**, with a 2-position methylene, retained both aerobic and anaerobic activities [32].

Schiff's base derivatives (**Fig. 4, Table 3**) have been shown to exert effective antibacterial activity as compared to the standards penicillin G and kanamycin B [44]. Against the Gram-negative bacteria *Pseudomonas aeruginosa*, compound **61b** was found to be more potent (MIC = 3.13 µg/ml) than penicillin G (MIC = 6.25 µg/ml) and showed comparable activity with kanamycin B. Moreover, compounds **61c** and **61h** showed activity (MIC = 3.13 µg/ml) against the Gram-negative bacteria *Escherichia coli* comparable with both standards used (MIC = 3.13 µg/ml). Compound **61f** showed effective activity (MIC = 3.13 µg/ml) against the Gram-positive bacteria *Bacillus subtilis* as compared to both standard (MIC = 1.56 µg/ml). The data suggest that a change in R substitution might lead to an activity change against the tested strains. The functional group at position R may therefore determine the activity against a particular species. Compounds having a 4-CH₃ and a 2-NH₂ at the benzene ring are found to be more effective as compared to compounds having Cl and NH₂ at 4-position. It is worth to mention that electron donating groups (CH₃ and NH₂) on a benzene ring is more effective than electron withdrawing groups (Cl). Furthermore, a hydroxyl group (**61d** and **61f**) is more effective than an amino group (**61g**). In conclusion, activity of antibacterial 5-nitroimidazole based derivatives not only depends not only on the bicyclic heteroaromatic pharmacophore, but also on the nature of the substituents [44, 45].

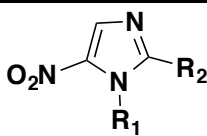




Compound	R	X
61a	H	C
61b	4-CH ₃	C
61c	4-Cl	C
61d	2-OH	C
61e	2-NH ₂	C
61f	4-OH	C
61g	4-NH ₂	C
61h	H	N

Figure 4: 5-nitroimidazole derivatives

Table 2: Minimum inhibitory concentration (MIC) of 5-nitroimidazoles against *Bacteroides fragillis*.

				
Compound	Compound name	R ₁	R ₂	MIC (μM)
Against <i>Bacteroides fragilis</i> ATCC 23745†				
47	Tinidazole	CH ₂ CH ₂ SO ₂ CH ₂ CH ₃	CH ₃	0.8
50	Panidazole	CH ₂ CH ₂ -(4)-pyridyl	CH ₃	2.2
45	Ornidazole	CH ₂ CH(OH)CH ₂ Cl	CH ₃	3.7
44	Mtz	CH ₂ CH ₂ OH	CH ₃	3.7
46	Secnidazole	CH ₂ CH(OH)CH ₃	CH ₃	3.7
49	Carnidazole	CH ₂ CH ₂ NHC(S)OCH ₃	CH ₃	6.3
50	Dimetridazole	CH ₃	CH ₃	10.0

Data from [41, 42]

Table 3: Antibacterial activity of compounds 61a-61h

Compounds	Gram positive bacteria		Gram negative bacteria	
	<i>B. subtilis</i> ATCC 6633	<i>S. aureus</i> ATCC 6538	<i>E. coli</i> ATCC 35218	<i>P. aeruginosa</i> ATCC 13525
Minimum inhibitory concentrations (MIC) expressed in μg/ml				
61a	25	100	100	100
61b	>100	6.25	50	3.13
61c	100	>100	3.13	100
61d	100	>100	100	50
61e	12.5	3.13	>100	6.25
61f	3.13	25	25	25
61g	100	100	100	25
61h	100	50	3.13	25
Kanamycin	1.56	1.56	3.13	3.13
B				
Penicilin G	1.56	6.25	3.13	6.25

Nitroimidazoles analogues as radiosensitizers and SAR studies

To overcome the resistance to radiotherapy within hypoxic tumor regions several nitroimidazole compounds, mimicking the effect of oxygen during irradiation, have been identified based on their electron affinity [46, 47]. In hypoxic tissues, as described above (**Fig. 1**) the nitro group is reduced by enzymatic nitroreductase catalysis, decomposed into radicals, bound to cellular macro-molecules and trapped therefore in hypoxic cells [16, 48-50]. A number of studies have been hitherto carried out to search electron-capturing chemical agents that show radiosensitizing ability.

The first generation of radiosensitizers includes nitroimidazole and Mtz **44** derivatives, bearing a hydroxyethyl side chain (**Fig. 4**). This family of agents was confirmed to show effective *in vitro* and *in vivo* radiosensitizing activity exclusively under hypoxic conditions [51]. The discovery of this family prompted the search for related analogues with higher radiosensitizing ability. Consequently, the more active compound misonidazole **62** was discovered [52]. Because of severe neurological toxicity clinical trials with misonidazole were halted, but this prototype agent confirms that compounds with electron affinity exhibit radiosensitizing properties towards hypoxic tumor cells [53, 54].

Second generation 2-nitroimidazole derivatives (**Fig. 5**) are mainly based on a modification of the side chain structures. Amongst a large number of synthesized 2-nitroimidazole derivatives etanidazole **63**, NLCQ-1 **64**, pimonidazole **65**, nimorazole **88** and KU2285 **66** provided encouraging results including suppression of neurotoxicity related side effects [55]. The less toxic 5-nitroimidazole derivative, nimorazole **88**, has been shown to reach similar sensitizer enhancement ratios (SER 1.26) in a fractionated radiation schedule (300 mg/kg) as compared to misonidazole (SER 1.32) but with far less toxicity [56] and is therefore now used in standard clinical treatment for head and neck cancer patients in Denmark [57]. Currently, a multicentric EORTC trial (NCT01880359) is ongoing to validate these results.

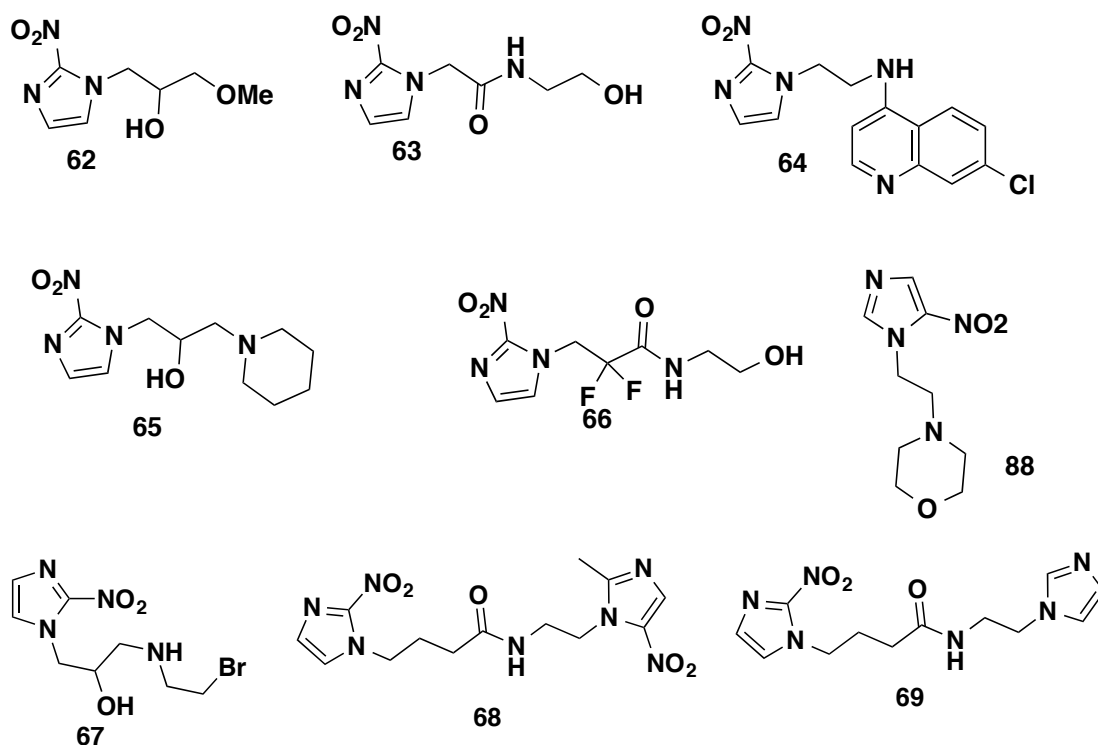


Figure 5: Structures of radiosensitizing 2-nitroimidazoles

A series of novel bis-(nitroimidazolyl) alkanecarboxamides has been synthesized and evaluated for their hypoxia-selective cytotoxicity and hypoxic cell radiosensitisation *in vitro* and *in vivo* [58]. The SER values for the bis- nitroimidazoles **70-79** (Fig. 6) containing one or more 2-nitroimidazole moieties were at least 2-fold lower compared to misonidazole, with no obvious structure activity relationships. Compound **80**, containing two 5-nitroimidazole moieties, was 5-fold more potent than the mono-5-nitroimidazole derivative **44**. Overall, the bis derivatives appear to be broadly similar to monomeric nitroimidazoles as hypoxic cell radiosensitizers with respect to potency and selectivity relative to aerobic toxicity [58, 59].

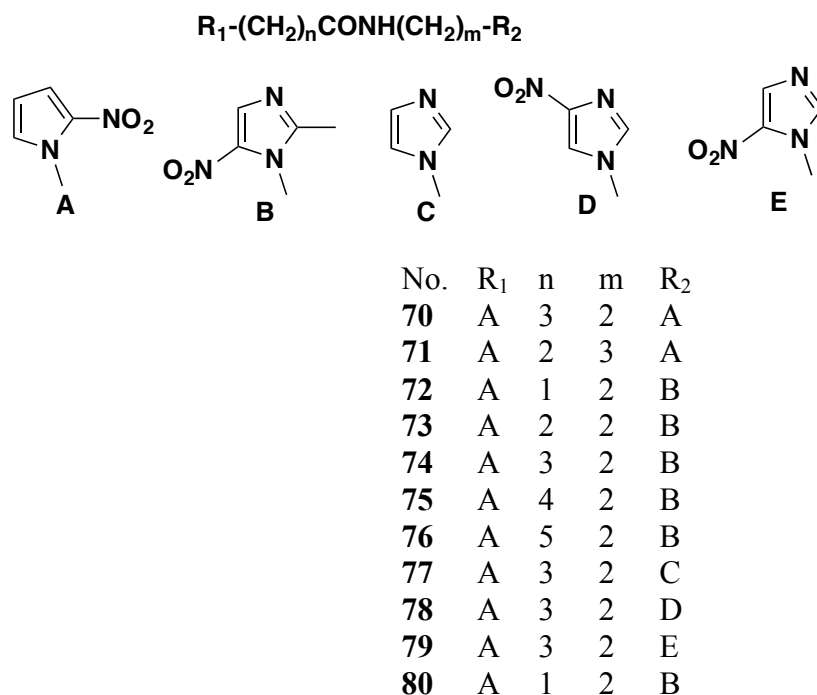


Figure 6: Structures of bis (nitroimidazolyl)alkanecarboxamides

To investigate the influence of aqueous solubility, lipophilicity and electron affinity on radiosensitizing efficacy a series of nitroimidazole alkylsulfonamides was synthesized (**Fig. 7**) [60]. Although a sulfonamide group provides an increased polar surface area (PSA), it has a negative effect on aqueous solubility. The solubility, although still in the millimolar range, of neutral 2-nitroimidazole sulfonamides **81**, **82–84**, **85** is considerably less than either misonidazole **62** or etanidazole **63**. The use of basic side chains, as done for derivative **86** and **87**, provides a two-fold increase in solubility over **85**, but solubility remains lower compared to **62** and **63**. Lipophilicity influences two important properties of nitroimidazole-based radiosensitizers: extravascular transport and normal tissue toxicity [61, 62]. The new analogues are at least as polar as misonidazole **62** with two analogues **84** and **86** being more polar than etanidazole **63**. The electron affinity of the nitroimidazole moiety dominates the in vitro SAR for radiosensitisation [63] and cytotoxicity [64]. The one-electron reduction potential E(1) values are correlated with electron affinity [62], making this the most relevant parameter for SAR studies. The E(1) value of the three possible regio-isomers determined by pulse radiolysis are summarized in **Table 4**. The reported potentials span the range for efficient reaction with DNA radicals (-503 to -342 mV) with the 2-nitroimidazole being more electron affinic than the corresponding 5- and 4-isomers. The sulfonamide group provides a strong electron-withdrawing

influence increasing the electron affinity, with the two 2-nitroimidazoles **81** and **84** having E(1) values raised by 36 and 46 mV, respectively, compared to etanidazole. Similarly, the 4-nitroimidazole **82** and the 5-nitroimidazole **83** have increased E(1) values compared to comparable nitroimidazoles (e.g., nimorazole **88** has an E(1) value of -457 mV, while the analogous 4-isomer has an E(1) of -554 mV) [65]. In contrast, the 5-nitroimidazole **85** has a slightly reduced E(1) compared to Mtz **44** (-480 mV) [64] reflecting the reduced electronic effect over the longer ethyl spacer unit. A positively charged solubilizing side chain **86** offsets this to some extent.

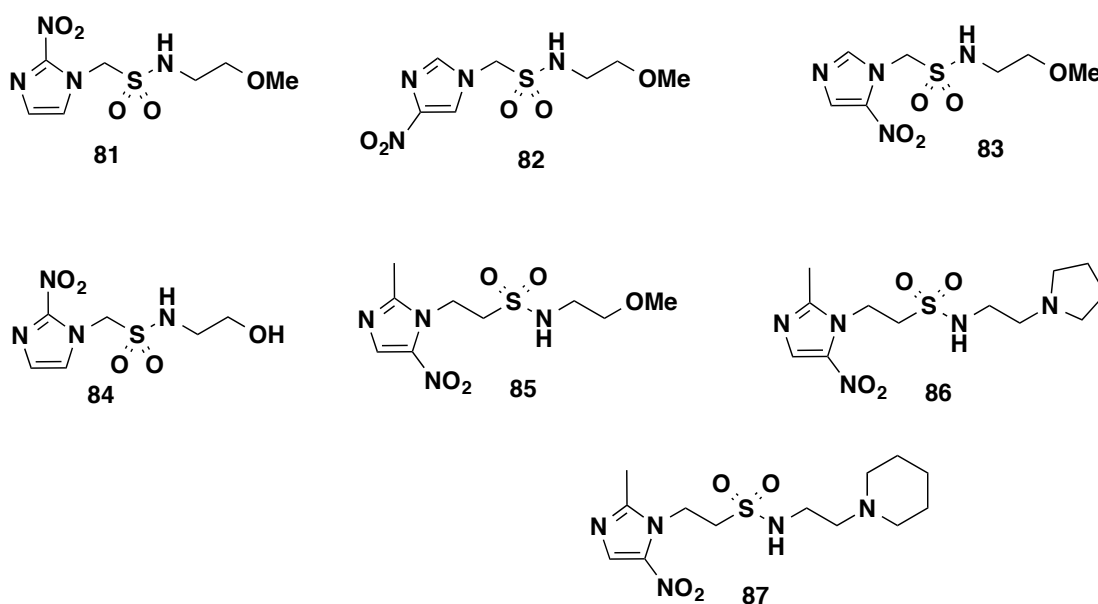


Figure 7: Structures of nitroimidazole alkylsulfonamides

Table 4: Physicochemical parameters of alkylsulfonamides

Compound	Solubility (mM)	LogD ^a	PSA ^b	E(1) mV	Reference E(1) ^d
Misonidazole (62)	>100	-0.41	93.1	-389 ^c	?
Etanidazole (63)	>100	-1.37	113.0	-388 ^c	?
81	6.5	-1.19	127.4	-352±10	BV
82	23.5	-0.83	127.4	-503±7	MV
83	>27	-0.64	127.4	-421±8	MV
84	18.1	-1.53	138.3	-342±8	MV
85	29.6	-0.84	127.4	-500±8	TQ
86	61.7	-1.87	121.4	-475±8	TQ
87	>51	-0.39	121.4	-554	

^aCalculated by ACD Lab LogD calculator v12.5; ^bACD/PhysChem v12; ^cReference compounds:BV, benzylviologen, MV, methylviologen, TQ, triquat

Novel bifunctional hypoxic radiosensitizers have been designed as hypoxia-targeting compounds (**Fig. 8**) [66]. TX-1845 (**89**), TX-1846 (**90**) and the corresponding optically active agents TX-1898 (**91**) and TX-1900 (**92**) comprising 2-nitroimidazole and haloacetyl carbamoyl groups at the side chain have been synthesized [54, 66, 67]. The haloacetyl group acts as an acceptor of intracellular nucleophiles such as mercapto and amino groups to form a covalent bond with DNA or proteins. Thus, these bifunctional haloacetyl carbamoyl compounds possess radiosensitizing and alkylating functionalities, exhibiting 100 times higher hypoxic radiosensitizing activity than conventional 2-nitroimidazole derivatives. The derivative TX-1877 (**93**), which is conjugated with an acetoamide unit, shows higher inhibitory activity against metastasis and angiogenesis, and causes greater enhancement of macrophage infiltration [66].

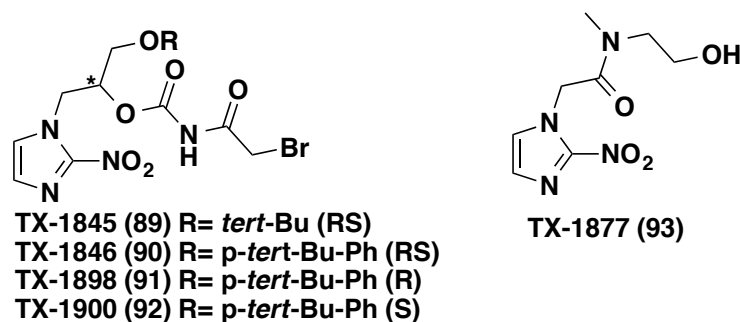


Figure 8: Structures of bifunctional 2-nitroimidazole radiosensitizers

Recently, synthesis and SAR studies on bifunctional alkylating and acylating radiosensitizers (**94a-l and 95**) (**Fig. 9**) have been described and only the compounds **94a, g, h, and 95** exhibited a SER >2.0. The compounds **92a, b, f, h and 95** yielding an SER \geq 1.8 were further evaluated in a dose–response study ($C_{1.6}$ determination). The $C_{1.6}$ of a compound is a measure of its radiosensitization efficiency and is defined as the concentration required to give a SER of 1.6. Despite being generally weak as radiosensitizers based on SER, the compounds **94f, h, 95** showed $C_{1.6}$ values comparable to or less than the reference agent **67** (**Table 5**) [68].

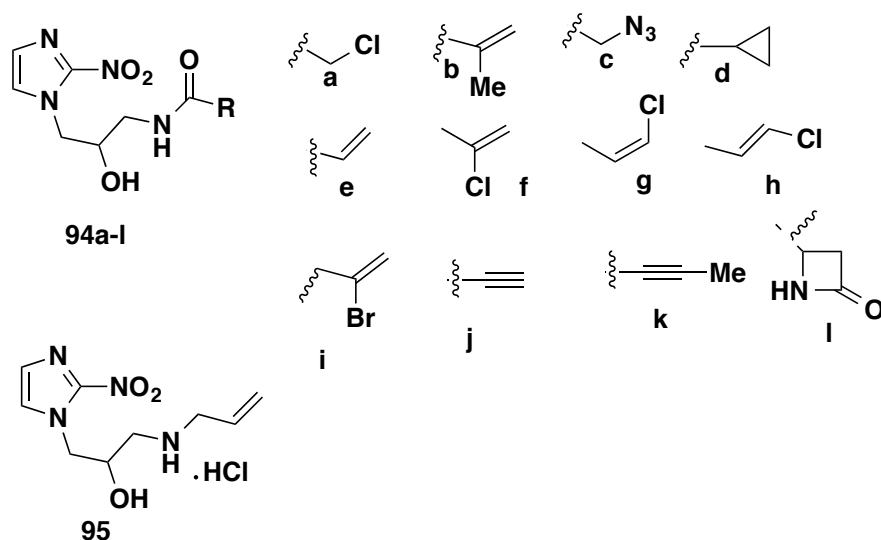


Figure 9: Structures of bifunctional nitroimidazole alkylating and acylating radiosensitizers

Table 5: *In Vitro* Radiosensitizing Activity^a and Alkylation Potential of 2-Nitroimidazoles^b

Compound	Max. tolerance conc. (mM)	SER	C _{1.6}
67	3.0	2.8	0.5
94a	3.0	2.4	0.71
94b	3.0	1.8	2.1
94c	3.0	1.5	ND ^c
94d	1.5	1.2	ND
94e	3.0	1.3	ND
94f	0.09	1.8	0.08
94g	3.0	2.4	0.98
94h	1.5	2.2	0.38
94i	0.02	1.2	ND
94j	3.0	1.6	ND
94k	3.0	1.4	ND
94l	3.0	1.0	ND
95	3.0	2.5	0.31

^aValues represent the mean of replicate experiments agreeing within $\pm 20\%$

^bSupplemental information for *in vitro* methods, ^cNot determined

Hypoxia causes acidification of the extracellular environment and studies have demonstrated that CAIX is the main contributor to this process [69-71], i.e. CAIX maintains intracellular pH at physiological values [72]. Previous studies show that CAIX inhibition is able to sensitize tumors towards radiation [69]. Designing new derivatives with well-known radiosensitizers (nitroimidazoles) coupled with CAIX inhibitors (dual target compounds) are able to reduce hypoxic extracellular acidification, to inhibit tumor growth at nontoxic doses and to sensitize tumors to radiation and chemotherapy in a CAIX dependent manner [73, 74]. Promising results

show that this dual targeting concept was a breakthrough to exploit nitroimidazoles radiosensitization property by modifying them to target tumor associated carbonic anhydrase IX (CAIX) [72], e.g. **96**, **97**, **98** and **99a-c** (Fig. 10). In this study, CAIX-specific dual targeting sulfamide (**96**) enhanced the therapeutic effect of radiation in a CAIX dependent manner (SER 1.45 in tumors expressing CAIX vs SER 1.04 in tumors with CAIX knockdown) without systemic toxicity as evaluated by body weight loss. Dual target nitroimidazole derivative **96** showed higher SER than **81** (SER 1.32) and **88** (1.26). The SER of the dual targeting compound **96** (10 mg/kg) was also higher than the well-established hypoxic radiosensitizers misonidazole **81** and nimorazole **88** (300 mg/kg) for which a minimal dose of 100 mg/kg was needed to achieve an SER above unity [56].

SAR studies on these dual targeting derivatives would help to develop potent radiosensitizers with low cytotoxicity. Therapeutic targets expressed in hypoxic tumor microenvironment also open a wide range of opportunities to develop optimal radiosensitizers.

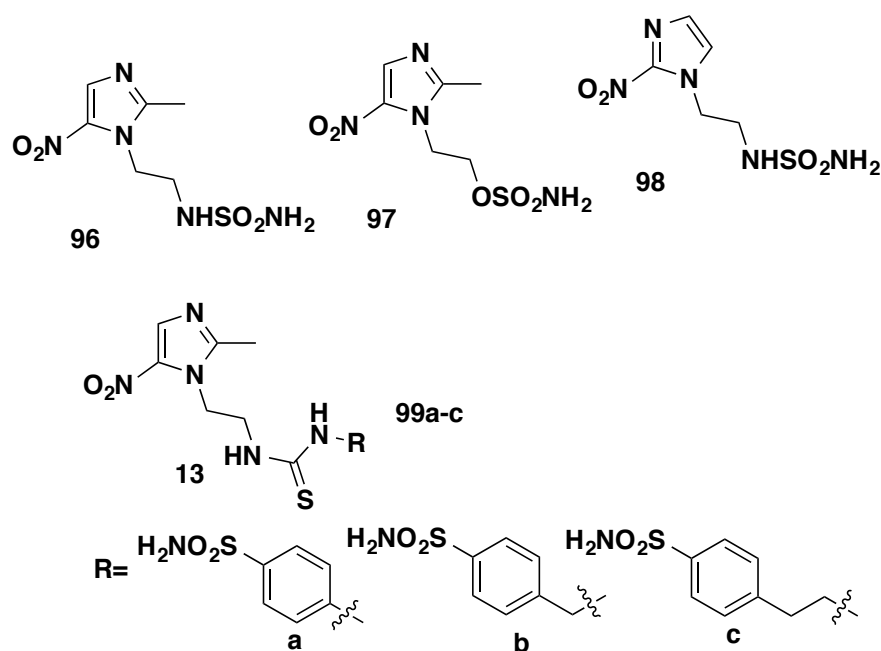


Figure 10: Structures of dual targeting derivatives

Future perspectives

The nitroimidazoles activation depends on reduction by ferredoxin or flavodoxin. Increased use of nitroheterocyclic drugs, in response to drug resistance to other commonly used antibiotics has in turn resulted in drug resistance to a number of nitroheterocyclic drugs. *Bacteroides* strains and other bacteria, including *Helicobacter*, have developed resistance to Mtz via a number of mechanisms, especially a decrease in drug reduction as a result of alterations in the electron transport pathways. Although resistance to these drugs is not widespread, their increased use worldwide as a prophylaxis and in chemotherapy will inevitably result in increased resistance in organisms commonly found in bacterial infections. However, the variety of substitutions which can be attached to the ring structures has led to a great variety of drugs being synthesized, some of which are many-fold more active than the commonly prescribed nitroheterocycles [13]. The recent development of molecular genetic techniques for *Trichomonas vaginalis* has opened the possibility for definitive studies of drug resistance as transient and selectable transformation methods are now available. Reverse genetic approaches will allow testing the function of specific molecules and postulated pathways leading to Mtz resistance. A clearer understanding of the mechanism(s) of Mtz resistance should provide a foundation for the development of alternative chemotherapies for treatment-refractory cases of infection caused by these organisms [75]. SAR studies and minimal resistance of nitroimidazole to a plethora of bacteria shows that this area of research is still thriving research interest for future antibiotic development.

A potential explanation for the failure of treatment to improve outcomes of hypoxic solid tumor is the heterogeneity of therapy resistant hypoxic tumor cells. Transient tumor hypoxia and subsequent reperfusion may result in cells that are viable yet also radio- and drug-resistant [76]. Oxygen mimicking small molecules has the potential to sensitize hypoxic tumors to radiation. To develop a good radiosensitizer aqueous solubility, electron affinity and reduction potentials play a key role. Altering one of these parameters and SAR studies would help to develop potent radiosensitizer with minimal side effects.

Acknowledgements

Authors acknowledge financial support from ERC advanced grant (ERC-ADG-2015, No. 694812 - Hypoximmuno).

References

1. Brown, J.M., *Tumor hypoxia in cancer therapy*. Methods in enzymology, 2007. **435**: p. 297-321.
2. Hirn, M., *Hyperbaric oxygen in the treatment of gas gangrene and perineal necrotizing fasciitis. A clinical and experimental study*. The European journal of surgery. Supplement. := Acta chirurgica. Supplement, 1993(570): p. 1-36.
3. Hall, E.J., et al., *The nitroimidazoles as radiosensitizers and cytotoxic agents*. The British journal of cancer. Supplement, 1978. **3**: p. 120-3.
4. O'Connor, J.P., et al., *Imaging biomarker roadmap for cancer studies*. Nature reviews. Clinical oncology, 2017. **14**(3): p. 169-186.
5. Zegers, C.M., et al., *In vivo quantification of hypoxic and metabolic status of NSCLC tumors using [18F]HX4 and [18F]FDG-PET/CT imaging*. Clinical cancer research : an official journal of the American Association for Cancer Research, 2014. **20**(24): p. 6389-97.
6. Peeters, S.G., et al., *Current preclinical and clinical applications of hypoxia PET imaging using 2-nitroimidazoles*. The quarterly journal of nuclear medicine and molecular imaging : official publication of the Italian Association of Nuclear Medicine, 2015. **59**(1): p. 39-57.
7. Yaromina, A., et al., *A novel concept for tumour targeting with radiation: Inverse dose-painting or targeting the "Low Drug Uptake Volume"*. Radiotherapy and oncology : journal of the European Society for Therapeutic Radiology and Oncology, 2017.
8. Peeters, S.G., et al., *TH-302 in Combination with Radiotherapy Enhances the Therapeutic Outcome and Is Associated with Pretreatment [18F]HX4 Hypoxia PET Imaging*. Clinical cancer research : an official journal of the American Association for Cancer Research, 2015. **21**(13): p. 2984-92.
9. Mukherjee, T. and H. Boshoff, *Nitroimidazoles for the treatment of TB: past, present and future*. Future medicinal chemistry, 2011. **3**(11): p. 1427-54.
10. Brook, I., *Antimicrobial treatment of anaerobic infections*. Expert opinion on pharmacotherapy, 2011. **12**(11): p. 1691-707.
11. Chow, A.W., V. Patten, and L.B. Guze, *Susceptibility of anaerobic bacteria to metronidazole: relative resistance of non-spore-forming gram-positive bacilli*. The Journal of infectious diseases, 1975. **131**(2): p. 182-5.

12. Sutter, V.L. and S.M. Finegold, *Susceptibility of anaerobic bacteria to 23 antimicrobial agents*. Antimicrobial agents and chemotherapy, 1976. **10**(4): p. 736-52.
13. Townson, S.M., et al., *Resistance to the nitroheterocyclic drugs*. Acta tropica, 1994. **56**(2-3): p. 173-94.
14. Upcroft, J.A., et al., *Efficacy of new 5-nitroimidazoles against metronidazole-susceptible and -resistant Giardia, Trichomonas, and Entamoeba spp.* Antimicrobial agents and chemotherapy, 1999. **43**(1): p. 73-6.
15. Muller, M., *Mode of action of metronidazole on anaerobic bacteria and protozoa*. Surgery, 1983. **93**(1 Pt 2): p. 165-71.
16. Edwards, D.I., *Nitroimidazole drugs--action and resistance mechanisms. I. Mechanisms of action*. The Journal of antimicrobial chemotherapy, 1993. **31**(1): p. 9-20.
17. Blower, P.J., et al., *Towards new transition metal-based hypoxic selective agents for therapy and imaging*. Journal of inorganic biochemistry, 2001. **85**(1): p. 15-22.
18. Knox, R.J., R.C. Knight, and D.I. Edwards, *Interaction of nitroimidazole drugs with DNA in vitro: structure-activity relationships*. British journal of cancer, 1981. **44**(5): p. 741-5.
19. Van Aerschot, A., et al., *An acyclic 5-nitroimidazole nucleoside analogue as ambiguous nucleoside*. Nucleic acids research, 1995. **23**(21): p. 4363-70.
20. Via, L.E., et al., *Tuberculous granulomas are hypoxic in guinea pigs, rabbits, and nonhuman primates*. Infection and immunity, 2008. **76**(6): p. 2333-40.
21. Boshoff, H.I. and C.E. Barry, 3rd, *Tuberculosis - metabolism and respiration in the absence of growth*. Nature reviews. Microbiology, 2005. **3**(1): p. 70-80.
22. Blair, J.M., et al., *Molecular mechanisms of antibiotic resistance*. Nature reviews. Microbiology, 2015. **13**(1): p. 42-51.
23. Voogd, C.E., *On the mutagenicity of nitroimidazoles*. Mutation research, 1981. **86**(3): p. 243-77.
24. Cavalleri, B., et al., *New 5-substituted 1-alkyl-2-nitroimidazoles*. Journal of medicinal chemistry, 1973. **16**(5): p. 557-60.
25. Alka, M., *Synthetic Nitroimidazoles: Biological Activities and Mutagenicity Relationships*. Sci Pharm. , 2009. **77**: p. 497-520.

26. Cavalleri, B., G. Volpe, and V. Arioli, *Synthesis and biological activity of some vinyl-substituted 2-nitroimidazoles*. Journal of medicinal chemistry, 1977. **20**(5): p. 656-60.
27. Cavalleri, B., et al., *Synthesis and biological activity of two metabolites of 1-methyl-5-(1-methylethyl)-2-nitro-1 H-imidazole, an antiprotozoal agent*. Journal of medicinal chemistry, 1977. **20**(11): p. 1522-5.
28. Chopra, S., et al., *Discovery and optimization of benzotriazine di-N-oxides targeting replicating and nonreplicating Mycobacterium tuberculosis*. Journal of medicinal chemistry, 2012. **55**(13): p. 6047-60.
29. Cavalleri, B., et al., *Synthesis and biological activity of some 2-aminoimidazoles*. Arzneimittel-Forschung, 1977. **27**(10): p. 1889-95.
30. Cavalleri, B., et al., *1-Methyl-2-nitroimidazol-5-yl derivatives. IIIrd communication*. Arzneimittel-Forschung, 1977. **27**(6): p. 1131-34.
31. Tyagi, S., et al., *Bactericidal activity of the nitroimidazopyran PA-824 in a murine model of tuberculosis*. Antimicrobial agents and chemotherapy, 2005. **49**(6): p. 2289-93.
32. Kim, P., et al., *Structure-activity relationships of antitubercular nitroimidazoles. 1. Structural features associated with aerobic and anaerobic activities of 4- and 5-nitroimidazoles*. Journal of medicinal chemistry, 2009. **52**(5): p. 1317-28.
33. Thompson, A.M., et al., *Synthesis, reduction potentials, and antitubercular activity of ring A/B analogues of the bio-reductive drug (6S)-2-nitro-6-{[4-(trifluoromethoxy)benzyl]oxy}-6,7-dihydro-5H-imidazo[2,1-b][1, 3]oxazine (PA-824)*. Journal of medicinal chemistry, 2009. **52**(3): p. 637-45.
34. Bagan, E.S.M., G.T. , *Uniquely non-mutagenic substituted nitroimidazole*. . US4728664 A. , 1988.
35. Nagarajan, K.A., V.P.; George, T.; Sudarsanam, V.; Shah, R.K.; Goud, A.N.; Shenov, S.J.; Honkan, V.; Kulkarni, Y.S.; Rao, M.L. , *Nitroimidazoles. IV. 1-1-Methyl-5-nitroimidazolyl (2)-2-oxo-3-sulphonyl (carbamoylthiocarbamoyl) tetrahydro imidazoles*. . Ind. J. Chem. , 1982. **21**: p. 928-940.
36. WHO, *model list of essential medicines*. . www.who.int/entity/medicines/publications/essentialmedicines Updated sixteenth adult list en.pdf.

37. Wayne, L.G. and H.A. Sramek, *Metronidazole is bactericidal to dormant cells of Mycobacterium tuberculosis*. Antimicrobial agents and chemotherapy, 1994. **38**(9): p. 2054-8.
38. Barry, C.E., 3rd, et al., *The spectrum of latent tuberculosis: rethinking the biology and intervention strategies*. Nature reviews. Microbiology, 2009. **7**(12): p. 845-55.
39. Young, D.B., et al., *Confronting the scientific obstacles to global control of tuberculosis*. The Journal of clinical investigation, 2008. **118**(4): p. 1255-65.
40. Hof, H., *Antibacterial activities of the antiparasitic drugs nifurtimox and benznidazole*. Antimicrobial agents and chemotherapy, 1989. **33**(3): p. 404-5.
41. Jokipii, L. and A.M. Jokipii, *Comparative evaluation of the 2-methyl-5-nitroimidazole compounds dimetridazole, metronidazole, secnidazole, ornidazole, tinidazole, carnidazole, and panidazole against Bacteroides fragilis and other bacteria of the Bacteroides fragilis group*. Antimicrobial agents and chemotherapy, 1985. **28**(4): p. 561-4.
42. Hof, H. and J. Stroder, *Antibacterial activity of GO 10213, a nitroimidazole derivative*. Antimicrobial agents and chemotherapy, 1986. **29**(5): p. 953-4.
43. Arredondo, Y., et al., *Preparation, antimicrobial evaluation and mutagenicity of differently substituted [2-hydroxyaryl]-[1-methyl-5-nitro-1H-2-imidazolyl]methanols*. Bioorganic & medicinal chemistry letters, 1996. **6**(15): p. 1781-1784.
44. Makawana, J.A., J. Sun, and H.L. Zhu, *Schiff's base derivatives bearing nitroimidazole moiety: new class of antibacterial, anticancer agents and potential EGFR tyrosine kinase inhibitors*. Bioorganic & medicinal chemistry letters, 2013. **23**(23): p. 6264-8.
45. Haythem, A.S.I., M.M.; Amal, G.A.; Mohammad, S.M., *Synthesis and antimicrobial activity of new 1,2,4-triazole-3-thiol metronidazole derivatives*. . Montash. Chem, 2010. **141**: p. 471-478.
46. Adams, D.E.F., J. F.; Wardman, P., *HYPOXIC CELL SENSITIZERS IN RADIOBIOLOGY AND RADIOTHERAPY*. The British journal of cancer. Supplement, 1978. **37**: p. 1-132.
47. Asquith, J.C., et al., *Electron affinic sensitization. V. Radiosensitization of hypoxic bacteria and mammalian cells in vitro by some nitroimidazoles and nitropyrazoles*. Radiation research, 1974. **60**(1): p. 108-18.

48. Edwards, D.I., *Nitroimidazole drugs--action and resistance mechanisms. II. Mechanisms of resistance*. The Journal of antimicrobial chemotherapy, 1993. **31**(2): p. 201-10.
49. Hodgkiss, R.J., *Use of 2-nitroimidazoles as bioreductive markers for tumour hypoxia*. Anti-cancer drug design, 1998. **13**(6): p. 687-702.
50. Taiwei, M.L.C., *[(99m)Tc(CO)₃]⁺ labeled histidine derivative containing 4-nitroimidazole: Synthesis, biodistribution as a tumor hypoxia imaging agent*. Nuclear Science and Techniques 2011. **22**(2): p. 105-110.
51. Willson, R.L., W.A. Cramp, and R.M. Ings, *Metronidazole ('Flagyl'): mechanisms of radiosensitization*. International journal of radiation biology and related studies in physics, chemistry, and medicine, 1974. **26**(6): p. 557-69.
52. Dische, S., et al., *Misonidazole-a drug for trial in radiotherapy and oncology*. International journal of radiation oncology, biology, physics, 1979. **5**(6): p. 851-60.
53. Brown, J.M., *Modification of Radiosensitivity in Cancer Treatment*. ed. S. Sugahara, Academic Press, Tokyo, 1984: p. 139-174.
54. Tanabe, K., et al., *Current molecular design of intelligent drugs and imaging probes targeting tumor-specific microenvironments*. Organic & biomolecular chemistry, 2007. **5**(23): p. 3745-57.
55. Keisuke Sasai, H.I., Toru Yoshizawa, Sei-Ichi Nishimoto, Yuta Shibamoto, Natsuo Oya, Toru Shibata, Mitsuyuki Abe, *Fluorinated 2-nitroimidazole derivative hypoxic cell radiosensitizers: Radiosensitizing activities and pharmacokinetics*. International journal of Radiation Oncology biology physics, 1994. **29**(3): p. 579-582.
56. Overgaard, J., et al., *A comparative investigation of nimorazole and misonidazole as hypoxic radiosensitizers in a C3H mammary carcinoma in vivo*. British journal of cancer, 1982. **46**(6): p. 904-11.
57. Overgaard, J., et al., *A randomized double-blind phase III study of nimorazole as a hypoxic radiosensitizer of primary radiotherapy in supraglottic larynx and pharynx carcinoma. Results of the Danish Head and Neck Cancer Study (DAHANCA) Protocol 5-85*. Radiotherapy and oncology : journal of the European Society for Therapeutic Radiology and Oncology, 1998. **46**(2): p. 135-46.
58. Hay, M.P., et al., *Hypoxia-selective antitumor agents. 8. Bis(nitroimidazolyl)alkanecarboxamides: a new class of hypoxia-selective cytotoxins and hypoxic cell radiosensitisers*. Journal of medicinal chemistry, 1994. **37**(3): p. 381-91.

59. Moselen, J.W., et al., *N-[2-(2-methyl-5-nitroimidazolyl)ethyl]-4-(2-nitroimidazolyl)butanamide (NSC 639862), a bisnitroimidazole with enhanced selectivity as a bioreductive drug*. *Cancer research*, 1995. **55**(3): p. 574-80.
60. Bonnet, M., et al., *Novel nitroimidazole alkylsulfonamides as hypoxic cell radiosensitisers*. *Bioorganic & medicinal chemistry*, 2014. **22**(7): p. 2123-32.
61. Frederik B. Pruijn, K.P., Michael P. Hay, William R. Wilson, and Kevin O. Hicks, *Prediction of Tumour Tissue Diffusion Coefficients of Hypoxia-Activated Prodrugs from Physicochemical Parameters*. *Australian journal of Chemistry*, 2008. **61**: p. 687-693.
62. J Martin Brown, N.Y.Y., Dennis M Brown, William W Lee., *SR-2508: A 2-nitroimidazole amide which should be superior to misonidazole as a radiosensitizer for clinical use*. *International Journal of Radiation Oncology Biology Physics*, 1981. **7**(6): p. 695-703.
63. Adams, G.E., et al., *Structure-activity relationships in the development of hypoxic cell radiosensitizers. I. Sensitization efficiency*. *International journal of radiation biology and related studies in physics, chemistry, and medicine*, 1979. **35**(2): p. 133-50.
64. Adams, G.E., et al., *Structure-activity relationships in the development of hypoxic cell radiosensitizers. II. Cytotoxicity and therapeutic ratio*. *International journal of radiation biology and related studies in physics, chemistry, and medicine*, 1979. **35**(2): p. 151-60.
65. Wardman, P., *Reduction Potentials of One-Electron Couples Involving Free-Radicals in Aqueous-Solution*. *Journal of Physical and Chemical Reference Data*, 1989. **18**(4): p. 1637-1755.
66. Hori, H., et al., *Design, synthesis, and biological activity of anti-angiogenic hypoxic cell radiosensitizer haloacetylcarbamoyl-2-nitroimidazoles*. *Bioorganic & medicinal chemistry*, 1997. **5**(3): p. 591-599.
67. Jin, C.Z., et al., *Angiogenesis inhibitor TX-1898: syntheses of the enantiomers of sterically diverse haloacetylcarbamoyl-2-nitroimidazole hypoxic cell radiosensitizers*. *Bioorganic & medicinal chemistry*, 2004. **12**(18): p. 4917-4927.
68. Thomas Winters, A.S., Carla Suto, William Elliott, Wilbur Leopold, Judith Leopold, Hollis Showalter, *Design and Synthesis of 2-Nitroimidazoles with Variable Alkylating and Acylating Functionality* *Chemical and Pharmaceutical Bulletin*, 2014. **62**(3): p. 301-303.

69. Dubois, L., et al., *Specific inhibition of carbonic anhydrase IX activity enhances the in vivo therapeutic effect of tumor irradiation*. Radiotherapy and oncology : journal of the European Society for Therapeutic Radiology and Oncology, 2011. **99**(3): p. 424-31.
70. Svastova, E., et al., *Hypoxia activates the capacity of tumor-associated carbonic anhydrase IX to acidify extracellular pH*. FEBS letters, 2004. **577**(3): p. 439-45.
71. van den Beucken, T., et al., *Deficient carbonic anhydrase 9 expression in UPR-impaired cells is associated with reduced survival in an acidic microenvironment*. Radiotherapy and oncology : journal of the European Society for Therapeutic Radiology and Oncology, 2009. **92**(3): p. 437-42.
72. Potter, C.P. and A.L. Harris, *Diagnostic, prognostic and therapeutic implications of carbonic anhydrases in cancer*. British journal of cancer, 2003. **89**(1): p. 2-7.
73. Dubois, L., et al., *Targeting carbonic anhydrase IX by nitroimidazole based sulfamides enhances the therapeutic effect of tumor irradiation: a new concept of dual targeting drugs*. Radiotherapy and oncology : journal of the European Society for Therapeutic Radiology and Oncology, 2013. **108**(3): p. 523-8.
74. Rami, M., et al., *Hypoxia-targeting carbonic anhydrase IX inhibitors by a new series of nitroimidazole-sulfonamides/sulfamides/sulfamates*. Journal of medicinal chemistry, 2013. **56**(21): p. 8512-20.
75. Land, K.M. and P.J. Johnson, *Molecular mechanisms underlying metronidazole resistance in trichomonads*. Experimental parasitology, 1997. **87**(3): p. 305-8.
76. Janssen, H.L., et al., *Hypoxia in head and neck cancer: how much, how important?* Head & neck, 2005. **27**(7): p. 622-38.

Chapter 3

Hypoxia-targeting Carbonic Anhydrase IX inhibitors by a new series of nitroimidazole-sulfonamides/sulfamides/ sulfamates

Published in J Med Chem. 2013, 56, 8512–8520
Marouan Rami, Ludwig Dubois, Nanda Kumar Parvathaneni, Vincenzo Alterio,
Simon van Kuijk, Simona Maria Monti, Philippe Lambin, Giuseppina De Simone,
Claudiu T. Supuran and Jean-Yves Winum

Abstract

A series of nitroimidazoles incorporating sulfonamide/sulfamide/sulfamate moieties were designed and synthesized as radio/chemosensitizing agent targeting the tumor-associated carbonic anhydrase (CA) isoforms IX and XII. Most of the new compounds were nanomolar inhibitors of these isoforms. Crystallographic studies on the complex of hCA II with the lead sulfamide derivative of this series, clarified the binding mode of this type of inhibitors in the enzyme active site cavity. Some of the best nitroimidazole CA IX inhibitors showed significant activity *in vitro* by reducing hypoxia-induced extracellular acidosis in HT-29 and HeLa cell lines. *In vivo* testing of the lead molecule in the sulfamide series, in co-treatment with doxorubicin, demonstrated a chemosensitization of CA IX containing tumors. Such CA inhibitors, specifically targeting the tumor-associated isoforms, are candidates for novel treatment strategies against hypoxic tumors overexpressing extracellular CA isozymes.

Introduction

Hypoxia is a strong oncogenic phenotype occurring in all solid tumors, which is responsible for enhanced malignancy and is associated with resistance to ionizing radiation and chemotherapy. This inherent feature provides significant opportunities for drug discovery especially for specific tumor-targeting agents [1, 2].

Among the proteins whose expression is induced by hypoxia, *via* the hypoxia inducible factor 1 α (HIF-1 α), membrane-associated carbonic anhydrase IX (CA IX, (CA, EC 4.2.1.1)) [1] is the most strongly induced one in human cancer cells [4]. CA IX is also the most active CA isoform for the CO₂ hydration reaction, playing a major role in regulating the tumor acid-base balance [4, 5]. It is strongly overexpressed in a broad range of tumor types, and its expression negatively correlates with the prognosis of cancer patients. Moreover, this isoform exhibits a very limited expression in normal tissues, thus its inhibition may lead to significantly fewer side effects compared to classical anticancer agents in clinical use [4].

CA IX is now a validated antitumor target, and its inhibition with antibodies, sulfonamide and coumarin inhibitors has been undoubtedly proven to reverse the effect of tumor acidification, leading to the inhibition of the cancer cells growth *in vivo* [4,6-10].

In order to improve the potency of tumors treatment with CA inhibitors, we have recently focused our attention on the development of dual drugs able to inhibit selectively CA IX and to enhance hypoxic tumor sensitization towards therapy. At this aim we decided to utilize nitroimidazole scaffolds as they are well known as radiosensitizers, and have been subject of investigation for several decades with a number of such derivatives being clinically used [11]. Thus, the present article deals with the development of novel nitroimidazole compounds whose properties have been optimized by conjugation with pharmacophoric moieties targeting CA IX. In particular, we report here the synthesis and carbonic anhydrase inhibitory activity of a panel of sulfonamide/sulfamide/sulfamate derivatives containing 2- or 5-nitroimidazoles moieties. The crystallographic structures of the lead sulfamide derivative in adduct with isoform II was studied. Validation in *in vitro* studies identified compounds that selectively inhibit CA IX activity, thereby reducing hypoxia-induced extracellular acidosis. From this inhibitor library a lead compound

was taken forward into *in vivo* demonstrating to be able to chemosensitize tumors (HT-29 colorectal carcinoma) to clinically available treatment schedules.

Results and Discussion

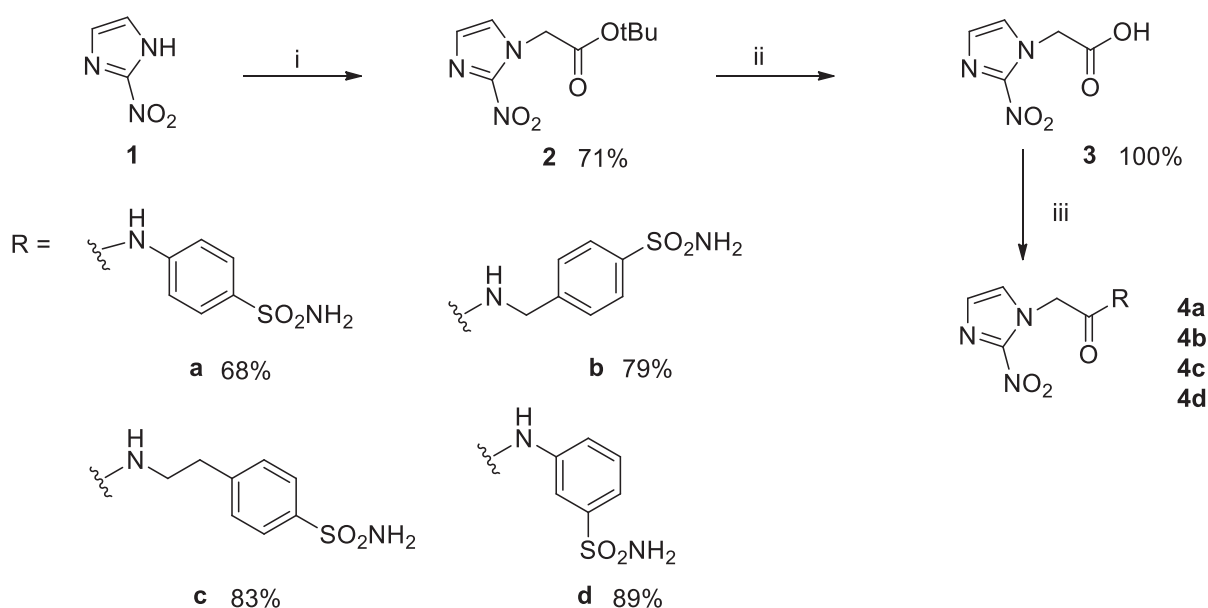
Several studies have emphasized that specific inhibitors of CA IX activity are promising to pursue for their tumor-specific therapeutic properties also in combination with conventional therapies [3-5]. A different approach to sensitize tumors is the use of nitroimidazole, although high clinical toxicity has been observed upon therapeutic efficacy [11-12]. An important requisite for newly designed compounds is therefore the more specific targeting towards the hypoxic tumor regions using lower doses.

On the basis of these considerations, the rationale of this work for designing new CAIs was to incorporate in the same scaffold two different functionalities: (i) the sulfonamide/sulfamate/sulfamide one which is responsible for binding to the Zn (II) within the CA active site and whence inhibition of the enzyme, and (ii) a nitroazole moiety which is responsible for radiosensitization in tumors (such moiety is found in agents such as pimonidazole, and has proved to be an effective and non-toxic hypoxia marker for several human squamous cell carcinomas). A comparable approach has been in fact reported earlier by one of our groups [13] by combining benzenesulfonamide and aromatic nitroderivatives in the same molecule. Indeed, the derivatives of this type reported by D'Ambrosio et al. were highly effective CA IX/XII inhibitors.

Chemistry

Different libraries of inhibitors were synthesized incorporating 2- or 5-nitroimidazole moieties. Starting from the 2-nitroimidazole **1**, we introduced the acetic acid moiety on position 1 of the imidazole ring by reacting *tert*-butyl bromoacetate on **1** in basic medium followed by deprotection of the resulting ester **2** by trifluoroacetic acid to give compound **3**. The latter was then reacted with different aminobenzenesulfonamide derivatives using carbodiimide as coupling agent to give compounds **4** in good yield (Scheme 1) [10-11].

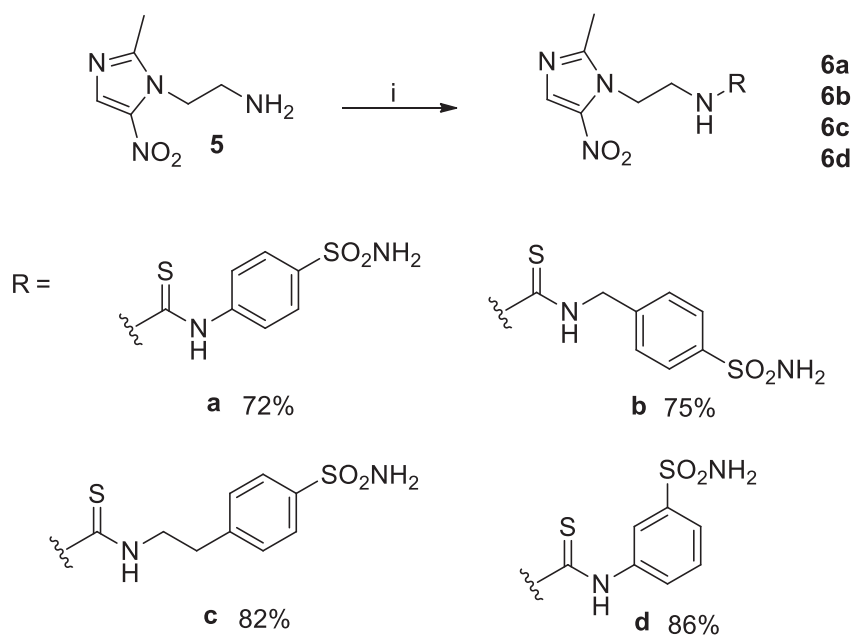
Scheme 1



Scheme 1: Reagents and conditions: (i) 1 equiv. of 2-nitroimidazole, 1 equiv. of *tert*-butyl bromoacetate, 4 equiv. of potassium carbonate, MeCN, RT, 1 night; (ii) cocktail of trifluoroacetic acid/ water/ thioanisole 95/2.5/2.5 v/v, rt, 1 night; (iii) 1 equiv. of 4-dimethylaminopyridine (DMAP), 1 equiv. of 1-(3-dimethylaminopropyl)-3-ethylcarbodiimide hydrochloride (EDC), *N,N*-dimethylacetamide (DMA), RT, 2 days.

The synthesis of the 5-nitroimidazole series was realized following classical strategies used for the preparation of CA inhibitors. Starting from the amine analogue of metronidazole **5**, we reacted different benzene sulfonamide isothiocyanates to lead to the series of thioureas compounds **6** (Scheme 2) [14-15].

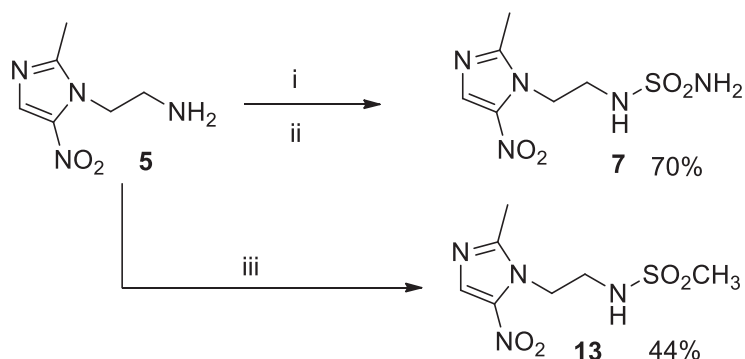
Scheme 2



Scheme 2: Reagents and conditions: (i) 1 equiv. of 1-(2-aminoethyl)-2-methyl-5-nitroimidazole dihydrochloride monohydrate, 1 equiv. SCN-Ph-SO₂NH₂, 2 equiv. of triethylamine, MeCN, RT, 1 hour.

Sulfamide derivative **7** and methylsulfonamide analogue **13** (Scheme 3) were obtained from the same starting material **5** by a procedure previously reported by this group [16]. Sulfamate analogue **9** was prepared starting from the metronidazole **8** using a direct sulfamoylation procedure as described previously (Scheme 4) [17].

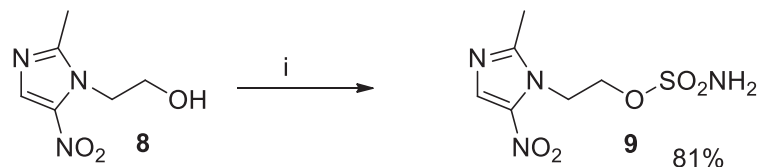
Scheme 3



Scheme 3: Reagents and conditions: (i) 1 equiv. of 1-(2-aminoethyl)-2-methyl-5-nitroimidazole dihydrochloride monohydrate, 4 equiv. of triethylamine, 1 equiv. of chlorosulfonylisocyanate, 1 equiv. of *tert*-butanol, CH₂Cl₂, rt, 1 hour; (ii)

trifluoroacetic acid -CH₂Cl₂ 7-3 v-v, RT, 6 hours. (iii) 2 equiv. of methane sulfonyl chloride, 2 equiv. of triethylamine, CH₂Cl₂.

Scheme 4

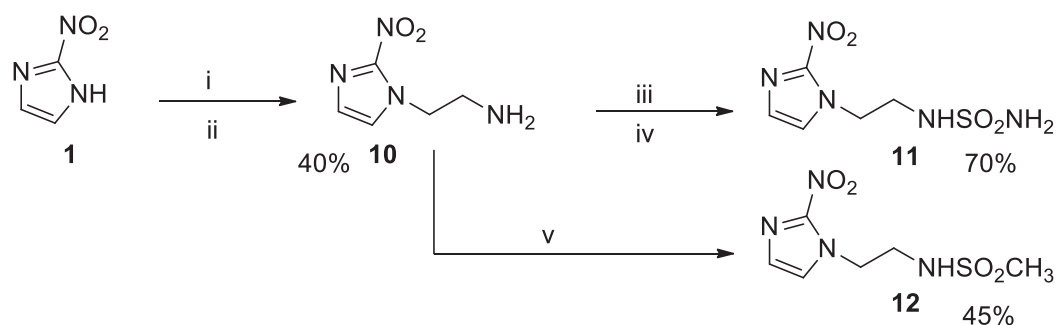


Scheme 4: Reagents and conditions: (i) 1 equiv. of 2-methyl-5-nitro-1H-imidazole-3-ylmethanol, N, N-dimethylacetamide, 3 equiv. sulfamoyl chloride, RT, 1 night.

Compounds **11** and **12** were obtained in the same manner as compounds **7** and **13** starting from compound **10** obtained as previously described by Hoigebazar *et al.* [18] (Scheme 5).

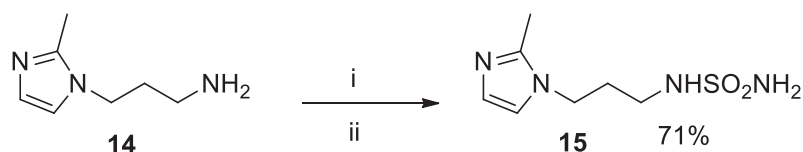
Sulfamide **15** was prepared from the commercially available compound **14** following the sulfamoylation process used for compound **7** (Scheme 6).

Scheme 5



Scheme 5: Reagents and conditions: (i) 1 equiv. of 2-nitroimidazole, Dry DMF, 1 equiv. K₂CO₃, 1.5 equiv. *tert*-butyl 2-bromoethylcarbamate. (ii) trifluoroacetic acid-CH₂Cl₂ 8-2 v-v, RT, 2 hours. (iii) 4 equiv. of triethylamine, 1.5 equiv. of chlorosulfonylisocyanate, 1.5 equiv. of *tert*-butanol, CH₂Cl₂, rt, 12 hours. (iv) trifluoroacetic acid-CH₂Cl₂ 8-2 v-v, RT, 2 hours. (v) 2 equiv. of methane sulfonyl chloride, 2 equiv. of triethylamine, CH₂Cl₂.

Scheme 6



Scheme 6: Reagents and conditions: (i) 4 equiv. of triethylamine, 1.5 equiv. of chlorosulfonylisocyanate, 1.5 equiv. of *tert*-butanol, CH₂Cl₂, rt, 12 hours. (ii) trifluoroacetic acid-CH₂Cl₂ 8-2 v-v, RT, 2 hours.

The new compounds were characterized extensively by spectral and physico-chemical methods, which confirmed their structures (supplementary data).

CA inhibition assays

All compounds reported here were assayed as inhibitors of four physiologically relevant CA isoforms, the cytosolic hCA I and II (h=human isoform), and the transmembrane, tumor-associated hCA IX and XII using the CO₂ hydrase assay (Table 1) [19]. The clinically employed sulfonamide acetazolamide (**AAZ**, 5-acetamido-1, 3,4-thiadiazole-2-sulfonamide) has been used as standard in these measurements, for comparison reasons.

Analysis of these inhibition data shows a very interesting inhibition profile for this newly designed series of compounds. Indeed, all compounds, except **12** and **13** which were prepared as negative control molecules, acted as effective inhibitors against isoforms hCA I, II, IX and XII.

Against the abundant, cytosolic isoform hCA I the new compounds reported here behaved as medium/weak potency inhibitors, with K_Is in the range of 79 nM – 9.57 μM. For the benzenesulfonamides **4** and **6**, the main factor influencing hCA I inhibition was the substitution pattern of the benzenesulfonamide and the length of the linker between this and the rest of the molecule. Indeed, for compounds of subseries 4, the sulfanilamide derivative **4a** was a much weaker hCA I inhibitor compared to the congeners with a larger linker (n = 1 and 2) between the benzenesulfonamide functionality and the nitroazole-acetamido moiety. Indeed, the derivatives **4b** and **4c** having these longer linkers, as well as the metanilamide derivative **4d** were much more effective hCA I inhibitors (K_Is of 79-107 nM) compared to the sulfanilamide derivative **4a** (K_I of 3203 nM). In the case of the thioureas **6**, the SAR is slightly different, in the sense that the least effective derivative was the homosulfanilamide

derivative **6b** (K_I of 483 nM) whereas the remaining ones (**6a**, **6c** and **6d**) showed a similar behavior of medium potency inhibitors (K_I of 79-105 nM). Finally, sulfamates, sulfamides and methylsulfonamide **7**, **9**, **11-15**, were either very weak hCA I inhibitors or devoid of such an activity (Table 1).

The physiologically dominant off-target isoform hCA II was highly inhibited by most of the new sulfonamides reported here (**4b-4d**, **6a-6d**) which had K_{IS} in the range of 2.9 – 7.4 nM (better than that of **AAZ** of 12 nM). Compounds in the sulfamide and sulfamate series were medium potency inhibitor (K_{IS} of 33.8-58 nM) except **7**, which showed activity in the same range as **AAZ**. Derivatives **12** and **13** were not inhibitory also against this isoform (Table 1). Again SAR is straightforward, as for the discussion of hCA I inhibition above. For amides **4** the length of the spacer between the benzenesulfonamide and nitroazole functionalities was the main factor influencing activity, whereas for thioureas **6** all substitution patterns were equal in generating potent hCA II inhibitors. The aliphatic derivatives **7-15** possessing a ZBG were effective or medium potency hCA II inhibitors whereas those without such a moiety (the methylsulfonamides) were ineffective as hCA II inhibitors.

The tumor-associated transmembrane isoforms hCA IX and hCA XII were both potently inhibited by all sulfonamides series **4** and **6** (except **4a**) reported here, which showed inhibition constants <10 nM, more precisely, in the range of 7.2 – 8.3 nM against hCA IX, and of 6.7 – 8.5 against hCA XII, respectively. Sulfamides **7**, **11**, **15** and sulfamate **9** displayed also high potency at nanomolar levels for these isoforms. SAR for hCA IX inhibition is similar to what discussed above for hCA I and II inhibition whereas in the case of hCA XII all compounds (except those without a ZBG, i.e., **12** and **13**) were highly effective inhibitors, proving that all substitution patterns explored here led to highly effective CAIs.

Selectivity ratios for inhibiting hCA IX over hCA II and hCA XII over hCA II were in the range of 0.4 to 5. The inhibition profiles of CA II and IX (or CA II and XII) were generally rather similar for all the series of compounds; indeed, only inhibitors **4a**, **4b** and **9** were shown to have a moderate CA IX/XII selectivity. Nevertheless considering the difficulty to obtain small compounds with a better affinity for the tumor-associated isozymes over CA II, the selectivity obtained for these series is comparable or better with those of all the clinically used CA inhibitors which have selectivity ratios for the inhibition of CA II over CA IX <1 .

Table 1: hCA I, II, IX, and XII Inhibition data with compounds 4–15 and standard inhibitor acetazolamide AAZ by a Stopped-Flow, CO₂ Hydration Assay Method [19]. Selectivity ratios for the inhibition of the tumor-associated (CA IX and XII) over the cytosolic (CA II) isozyme are also reported.

Compounds	K _i (nM) ^a				Selectivity ratios	
	hCA I ^b	hCA II ^b	hCA IX ^c	hCA XII ^c	K _i hCA II/ K _i hCA IX	K _i hCA II/ K _i hCA XII
AAZ	250	12	25	5.6	0.48	2.14
4a	3203	330	70	64	4.71	5.15
4b	107	37	7.9	8.1	4.68	4.56
4c	79	4.8	8.0	6.7	0.6	0.71
4d	101	3.8	7.3	8.0	0.52	0.47
6a	105	5.5	7.3	8.0	0.75	0.68
6b	483	7.4	7.2	7.7	1.02	0.96
6c	79	2.9	8.3	8.5	0.35	0.34
6d	84	6.6	7.8	7.6	0.84	0.86
7	9576	10.1	20.4	8.1	0.49	1.24
9	4435	33.8	8.3	8.9	4.07	3.79
11	9120	58	41	38	1.41	1.52
12	>20000	>20000	>20000	>20000	-	-
13	>20000	>20000	>20000	>20000	-	-
15	8718	52	21	37	2.47	1.40

^aErrors in the range of ±5–10% of the reported value from three different determinations. ^bFull length, cytosolic isoform. ^cCatalytic domain, recombinant enzyme.

***In vitro* extracellular acidification tests.**

To investigate the efficacy of different dual targeting compounds, their effects on hypoxia-induced extracellular acidification was evaluated by measuring changes in pH before and after exposure to the dual compounds [20]. For this purpose, HeLa cervical and HT29 colorectal carcinoma cells were grown under ambient air or lowered oxygen concentrations and exposed to compounds in a 0.1 and 1 mM concentration. HeLa demonstrated increased CA IX expression upon hypoxia, while HT29 also had a high expression under ambient air [20]. Previously, we have demonstrated that inhibitor binding to CA IX requires both its expression and its activation and this was only observed exclusively during hypoxia, irrespective of the CA IX expression levels [9, 20]. The 5-nitroimidazole series was selected for further investigation based on the more favorable toxicity profile compared with 2-nitroimidazoles [12]. For all compounds, a concentration of 1 mM resulted in a significant reduction ($P < 0.05$) in hypoxia-induced extracellular acidosis, while the effect on cells exposed to ambient air was negligible (Figure 1). Only for **7**, a significant ($P < 0.05$) dose-dependent effect was observed, while a lower concentration was not effective for the other compounds. For **6c**, a strong alkalization was observed only for the HeLa cells. Previously, we have shown that for the single targeting compound **13** and **15**, only **15** was able to reduce the extracellular acidification [21]. These data indicated that the efficacy of the dual targeting compound is attributed to the CA IX inhibiting moiety. Based on these and the current results, **7** was selected as the lead compound for further *in vivo* investigations.

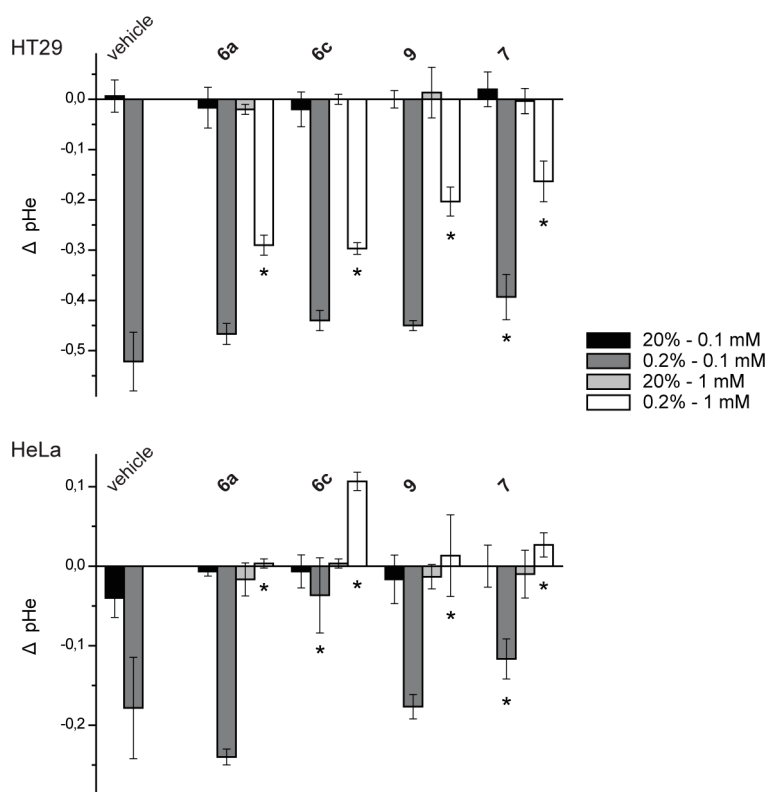


Figure 1: Extracellular acidification of cells exposed to normoxia (20%) or hypoxia (0.2%) upon treatment with dual targeting compounds (0.1 or 1 mM). Data are expressed as the difference between medium pH values ($\Delta\text{pHe} = \text{pH}_{\text{after incubation}} - \text{pH}_{\text{before incubation}}$) and show the mean \pm SD of at least three independent experiments. Asterisks indicate significant difference (* $P < 0.05$).

***In vivo* tests**

To investigate whether **7** exerted a chemosensitizing effect, HT-29 tumour bearing mice were treated with **7** according to previously described strategies [9,10,21] and subsequently exposed to chemotherapy. **7**-treated ($P < 0.01$) or doxorubicin-treated ($P < 0.001$) mice demonstrated a significantly reduction in tumour growth, with an average time to reach 4x starting volume (T4xSV) of 25.43 and 23.39 days for **7** and doxorubicin respectively, compared to vehicle treatment only (14.07 days). T4xSV was further enhanced (40.66 days, $P < 0.05$) upon combination of **7** with doxorubicin (Fig. 2). None of the treatment schedules caused observable toxicity assessed by body weight loss. Furthermore, recently we have demonstrated that **7** also exerted a radiosensitizing effect in a CA IX dependent manner. A significant higher

sensitization enhancement ratio (SER) was observed upon pre-treatment with **7** before radiotherapy compared to vehicle pre-treatment only for CA IX expressing tumors.²¹ Derivative **7** sensitizes tumors towards radiotherapy and doxorubicin based chemotherapy, indicating the potential utility of nitroimidazole based CA IX targeting compounds as novel anticancer agents. The sensitization effects of the “dual drug” were markedly higher compared with single CA IX targeting agents⁹ or nitroimidazole-based drugs.¹²

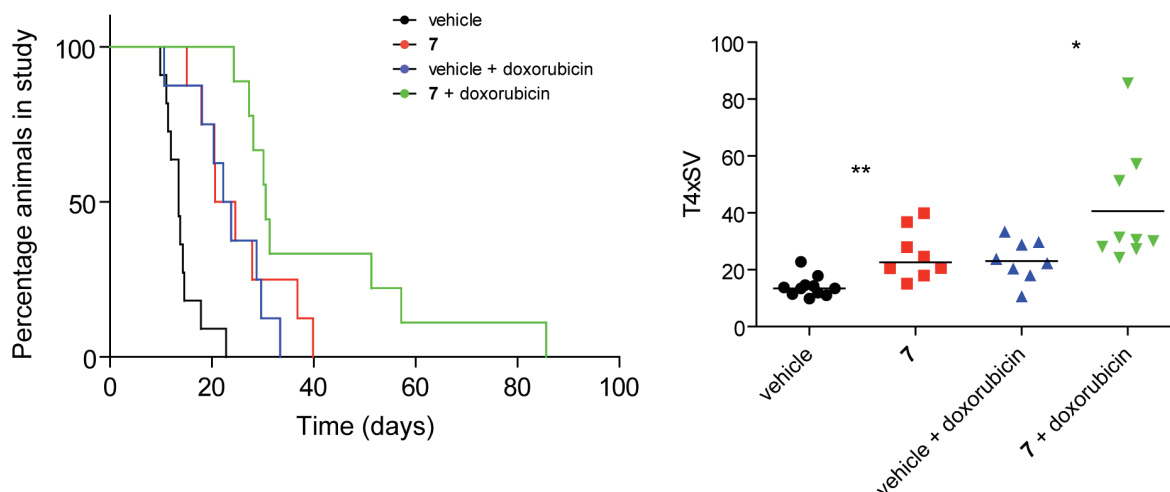


Figure 2: **7** (10 mg/kg 3 days) and doxorubicin (5 mg/kg at day 3) were injected intravenously when tumours reached a volume of 250 mm³. The treatment schedule was repeated for 3 consecutive weeks. Tumour growth was monitored until reaching 4x the volume at treatment time (T4xSV). Data represent the mean \pm SD of eight to eleven independent animals. Asterisks indicate statistical significance (*P < 0.05; **P < 0.01).

X-ray Crystallography

To determine the molecular features responsible of the CA inhibitory properties of the dual drug **7**, the crystal structure of such molecule in complex with the cytosolic dominant isoform hCA II has been solved. Crystals of the hCA II–**7** adduct were isomorphous with those of the native protein [22], allowing for the analysis of the three-dimensional structure by difference Fourier techniques. Data collection and refinement statistics are shown in Table 2.

Table 2: Crystal parameters, data collection and refinement statistics. Values in parentheses

refer to the highest resolution shell (1.92-1.85 Å).

Crystal parameters	
<i>Space group</i>	<i>P2₁</i>
<i>a</i> (Å)	42.17
<i>b</i> (Å)	41.22
<i>c</i> (Å)	71.95
<i>γ</i> (°)	104.22
<i>Number of independent molecules</i>	1
Data collection statistics	
<i>Resolution</i> (Å)	20.00-1.85
<i>Wavelength</i> (Å)	1.54178
<i>Temperature</i> (K)	100
<i>R_{merge}</i> (%) ^a	4.7 (13.2)
<i>Mean I/σ(I)</i>	25.7 (6.6)
<i>Total reflections</i>	94974
<i>Unique reflections</i>	20161
<i>Redundancy</i> (%)	4.7 (2.4)
<i>Completeness</i> (%)	97.2 (82.2)
Refinement	
<i>Resolution</i> (Å)	20.00-1.85
<i>R_{factor}</i> (%) ^b	16.3
<i>R_{free}</i> (%) ^b	19.6
RMSD from ideal geometry:	
<i>Bond lengths</i> (Å)	0.011
<i>Bond angles</i> (°)	1.7
<i>Number of protein atoms</i>	2177
<i>Number of water molecules</i>	199
<i>Number of inhibitor atoms</i>	16
Average B factor (Å ²):	
<i>All atoms</i>	14.1
<i>Protein atoms</i>	13.6
<i>Inhibitor atoms</i>	20.1
<i>Water molecules</i>	22.9

$$^a R_{\text{merge}} = \frac{\sum_{hkl} \sum_i |I_i(hkl) - \langle I(hkl) \rangle|}{\sum_{hkl} \sum_i I_i(hkl)}.$$

$$^b R_{\text{factor}} = \frac{\sum_{hkl} \left| |F_o(hkl)| - |F_c(hkl)| \right|}{\sum_{hkl} |F_o(hkl)|}; R_{\text{free}} \text{ calculated with 5\% of data}$$

withheld from refinement.

Inhibitor binding did not generate significant changes in hCA II structure, indeed the rmsd for the superposition of the corresponding C α atoms between the native enzyme and the enzyme-inhibitor adduct was 0.3 Å. The analysis of the electron density maps showed the presence of one inhibitor molecule bound within the active site. The main protein-inhibitor interactions are schematically depicted in Figure 3. Analysis of this figure reveals that the tetrahedral coordination geometry of the Zn²⁺ ion and the key hydrogen bonds between the sulfamide moiety of the inhibitor and the enzyme active site are all retained with respect to other hCA II–sulfamide complexes solved so far [23,24]. In particular, the ionized sulfamide NH⁻ group coordinates to Zn²⁺ ion and donates a hydrogen bond to Thr199OG1, while one of the two sulfamide oxygens accepts a hydrogen bond from the backbone NH group of Thr199. An additional H-bond interaction is observed between the Thr200OG1 atom and the second nitrogen atom of the sulfamide moiety. The imidazole ring of the inhibitor is located in the middle of the active site cavity, with the nitro group oriented toward the hydrophilic part [25], establishing strong direct hydrogen bond interactions with residues Thr200 and His64, stabilized in its *in* conformation (Figure 3). The inhibitor binding is further stabilized by additional water mediated hydrogen bonds and a large number of van der Waals interactions with the side chains of residues Trp5, Gln92, Val121, Phe131, Leu198, Thr199, Thr200, and Pro201.

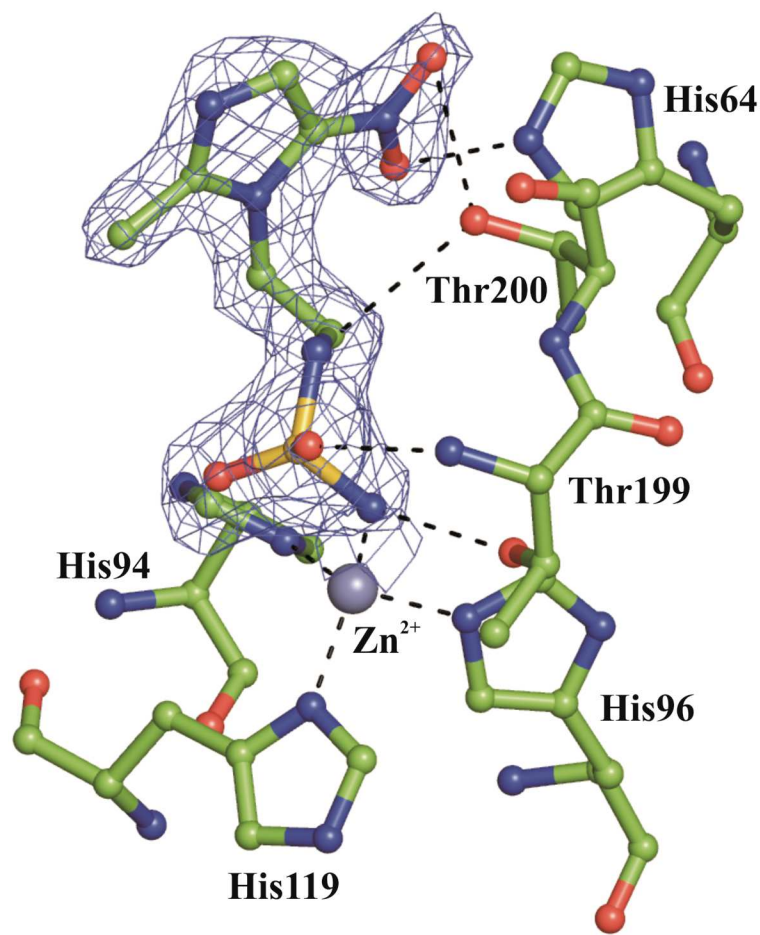


Figure 3: Active site region in the hCAII-7 complex. Active site Zn^{2+} coordination and direct hydrogen bonds between inhibitor and enzyme residues are reported as dashed lines. The sigma-A weighted $|2Fo-Fc|$ simulated annealing omit map (at 1.0 sigma) relative to the inhibitor molecule is also shown.

Conclusion

We designed and synthesized a new class of CA IX inhibitors containing nitroimidazole moieties. These molecules showed efficacy *in vitro* for the inhibition of extracellular tumor acidification in two cell lines overexpressing CA IX, namely the colorectal HT-29 and the cervical HeLa carcinoma cell lines. In both tumor types, a significant reduction of tumor acidosis was detected. Moreover, one of the lead molecule, the sulfamide derivative **7**, was demonstrated to enhance sensitization towards radiotherapy and chemotherapy with doxorubicin *in vivo*. The X-ray crystal structure of the hCA II/7 adduct was also solved showing that the binding of **7** in the middle of the enzyme active site cavity was mainly driven by the canonical interactions of the sulfamide group, two H-bond interactions between the nitro group

of **7** and residues His64 and Thr200, as well as several water mediated hydrogen bonds and hydrophobic interactions. Altogether these data indicate the potential utility of nitroimidazole compounds and open the way to their use as novel anticancer agents targeting the tumor-associated CA isoforms IX and XII.

Experimental Section

Chemistry

General: All reagents and solvents were of commercial quality and used without further purification, unless otherwise specified. All reactions were carried out under an inert atmosphere of nitrogen. TLC analyses were performed on silica gel 60 F₂₅₄ plates (Merck Art.1.05554). Spots were visualized under 254nm UV illumination, or by ninhydrin solution spraying. Melting points were determined on a Büchi Melting Point 510 and are uncorrected. ¹H and ¹³C NMR spectra were recorded on Bruker DRX-400 spectrometer using DMSO-*d*₆ as solvent and tetramethylsilane as internal standard. For ¹H NMR spectra, chemical shifts are expressed in δ (ppm) downfield from tetramethylsilane, and coupling constants (*J*) are expressed in Hertz. Electron Ionization mass spectra were recorded in positive or negative mode on a Water MicroMass ZQ. High-resolution ESI mass spectra (HRMS) were recorded on a Q-ToF I mass spectrometer fitted with an electrospray ion source.

***tert*-butyl-(2-nitro-imidazol-1-yl) acetate (2):** A solution of *tert*-butylbromoacetate (17.7 mmol, 1 equiv.) in 10 ml of acetonitrile is added dropwise to a mixture of 2-nitroimidazole **1** (17,7 mmol, 1 equiv.) and anhydrous potassium carbonate (70.74 mmol, 4 equiv.) in 20 mL of acetonitrile. The mixture is stirred one night at room temperature and concentrated under vacuum. The residue is purified by chromatography on silica gel using a mixture CH₂Cl₂/ MeOH 95/5 as eluent to give the expected compound as white powder in 71 % yield. mp 95-97°C; ¹H NMR (DMSO-*d*₆, 400 MHz) δ 1.46 (s, 9H), 4.99 (s, 2H), 7.06 (d, 1H, *J*=1.01 Hz), 7.17 (d, 1H, *J*=1.01 Hz). MS (ESI⁺/ESI⁻) *m/z* 226.15 [2]⁻, 262.13 [M+Cl]⁻, 250.20 [M+H]⁺.

(2-nitro-imidazol-1-yl) acetic acid (3): Compound **2** (2.5g) is dissolved in 20 mL of a cocktail of TFA, water, thioanisole 95-2.5-2.5 and stirred at room temperature for one night. The mixture is then concentrated under vacuum and co-evaporated several

times with diethyl ether until formation of a powder. After filtration, the precipitate is washed with dichloromethane and acetonitrile to give quantitatively the expected product. Mp 143°C (decomposition); ¹H NMR (DMSO-*d*₆, 400 MHz) δ 5.21 (s, 2H), 7.21 (d, 1H, *J*=1.01 Hz), 7.64 (d, 1H, *J*=1.01Hz). ¹³C (DMSO-*d*₆, 101 MHz) δ 50.65, 127.69, 128.44, 168.56, 168.57; MS (ESI⁺/ESI⁻) *m/z* 170.12 [2]⁻, 341.05 [2M-H]⁻, 194.14 [M+Na]⁺.

General procedure for the preparation of compounds (4a-d)

The aminoalkylbenzene sulfonamide (1.17 mmol, 1 equiv.), 4-dimethylaminopyridine (1.17 mmol, 1 equiv.) and 1-ethyl-3-(3-dimethylaminopropyl) carbodiimide (1.17 mmol, 1 equiv.) were added to a solution of compound **3** (1.17 mmol, 1 equiv.) in 8 mL of N,N-dimethylacetamide. The mixture was stirred two days at room temperature, then diluted with ethyl acetate and washed three times with water. The organic layer was dried over anhydrous magnesium sulfate, filtrated and concentrated under vacuum. The residue was then purified by chromatography on silica gel using methylene chloride – methanol 98-2 v-v as eluent.

2-(2-nitro-imidazol-1-yl)-N-(4-sulfamoylphenyl)acetamide (4a): Yield: 68%; mp 163-165°C; ¹H NMR (DMSO-*d*₆, 400 MHz) δ 5.36 (s, 2H), 7.24 (d, 1H, *J*=1.01Hz), 7.28 (s, 2H), 7.67 (d, 1H, *J*=1.01Hz), 7.70 (d, 2H, *J*=8.9Hz), 7.77 (d, 2H, *J*=8.9Hz), 10.7 (s, 1H); ¹³C (DMSO-*d*₆, 101 MHz) δ 52.20, 118.70, 126.81, 127.57, 128.84, 138.76, 141.18, 144.79, 165.02; MS (ESI⁺/ESI⁻) *m/z* 324.09 [2]⁻, 359.92 [M+Cl]⁻, 649.15 [2M-H]⁻, 685.01 [2M+Cl]⁻, 348.14 [M+Na]⁺. HRMS (ESI) [M+H]⁺ calculated for [C₁₁H₁₂N₅O₅S]⁺: 326.0559, found 326.0563.

2-(2-nitro-imidazol-1-yl)-N-(4-sulfamoylbenzyl)acetamide (4b): Yield: 83%; mp 181-183°C; ¹H NMR (DMSO-*d*₆, 400 MHz) δ 4.37 (d, 2H, *J*=5.7Hz), 5.22 (s, 2H), 7.18 (d, 1H, *J*=1.01Hz), 7.35 (s, 2H), 7.43 (d, 2H, *J*=8.4Hz), 7.67 (d, 1H, *J*=1.01Hz), 7.76 (d, 2H, *J*=8.4Hz), 9.15 (t, 1H, *J*=6.06Hz); ¹³C (DMSO-*d*₆, 101 MHz) δ 41.81, 51.55, 106.87, 125.58, 127.39, 138.91, 142.66, 142.99, 156.82, 165.88; MS (ESI⁺/ESI⁻) *m/z* 338.15 [2]⁻, 374.22 [M+Cl]⁻, 713.16 [2M+Cl]⁻, 340.15 [M+H]⁺, 362.17 [M+Na]⁺. HRMS (ESI) [M+H]⁺ calculated for [C₁₂H₁₄N₅O₅S]⁺: 340,0716, found 340.0723.

2-(2-nitroimidazol-1-yl)-N-[2-(4-sulfamoylphenyl)ethyl]acetamide (4c): Yield: 89%; mp 139-141°C; ¹H NMR (DMSO-*d*₆, 400 MHz) δ 2.80 (t, 2H, *J*=6.9Hz), 3.16 (m 2H), 5.07 (s, 2H), 7.18 (d, 1H, *J*=1.01Hz), 7.30 (s, 2H), 7.40 (d, 2H, *J*=8.2Hz), 7.61 (d, 1H, *J*=1.01Hz), 7.74 (d, 2H, *J*=8.2Hz), 8.46 (t, 1H, *J*=5.6Hz); ¹³C (DMSO-*d*₆, 101 MHz) δ 34.59, 51.49, 125.64, 127.38, 128.74, 129.09, 142.05, 143.39, 144.87, 165.57; MS (ESI⁺/ESI⁻) *m/z* 352.19 [2]⁻, 388.07 [M+Cl]⁻, 354.12 [M+H]⁺, 376.09 [M+Na]⁺, 729.21 [2M+Na]⁺. HRMS (ESI) [M+H]⁺ calculated for [C₁₃H₁₆N₅O₅S]⁺: 354.0872, found 354.0873.

2-(2-nitroimidazol-1-yl)-N-(3-sulfamoylphenyl)acetamide (4d): Yield: 79%; mp 195-197°C; ¹H NMR (DMSO-*d*₆, 400 MHz) δ 5.35 (s, 2H), 7.24 (d, 1H, *J*=1.01Hz), 7.38 (s, 2H), 7.52 (m, 2H), 7.65 (m, 1H), 7.67 (d, 1H, *J*=1.01Hz), 8.14 (s, 1H), 10.81 (s, 1H); ¹³C (DMSO-*d*₆, 101 MHz) δ 52.16, 116.10, 120.72, 121.92, 127.59, 128.86, 129.67, 138.67, 144.72, 164.87, 167.75; MS (ESI⁺/ESI⁻) *m/z* 324.24 [2]⁻, 360.18 [M+Cl]⁻, 685.13 [2M+Cl]⁻, 326.24[M+H]⁺, 348.07 [M+Na]⁺, 364.17 [M+K]⁺, 673.18 [2M+Na]⁺. HRMS (ESI) [M+H]⁺ calculated for [C₁₁H₁₂N₅O₅S]⁺: 326.0559, found 326.0553.

General procedure for the preparation of compounds (6a-d): isothiocyanate (0.76 mmol, 1 equiv.) was added to a solution of the commercially available compound **5** (0.76 mmol, 1 equiv.) in 10 mL of acetonitrile. The reaction was stirred for one hour at room temperature and then filtered. The filtrate was concentrated under vacuum, and the residue obtained purified by chromatography on silica gel using methylene chloride – methanol 95 – 5 as eluent.

N-(4-sulfamoylphenyl)-N-((2-aminoethyl)-2-methyl-5-nitroimidazolyl) thiourea (6a): Yield: 72%; mp 186-188°C; ¹H NMR (DMSO-*d*₆, 400 MHz) δ 2.42 (s, 3H), 3.91 (m, 2H), 4.5 (t, 2H, *J*=5.68Hz), 7.3 (s, 2H), 7.46 (d, 2H, *J*=8.7Hz), 7.71 (d, 2H, *J*=8.7Hz), 8.05 (s, 2H), 10.0 (s, 1H); ¹³C (DMSO-*d*₆, 101 MHz) δ 13.81, 42.87, 44.86, 122.46, 126.30, 133.19, 138.66, 139.14, 141.88, 151.35, 180.88; MS (ESI⁺/ESI⁻) *m/z* 385.17 [M+H]⁺, 407.07 [M+Na]⁺, 769.22 [2M+H]⁺, 383.21 [2]⁻, 419.18 [M+Cl]⁻, 767.16. [2M-H]⁻. HRMS (ESI) [M+H]⁺ calculated for [C₁₃H₁₇N₆O₄S₂]⁺: 385.0753, found 385.0756.

N-(4-sulfamoylbenzyl)-N-((2-aminoethyl)-2-methyl-5-nitroimidazolyl) thiourea (6b): Yield: 82%; mp 67-69°C; ¹H NMR (DMSO-*d*₆, 400 MHz) δ 2.37 (s, 3H), 2.87

(m, 2H), 4.43 (t, 2H, $J=5.18\text{Hz}$), 4.70 (br s, 2H), 7.32 (s, 2H), 7.34 (d, 2H, $J=8.4\text{Hz}$), 7.68 (s, 1H), 7.75 (d, 2H, $J=8.4\text{Hz}$), 8.03 (s, 1H), 8.15 (s, 1H); ^{13}C (DMSO- d_6 , 101 MHz) δ 13.84, 30.64, 42.70, 45.44, 125.52, 127.23, 133.17, 138.61, 142.48, 151.41, 181.44; MS (ESI $^+$ /ESI $^-$) m/z 399.23 [M+H] $^+$, 421.16 [M+Na] $^+$, 797.08 [2M+H] $^+$, 819.26 [2M+Na] $^+$, 397.10 [2] $^-$, 433.09 [M+Cl] $^-$, 795.33 [2M-H] $^-$. HRMS (ESI) [M+H] $^+$ calculated for [C $_{14}$ H $_{19}$ N $_6$ O $_4$ S $_2$] $^+$: 399,0909, found 399.0912.

N-(4-sulfamoylphenylethyl)-N-((2-aminoethyl)-2-methyl-5-nitroimidazolyl) thiourea (6c):

Yield: 86%; mp 75-77°C; ^1H NMR (DMSO- d_6 , 400 MHz) δ 2.35 (s, 3H), 2.83 (m, 2H), 3.62 (m, 2H), 3.82 (m, 2H), 4.41 (m, 2H), 7.31 (s, 2H), 7.37 (d, 2H, $J=8.2\text{Hz}$), 7.52 (s, 1H), 7.63 (s, 1H), 7.74 (d, 2H, $J=8.2\text{Hz}$), 8.03 (s, 1H); ^{13}C (DMSO- d_6 , 101 MHz) δ 13.78, 30.64, 45.4, 125.65, 129.05, 133.18, 138.54, 142.03, 143.45, 151.42, 180.83; MS (ESI $^+$ /ESI $^-$) m/z 413.06 [M+H] $^+$, 435.02 [M+Na] $^+$, 825.09 [2M+H] $^+$, 847.21 [2M+Na] $^+$, 411.06 [2] $^-$, 447.20 [M+Cl] $^-$, 822.99 [2M-H] $^-$, 859.26 [2M+Cl] $^-$. HRMS (ESI) [M+H] $^+$ calculated for [C $_{15}$ H $_{21}$ N $_6$ O $_4$ S $_2$] $^+$: 413.1066, found 413.1069.

N-(3-sulfamoylphenyl)-N-((2-aminoethyl)-2-methyl-5-nitroimidazolyl) thiourea (6d):

Yield: 75%; mp 66-68°C; ^1H NMR (DMSO- d_6 , 400 MHz) δ 2.43 (s, 3H), 3.91 (m, 2H), 4.49 (t, 2H, $J=5.68\text{Hz}$), 7.39 (s, 2H), 7.51 (m, 1H), 7.55 (s, 1H), 7.57 (m, 1H), 7.81 (s, 1H, 1H), 7.93 (m, 1H), 8.04 (s, 1H), 9.94 (s, 1H); ^{13}C (DMSO- d_6 , 101 MHz) δ 13.81, 42.82, 44.99, 120.29, 121.39, 126.62, 129.09, 133.18, 138.65, 139.51, 144.35, 151.37, 181.28; MS (ESI $^+$ /ESI $^-$) m/z 385.23 [M+H] $^+$, 406.94 [M+Na] $^+$, 791.19 [2M+Na] $^+$, 383.12 [2] $^-$, 419.09 [M+Cl] $^-$, 767.26 [2M-H] $^-$. HRMS (ESI) [M+H] $^+$ calculated for [C $_{13}$ H $_{17}$ N $_6$ O $_4$ S $_2$] $^+$: 385.0753, found 385.0746.

N-[2-(2-methyl-5-nitro-imidazol-1-yl)ethyl]sulfamide (7): A solution of chlorosulfonyl isocyanate (4.59 mmol, 1.2 equiv) and *tert*-butanol (4.59 mmol, 1.2 equiv.) in 2 mL of methylene chloride (prepared *ab-initio*) was added to a solution of **5** (3.83 mmol, 1 equiv.) and triethylamine (30.63 mmol, 4 equiv.) in 10 mL of methylene chloride. The mixture was stirred at room temperature for one hour, then diluted with ethyl acetate and washed with water. The organic layer was dried over anhydrous sodium sulfate, filtered and concentrated under vacuum. The residue was purified by chromatography on silica gel using methylene chloride – methanol 98-2 as eluent. This intermediate was then diluted in a solution of trifluoroacetic acid in

methylene chloride (30 % volume), and stirred at room temperature for 6 hours. The mixture was then concentrated under vacuum and co-evaporated several times with diethyl ether to give the expected sulfamide as a white powder. Overall Yield: 70%; mp 122°C; ¹H NMR (DMSO-*d*₆, 400 MHz) δ 2.52 (s, 3H), 3.26 (m, 2H), 4.37 (t, 2H, *J*=5.81Hz), 6.65 (s, 2H), 6.86 (s, 1H), 8.1 (s, 1H); ¹³C (DMSO-*d*₆, 101 MHz) δ 14.03, 41.8, 46.0, 132.68, 138.26, 151.65; MS (ESI⁺/ESI⁻) *m/z* 250.19 [M+H]⁺, 272.34 [M+Na]⁺, 499.32 [2M+H]⁺, 249.09 [2]⁻, 284.12 [M+Cl]⁻, 533.14 [2M+Cl]⁻. HRMS (ESI) [M+H]⁺ calculated for [C₆H₁₂N₅O₄S]⁺: 250.0610, found 250.0616.

***N*-[2-(2-methyl-5-nitro-imidazol-1-yl)ethyl]sulfamate (9):** Sulfamoyl chloride (5.25 mmol, 3 equiv.) was added to a solution of the commercially available compound **8** (1.75 mmol, 1 equiv.) in *N,N*-dimethylacetamide. The mixture was stirred at room temperature for one night, then diluted with ethyl acetate, and washed three times with water. The organic layer was dried over anhydrous magnesium sulphate, filtered and concentrated under vacuum. The residue was purified by chromatography on silica gel using methylene chloride – methanol 9-1 as eluent. Yield: 81%; mp 166-168°C; ¹H NMR (DMSO-*d*₆, 400 MHz) δ 2.45 (s, 3H), 4.35 (t, 2H, *J*=5.05Hz), 4.61 (t, 2H, *J*=5.05Hz), 7.57 (s, 2H), 8.06 (s, 1H); ¹³C (DMSO-*d*₆, 101 MHz) δ 14.04, 44.98, 57.21, 133.10, 138.32, 151.82; MS (ESI⁺/ESI⁻) *m/z* 250.3 [M+H]⁺, 272.32 [M+Na]⁺, 521.30 [2M+Na]⁺, 770.16 [3M+Na]⁺. HRMS (ESI) [M+H]⁺ calculated for [C₆H₁₁N₄O₅S]⁺: 251.0450, found 251.0456.

2-(2-nitro-imidazol-1-yl)ethylamine (10): *Tert*-butyl 2-bromoethylcarbamate (3.3 mmol, 1.5 equiv.) was added at room temperature to a solution of 2-nitroimidazole (2.2 mmol, 1 equiv.) and K₂CO₃ (2.2 mmol, 1 equiv.) in 3 ml of DMF. The reaction mixture was stirred at room temperature overnight then filtered and the filtrate was concentrated under vacuum. The solid obtained was dissolved with ethyl acetate and washed with water. The organic layer was dried over anhydrous sodium sulfate, and concentrated. The residue was purified on silica column chromatography using methylene chloride – methanol 9-1 as eluent. The pure Boc protected compound was then dissolved in 20% trifluoroacetic acid – methylene chloride (16 equiv.TFA) solution and stirred at room temperature for 2 hrs. The reaction mixture was then concentrated in vacuo and co-evaporated with methanol. The pure expected compound (under trifluoroacetate salt) was then obtained after precipitation in diethyl

ether and filtration. Yield: 40%; mp 166-168°C; ¹H NMR (DMSO-*d*₆, 400 MHz) δ 3.33 (t, 2H, *J*=6.0Hz), 4.64 (t, 2H, *J*=6.0Hz), 7.23 (d, 1H, *J*=0.6Hz), 7.65 (d, 1, *J*=0.5Hz), 8.17 (s, 2H); MS (ESI⁺) *m/z* 157.09 [M+H]⁺, 313.35 [2M+H]⁺.

***N*-[2-(2-nitro-imidazol-1-yl)ethyl]sulfamide (11):** Same protocol as for the synthesis of compound **7** starting from **10**. Overall Yield: 70%; mp 78-80°C; ¹H NMR (DMSO-*d*₆, 400 MHz) δ 3.39 (q, 2H, *J*=6.2Hz), 4.46 (t, 2H, *J*=5.9Hz), 6.64 (s, 2H), 7.18 (d, 1H, *J*=1Hz), 7.23 (t, 1H, *J*=6.2Hz), 7.59 (d, 1H, *J*=1Hz); ¹³C (DMSO-*d*₆, 101 MHz) δ 41.85, 49.45, 127.63, 128.52; MS (ESI⁺/ESI⁻) *m/z* 236.15 [M+H]⁺.]⁺. HRMS (ESI) [M+H]⁺ calculated for [C₅H₁₀N₅O₄S]⁺: 236.0453, found 236.0456.

***N*-methanesulfonyl 2-(2-nitro-imidazol-1-yl)ethylamine (12):** compound **10** (1 equiv.) was suspended in methylene chloride and triethylamine (2 equiv. 2.56 mmol) was added at 0°C. Methanesulfonyl chloride (2 equiv. 2.56 mmol) was added dropwise to the resulting solution. Reaction was monitored by TLC until completion. Then the reaction mixture was diluted with methylene chloride and washed with water. The organic phase was dried over sodium sulfate and concentrated under vacuum. The residue was purified on silica gel column chromatography (eluent methylene chloride – methanol 9 – 1 v-v) to afford the pure expected compound as a white powder. Yield: 45%; mp 122-125°C; ¹H NMR (DMSO-*d*₆, 400 MHz) δ 2.87 (s, 3H), 3.39 (q, 2H, *J*=6.2Hz), 4.47 (t, 2H, *J*=5.9Hz), 7.19 (d, 1H, *J*=1.0Hz), 7.24 (t, 1H, *J*=6.2Hz), 7.60 (d, 1H, *J*=1.0Hz); ¹³C (DMSO-*d*₆, 101 MHz) δ 128.52, 127.63, 49.45, 41.85, 39.64; MS (ESI⁺/ESI⁻) *m/z* 235.13 [M+H]⁺. HRMS (ESI) [M+H]⁺ calculated for [C₆H₁₁N₄O₄S]⁺: 235.0501, found 235.0507.

***N*-methanesulfonyl 1-(2-aminoethyl)-2-methyl-5-nitroimidazole (13):** Same protocol as for the synthesis of compound **12** starting from **5**. Yield: 44%; mp 132-135°C; ¹H NMR (DMSO-*d*₆, 400 MHz) δ 2.47 (s, 3H), 2.87 (s, 3H), 3.33 (q, 2H, *J*=6.2Hz), 4.34 (t, 2H, *J*=5.9Hz), 7.33 (t, 1H, *J*=6.4Hz), 8.05 (s, 1H); ¹³C (DMSO-*d*₆, 101 MHz) δ 151.72, 138.35, 133.17, 46.33, 41.66, 39.40, 14.16; MS (ESI⁺/ESI⁻) *m/z* 249.20 [M+H]⁺. HRMS (ESI) [M+H]⁺ calculated for [C₇H₁₃N₄O₄S]⁺: 249.0658, found 249.0657.

***N*-[2-(2-methyl-imidazol-1-yl)propyl]sulfamide (15):** Same protocol as for the synthesis of compound 7 starting from 14. Overall Yield: 71%; mp 133-135°C; ¹H NMR (DMSO-*d*₆, 400 MHz) δ 2.47 (s, 3H), 2.86 (m, 2H), 3.38 (q, 2H, *J*=6.1Hz), 4.46 (t, 2H, *J*=5.9Hz), 6.64 (s, 2H), 7.18 (d, 1H, *J*=1.0Hz), 7.23 (t, 1H, *J*=6.2Hz), 7.59 (d, 1H, *J*=1.0Hz); ¹³C (DMSO-*d*₆, 101 MHz) δ 151.72, 138.35, 133.17, 46.33, 41.66, 38.81, 14.16; MS (ESI⁺/ESI) *m/z* 219.28 [M+H]⁺. HRMS (ESI) [M+H]⁺ calculated for [C₇H₁₅N₄O₂S]⁺: 219.0916, found 219.0917.

CA inhibition assays

An Applied Photophysics stopped-flow instrument has been used for assaying the CA-catalyzed CO₂ hydration activity [19]. Phenol red (at a concentration of 0.2 mM) has been used as an indicator, working at the absorbance maximum of 557 nm, with 20 mM Hepes (pH 7.5) as buffer, and 20 mM Na₂SO₄ (for maintaining constant the ionic strength), following the initial rates of the CA-catalyzed CO₂ hydration reaction for a period of 10–100 s. The CO₂ concentrations ranged from 1.7 to 17 mM for the determination of the kinetic parameters and inhibition constants. For each inhibitor, at least six traces of the initial 5–10% of the reaction have been used for determining the initial velocity. The uncatalyzed rates were determined in the same manner and subtracted from the total observed rates. Stock solutions of inhibitor (0.1 mM) were prepared in distilled–deionized water, and dilutions up to 0.01 nM were done thereafter with distilled–deionized water. Inhibitor and enzyme solutions were preincubated together for 15 min at room temperature prior to assay, to allow for the formation of the E–I complex. The inhibition constants were obtained by nonlinear least squares methods using PRISM 3 and represent the mean from at least three different determinations. CA isoforms were recombinant ones obtained in house as reported earlier.

Biological assays

Cells

Exponentially growing colorectal (HT-29, ATCC HTB-38) and cervical (HeLa, ATCC CCL-2) carcinoma cells were cultured in Dulbecco's modified Eagle's medium supplemented with 10% foetal bovine serum. Low oxygen conditions were

acquired in a hypoxic workstation (Ruskinn INVIVO2 1000). The atmosphere in the chamber consisted of 0.2% O₂ (hypoxia), 5% CO₂ and residual N₂. In parallel, normoxic (20% O₂) dishes were incubated in air with 5% CO₂. pH of the culture medium was immediately measured at the end of each experiment as previously described [9, 20].

Compounds preparation

Compounds were dissolved in culture medium containing 1% DMSO at the indicated final concentrations just before addition to the cells. For the animal experiments, **7** was dissolved in NaCl 0.9% containing 1% DMSO to a final concentration of 10 mg/kg and injected intravenously *via* a lateral tail vein.

Animals

Cells were resuspended in matrigel (BD Biosciences) and injected subcutaneously into the lateral flank of adult NMRI-nu mice (28-32 g). Intravenous **7** and doxorubicin treatment started at a tumor volume of 250 mm³ for 3 days (10 mg/kg daily) and at day 3 (5 mg/kg) respectively. This schedule was repeated during 3 weeks. Tumour growth was monitored until reaching 4x the volume at treatment time (T4xSV) and treatment toxicity was scored by body weight measurements. All experiments were in accordance with local institutional guidelines for animal welfare and were approved by the Animal Ethical Committee of the University (2008-025).

Statistics

All statistical analyses were performed with GraphPad Prism version 5.03 for Windows (GraphPad Software, 2009, California, USA). A non-parametric Mann-Whitney U test for small groups was used to determine the statistical significance of differences between two independent groups of variables. For all tests, a $P < 0.05$ was considered significant.

X-ray studies

The hCA II-**7** complex was obtained by adding a 5-molar excess of inhibitor to a 10 mg/mL protein solution in 20 mM Tris-HCl pH 8, 0.1% DMSO. Crystals of the complex were obtained using the hanging drop vapor diffusion technique. In

particular 2 μL of complex solution and 2 μL of precipitant solution (1.4 M Na-Citrate, 100 mM Tris-HCl pH 8.0) were mixed and suspended over a reservoir containing 1 mL of precipitant solution at 20°C. Crystals grew within 3 days. A complete dataset was collected at 1.85 Å resolution from a single crystal, at 100 K, with a copper rotating anode generator developed by Rigaku and equipped with Rigaku Saturn CCD detector. Prior to cryogenic freezing crystals were transferred to the precipitant solution with the addition of 20% (v/v) glycerol. Diffracted intensities were processed using the HKL2000 crystallographic data reduction package (Denzo/Scalepack) [26]. Crystal parameters and data processing statistics are summarized in Table 2. The structure of the complex was analyzed by difference Fourier techniques using hCA II crystallized in the $P2_1$ space group (PDB code 1CA2) [22] as the starting model after deletion of non-protein atoms. An initial round of rigid body refinement followed by simulated annealing and individual B factor refinement was performed using the program CNS [27]. Model visualization and rebuilding was performed using the graphics program O [28]. After an initial refinement, limited to the enzyme structure, a model for the inhibitor was easily built and introduced into the atomic coordinates set for further refinement. Restraints on inhibitor bond angles and distances were taken from the Cambridge Structural Database [29] and standard restraints were used on protein bond angles and distances throughout refinement. Water molecules were built into peaks $>3\sigma$ in $|F_o| - |F_c|$ maps that demonstrated appropriate hydrogen-bonding geometry. Final crystallographic R-factor and R-free values were 0.163 and 0.196, respectively. Statistics for refinement are summarized in Table 2. Coordinates and structure factors have been deposited with the Protein Data Bank (accession code 4MO8).

Acknowledgements

This work has been funded with the support of the EU 6th framework Program (Euroxy project ref. 2003-502932), the EU 7th framework (Metoxia project ref. 2008-222741), the KWF UM2012-5394, the NGI Life Science Pre-Seed grant 93613002 and also the CNRS/CNR (CoopIntEER program, Grant No. 131999)

References

1. Wilson, W.R.; Hay, M.P. Targeting hypoxia in cancer therapy. *Nat. Rev. Cancer* 2011, **11**, 393-410.
2. Bennewith, K.L.; Dedhar, S. Targeting hypoxic tumour cells to overcome metastasis. *BMC Cancer* 2011, **11**, 504.
3. Supuran, C.T. Carbonic anhydrases: novel therapeutic applications for inhibitors and activators. *Nat. Rev. Drug Discov.* 2008, **7**, 168-81.
4. McDonald, P.C.; Winum, J-Y.; Supuran, C.T.; Dedhar, S. Recent developments in targeting carbonic anhydrase IX for cancer therapeutics. *Oncotarget* 2012, **3**, 84-97.
5. Neri, D.; Supuran, C.T. Interfering with pH regulation in tumours as a therapeutic strategy. *Nat. Rev. Drug Discov.* 2011, **10**, 767-77.
6. Pacchiano, F.; Carta, F.; McDonald, P.C.; Lou, Y.; Vullo, D.; Scozzafava, A.; Dedhar, S.; Supuran, C.T. Ureido-substituted benzenesulfonamides potently inhibit carbonic anhydrase IX and show antimetastatic activity in a model of breast cancer metastasis. *J. Med. Chem.* 2011, **54**, 1896-902.
7. Touisni, N.; Maresca, A.; McDonald, P.C.; Lou, Y.; Scozzafava, A.; Dedhar, S.; Winum, J-Y, Supuran, C.T. Glycosyl coumarin carbonic anhydrase IX and XII inhibitors strongly attenuate the growth of primary breast tumors. *J. Med. Chem.* 2011, **54**, 8271-7.
8. Lou, Y.; McDonald, P.C.; Oloumi, A.; Chia, S.; Ostlund, C.; Ahmadi, A.; Kyle, A.; Auf dem Keller, U.; Leung, S.; Huntsman, D.; Clarke, B.; Sutherland, B.W.; Waterhouse, D.; Bally, M.; Roskelley, C.; Overall, C.M.; Minchinton, A.; Pacchiano, F.; Carta, F.; Scozzafava, A.; Touisni, N.; Winum, J-Y.; Supuran, C.T.; Dedhar, S. Targeting tumor hypoxia: suppression of breast tumor growth and metastasis by novel carbonic anhydrase IX inhibitors. *Cancer Res.* 2011, **71**, 3364-76.
9. Dubois, L.; Peeters, S.; Lieuwes, N.G.; Geusens, N.; Thiry, A.; Wigfield, S.; Carta, F.; McIntyre, A.; Scozzafava, A.; Dogné, J-M.; Supuran, C.T.; Harris, A.L.; Masereel, B.; Lambin, P. Specific inhibition of carbonic anhydrase IX activity enhances the in vivo therapeutic effect of tumor irradiation. *Radiother. Oncol.* 2011, **99**, 424-31.
10. Gieling, R.G.; Babur, M.; Mamnani, L.; Burrows, N.; Telfer, B.A.; Carta, F.; Winum, J-Y.; Scozzafava, A.; Supuran, C.T.; Williams, K.J. Antimetastatic effect of

- sulfamate carbonic anhydrase IX inhibitors in breast carcinoma xenografts. *J. Med. Chem.* 2012, **55**, 5591-600.
11. Liu, K.; Zhu, H.L. Nitroimidazoles as anti-tumor agents. *Anticancer Agents Med. Chem.* 2011, **11**, 687-91.
12. Overgaard, J.; Overgaard, M.; Nielsen, O.S.; Pedersen, A.K.; Timothy, A.R. A comparative investigation of nimorazole and misonidazole as hypoxic radiosensitizers in a C3H mammary carcinoma in vivo. *Br. J. Cancer* 1982, **46**, 904-11.
13. D'Ambrosio, K.; Vitale, R.M.; Dogné, J.M.; Masereel, B.; Innocenti, A.; Scozzafava, A.; De Simone, G.; Supuran, C.T. Carbonic anhydrase inhibitors: bioreductive nitro-containing sulfonamides with selectivity for targeting the tumor associated isoforms IX and XII. *J Med Chem.* 2008, **51**, 3230-37
14. Rami, M.; Cecchi, A.; Montero, J-L.; Innocenti, A.; Vullo, D.; Scozzafava, A.; Winum, J-Y.; Supuran, C.T. Carbonic anhydrase inhibitors: design of membrane-impermeant copper(II) complexes of DTPA-, DOTA-, and TETA-tailed sulfonamides targeting the tumor-associated transmembrane isoform IX. *ChemMedChem.* 2008, **3**, 1780-8.
15. Rami, M.; Montero, J-L.; Dubois, L.; Lambin, P.; Scozzafava, A.; Winum, J-Y.; Supuran, C.T. Carbonic anhydrase inhibitors: Gd(III) complexes of DOTA- and TETA-sulfonamide conjugates targeting the tumor associated carbonic anhydrase isozymes IX and XII. *New J. Chem.*, 2010, **34**, 2139.
16. D'Ambrosio, K.; Smaine, F.Z.; Carta, F.; De Simone, G.; Winum, J-Y.; Supuran, C.T. Development of potent carbonic anhydrase inhibitors incorporating both sulfonamide and sulfamide groups. *J. Med. Chem.* 2012, **55**, 6776-83.
17. Winum, J-Y.; Carta, F.; Ward, C.; Mullen, P.; Harrison, D.; Langdon, S.P.; Cecchi, A.; Scozzafava, A.; Kunkler, I.; Supuran, C.T. Ureido-substituted sulfamates show potent carbonic anhydrase IX inhibitory and antiproliferative activities against breast cancer cell lines. *Bioorg. Med. Chem. Lett.* 2012, **22**, 4681-5.
18. Hoigebazar, L.; Jeong, J.M.; Choi, S.Y.; Choi, J.Y.; Shetty, D.; Lee, Y.S.; Lee, D.S.; Chung, J.K.; Lee, M.C.; Chung, Y.K. Synthesis and characterization of nitroimidazole derivatives for ⁶⁸Ga-labeling and testing in tumor xenografted mice. *J. Med. Chem.* 2010, **53**, 6378-85.
19. Khalifah, R. G. The carbon dioxide hydration activity of carbonic anhydrase. I. Stop-flow kinetic studies on the native human isoenzymes B and C. *J. Biol. Chem.* 1971, **246**, 2561-2573.

20. Dubois, L.; Douma, K.; Supuran, C.T.; Chiu, R.K.; van Zandvoort, M.A.; Pastoreková, S.; Scozzafava, A.; Wouters, B.G.; Lambin, P. Imaging the hypoxia surrogate marker CA IX requires expression and catalytic activity for binding fluorescent sulfonamide inhibitors. *Radiother. Oncol.* 2007, **83**, 367-73.
21. Dubois, L.; Peeters, S.G.; van Kuijk, S.J.; Yaromina, A.; Lieuwes, N.G.; Saraya, R.; Biemans, R.; Rami, M.; Parvathaneni, N.K.; Vullo, D.; Vooijs, M.; Supuran, C.T.; Winum, J.-Y.; Lambin, P. Targeting carbonic anhydrase IX by nitroimidazole based sulfamides enhances the therapeutic effect of tumor irradiation: a new concept of dual targeting drugs. *Radiother. Oncol.* 2013, *in press*. DOI: 10.1016/j.radonc.2013.06.018.
22. Eriksson, A.E.; Jones, T.A.; Liljas, A. Refined structure of human carbonic anhydrase II at 2.0 Å resolution. *Proteins.* 1988, **4**, 274-82.
23. Winum, J.-Y.; Temperini, C.; El Cheikh, K.; Innocenti, A.; Vullo, D.; Ciattini, S.; Montero, J.L.; Scozzafava, A.; Supuran, C.T. Carbonic anhydrase inhibitors: clash with Ala65 as a means for designing inhibitors with low affinity for the ubiquitous isozyme II, exemplified by the crystal structure of the topiramate sulfamide analogue. *J. Med. Chem.* 2006, **49**, 7024-31.
24. Di Fiore, A.; Monti, S.M.; Innocenti, A.; Winum, J.Y.; De Simone, G.; Supuran, C.T. Carbonic anhydrase inhibitors: crystallographic and solution binding studies for the interaction of a boron-containing aromatic sulfamide with mammalian isoforms I-XV. *Bioorg. Med. Chem. Lett.* 2010, **20**, 3601-5.
25. De Simone, G.; Alterio, V.; Supuran, C.T. Exploiting the hydrophobic and hydrophilic binding sites for designing carbonic anhydrase inhibitors. *Expert Opin. Drug Discov.* 2013, **8**, 793-810.
26. Otwinowski, Z.; Minor, W. Processing of X-ray diffraction data collected in oscillation mode. *Methods Enzymol.* 1997, **276**, 307-26.
27. Brünger, A.T.; Adams, P.D.; Clore, G.M.; DeLano, W.L.; Gros, P.; Grosse-Kunstleve, R.W.; Jiang, J.S.; Kuszewski, J.; Nilges, M.; Pannu, N.S.; Read, R.J.; Rice, L.M.; Simonson, T.; Warren, G.L. *Acta Crystallogr. Sect. D.* 1998, **54**, 905-21.
28. Jones, T.A.; Zou, J.Y.; Cowan, S.W.; Kjeldgaard, M. *Acta Crystallogr. Sect. A.* 1991, **47**, 110-19.
29. Allen, F.H. The Cambridge Structural Database: a quarter of a million crystal structures and rising. *Acta Cryst. sect. B.* 2002, **58**, 380-8.

Chapter 4

New approach of delivering cytotoxic drugs towards CAIX expressing cells: A concept of dual-target drugs

Published in: Eur. J. Med. Chem., 2017. 127: p. 691-702.

Simon J.A. van Kuijk* Nanda Kumar Parvathaneni*, Raymon Niemans*, Marike W. van Gisbergen*, Fabrizio Carta, Daniela Vullo, Silvia Pastorekova, Ala Yaromina, Claudiu T. Supuran, Ludwig J. Dubois**, Jean-Yves Winum**, Philippe Lambin**

* contributed equally

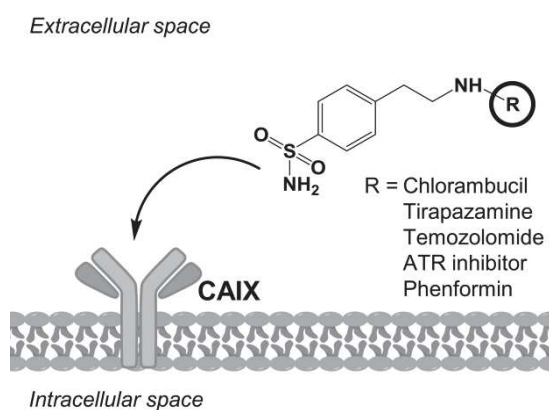
** contributed equally

Highlights

- New dual-target drugs combining cytotoxic agents with CAIX inhibitors were designed.
- Dual-targeting drugs may allow for specific drug delivery to hypoxic tumor areas.
- Increased binding affinity to CAIX was found for most of the dual-targeting drugs.
- Higher efficacy of dual-target ATR inhibitor was found in CAIX overexpressing cells.
- Design of alternative CAIX-targeting drugs may increase their therapeutic window.

Abstract

Carbonic anhydrase IX (CAIX) is a hypoxia-regulated and tumor-specific protein that maintains the pH balance of cells. Targeting CAIX might be a valuable approach for specific delivery of cytotoxic drugs, thereby reducing normal tissue side effects. A series of dual-target compounds were designed and synthesized incorporating a sulfonamide, sulfamide, or sulfamate moiety combined with several different anti-cancer drugs, including the chemotherapeutic agents chlorambucil, tirapazamine, and temozolomide, two Ataxia Telangiectasia and Rad3-related protein inhibitors (ATRi), and the anti-diabetic biguanide agent phenformin. An ATRi derivative (12) was the only compound to show a preferred efficacy in CAIX overexpressing cells versus cells without CAIX expression when combined with radiation. Its efficacy might however not solely depend on binding to CAIX, since all described compounds generally display low activity as carbonic anhydrase inhibitors. The hypothesis that dual-target compounds specifically target CAIX expressing tumor cells was therefore not confirmed. Even though dual-target compounds remain an interesting approach, alternative options should also be investigated as novel treatment strategies.



Introduction

Solid tumors are characterized by a hypoxic microenvironment caused by their immature and inadequate vascular supply of oxygen and nutrients. These hostile hypoxic conditions result in a phenotype that is associated with a worse prognosis [1] and resistance to standard treatment options such as radiotherapy, chemotherapy, and surgery [2-4]. Several different approaches are currently being investigated to target these hypoxic areas to make tumors more sensitive to standard treatment modalities [5-7].

Carbonic anhydrase IX (CAIX) can be a valuable therapeutic target since it plays an important role in maintaining the intracellular pH homeostasis [8, 9]. Furthermore its expression is predominantly tumor specific [5, 8, 10] and directly regulated via the hypoxia-inducible factor (HIF) pathway [11]. Even though alternative pathways are also able to modulate CAIX expression [12-14], its significant prognostic value in many different tumor types [15] has promoted investigations in its use as an imaging agent for diagnostic and prognostic purposes [5, 16-19]. Together these characteristics of CAIX support investigations into the therapeutic targeting of CAIX to improve efficacy of standard treatments. The function of CAIX is evolutionary conserved and catalyzes the hydration of carbon dioxide to bicarbonate at the cell membrane. The bicarbonate is transported back intracellular from the extracellular space, whereas the free proton is extruded in the extracellular space. CAIX thereby maintains the balance between an acidic extracellular and alkaline intracellular pH of tumor cells, the latter of which would otherwise acidify due to the increased acid production resulting from their glycolytic metabolism [8, 9]. Many different inhibitors are currently being developed to specifically target the tumor-associated CAIX isoform and have shown promise in reducing tumor cell survival, migration, invasion, and reduce tumor xenograft growth and metastases formation [20-23]. Furthermore, the combination therapy of CAIX inhibitors (CAIXi) with standard treatment options was previously found to increase the efficacy of radiotherapy [24] and of weakly basic chemotherapeutic agents such as doxorubicin [25].

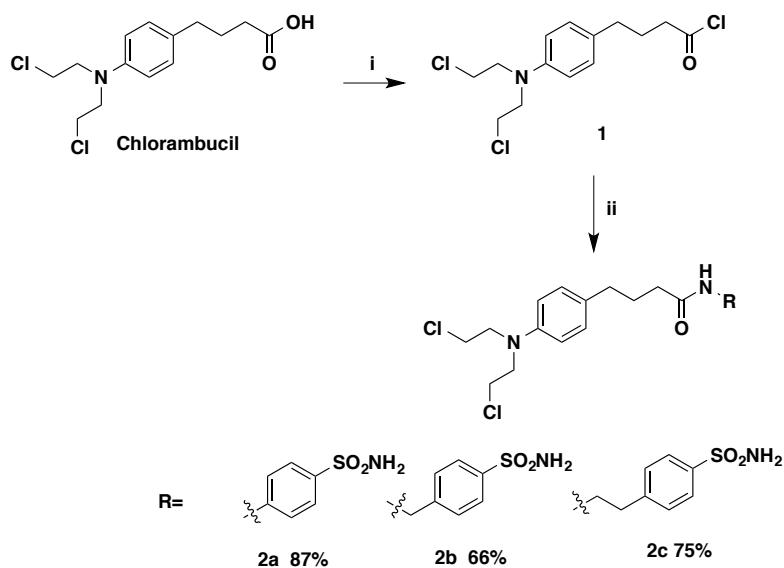
The predominant expression of CAIX on hypoxic tumor cells can also be exploited to direct cytotoxic agents specifically to those CAIX expressing cancer cells thereby possibly minimizing normal tissue toxicity. This can be achieved by conjugating anti-

cancer drugs with CAIX inhibiting molecules that bind to the Zn^{2+} active site of CAIX and hence inhibit its enzymatic function [8, 26, 27], *i.e.* a so-called dual-targeting approach. Our group showed previously that such a dual-target approach with a sulfamide CAIXi moiety coupled to the radiosensitizing compound nitroimidazole to be a more effective radiosensitizer than an indanesulfonamide CAIXi [28]. Alternative novel dual-target compounds have been developed to investigate this strategy of dual-targeting further in the context of anti-cancer agents to target CAIX. Here we have designed five different classes of dual-target compounds conjugated to CAIXi (sulfonamide, sulfamide, or sulfamate), which included the chemotherapeutic anti-cancer agents chlorambucil, tirapazamine, and temozolomide, two ataxia telangiectasia and Rad3-related protein inhibitors (ATRi), and the biguanide agent phenformin, previously used in diabetes treatment. We hypothesize that these new dual-target compounds will have the ability to specifically target CAIX expressing cells and modulate their efficacy in a CAIX-dependent manner.

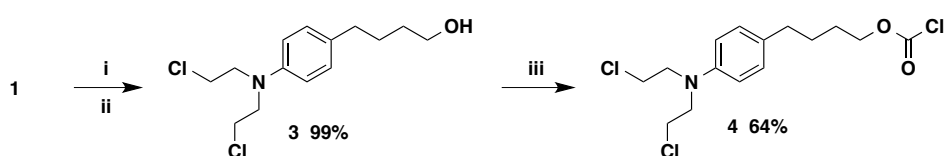
Results and discussion

Chemistry

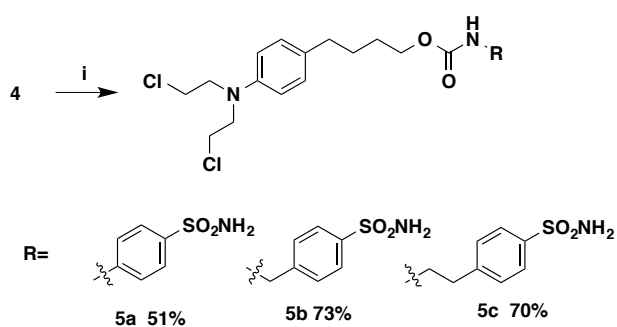
Chlorambucil was converted to its acid chloride [29] **1** by using oxalyl chloride. This chlorambucil acid chloride reacted with different benzene sulfonamides under basic condition to obtain good yields of chlorambucil derivatives **2a**, **2b** and **2c**. Chlorambucil carbamate derivatives were obtained by converting compound **1** into a methyl ester [30] using methanol. This ester was reduced to alcohol [31], *i.e.* compound **3**, after treating with lithium aluminium hydride. Compound **3** was treated with triphosgene to obtain its respective chloroformate [32], *i.e.* compound **4** (Scheme 2). The reaction of chlorambucil chloroformate (**4**) with different benzene sulfonamides resulted in compounds **5a**, **5b** and **5c** (Scheme 3).



Scheme 1. Reagents and conditions: (i) $(\text{COCl})_2$, DMF, DCM, 0 °C–rt; (ii) DIPEA, THF, 0 °C–rt.

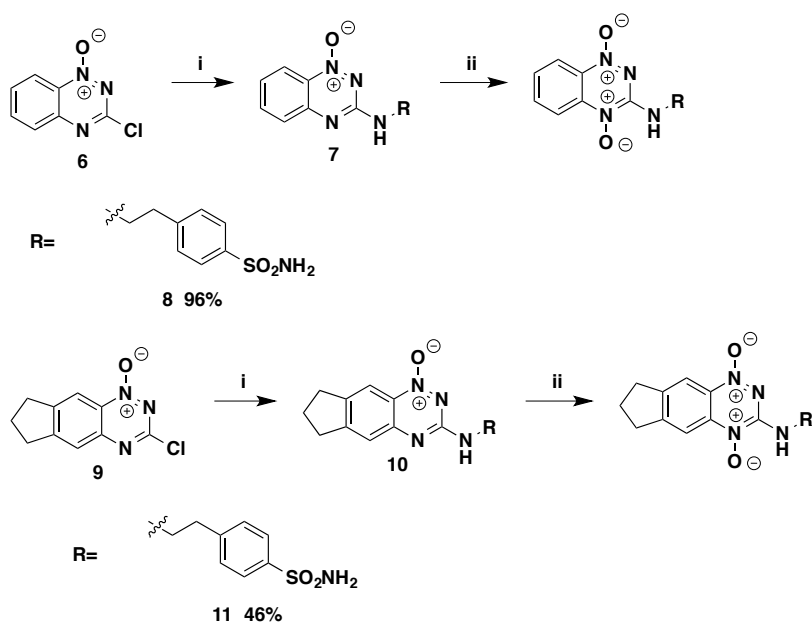


Scheme 2. Reagents and conditions: (i) MeOH, DCM; (ii) LAH, THF; (iii) Triphosgene, Na_2CO_3 , Toluene, DMF.



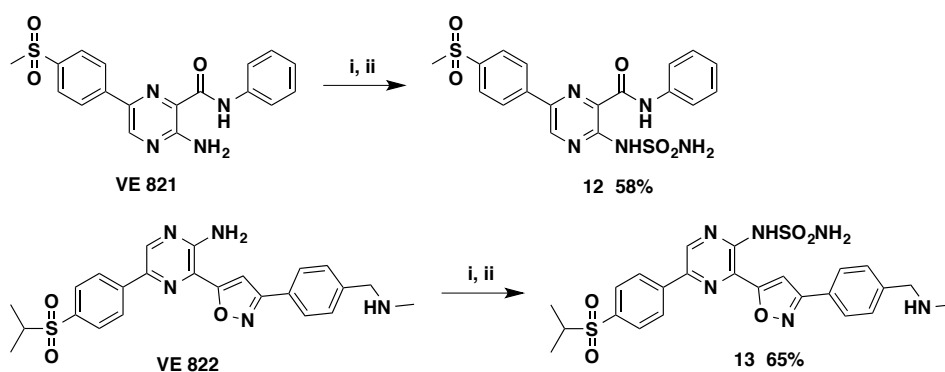
Scheme 3. Reagents and conditions: (i) DIPEA, THF, 0 °C–rt.

Tirapazamine derivatives **8** and **11** were synthesized from **6** and **9** with the previously described procedure [33]. In short, **6** and **9** reacted with 4-(2-aminoethyl) benzene sulfonamide under reflux conditions and was followed by oxidation of the mono-oxides (Scheme 4).



Scheme 4. Reagents and conditions: (i) RNH₂ (3 equiv.), DME, reflux; (ii) TFAA, H₂O₂, DCM, rt.

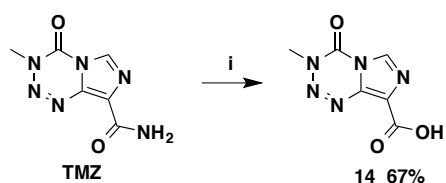
The ATRi derivatives **12** and **13** were synthesized from commercially available VE-821 and VE-822 (MedChemTronica) using a classical synthetic strategy described previously [25] (Scheme 5).



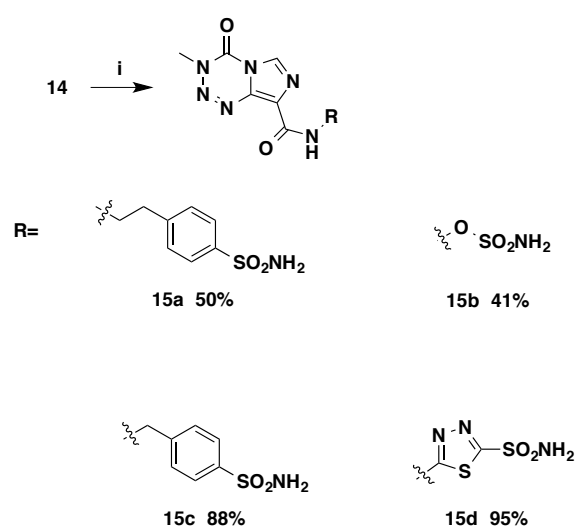
Scheme 5. Reagents and conditions: (i) ClSO₂NCO, tBuOH, NEt₃, DCM, 0 °C to rt; (ii) 20% TFA-DCM.

Commercially purchased temozolomide (SelleckChem) was converted into its respective acid by treating with concentrated sulfuric acid and sodium nitrate at 0 °C–15 °C (Scheme 6) [34]. Reacting the temozolomic acid with different benzenesulfonamides, aminoxysulfonamide [35] and 5-amino-1, 3,4-thiadiazole-2-

sulfonamide hydrochloride under known amide bond formation conditions [34] resulted in compounds **15a**, **15b**, **15c** and **15d** (Scheme 7).

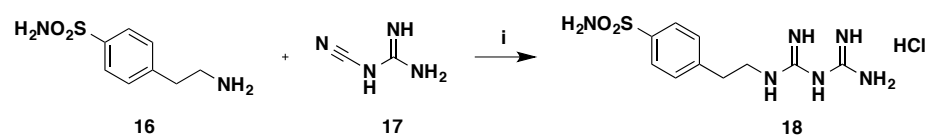


Scheme 6. Reagents and conditions: (i) Con. H₂SO₄, NaNO₂, 0 °C to 15 °C



Scheme 7. Reagents and conditions: (i) BOP, NEt₃, DCM, rt.

The compound **18** was obtained by a slight modification based on the method reported by Kelarev et al. [36]. The commercially available compounds 4-(2-aminoethyl) benzenesulfonamide **16** and cyanoguanidine **17** were coupled in n-butanol using a stoichiometric amount of hydrochloric acid (Scheme 8).



Scheme 8. Reagents and conditions: (i) 6.0 M HCl aq, nBuOH, reflux.

Binding affinity human CAs

Increased binding affinity to human carbonic anhydrases (CAs) as compared with their respective parental compound are observed (Table 1) for most of the

compounds, except for the CAIXi conjugated ATRi (**12** and **13**), which do not bind to any of the four tested human CA isoforms included ($K_i > 50000$ nM). The K_i values of the other dual-targeting compounds are higher than of the previously reported CAIXi [20] with **15a** showing relatively good K_i for the CAII and CAIX isoforms, but not for CAXII. Only the phenformin derivative **18** was found to be selective for the transmembrane CAIX and CAXII isoforms. To investigate whether the biological efficacy of the functionalized compounds is dependent on CAIX expression, canine kidney epithelial (MDCK) cells without CAIX (CAIX⁻), *i.e.* both human and canine [37], or MDCK cells transfected with human CAIX [37], *i.e.* overexpressing CAIX (CAIX⁺), were used. Western blotting confirmed differential expression of CAIX in these cells both under normoxic and hypoxic conditions (Supplementary Fig. S1).

Table 1: Binding affinity (K_i) to human CAI, CAII, CAIX, and CAXII of the parental compounds (bold) and their CAIXi conjugated derivatives.

Compound	K_i (nM) ^a				Selectivity Ratios ^b	
	hCAI	hCAII	hCAIX	hCAXII	K_i hCAII / K_i hCAIX	K_i hCAII / K_i hCAXII
Chlorambucil	>50000	>50000	>50000	>50000		
2a	73.0	9.0	172	689	0.05	0.01
2b	5950	747	8970	7340	0.08	0.10
2c	8400	450	4610	10160	0.10	0.04
5a	5580	553	2740	9380	0.20	0.06
5c	6140	265	4130	9570	0.06	0.03
5c	5670	504	3850	13600	0.13	0.04
Tirapazamine	>50000	>50000	>50000	>50000		
8	567	7.1	383	14600	0.02	<0.01
11	428	8.1	307	624	0.03	0.01
Temozolomide	>50000	>50000	>50000	>50000		
15a	91.3	9.2	37.1	9300	0.25	<0.01

Compound	K_i (nM) ^a				Selectivity Ratios ^b	
	hCAI	hCAII	hCAI X	hCAXI I	K_i hCAII / K_i hCAIX	K_i hCA II / K_i hCA XII
15b	>50000	>50000	>50000	>50000		
15c	539	90.5	271	12400	0.33	0.01
15d	743	15.7	176	92.7	0.09	0.17
ATRi VE-821	>50000	>50000	>50000	>50000		
12	>50000	>50000	>50000	>50000		
ATRi VE-822	>50000	>50000	>50000	>50000		
13	>50000	>50000	>50000	>50000		
Phenformin	>50000	>50000	>50000	>50000		
18	4435	501	20.2	1.7	24.8	295
Acetazolamide^c	250	12.1	25.3	5.7	0.48	2.12

^aValues reported (in nM) are the average of three different estimations with errors between 5–10% of the reported values. Reported values >50000 indicates no binding of the compound towards the CA isoforms.

^bSelectivity ratios of the cytosolic hCAII over the tumor-associated hCAIX and hCAXII isoforms.

^cNon-specific CAi acetazolamide is included as a reference.

Chlorambucil derivatives

Chlorambucil (4-[p-[bis(2-chloroethyl)amino]phenyl]butyric acid) is a nitrogen mustard that acts as a bifunctional alkylating agent used for decades to treat cancers originating in the blood and lymphatic system, e.g. chronic lymphocytic leukemia and lymphomas [38]. Even though reported data suggest chlorambucil efficacy to increase in an acidic microenvironment [39], the CAIXi moiety (benzenesulfonamides) with different linkers (*i.e.* amide, carbamate) might allow for specific targeting of the

compounds to these areas in the tumor. The six CAIXi conjugated chlorambucil derivatives (**2a**, **2b**, **2c**, **5a**, **5b**, and **5c**, Scheme 1 and Scheme 2) lead to reduced cell viability as compared to the parental compound, which was only marginally effective (Table 2, Supplementary Fig. S1). The therapeutic efficacy of these compounds however was not increased in the CAIX⁺ MDCK cells as compared with the CAIX⁻ MDCK cells. Furthermore, none of the six compounds showed an increased efficacy upon hypoxia exposure (0.2% O₂). In contrast, some of the chlorambucil dual-target derivatives were less cytotoxic (*i.e.* higher IC₅₀, Table 2) in CAIX expressing cells independent of oxygen levels, which contradicts the studies demonstrating an increased efficacy of chlorambucil in an acidic micromilieu [39]. All together from these results it can be concluded that the CAIXi conjugated chlorambucil derivatives do not show an increased efficacy in a CAIX or hypoxia dependent manner.

Table 2. Estimated IC₅₀ of the cytotoxic parental compounds (bold) and their CAIXi conjugated derivatives obtained with cell viability assays for MDCK CAIX⁻ and MDCK CAIX⁺ cells exposed to normoxic and hypoxic conditions.

Compound	Normoxia (μM) ^a		Hypoxia (μM) ^a	
	CAIX ⁻	CAIX ⁺	CAIX ⁻	CAIX ⁺
Chlorambucil ^b	93	>100	~100	>100
2a	~100	87	~100	95
2b	18	98	14	92
2c	18	~100	18	~100
5a	8	56	8	62
5b	86	98	52	100
5c	89	99	81	~100
Tirapazamine ^c	>300	>300	<50	95
8	>300	>300	~300	>300
11	>300	>300	>300	>300
Temozolomide ^d	775	>1000	~1000	>1000
15a	>1000	>1000	>1000	>1000
15b	719	>1000	~1000	>1000
15c	>1000	>1000	>1000	>1000

15d	>1000	>1000	>1000	>1000
------------	-------	-------	-------	-------

^aNo IC₅₀ reached is indicated with >. Estimated IC₅₀ value higher than the maximum concentration included is indicated with ~.

^bIncluded concentrations for chlorambucil were 1, 10, and 100 μM.

^cIncluded concentrations for tirapazamine were 50, 100, 200, and 300 μM.

^dIncluded concentrations for temozolomide were 100, 400, 700, and 1000 μM.

Tirapazamine derivatives

The hypoxia-activated prodrug tirapazamine (3-amino-1,2,4-benzotriazine-1,4-dioxide) has been tested in several clinical trials in combination with chemo- and/or radiotherapy [40]. The cytotoxicity of tirapazamine results from activation by reductive enzymes that add an electron to the parent drug to produce a radical species that causes DNA damage. Nevertheless, no definitive conclusions regarding its clinical efficacy can be drawn since addition of tirapazamine to standard treatment (*i.e.* radio-chemotherapy) did not result in an increased benefit in phase III clinical trials. In addition, tirapazamine treatment was often characterized by toxic side-effects, such as nausea, vomiting, and diarrhea, which limited its therapeutic gain [40]. Targeting tirapazamine towards the CAIX expressing (hypoxic) areas in tumors by conjugating tirapazamine with the benzenesulfonamide CAIXi might thereby prove a valuable approach to reduce normal tissue toxicity and increase the efficacy of the compounds (**8** and **11**) in CAIX expressing (hypoxic) cells. Cell viability assays (Table 2, Supplementary Fig. S2) confirmed that the parental compound was specifically effective in hypoxic cells, and more effective in CAIX⁻ cells (IC₅₀ < 50 versus 95 μM, p = 0.037). The CAIXi conjugated tirapazamine derivatives however abrogated the effect observed for the parental compound, both during hypoxia and normoxia, which was independent of CAIX levels (Table 2).

Temozolomide derivatives

The current treatment of glioblastoma is based on radiotherapy combined with temozolomide, which has been shown to increase survival in phase III clinical trials [41]. Temozolomide is a methylating agent that spontaneously hydrolyzes to its active metabolite 3-methyl-(triazene-1-yl)imidazole-4-carboxamide (MTIC) at physiological pH [42]. The acidic extracellular pH in tumors might therefore reduce spontaneous temozolomide conversion and thereby decrease its efficacy. Inhibiting CAIX function is known to decrease extracellular acidification *in vitro* [24, 25, 28, 43], and we

hypothesized that conjugating temozolomide with a sulfonamide or sulfamate moiety (**15a**, **15b**, **15c**, and **15d**) will specifically target hypoxic tumors and increase temozolomide conversion and thereby its efficacy. Nevertheless, while temozolomide resulted in lower cell viability in CAIX⁻ cells, consistent with the pH-dependent mechanism of activation, the CAIXⁱ conjugated temozolomide derivatives **15a**, **15c**, and **15d** were ineffective in reducing cell viability in both MDCK cell lines during normoxic and hypoxic conditions within the concentration range tested in the present study (Table 2, Supplementary Fig. S3). In contrast, **15b** was similarly effective as the parental temozolomide compound (Table 2).

This dual-target compound was therefore investigated further in clonogenic survival assays in which the medium of the cells was acidified because of CAIX function during hypoxic conditions (Supplementary Fig. S1) [44]. Temozolomide was again more effective in reducing clonogenic cell survival in the CAIX⁻ MDCK cells as compared with the CAIX⁺ MDCK cells (Fig. 1), similarly to its efficacy on cell viability. During hypoxia however temozolomide caused no difference in clonogenic survival as compared to normoxia, even though hypoxia is required to activate CAIX and cause extracellular acidification [43, 45] and is therefore hypothesized to reduce temozolomide conversion and efficacy. In contrast, the CAIXⁱ conjugated derivative **15b** significantly reduced clonogenic cell survival in hypoxic versus normoxic conditions in the CAIX⁺ cells (surviving fraction is 46.1 ± 3.1 versus $26.1\% \pm 7.9$ during normoxia and hypoxia respectively, $p < 0.05$). Nevertheless, the effect of **15b** on survival was not significantly different from the parental temozolomide compound. In addition, the low binding affinity of the compound (Table 1) combined with its relatively low efficacy in the CAIX⁺ as compared to the CAIX⁻ cells minimizes its potential for further development. These results furthermore suggest that temozolomide efficacy is not affected by CAIX dependent changes in extracellular pH during hypoxia. A reduction of temozolomide conversion and efficacy might require lower pH levels, *i.e.* $\text{pH} < 6.6$, which may have not been achieved in the present experiments [8, 9, 39].

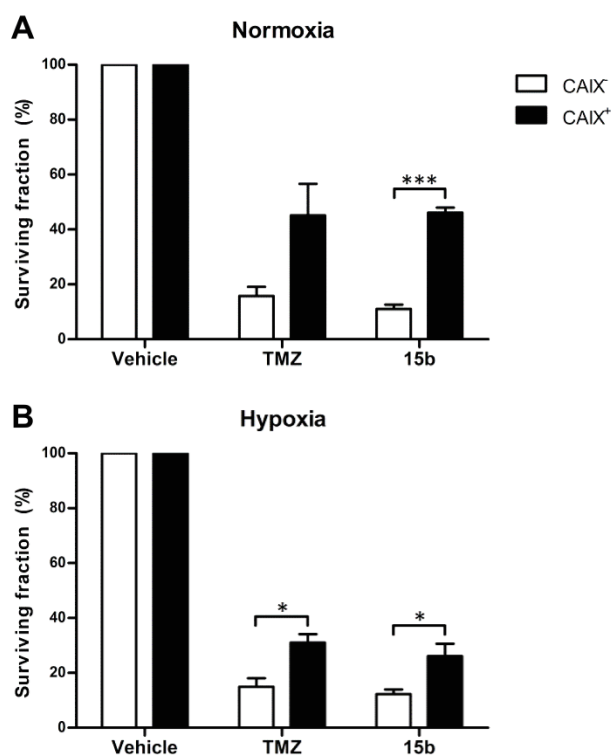


Figure 1. Clonogenic cell survival of confluent MDCK CAIX⁻ and CAIX⁺ cells during normoxia (21% O₂) and hypoxia (0.02% O₂) when exposed to temozolomide (TMZ) and the CAIXi conjugated derivative **15b**. Surviving fraction (%) was normalized to vehicle control. Average \pm SEM of three independent biological repeats is shown. Asterisks indicate statistical significance (* p <0.05; *** p <0.001).

ATR inhibitor derivatives

Preclinical experiments have shown that Ataxia Telangiectasia and Rad3-related protein inhibitors (ATRi) reduce the DNA repair capacity resulting in enhanced cell death and decreased tumor growth when combined with either chemo- or radiotherapy [46-48]. However, ATRi are not highly tumor specific, thus targeting these compounds towards the CAIX expressing areas of a tumor might increase their therapeutic benefit. The effect on cell viability of the parental ATRi (VE-821 and VE-822) and their CAIXi conjugated derivatives (**12** and **13**) was tested in combination with radiotherapy to induce DNA damage where a higher radiation dose was applied to anoxic cells, since those are more radioresistant [49, 50]. The parental ATRi and the CAIXi conjugated derivatives in combination with radiation decreased cell viability as compared to radiation only in the CAIX⁺ cells (p <0.05) under both normoxic and anoxic conditions, but not in the CAIX⁻ cells (Fig. 2). The only

exception is the derivative **13**, which had no significant effect on cell viability during anoxic conditions in both cell lines as compared to radiation alone ($p=0.09$ and $p=0.08$ for CAIX⁻ and CAIX⁺ cells, respectively). More importantly, the CAIXi conjugated derivative **12** was more effective than its respective parental ATRi (VE-821) in the CAIX⁺ ($p<0.01$ during normoxia and anoxia), but not the CAIX⁻ cells ($p=0.52$ and $p=0.72$ for normoxia and anoxia, respectively), suggesting a CAIX specific effect. In contrast, the CAIXi conjugated derivative **13** in combination with radiation was less effective in reducing cell viability than the parental compound VE-822 in CAIX⁺ cells ($p<0.001$ and $p<0.01$ during normoxic and anoxic conditions, respectively). Although radiation induced similar effects on cell viability during normoxic and anoxic conditions, the efficacy of derivative **12** did not increase further during anoxic conditions as compared to normoxic conditions, even though CAIX expression is upregulated under hypoxic conditions (Supplementary Fig. S1) and these conditions are essential for CAIXi binding [43, 45]. Although derivative **12** indeed proved to be more effective in CAIX⁺ than in CAIX⁻ cells in combination with radiation, its efficacy might however not be solely dependent on binding to CAIX, which is consistent with unfavorable K_i values of the compound (Table 1). Exposing both cell lines to ATRi without irradiation decreased cell viability of both cell lines during normoxic and anoxic conditions, although this effect appeared to be slightly more pronounced in the CAIX⁻ cells (Supplementary Fig. S5). Differences in ATRi response between the cell lines when combined with radiation might be explained by a lower number of cells in the resistant S-phase of the cell cycle [51], or by a decreased DNA repair capacity in cells with lower intracellular pH [52-54], *i.e.* those that do not express CAIX. This may also explain the difference in sensitivity to cytotoxic drugs between both cell lines, although further investigations are required to prove this causal relationship.

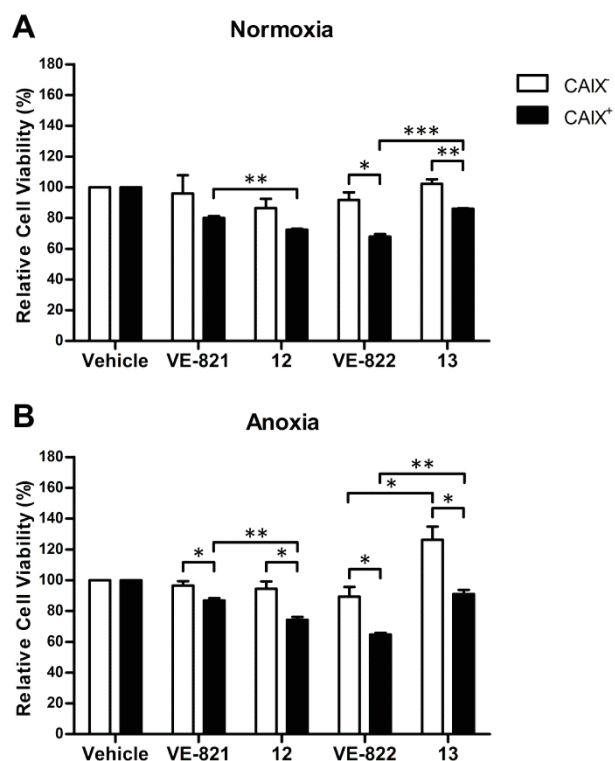


Figure 2. Relative cell viability (%) in MDCK CAIX⁻ and CAIX⁺ cells exposed to ATR inhibitors (VE-821 and VE-822) or the CAIXi conjugated derivatives (**12** and **13**) in combination with radiation during normoxia (21% O₂) and anoxia (<0.02% O₂). Normoxic cells were irradiated with 2 Gy and anoxic cells with 4 Gy to induce similar effects on cell viability. Cells were exposed to 500 nM VE-821 and **12**, and to 50 nM VE-822 and **13**. Average ± SEM of three independent biological repeats is shown. Asterisks indicate statistical significance (*p<0.05; **p<0.01; ***p<0.001).

Phenformin derivatives

Phenformin (1-(diaminomethylidene)-2-(2-phenylethyl) guanidine) is a drug used to treat diabetes, but was withdrawn from the North-American market in the 1970s by the Food and Drug Administration (FDA) due to a high risk of developing lactic acidosis [55]. Treating patients with a similar but less potent drug metformin was found to be associated with a decrease in cancer incidence and an increased life span of cancer patients [56]. The repurposing of these compounds as anti-cancer agents is therefore being investigated where phenformin is found to be more lipophilic, thereby requiring less active transport than metformin [57]. The proposed mechanism of

action of phenformin is its ability to inhibit mitochondrial respiration, which will consequently result in a decreased ATP production, thereby reducing tumor cell growth and improving tumor oxygenation as a result of decreased oxygen consumption [58, 59]. Conjugating phenformin with CAIXi might make the drug more tumor-specific leading to reduced normal tissue toxicity. Since tumor cells are more sensitive to phenformin treatment due to their altered energy metabolism, human colorectal HCT116 cells, with or without CAIX knockdown [24, 28] were used to study the effect of phenformin and its CAIXi conjugated derivative **18** on mitochondrial respiration. Western blotting confirms low expression of CAIX in CAIX KD cells under hypoxic conditions as compared with control cells (Supplementary Fig. S1B). As expected, CAIX levels were low in both cell lines under normoxic conditions. Phenformin significantly reduced Oxygen Consumption Rate (OCR) in both cell lines ($p < 0.05$), independent of CAIX expression levels (Fig. 3). In contrast, the CAIXi conjugated derivative **18** was ineffective in reducing OCR, even when a fourfold higher concentration was used.

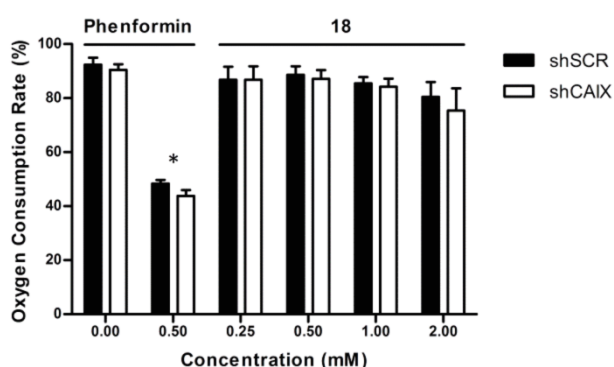


Figure 3. Oxygen consumption rate (OCR) of HCT116 cells with CAIX (shSCR) or without CAIX expression (shCAIX) exposed to phenformin or the CAIXi conjugated derivative **18**. OCR was normalized to baseline OCR levels before compound injection. Average \pm SEM of four independent biological repeats is shown. Asterisks indicate statistical significance ($*p < 0.05$).

Conclusion

Overall our hypothesis that newly designed dual-target drugs are more selective for CAIX expressing cells and are able to modulate their own efficacy by inhibiting CAIX function was not confirmed. Of all derivatives included, only one (*i.e.* the ATRi derivative **12**) proved more effective than its parental compound when combined with irradiation in CAIX⁺ cells versus CAIX⁻ cells. Nevertheless, the effect of this compound may not only be related to binding of the compound to CAIX due to limited binding affinity and the lack of further increase in its efficacy under hypoxic conditions. The rest of the derivatives included in this study did not show an increased efficacy in CAIX⁺ versus CAIX⁻ cells, or an efficacy that depended on oxygen levels, *i.e.* hypoxia versus normoxia. Nevertheless, since the parental compounds proved effective in these experiments the conjugation of the CAIXi moiety with the cytotoxic compounds may have caused conformational changes, thereby altering the compounds efficacy. In addition, these conformational changes may have also limited the binding of the CAIXi moiety (sulfonamide, sulfamide or aminoxysulfonamide) into the Zn²⁺ containing active pocket of CAIX, which explains the lack of CAIX specificity and binding affinity for human CAs (Table 1) of the compounds. Alternative strategies to target the CAIX expressing cells in a tumor, e.g. antibody targeting or an increased number of CAIXi conjugated molecules [60], might therefore be more promising options to pursue in the future.

Experimental section

Chemistry

General

Unless otherwise specified, reagents and solvents were of commercial quality and were used without further purification. All reactions were carried out under an inert atmosphere of nitrogen. TLC analyses were performed on silica gel 60 F₂₅₄ plates (Merck Art.1.05554). Spots were visualized under 254 nm UV illumination, or by ninhydrin solution spraying. Melting points (mp) were determined on a Büchi Melting Point 510 and are uncorrected. ¹H and ¹³C NMR spectra were recorded on Bruker DRX-400 spectrometer using DMSO-_d₆ as a solvent and tetramethylsilane as an internal standard. For ¹H NMR spectra, chemical shifts are expressed in δ (ppm) downfield from tetramethylsilane, and coupling constants (*J*) are expressed in Hertz.

Electron Ionization mass spectra were recorded in positive or negative mode on a Waters MicroMass ZQ. All compounds that were tested in the biological assays were analyzed by High-resolution ESI mass spectra (HRMS) using on a Q-ToF I mass spectrometer fitted with an electrospray ion source in order to confirm the purity of >95%.

4-(4-(Bis(2-chloroethyl)amino)phenyl)butanoyl chloride (1):

Oxalyl chloride (32.8 mmol, 2.0 equiv.) was added slowly over a period of 1.0 h at 5–10 °C to a stirred solution of chlorambucil (16.4 mmol, 1.0 equiv.) in DCM (25.0 mL, 5.0 vol) and a catalytic amount of N, N-dimethylformamide. The reaction mixture was stirred at ambient temperature for 2–3 h, after which excess oxalyl chloride and DCM were removed under reduced pressure. The chlorambucil acid chloride that was obtained was a pale green solid in quantitative yield, which was used as such for the synthesis of Compounds **2a–c**.

4-(4-(Bis(2-chloroethyl)amino)phenyl)butan-1-ol (3):

Compound **1** (15.5 mmol, 1.0 equiv.) was dissolved in DCM (125 mL) and methanol (75 mL, 3 vol) was slowly added over a period of 1 h at 15–20 °C. The reaction mixture was stirred at ambient temperature for 2 h. The reaction mixture was concentrated and the residue was dissolved in ethyl acetate (125 mL, 5 vol) and washed successively with a 5% aq. NaHCO₃. Evaporation of the solvent under reduced pressure resulted in the chlorambucil methyl ester (16.4 mmol, 1.0 equiv.) in 95% yield as a light brown oil, which was added to a suspension of lithium aluminium hydride (32.8 mmol, 2 equiv.) in anhydrous THF (100 mL, 4 vol) at 0–5 °C for a period of 1 h. The reaction mixture was thereafter allowed to stir at ambient temperature for 2–3 h. Next, the reaction mixture was cooled to 0–5 °C and quenched slowly with ethyl acetate (250 mL, 10 vol) followed by water (100 mL, 4 vol). The reaction mixture was filtered through celite and ethyl acetate (50 mL, 2 vol) was used to wash the celite bed. The organic layer was washed with water (100 mL, 4 vol), dried over anhydrous Na₂SO₄, and filtered. Evaporation of the solvent under reduced pressure resulted in 99% yield of the crude alcohol as a pale yellow oil, which was used in the next step.

4-(4-(Bis(2-chloroethyl)amino)phenyl)butyl carbonochloridate (4):

DMF (1.4 g) and sodium carbonate (75.79 mmol, 1.1 equiv.) were added to a solution of triphosgene (37.89 mmol, 0.55 equiv.) in toluene (300 mL, 15 vol) at ambient temperature. The reaction mixture was cooled to 0–5 °C and maintained at the same temperature for 30 min. Next, a solution of **3** (68.9 mmol, 1.0 equiv.) in toluene (100 mL, 5 vol) was added to the stirred reaction mixture at 0–5 °C during 30 min. This reaction mixture was stirred for 4–5 h at room temperature. The reaction mixture was filtered thereafter and the solid was washed with toluene (100 mL, 5 vol). Evaporation of the solvent under reduced pressure resulted in the chloroformate **4** with a 64% yield as a yellow viscous liquid, which was used for the synthesis of carbamates (compounds **5a–c**).

General procedure for the preparation of compounds (2a–c and 5a–c):

To a solution of aminoalkylbenzene sulfonamide (1.0 equiv.) in acetonitrile (225 mL, 15 vol) and N,N-diisopropylethylamine (2.5 equiv.) a solution of compound **1** (**2a–c**) or compound **4** (**5a–c**) (1.0 equiv.) in acetonitrile (75 mL, 5 vol) was added over a period of 1 h and stirred overnight at ambient temperature. After completion, the reaction mixture was concentrated and the residue obtained was dissolved in ethyl acetate (150 mL, 10 vol). The organic layer was successively washed with 2 N HCl solution (100 mL × 2) in water, dried over anhydrous Na₂SO₄, and filtered. After evaporation of the solvent under reduced pressure a pale yellow solid was obtained as a crude product. This crude product was purified with column chromatography using a silica gel (40% ethyl acetate in hexane) to obtain compound **2a–c** and **5a–c** in a 51–87% yield.

General procedure for amination of 3-Chlorobenzotriazine-1,4-di-N-oxides (7 and 10):

4-(2-Aminoethyl) benzene sulfonamide (8.25 mmol, 3.0 equiv.) was added to a stirring solution of 3 chlorobenzotriazine-1,4-di-N-oxide (2.75 mmol, 1.0 equiv.) in dimethoxyethane (30 mL) and the mixture was stirred overnight at reflux temperature. The next day mixture was cooled to room temperature and concentrated under vacuum, after which the residue was dissolved in ammonium hydroxide solution and extracted with ethyl acetate. The organic layer was dried over Na₂SO₄, filtered and concentrated under vacuum. The residue was purified by chromatography using a

silica gel with methylene chloride-methanol 98:2 v-v as an eluent to obtain the expected compound as a yellow powder with an 85–94% yield.

General procedure for oxidation (8 and 11):

Hydrogen peroxide (12.9 mmol, 10 equiv.) was added dropwise to a stirred solution of trifluoroacetic anhydride (12.9 mmol, 10 equiv.) in DCM at 0 °C. This reaction mixture was stirred at 0 °C for 5 min, warmed to room temperature for 10 min, and cooled to 5 °C. Next, the mixture was added to a stirred solution of mono oxide (1.29 mmol, 1.0 equiv.) in DCM at 0 °C and stirred at room temperature for 2–3 days. The reaction mixture was carefully diluted with water and basified with aqueous NH₄OH and extracted with CHCl₃. The organic fraction was dried over anhydrous Na₂SO₄, filtered and evaporated to obtain the residue. This residue was purified by chromatography using a silica gel with methylene chloride-methanol 98:2 v-v as an eluent to obtain the expected compound as an orange red powder with a 46–96% yield.

General procedure for synthesis of ATRi derivatives (12 and 13):

A solution of VE-821 or VE-822 (0.54 mmol, 1.0 equiv.) and triethylamine (1.62 mmol, 3.0 equiv.) in 10 mL of methylene chloride was added to a mixture of chlorosulfonyl isocyanate (0.68 mmol, 1.2 equiv.) and tert-butanol (0.648 mmol, 1.2 equiv.) in 2 mL of methylene chloride. The mixture was stirred at room temperature for 1.0 h, diluted with ethyl acetate, and washed with water. The organic layer was then dried over anhydrous Na₂SO₄, filtered and concentrated under vacuum. The residue was purified by chromatography with a silica gel and methylene chloride-methanol 98:2 as an eluent. This intermediate was thereafter diluted in a solution of trifluoro acetic acid in methylene chloride (20% vol.) and stirred at room temperature for 6 h. Next, the mixture was concentrated under vacuum and co-evaporated with diethyl ether multiple times to obtain the expected compound with a 58–65% yield.

General procedure for synthesis of temozolomide derivatives:

To a slurry of 3-methyl-4-oxo-3,4-dihydroimidazo[5,1-d][1,2,3,5] tetrazine-8-carboxylic acid (1.0 mmol, 1.0 equiv.) in DCM, BOP (1.0 mmol, 1.0 equiv.), amine (1.1 mmol, 1.1 equiv.) and triethylamine (2.5 mmol, 2.5 equiv.) were added. This reaction mixture was stirred overnight at room temperature and filtered to obtain the expected compounds with a 41–95% yield.

4-(4-(Bis(2-chloroethyl)amino)phenyl)-N-(4-sulfamoylphenyl)butanamide (2a):

mp: 155–157 °C; ¹H NMR (400 MHz, DMSO-d₆), δ 10.22 (s, 1H), 7.73 (d, *J* = 4.4, 4H), 7.23 (s, 2H), 7.05 (d, *J* = 8.7, 2H), 6.67 (d, *J* = 8.7, 2H), 3.70 (d, *J* = 8.6, 8H), 2.54–2.50 (m, 2H), 2.34 (t, *J* = 8.6, 2H), 1.90–1.78 (m, 2H); ¹³C NMR (101 MHz, DMSO-d₆), δ 171.68, 144.46, 142.23, 138.03, 129.53, 126.65, 118.51, 111.90, 52.22, 41.17, 35.84, 33.54, 26.87; MS (ESI⁺) *m/z* 458.11 [M+H]⁺, 460.10 [M+2]⁺. HRMS (ESI⁺) [M+H]⁺ calculated for [C₂₀H₂₆N₃O₃SCl₂]⁺: 458.1072, found: 458.1075.

4-(4-(bis(2-chloroethyl)amino)phenyl)-N-(4-sulfamoylbenzyl)butanamide (2b):

mp: 130–132 °C; ¹H NMR (400 MHz, DMSO-d₆), δ 8.41 (t, *J* = 5.9, 1H), 7.76 (d, *J* = 8.3, 2H), 7.41 (d, *J* = 8.3, 2H), 7.31 (s, 2H), 7.02 (d, *J* = 8.6, 2H), 6.66 (d, *J* = 8.6, 2H), 4.31 (d, *J* = 5.9, 2H), 3.69 (s, 8H), 2.45 (t, *J* = 7.5, 2H), 2.15 (t, *J* = 7.5, 2H), 1.82–0.72 (m, 2H); ¹³C NMR (101 MHz, DMSO-d₆), δ 172.15, 144.42, 143.92, 142.54, 129.86, 129.33, 127.46, 125.68, 111.89, 52.22, 41.67, 41.17, 34.84, 33.66, 27.39; MS (ESI⁺) *m/z* 472.12 [M+H]⁺, 474.12 [M+2]⁺. HRMS (ESI⁺) [M+H]⁺ calculated for [C₂₁H₂₈N₃O₃SCl₂]⁺: 472.1228, found: 472.1236.

4-(4-(Bis(2-chloroethyl)amino)phenyl)-N-(4-sulfamoylphenethyl)butanamide (2c):

mp: 108–110 °C; ¹H NMR (400 MHz, DMSO-d₆), δ 7.89 (t, *J* = 5.6, 1H), 7.74 (d, *J* = 8.3, 2H), 7.38 (d, *J* = 8.3, 2H), 7.30 (s, 2H), 7.00 (d, *J* = 8.6, 2H), 6.66 (d, *J* = 8.6, 2H), 3.70 (d, *J* = 8.9, 8H), 3.29 (dd, *J* = 13.0, 5.6, 2H), 2.78 (t, *J* = 7.5, 2H), 2.41 (t, *J* = 7.5, 2H), 2.08–1.98 (m, 2H), 1.76–1.65 (m, 2H); ¹³C NMR (101 MHz, DMSO-d₆), δ 171.95, 144.39, 143.80, 142.01, 129.89, 129.21, 125.67, 111.87, 52.23, 41.17, 34.87, 33.61, 27.32; MS (ESI⁺) *m/z* 486.14 [M+H]⁺, 488.14 [M+2]⁺. HRMS (ESI⁺) [M+H]⁺ calculated for [C₂₂H₃₀N₃O₃SCl₂]⁺: 486.1385, found 486.1387.

4-(4-(Bis(2-chloroethyl)amino)phenyl)butyl (4-sulfamoylphenyl)carbamate(5a):

mp: 156–158 °C; ¹H NMR (400 MHz, DMSO-d₆), δ 10.01 (s, 1H), 7.76–7.69 (m, 2H), 7.64–7.56 (m, 2H), 7.22 (s, 2H), 7.04 (d, *J* = 8.7, 2H), 6.66 (d, *J* = 8.7, 2H), 4.12 (t, *J* = 6.0, 2H), 3.77–3.63 (m, 8H), 1.70–1.54 (m, 4H); ¹³C NMR (101 MHz, DMSO-d₆), δ 153.50, 144.40, 142.34, 137.48, 130.06, 129.30, 126.77, 117.50, 111.89, 64.43, 52.22, 41.17, 33.68, 28.09, 27.62; MS (ESI⁺) *m/z* 488.12 [M+H]⁺, 490.12 [M+2]⁺. HRMS (ESI⁺) [M+H]⁺ calculated for [C₂₁H₂₈N₃O₄SCl₂]⁺: 488.1178, found: 488.1184.

4-(4-(Bis(2-chloroethyl)amino)phenyl)butyl (4-sulfamoylbenzyl)carbamate(5b):

mp: 98–100 °C; ¹H NMR (400 MHz, DMSO-d₆), δ 7.76 (t, *J* = 8.5, 3H), 7.41 (d, *J* = 8.5, 2H), 7.31 (s, 2H), 7.02 (d, *J* = 8.6, 2H), 6.66 (d, *J* = 8.6, 2H), 4.23 (d, *J* = 6.1, 2H), 3.98 (s, 2H), 3.75–3.63 (m, 8H), 2.47 (s, 2H), 1.55 (m, 4H); ¹³C NMR (101 MHz, DMSO-d₆), δ 156.63, 144.37, 143.97, 142.61, 130.13, 129.26, 127.27, 125.70, 111.88, 63.84, 52.23, 43.37, 41.18, 33.68, 28.31, 27.64; MS (ESI⁺) *m/z* 502.13 [M+H]⁺, 504.13 [M+2]⁺. HRMS (ESI⁺) [M+H]⁺ calculated for [C₂₂H₃₀N₃O₄SCl₂]⁺: 502.1334, found: 502.1338.

4-(4-(Bis(2-chloroethyl)amino)phenyl)butyl (4-sulfamoylphenethyl)carbamate(5c):

mp: 100–102 °C; ¹H NMR (400 MHz, DMSO-d₆), δ 7.77–7.70 (m, 2H), 7.37 (d, *J* = 8.2, 2H), 7.30 (s, 2H), 7.19 (t, *J* = 5.5, 1H), 7.02 (d, *J* = 8.6, 2H), 6.66 (d, *J* = 8.6, 2H), 3.94 (d, *J* = 5.5, 2H), 3.69 (s, 8H), 3.21 (dd, *J* = 13.3, 6.6, 2H), 2.76 (dd, *J* = 16.9, 9.8, 2H), 2.46 (s, 2H), 1.52 (s, 4H); ¹³C NMR (101 MHz, DMSO-d₆), δ 156.30, 144.37, 143.58, 142.03, 130.15, 129.19, 125.67, 111.88, 63.51, 52.23, 41.28, 35.09, 33.67, 28.32, 27.63; MS (ESI⁺) *m/z* 516.15 [M+H]⁺, 518.15 [M+2]⁺. HRMS (ESI⁺) [M+H]⁺ calculated for [C₂₃H₃₂N₃O₄SCl₂]⁺: 516.1491, found: 516.1490.

3-(4-Sulfamoylphenethylamino) benzo [e][1,2,4] triazine 1-oxide (7):

Compound **7** was synthesized from **6** by a general amination method and resulted in a yellow solid with a yield of 94%. mp: 250–252 °C; ¹H NMR (400 MHz, DMSO-d₆), δ 8.15 (s, 1H), 8.13 (s, 1H), 8.03 (s, 1H), 7.82–7.71 (m, 3H), 7.60 (d, *J* = 8.0, 1H), 7.47 (d, *J* = 8.0, 2H), 7.38–7.30 (m, 1H), 7.28 (s, 2H), 3.60 (d, *J* = 6.2, 2H), 3.01 (dd, *J* = 6.2, 2H); ¹³C NMR (101 MHz, DMSO-d₆) δ 158.80, 143.70, 142.07, 135.76, 129.25, 125.92, 124.66, 119.93, 41.92, 34.09; MS (ESI⁺) *m/z* 346.10 [M+H]⁺. HRMS (ESI⁺) [M+H]⁺ calculated for [C₁₅H₁₆N₅O₃S]⁺: 346.0974, found: 346.0973.

3-((4-Sulfamoylphenethyl)amino)benzo[e][1,2,4]triazine 1,4-dioxide (8):

Compound **8** was synthesized from **7** by a general oxidation method, resulting in an orange red solid with a yield of 96%. mp: 210–212 °C; ¹H NMR (400 MHz, DMSO-d₆), δ 8.31 (t, *J* = 6.1, 1H), 8.22 (d, *J* = 8.1, 1H), 8.13 (d, *J* = 8.1, 1H), 7.97–7.89 (m, 1H), 7.75 (d, *J* = 8.3, 2H), 7.61–7.53 (m, 1H), 7.47 (d, *J* = 8.3, 2H), 7.29 (s, 2H), 3.67 (dd, *J* = 7.2, 6.1, 2H), 3.03 (t, *J* = 7.2, 2H); ¹³C NMR (101 MHz, DMSO-d₆), δ 149.67, 143.19, 142.16, 138.19, 135.48, 130.07, 129.26, 127.04, 125.71, 121.13,

116.89, 41.76, 34.18; MS (ESI⁺) m/z 362.09 [M+H]⁺. HRMS (ESI⁺) [M+H]⁺ calculated for [C₁₅H₁₆N₅O₄S]⁺: 362.0923, found: 362.0928.

3-(4-Sulfamoylphenethylamino)-7,8-dihydro-6H-indeno [5,6-e][1,2,4] triazine 1-oxide (10):

Compound **10** was synthesized from **9** by using a general amination method, which resulted in a yellow solid with a 85% yield. mp: 238–240 °C; ¹H NMR (400 MHz, DMSO-d₆), δ 7.95 (s, 1H), 7.82 (s, 1H), 7.74 (t, *J* = 10.0, 2H), 7.49–7.39 (m, 3H), 7.28 (s, 2H), 3.57 (dd, *J* = 13.0, 6.8, 2H), 3.02–2.90 (m, 6H), 2.11–1.99 (m, 2H); ¹³C NMR (101 MHz, DMSO-d₆), δ 157.56, 153.64, 142.79, 141.97, 130.10–127.99, 125.35, 112.78, 41.77, 32.35, 31.60, 25.25; MS (ESI⁺) m/z 386.13 [M+H]⁺. HRMS (ESI⁺) [M+H]⁺ calculated for [C₁₈H₂₀N₅O₃S]⁺: 386.1287, found: 386.1291.

3-((4-Sulfamoylphenethyl) amino)-7,8-dihydro-6H-indeno [5,6-e][1,2,4] triazine 1,4-dioxide (11):

Compound **11** was synthesized from **10** by using a general oxidation method resulting in an orange red solid with a yield of 46%. mp: 218–220 °C; ¹H NMR (400 MHz, DMSO-d₆), δ 8.19 (s, 1H), 7.98 (d, *J* = 24.2, 2H), 7.75 (d, *J* = 7.8, 2H), 7.46 (d, *J* = 7.7, 2H), 7.29 (s, 2H), 3.65 (d, *J* = 6.2, 2H), 3.12–2.92 (m, 6H), 2.17–1.99 (m, 2H); ¹³C NMR (101 MHz, DMSO-d₆), δ 154.56, 149.25, 145.07, 143.22, 142.15, 129.23, 125.71, 41.76, 32.74, 31.80, 25.24; MS (ESI⁺) m/z 402.12 [M+H]⁺. HRMS (ESI⁺) [M+H]⁺ calculated for [C₁₈H₂₀N₅O₄S]⁺: 402.1236, found: 402.1234.

6-(4-(Methylsulfonyl)phenyl)-N-phenyl-3-(sulfamoylamino)pyrazine-2-carboxamide (12):

Compound **12** was synthesized from commercially purchased VE-821 by using the general procedure described above, which resulted in a yellow solid with an overall yield of 58%. mp: 233–235 °C; ¹H NMR (400 MHz, DMSO-d₆), δ 11.27 (s, 1H), 10.82 (s, 1H), 9.28 (s, 1H), 8.64 (d, *J* = 8.6, 2H), 8.08 (d, *J* = 8.6, 2H), 7.83–7.76 (m, 2H), 7.68 (s, 2H), 7.48–7.39 (m, 2H), 7.23 (dd, *J* = 14.0, 6.6, 1H), 3.30 (s, 3H); ¹³C NMR (101 MHz, DMSO-d₆), δ 164.59–163.27, 149.32–147.73, 144.46–143.38, 141.16, 139.57, 137.17–136.45, 128.69, 127.46, 125.15, 122.08, 43.46; MS (ESI⁺) m/z 448.07 [M+H]⁺. HRMS (ESI⁺) [M+H]⁺ calculated for [C₁₈H₁₈N₅O₂S₂]⁺: 448.0749, found: 448.0748.

5-(4-(Isopropylsulfonyl) phenyl)-3-(3-(4-((methylamino) methyl) phenyl) isoxazol-5-yl) pyrazin-2-carboxamide (13):

Compound **13** was synthesized from commercially purchased VE-822 by using the general procedure described above, which resulted in a yellow solid with an overall yield of 65%. mp: 242–244 °C; ¹H NMR (400 MHz, DMSO-d₆), δ 8.94 (s, 1H), 8.38 (d, *J* = 8.5, 2H), 8.02 (d, *J* = 8.2, 2H), 7.93 (d, *J* = 8.5, 2H), 7.79 (s, 1H), 7.54 (d, *J* = 8.2, 2H), 7.20 (s, 2H), 6.96 (s, 2H), 4.17 (s, 2H), 3.54–3.38 (m, 1H), 2.58 (s, 3H), 1.17 (t, *J* = 14.1, 6H); ¹³C NMR (101 MHz, DMSO-d₆), δ 167.67, 162.00, 151.75, 142.47, 141.04, 139.53, 137.62, 135.78, 129.00, 127.17, 125.69, 124.47, 102.16, 54.22, 53.49, 34.94, 15.19; MS (ESI⁺) *m/z* 543.15 [M+H]⁺. HRMS (ESI⁺) [M+H]⁺ calculated for [C₂₄H₂₇N₆O₅S₂]⁺: 543.1484, found: 543.1484.

3-Methyl-4-oxo-N-(4-sulfamoylphenethyl)-3,4-dihydroimidazo[5,1-d][1,2,3,5]tetrazine-8-carboxamide (15a):

Compound **15a** was synthesized from **14** by reacting it with 4-(2-aminoethyl) benzene sulfonamide using the general procedure for synthesizing temozolomide derivatives described above. This reaction resulted in a white solid with a yield of 50%. mp: 195–197 °C; ¹H NMR (400 MHz, DMSO-d₆), δ 8.83 (s, 1H), 8.58 (t, *J* = 5.9, 1H), 7.74 (d, *J* = 8.3, 2H), 7.44 (d, *J* = 8.3, 2H), 7.30 (s, 2H), 3.86 (s, 3H), 3.58 (dd, *J* = 13.4, 6.8, 2H), 2.96 (t, *J* = 7.1, 2H); ¹³C NMR (101 MHz, DMSO-d₆), δ 159.67, 143.64, 142.05, 139.20, 134.45, 130.30, 129.14, 128.46, 125.73, 36.16, 34.78; MS (ESI⁺) *m/z* 378.10 [M+H]⁺. HRMS (ESI⁺) [M+H]⁺ calculated for [C₁₄H₁₆N₇O₄S]⁺: 378.0984, found: 378.0986.

3-Methyl-4-oxo-N-(sulfamoyloxy)-3,4-dihydroimidazo[5,1-d][1,2,3,5]tetrazine-8-carboxamide (15b):

Compound **15b** was synthesized from **14** by reacting it with aminoxysulfonamide using the general procedure for synthesizing temozolomide derivatives described above. This reaction resulted in a white solid with a yield of 41%. mp: 195–197 °C; ¹H NMR (400 MHz, DMSO-d₆), δ 8.81 (s, 1H), 7.80 (s, 1H), 7.67 (s, 1H), 7.30 (s, 2H), 3.86 (s, 3H); ¹³C NMR (101 MHz, DMSO-d₆) δ 161.51, 139.16, 134.57, 130.51, 128.37, 45.72.

3-Methyl-4-oxo-N-(4-sulfamoylbenzyl)-3,4-dihydroimidazo [5,1-d][1,2,3,5]tetrazine-8-carboxamide (15c):

Compound **15c** was synthesized from **14** by reacting it with 4-(aminomethyl) benzene sulfonamide hydrochloride using the general procedure for synthesizing temozolomide derivatives described above. This reaction resulted in a white solid with a yield of 88%. mp: 185–187 °C; ¹H NMR (400 MHz, DMSO-d₆) δ 9.20 (t, *J* = 6.2, 1H), 8.87 (s, 1H), 7.77 (d, *J* = 8.3, 2H), 7.50 (d, *J* = 8.3, 2H), 7.31 (s, 2H), 4.55 (d, *J* = 6.3, 2H), 3.87 (s, 3H); ¹³C NMR (101 MHz, DMSO-d₆), δ 159.96, 143.85, 142.63, 142.63, 138.96, 134.69, 130.11, 129.28, 128.62, 127.68, 125.77, 41.94, 36.23; MS (ESI⁺) *m/z* 364.08 [M+H]⁺. HRMS (ESI⁺) [M+H]⁺ calculated for [C₁₃H₁₄N₇O₄S]⁺: 364.0828, found: 364.0826.

3-Methyl-4-oxo-N-(5-sulfamoyl-1,3,4-thiadiazol-2-yl)-3,4-dihydroimidazo[5,1-d][1,2,3,5]tetrazine-8-carboxamide (15d):

Compound **15d** was synthesized from **14** by reacting it with 5-amino-1, 3,4-thiadiazole-2-sulfonamide hydrochloride using the general procedure for synthesizing temozolomide derivatives described above. This reaction resulted in a light yellow solid with a yield of 95%. mp: 128–130 °C; ¹H NMR (400 MHz, DMSO-d₆), δ 8.63 (s, 1H), 8.06 (s, 1H), 7.81 (s, 1H), 7.35 (s, 2H), 3.83 (s, 3H); ¹³C NMR (101 MHz, DMSO-d₆), δ 171.73, 170.89, 165.39, 161.04, 157.91, 139.53, 134.24, 127.88; MS (ESI⁺) *m/z* 358.01 [M+H]⁺. HRMS (ESI⁺) [M+H]⁺ calculated for [C₈H₈N₉O₄S₂]⁺: 358.0141, found: 358.0140.

Synthesis of 4-(2-(3-carbamimidoylguanidino)ethyl)benzenesulfonamide hydrochloride salt (18):

4-(2-Aminoethyl)benzenesulfonamide **16** (0.5g, 1.0 equiv.) and cyanoguanidine **17** (0.21g, 1.0 equiv.) were suspended in n-butanol (5.0 mL) and treated with a 6.0 M aqueous hydrochloric acid solution (1.0 equiv., 0.4 mL). The mixture was treated at 100 °C overnight and the solvents were removed under vacuum. The residue was thereafter crystallized from isopropyl alcohol (IPA) to obtain compound **18** as a white solid with a 75% yield. mp: 154–159 °C; ¹H NMR (400 MHz, DMSO-d₆), δ 7.87 (d, 2H, *J* = 8.4, Ar-H), 7.82 (brs, 2H, exchangeable with D₂O), 7.50 (d, 2H, *J* = 8.4, Ar-H), 7.38 (brs, 1H, exchangeable with D₂O), 6.62 (brs, 2H, exchangeable with D₂O),

3.15 (t, 2H, $J = 6.7$), 2.98 (t, 2H, $J = 6.7$); ^{13}C NMR (101 MHz, DMSO- d_6), δ 164.0, 143.7, 142.0, 130.3, 127.0, 119.3, 61.4, 34.1; MS (ESI $^+$) m/z 285.11 $[\text{M}+\text{H}]^+$.

CA inhibition assays

To measure the CA-catalyzed CO_2 hydration activity an Applied Photophysics stopped-flow instrument was used [61]. To maintain ionic strength Na_2SO_4 (20 mM) was used with HEPES (20 mM, pH 7.5) as a buffer and Phenol red (0.2 mM) as an indicator working at the maximum absorbance of 557 nm, which was used to follow the initial rates of the CA-catalyzed CO_2 hydration for a duration of 10–100 s. To determine the kinetic parameters and inhibition constants varying CO_2 concentrations were included (1.7–17 mM). Initial velocity was assayed with at least six traces of the initial 5–10% of the reaction for each compound. Compounds were dissolved in distilled-deionized water (0.01 nM). The combined enzyme solutions and compounds were incubated for 15 min at room temperature to allow for the E-I complex formation prior to measurements. The nonlinear least-squares method of PRISM 3 was used to estimate the inhibition constants and the mean of three independent estimations is reported. The CA isoforms included are recombinant proteins obtained in house.

Biological assays

Cells

All cell lines used were cultured in DMEM supplemented with 10% fetal bovine serum. Canine kidney epithelial MDCK cells overexpressing human CAIX (CAIX $^+$) or a scrambled control vector (CAIX $^-$) have been described before [37, 44]. The HCT116 constitutive CAIX knockdown cell line and its scrambled control have also been described before and were kindly provided by Professor Adrien Harris (Weatherall Institute of Molecular Medicine, University of Oxford, John Radcliffe hospital, Oxford, UK) [24, 28, 62]. Cells were exposed to hypoxic or anoxic conditions in a hypoxic chamber (MACS VA500 microaerophilic workstation, Don Whitley Scientific, UK) with 0.2 or $\leq 0.02\%$ O_2 , respectively, and 5% CO_2 and residual N_2 to upregulate and activate CAIX. Normoxic cells were grown in normal incubators with 21% O_2 , 5% CO_2 at 37 °C.

Cell viability assays

The efficacy of the cytotoxic derivatives was compared to their respective parental compounds in cell viability assays using alamarBlue® (Invitrogen). In short, MDCK cells were seeded in 96-well plates and allowed to attach overnight. The next day plates were exposed to hypoxia and DMEM was replaced with pre-incubated hypoxic DMEM. In contrast, testing the ATRi was performed in anoxic conditions to decrease the radiosensitivity of the cells. In parallel normoxic 96-well plates were incubated in normal incubators with 21% O₂ and 5% CO₂. Compounds were dissolved in DMSO (0.5%, Sigma-Aldrich) and final concentrations were made with pre-incubated hypoxic or normoxic DMEM and added to the wells after 24 h of exposure. To test the ATR inhibitors cells were exposed to the compounds 1 h prior to irradiation and the 96-well plates were irradiated (225 kV Philips X-ray tube) with 2 Gy (normoxia) or 4 Gy (anoxia). Cells were exposed to compounds for a total of 2 h for chlorambucil and tirapazamine, or 72 h for temozolomide and the ATR inhibitors, after which medium was washed off and replaced with fresh medium. For chlorambucil, tirapazamine, and ATR inhibitor derivatives cells were allowed to grow for an additional 72 h under normoxic conditions prior to measurement, whereas cells exposed to temozolomide derivatives remained in hypoxic conditions prior to measurement. Cells were allowed to convert alamarBlue® for 2 h during normoxic conditions, which corresponds with their metabolic function and is a measure for cell viability.

Clonogenic assays

Clonogenic survival of MDCK cells was determined with high cell numbers to allow for CAIX-dependent extracellular acidification [44]. These cells were exposed to temozolomide or 15b for 24 h during normoxic or hypoxic conditions after which cells were trypsinized and reseeded in triplicate with known cell numbers. Cells were allowed to grow for 7 days to form colonies that were quantified after staining and fixation with 0.4% methylene blue in 70% ethanol. Surviving fraction was normalized to vehicle (0.5% DMSO).

Basal respiration measurements

Oxygen Consumption Rates (OCR) were determined using the Seahorse XF96 extracellular Flux analyzer (Agilent Technologies). Cells were seeded in a XF96 cell

plate with normal growth medium at an optimized cell density of 1.5×10^4 cells/well. Plates were placed in a 5% CO₂ incubator at 37 °C in order to let the cells attach. Subsequently cells were incubated for 18 h under hypoxic conditions (0.2% O₂). Culture medium was exchanged with DMEM containing 25 mM d-glucose, 4 mM l-glutamine and 1 mM sodiumpyruvate (GIBCO, Thermo Fisher) 60 min prior to the assay and plates were placed in a CO₂-free incubator at 37 °C. Prior to the first injection, baseline OCR was determined using a mixing period of 5 min and a measurement period of 3 min followed by 3 loops of mixing and measuring for 3 min each. Medium containing vehicle (PBS, Lonza), Phenformin Hydrochloride (Sigma-Aldrich), or the CAIXi conjugated phenformin derivative 18 were injected followed by several mixing and measurements cycles. Subsequently cells were washed with PBS and lysed in a 0.05% SDS (Sigma-Aldrich) solution. Protein quantification for normalization purposes was performed using Pierce™ BCA Protein Assay Kit (Thermo Fisher).

Western blot

To validate CAIX expression in the genetically modified cell lines protein immunoblotting was performed after 24 h of hypoxia exposure (0.2% O₂) as described previously [43]. Primary antibodies used included the anti-CAIX M75 antibody (kindly provided by Professor Silvia Pastorekova, Institute of Virology, Slovak Academy of Science, Slovak Republic), and anti-β-actin (MP Biomedicals, #691001) as a reference protein.

Statistical analyses

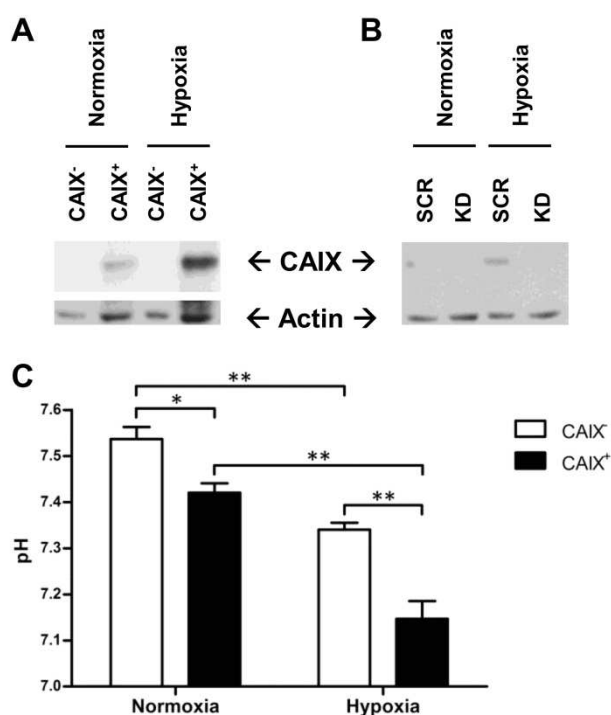
GraphPad Prism (version 5.03) was used for all statistical analyses. For the cytotoxic compounds IC₅₀ values were estimated with the curve of the log (inhibitor) vs. normalized response (Variable slope). Means between groups were compared using unpaired t-tests, where $p < 0.05$ indicated statistical significance.

Acknowledgements

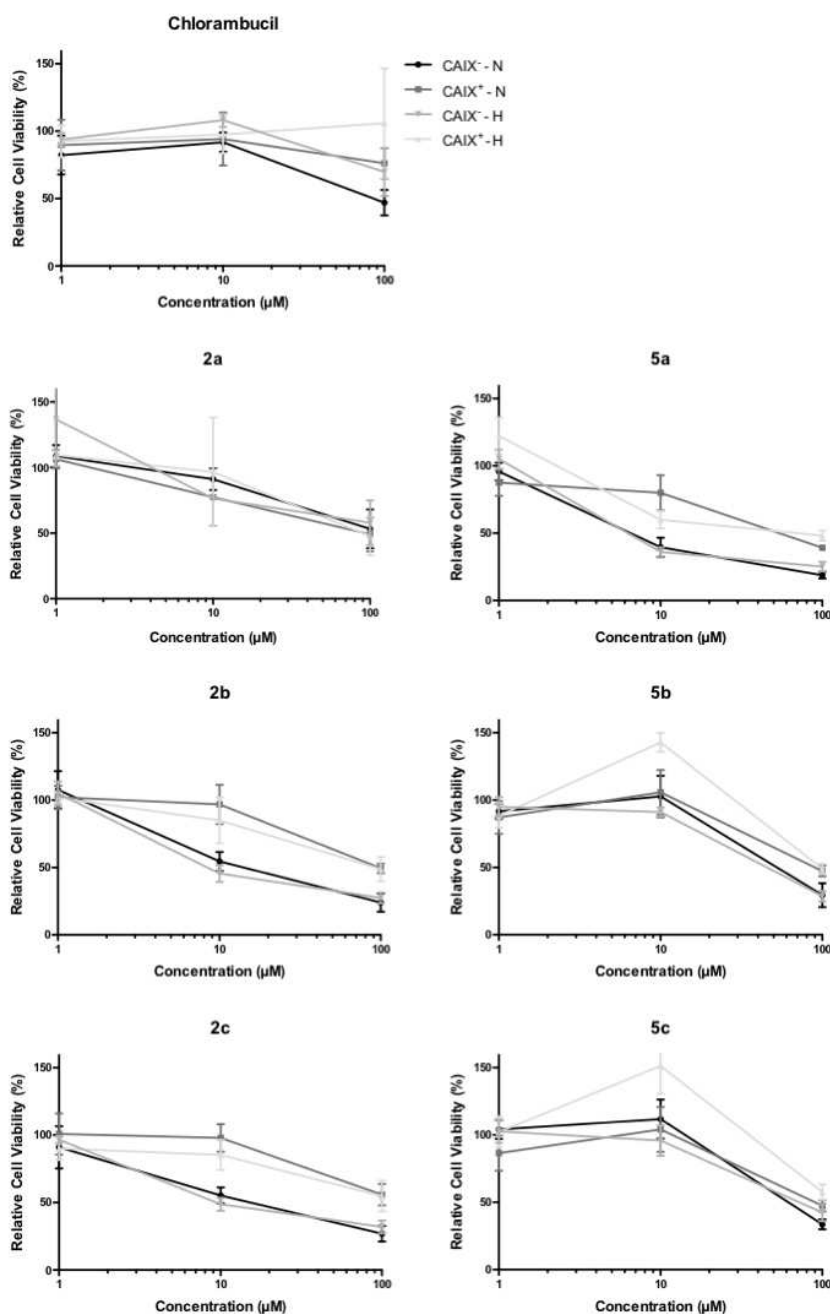
Authors acknowledge the aid of Advinus Therapeutics Ltd. for synthesis of compounds 1, 2a, 2b, 2c, 3, 4, 5a, 5b and 5c. This work was supported by METOXIA (Metastatic Tumors Facilitated by Hypoxic Micro-Environment; EU 7th Research Framework Programme - Theme HEALTH; Grant no.: 222741) NGI Pre-Seed grant (n° 93612005), Kankeronderzoekfonds Limburg from the Health Foundation Limburg

and the Dutch Cancer Society (KWF UM 2011–5020, KWF UM 2009–4454, KWF MAC 2013–6425, KWF MAC 2013–6089, KWF 2015–7635).

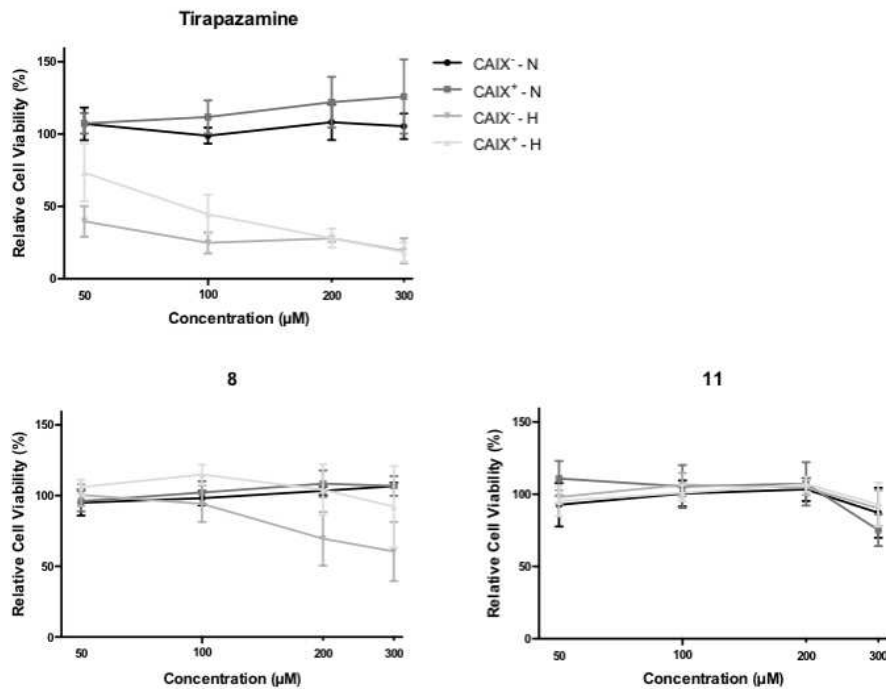
Supplementary data



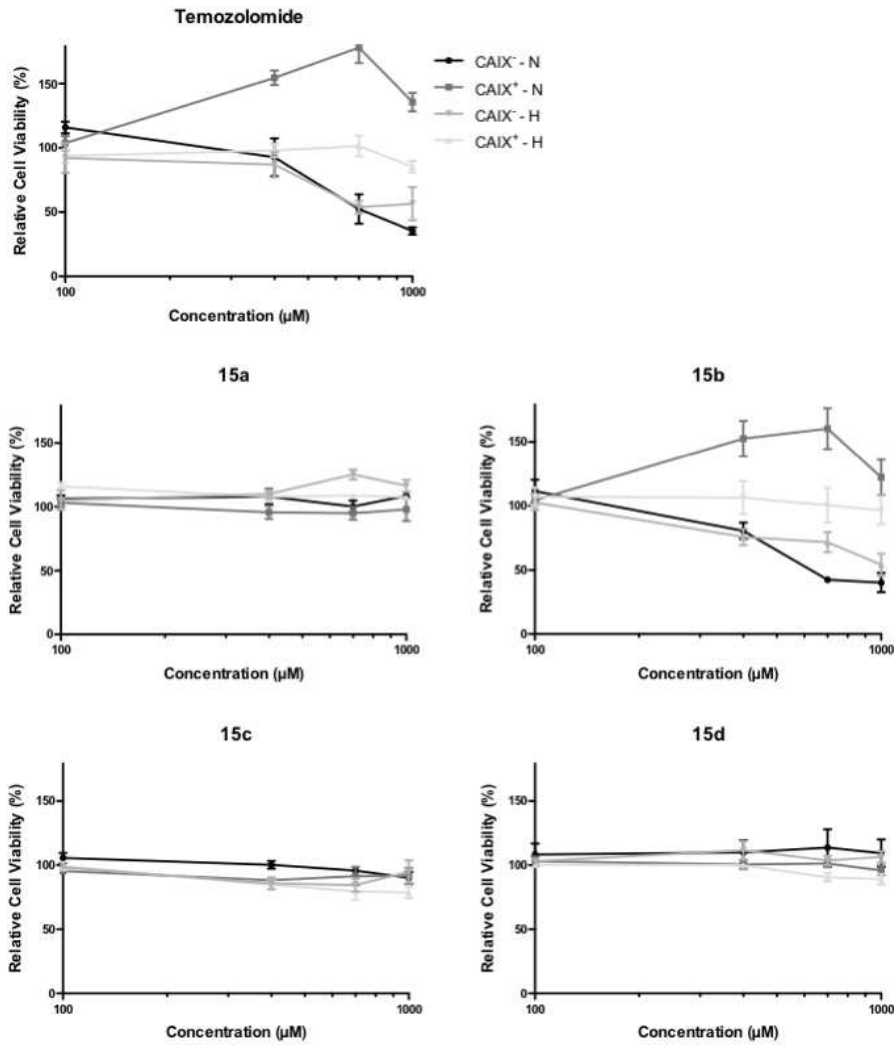
Supplementary Figure S1. CAIX protein expression during normoxia and hypoxia of the MDCK (A) and HCT116 (B) cells and pH measurements of MDCK cells (C). Expression of β -actin was included as a reference protein. CAIX⁺ MDCK cells are overexpressing CAIX, and CAIX⁻ cells are control cells lacking both human and canine CAIX expression. HCT116 scrambled control vector cells (SCR) show hypoxia-dependent CAIX expression, whereas CAIX knockdown (KD) cells do not. During normoxic conditions HCT116 SCR cells have no detectable levels of CAIX, since the dot (B) is an artefact on film. The pH of the culture medium was measured of the MDCK cells after 24 hours of normoxic or hypoxic exposure (C). Mean \pm SEM of three independent biological repeats are shown. Asterisks indicate statistical significance (* $p < 0.05$; ** $p < 0.01$).



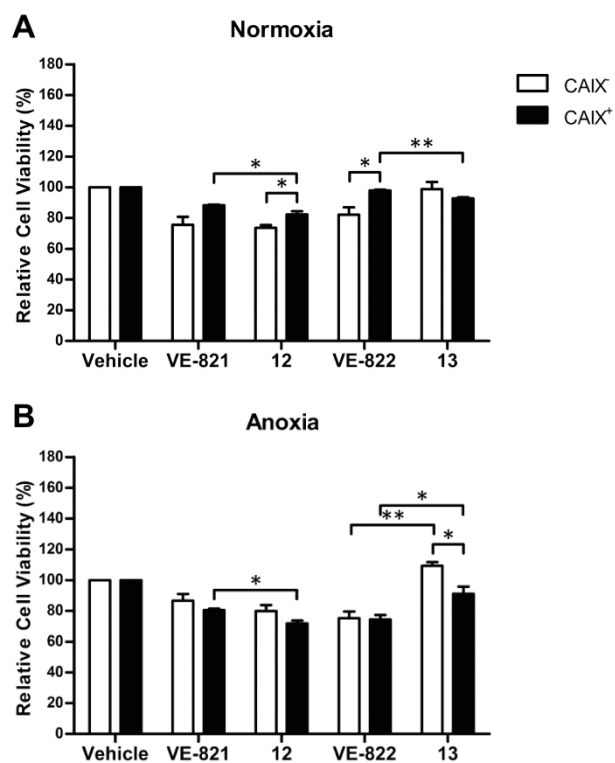
Supplementary Figure S2. Relative cell viability of CAIX⁺ and CAIX⁻ MDCK cells exposed to increasing concentrations of chlorambucil or the CAIXi conjugated derivatives during normoxic (N) and hypoxic (H) conditions. Relative cell viability was normalized to vehicle control (0.5% DMSO). Average \pm SEM of three independent biological repeats is shown.



Supplementary Figure S3. Relative cell viability of CAIX⁺ and CAIX⁻ MDCK cells exposed to increasing concentrations of tirapazamine or the CAIXi conjugated derivatives during normoxic (N) and hypoxic (H) conditions. Relative cell viability was normalized to vehicle control (0.5% DMSO). Average \pm SEM of three independent biological repeats is shown.



Supplementary Figure S4. Relative cell viability of CAIX⁺ and CAIX⁻ MDCK cells exposed to increasing concentrations of temozolomide or the CAIXi conjugated derivatives during normoxic (N) and hypoxic (H) conditions. Relative cell viability was normalized to vehicle control (0.5% DMSO). Average \pm SEM of three independent biological repeats is shown.



Supplementary Figure S5. Relative cell viability (%) in MDCK CAIX⁻ and CAIX⁺ cells exposed to ATR inhibitors (VE-821 and VE-822) or the CAIXi conjugated derivatives (**12** and **13**) without radiation during normoxia (21% O₂) and anoxia (<0.02% O₂). Cells were exposed to 500 nM VE-821 and **12**, and to 50 nM VE-822 and **13**. Average ± SEM of three independent biological repeats is shown. Asterisks indicate statistical significance (*p < 0.05; **p < 0.01; ***p < 0.001).

References

1. Nordsmark, M., et al., *Prognostic value of tumor oxygenation in 397 head and neck tumors after primary radiation therapy. An international multi-center study.* Radiotherapy and oncology : journal of the European Society for Therapeutic Radiology and Oncology, 2005. **77**(1): p. 18-24.
2. Hockel, M., et al., *Association between tumor hypoxia and malignant progression in advanced cancer of the uterine cervix.* Cancer research, 1996. **56**(19): p. 4509-15.
3. Wojtkowiak, J.W., et al., *Drug resistance and cellular adaptation to tumor acidic pH microenvironment.* Molecular pharmaceutics, 2011. **8**(6): p. 2032-8.
4. Good, J.S. and K.J. Harrington, *The hallmarks of cancer and the radiation oncologist: updating the 5Rs of radiobiology.* Clinical oncology, 2013. **25**(10): p. 569-77.
5. Dubois, L.J., et al., *New ways to image and target tumour hypoxia and its molecular responses.* Radiotherapy and oncology : journal of the European Society for Therapeutic Radiology and Oncology, 2015. **116**(3): p. 352-7.
6. Pettersen, E.O., et al., *Targeting tumour hypoxia to prevent cancer metastasis. From biology, biosensing and technology to drug development: the METOXIA consortium.* Journal of enzyme inhibition and medicinal chemistry, 2015. **30**(5): p. 689-721.
7. Ebbesen, P., et al., *Taking advantage of tumor cell adaptations to hypoxia for developing new tumor markers and treatment strategies.* Journal of enzyme inhibition and medicinal chemistry, 2009. **24 Suppl 1**: p. 1-39.
8. Neri, D. and C.T. Supuran, *Interfering with pH regulation in tumours as a therapeutic strategy.* Nature reviews. Drug discovery, 2011. **10**(10): p. 767-77.
9. Pastorek, J. and S. Pastorekova, *Hypoxia-induced carbonic anhydrase IX as a target for cancer therapy: from biology to clinical use.* Seminars in cancer biology, 2015. **31**: p. 52-64.
10. Pastorek, J., et al., *Cloning and characterization of MN, a human tumor-associated protein with a domain homologous to carbonic anhydrase and a putative helix-loop-helix DNA binding segment.* Oncogene, 1994. **9**(10): p. 2877-88.

11. Wykoff, C.C., et al., *Hypoxia-inducible expression of tumor-associated carbonic anhydrases*. *Cancer research*, 2000. **60**(24): p. 7075-83.
12. Kaluz, S., et al., *Lowered oxygen tension induces expression of the hypoxia marker MN/carbonic anhydrase IX in the absence of hypoxia-inducible factor 1 alpha stabilization: a role for phosphatidylinositol 3'-kinase*. *Cancer research*, 2002. **62**(15): p. 4469-77.
13. van den Beucken, T., et al., *Hypoxia-induced expression of carbonic anhydrase 9 is dependent on the unfolded protein response*. *The Journal of biological chemistry*, 2009. **284**(36): p. 24204-12.
14. Kopacek, J., et al., *MAPK pathway contributes to density- and hypoxia-induced expression of the tumor-associated carbonic anhydrase IX*. *Biochimica et biophysica acta*, 2005. **1729**(1): p. 41-9.
15. van Kuijk, S.J., et al., *Prognostic Significance of Carbonic Anhydrase IX Expression in Cancer Patients: A Meta-Analysis*. *Frontiers in oncology*, 2016. **6**: p. 69.
16. Peeters, S.G., et al., *[(18)F]VM4-037 MicroPET Imaging and Biodistribution of Two In Vivo CAIX-Expressing Tumor Models*. *Molecular imaging and biology : MIB : the official publication of the Academy of Molecular Imaging*, 2015. **17**(5): p. 615-9.
17. Akurathi, V., et al., *Development and biological evaluation of (9)(9)mTc-sulfonamide derivatives for in vivo visualization of CA IX as surrogate tumor hypoxia markers*. *European journal of medicinal chemistry*, 2014. **71**: p. 374-84.
18. Akurathi, V., et al., *Synthesis and biological evaluation of a 99mTc-labelled sulfonamide conjugate for in vivo visualization of carbonic anhydrase IX expression in tumor hypoxia*. *Nuclear medicine and biology*, 2010. **37**(5): p. 557-64.
19. Sneddon, D., et al., *Synthesis and in Vivo Biological Evaluation of 68Ga-Labeled Carbonic Anhydrase IX Targeting Small Molecules for Positron Emission Tomography*. *Journal of medicinal chemistry*, 2016.
20. Monti, S.M., C.T. Supuran, and G. De Simone, *Anticancer carbonic anhydrase inhibitors: a patent review (2008 - 2013)*. *Expert opinion on therapeutic patents*, 2013. **23**(6): p. 737-49.

21. Gieling, R.G., et al., *Antimetastatic effect of sulfamate carbonic anhydrase IX inhibitors in breast carcinoma xenografts*. Journal of medicinal chemistry, 2012. **55**(11): p. 5591-600.
22. Ward, C., et al., *Evaluation of carbonic anhydrase IX as a therapeutic target for inhibition of breast cancer invasion and metastasis using a series of in vitro breast cancer models*. Oncotarget, 2015. **6**(28): p. 24856-70.
23. Lock, F.E., et al., *Targeting carbonic anhydrase IX depletes breast cancer stem cells within the hypoxic niche*. Oncogene, 2013. **32**(44): p. 5210-9.
24. Dubois, L., et al., *Specific inhibition of carbonic anhydrase IX activity enhances the in vivo therapeutic effect of tumor irradiation*. Radiotherapy and oncology : journal of the European Society for Therapeutic Radiology and Oncology, 2011. **99**(3): p. 424-31.
25. Rami, M., et al., *Hypoxia-targeting carbonic anhydrase IX inhibitors by a new series of nitroimidazole-sulfonamides/sulfamides/sulfamates*. Journal of medicinal chemistry, 2013. **56**(21): p. 8512-20.
26. McDonald, P.C., et al., *Recent developments in targeting carbonic anhydrase IX for cancer therapeutics*. Oncotarget, 2012. **3**(1): p. 84-97.
27. Supuran, C.T., *Carbonic anhydrases: novel therapeutic applications for inhibitors and activators*. Nature reviews. Drug discovery, 2008. **7**(2): p. 168-81.
28. Dubois, L., et al., *Targeting carbonic anhydrase IX by nitroimidazole based sulfamides enhances the therapeutic effect of tumor irradiation: a new concept of dual targeting drugs*. Radiotherapy and oncology : journal of the European Society for Therapeutic Radiology and Oncology, 2013. **108**(3): p. 523-8.
29. Barman, S., et al., *Coumarin–benzothiazole–chlorambucil (Cou–Benz–Cbl) conjugate: an ESIPT based pH sensitive photoresponsive drug delivery system*. Journal of Materials Chemistry B, 2015. **3**(17): p. 3490-97.
30. Bekele, T., et al., *Catalytic, enantioselective [4 + 2]-cycloadditions of ketene enolates and o-quinones: efficient entry to chiral, alpha-oxygenated carboxylic acid derivatives*. Journal of the American Chemical Society, 2006. **128**(6): p. 1810-1.
31. Gill, M. and A.F. Smrdel, *Pigments of fungi, part 16. Synthesis of methyl (R)-(+)-tetrahydro-2-methyl-5-oxo-2-furanacetate and its (S)-(-)-antipode, chiroptical references for determination of the absolute stereochemistry of fungal pre-anthraquinones*. Tetrahedron Asymmetry, 1990. **1**(7): p. 453-64.

32. Deshmukh, A.R. and V. Gumaste, *Process for preparing alkyl/aryl chloroformates*, 2005, Google Patents.
33. Hay, M.P., et al., *Tricyclic [1,2,4]triazine 1,4-dioxides as hypoxia selective cytotoxins*. *Journal of medicinal chemistry*, 2008. **51**(21): p. 6853-65.
34. Arrowsmith, J., et al., *Antitumor imidazotetrazines. 41. Conjugation of the antitumor agents mitozolomide and temozolomide to peptides and lexitropsins bearing DNA major and minor groove-binding structural motifs*. *Journal of medicinal chemistry*, 2002. **45**(25): p. 5458-70.
35. Ombouma, J., et al., *Carbonic Anhydrase Glycoinhibitors belonging to the Aminoxysulfonamide Series*. *ACS medicinal chemistry letters*, 2015. **6**(7): p. 819-21.
36. Kelarev, V.I., et al., *Synthesis of N-substituted 6-alkyl-2,4-diamino-1,3,5-triazines containing long alkyl radicals*. *Zhurnal Organicheskoi Khimii*, 1988. **24**: p. 1100-1105.
37. Svastova, E., et al., *Carbonic anhydrase IX reduces E-cadherin-mediated adhesion of MDCK cells via interaction with beta-catenin*. *Experimental cell research*, 2003. **290**(2): p. 332-45.
38. Goede, V., et al., *Past, present and future role of chlorambucil in the treatment of chronic lymphocytic leukemia*. *Leukemia & lymphoma*, 2015. **56**(6): p. 1585-92.
39. Horsman, M.R. and P. Vaupel, *Pathophysiological Basis for the Formation of the Tumor Microenvironment*. *Frontiers in oncology*, 2016. **6**: p. 66.
40. Reddy, S.B. and S.K. Williamson, *Tirapazamine: a novel agent targeting hypoxic tumor cells*. *Expert opinion on investigational drugs*, 2009. **18**(1): p. 77-87.
41. Omuro, A. and L.M. DeAngelis, *Glioblastoma and other malignant gliomas: a clinical review*. *JAMA*, 2013. **310**(17): p. 1842-50.
42. Fukushima, T., H. Takeshima, and H. Kataoka, *Anti-glioma therapy with temozolomide and status of the DNA-repair gene MGMT*. *Anticancer research*, 2009. **29**(11): p. 4845-54.
43. Dubois, L., et al., *Imaging the hypoxia surrogate marker CA IX requires expression and catalytic activity for binding fluorescent sulfonamide inhibitors*. *Radiotherapy and oncology : journal of the European Society for Therapeutic Radiology and Oncology*, 2007. **83**(3): p. 367-73.

44. Ditte, P., et al., *Phosphorylation of carbonic anhydrase IX controls its ability to mediate extracellular acidification in hypoxic tumors*. *Cancer research*, 2011. **71**(24): p. 7558-67.
45. Dubois, L., et al., *Imaging of CA IX with fluorescent labelled sulfonamides distinguishes hypoxic and (re)-oxygenated cells in a xenograft tumour model*. *Radiotherapy and oncology : journal of the European Society for Therapeutic Radiology and Oncology*, 2009. **92**(3): p. 423-8.
46. Fokas, E., et al., *Targeting ATR in vivo using the novel inhibitor VE-822 results in selective sensitization of pancreatic tumors to radiation*. *Cell death & disease*, 2012. **3**: p. e441.
47. Josse, R., et al., *ATR inhibitors VE-821 and VX-970 sensitize cancer cells to topoisomerase I inhibitors by disabling DNA replication initiation and fork elongation responses*. *Cancer research*, 2014. **74**(23): p. 6968-79.
48. Hall, A.B., et al., *Potential of tumor responses to DNA damaging therapy by the selective ATR inhibitor VX-970*. *Oncotarget*, 2014. **5**(14): p. 5674-85.
49. Gray, L.H., et al., *The concentration of oxygen dissolved in tissues at the time of irradiation as a factor in radiotherapy*. *The British journal of radiology*, 1953. **26**(312): p. 638-48.
50. Wright, E.A. and P. Howard-Flanders, *The influence of oxygen on the radiosensitivity of mammalian tissues*. *Acta radiologica*, 1957. **48**(1): p. 26-32.
51. Doyen, J., et al., *Knock-down of hypoxia-induced carbonic anhydrases IX and XII radiosensitizes tumor cells by increasing intracellular acidosis*. *Frontiers in oncology*, 2012. **2**: p. 199.
52. Kulshrestha, A., et al., *Selective inhibition of tumor cell associated Vacuolar-ATPase 'a2' isoform overcomes cisplatin resistance in ovarian cancer cells*. *Molecular oncology*, 2016.
53. De Milito, A. and S. Fais, *Tumor acidity, chemoresistance and proton pump inhibitors*. *Future oncology*, 2005. **1**(6): p. 779-86.
54. Liao, C., et al., *Genomic screening in vivo reveals the role played by vacuolar H⁺ ATPase and cytosolic acidification in sensitivity to DNA-damaging agents such as cisplatin*. *Molecular pharmacology*, 2007. **71**(2): p. 416-25.
55. van Gisbergen, M.W., et al., *How do changes in the mtDNA and mitochondrial dysfunction influence cancer and cancer therapy? Challenges, opportunities and models*. *Mutation research. Reviews in mutation research*, 2015. **764**: p. 16-30.

56. Pollak, M., *Potential applications for biguanides in oncology*. The Journal of clinical investigation, 2013. **123**(9): p. 3693-700.
57. Pernicova, I. and M. Korbonits, *Metformin--mode of action and clinical implications for diabetes and cancer*. Nature reviews. Endocrinology, 2014. **10**(3): p. 143-56.
58. Liu, Z., et al., *Phenformin Induces Cell Cycle Change, Apoptosis, and Mesenchymal-Epithelial Transition and Regulates the AMPK/mTOR/p70s6k and MAPK/ERK Pathways in Breast Cancer Cells*. PloS one, 2015. **10**(6): p. e0131207.
59. Shackelford, D.B., et al., *LKB1 inactivation dictates therapeutic response of non-small cell lung cancer to the metabolism drug phenformin*. Cancer cell, 2013. **23**(2): p. 143-58.
60. Krall, N., et al., *A small-molecule drug conjugate for the treatment of carbonic anhydrase IX expressing tumors*. Angewandte Chemie, 2014. **53**(16): p. 4231-5.
61. Khalifah, R.G., *The carbon dioxide hydration activity of carbonic anhydrase. I. Stop-flow kinetic studies on the native human isoenzymes B and C*. The Journal of biological chemistry, 1971. **246**(8): p. 2561-73.
62. McIntyre, A., et al., *Carbonic anhydrase IX promotes tumor growth and necrosis in vivo and inhibition enhances anti-VEGF therapy*. Clinical cancer research : an official journal of the American Association for Cancer Research, 2012. **18**(11): p. 3100-11.

Chapter 5

Design and synthesis of Carbonic anhydrase IX inhibitors with different bio-reducible warheads

Submitted to J. Enzyme Inhb. Med. Chem.

Nanda Kumar Parvathaneni*, Ludwig Dubois, Ala Yaromina, Silvia Bua, Claudiu T. Supuran, Philippe Lambin, Jean-Yves Winum

Abstract

A series of 5-nitroimidazole, bio-reducible tirapazamine and DNA alkylating nitrogen mustard derivatives incorporating sulfonamide and sulfamate moieties have been designed and synthesized as radio, chemosensitizing and hypoxia-activated prodrugs targeting the tumor-associated carbonic anhydrase (CA) isoform IX. CAIX is a hypoxia-regulated and tumor-specific enzyme that maintains the pH balance of cells. Targeting CAIX might therefore be a valuable approach for tumor-specific delivery of cytotoxic drugs, sensitize radio, chemotherapy resistant tumors and reduce adverse effects on healthy tissues. All of the new compounds demonstrated low activity as CAIX inhibitors except compound **17**, a tirapazamine derivative, which showed nanomolar activity specifically towards CAII (7.1nM) and CAIX (93.3 nM). This differential inhibition capacity might be explained by the influence of the linker and sulfonamide or sulfamate substitution on the benzene ring. Same family compounds with different linkers and substitutions showed different binding capacity. Alternative strategies to target hypoxic tumors and increasing understanding of the CAIX conformation upon hypoxia would help to design novel CAIX inhibitors.

Introduction

Hypoxia is prevalent in a wide range of solid tumors [1, 2], is responsible for enhanced malignancy and is associated with resistance to ionizing radiation and chemotherapy [3, 4]. Under hypoxic conditions many metabolic pathways are altered and related target genes become upregulated. Among the proteins whose expression is induced by hypoxia, via transcriptional activation through hypoxia inducible factor 1 α (HIF-1 α), the membrane-associated carbonic anhydrase IX (CAIX, (CA, EC 4.2.1.1)) [5, 6] is the most strongly induced one in human cancer cells, making CAIX a potential anti-therapeutic target for the treatment of cancer [7]. Furthermore, CAIX overexpression occurs in the majority of solid tumors, whilst almost being absent in healthy tissue except for organs of the gastro-intestinal tract. Various strategies have been developed to exploit this exceptional feature. Hence, our group has developed a dual-target approach [8] with a sulfamide CAIX inhibitory moiety coupled to a 5-nitroimidazole as a more effective radiosensitizer than an indanesulfonamide CAIX inhibitor (CAIXi) [9].

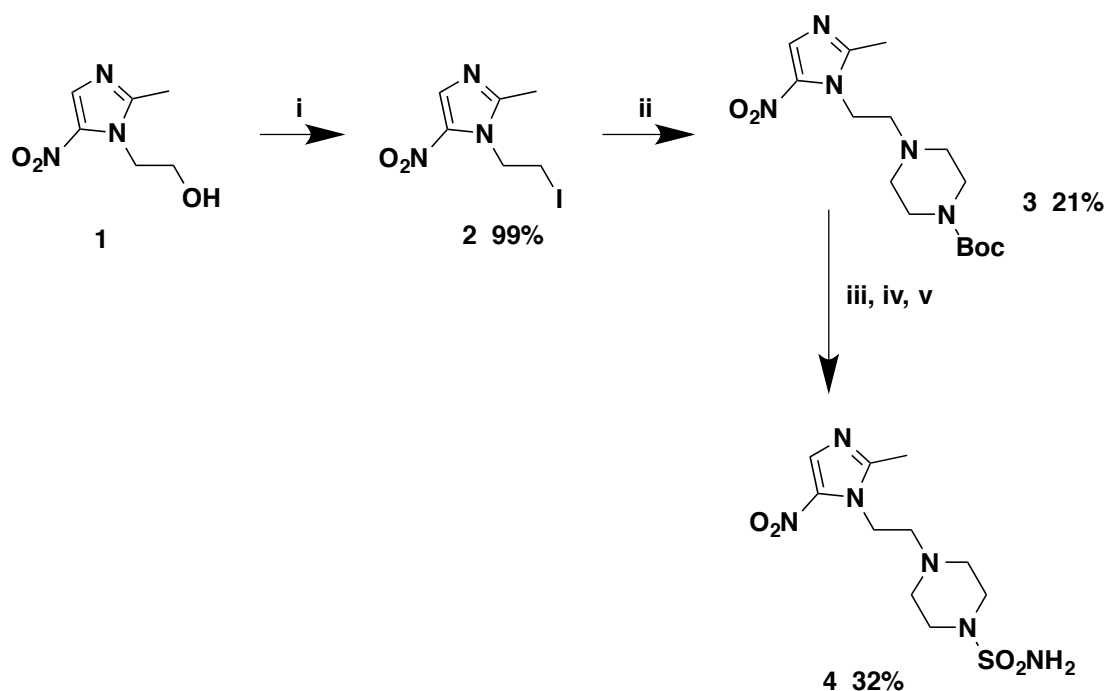
To investigate this strategy of CAIX dual-targeting further in the context of anti-cancer agents, alternative novel dual-target compounds have been developed by our group [10]. Here, we have designed three different classes of dual-target compounds conjugated to CAIXi (sulfonamide or sulfamate), i.e. 5-nitroimidazole derivatives as radiosensitizers, hypoxia-activated cytotoxic drugs and DNA alkylating agents.

Results and discussion:

Chemistry

Different libraries of inhibitors were synthesized by incorporating a 5-nitroimidazole, tirapazamine or nitrogen mustard moieties. Metronidazole **1** was converted to Iodo-metronidazole **2** at the hydroxyl position using basic conditions. Compound **3** was obtained by substitution with Boc-piperazine and converted to compound **4** by the procedure described by our group previously [11] with good yields (Scheme 1) [12].

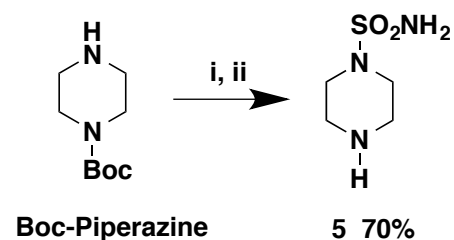
Scheme 1



Reagents and conditions: (i) PPh_3 , Imidazole, I_2 , DCM, rt; (ii) Boc-piperazine, THF, reflux; (iii) 20% TFA-DCM; (iv) ClSO_2NCO , tBuOH, NEt_3 , DCM, 0°C -rt; (v) 20% TFA-DCM.

Compound **5** was synthesized from commercially available Boc-piperazine by reacting with N-bocsulfamoyl chloride followed by Boc-deprotection under acidic conditions (Scheme 2).

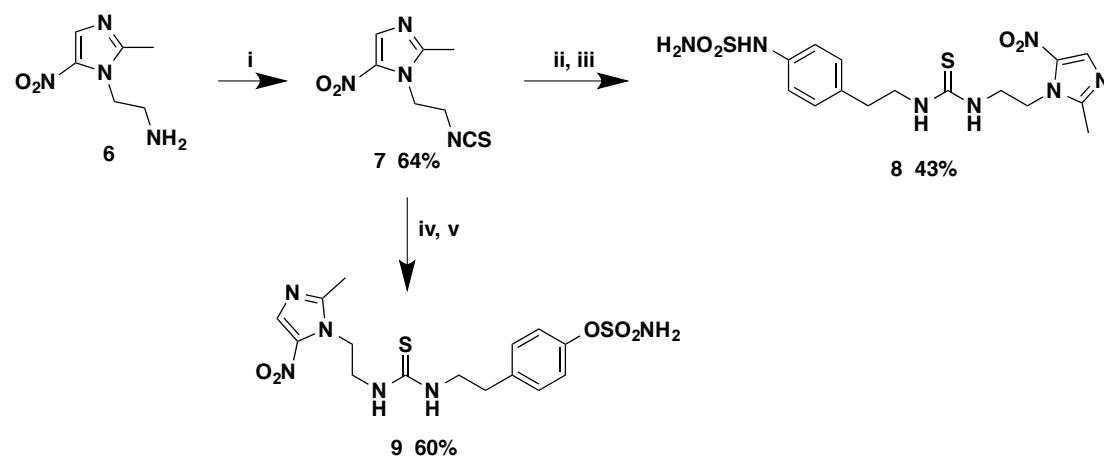
Scheme 2



Reagents and conditions: (i) ClSO₂NCO, tBuOH, NEt₃, DCM, 0°C-rt; (ii) 20% TFA-DCM.

Thiourea derivatives **8** and **9** were prepared similarly starting from the amino analogue of metronidazole **6** converted to isothiocyanate using thiophosgene under basic conditions, finally reacting with respectively 4-(2-aminoethyl) aniline and 4-(2-aminoethyl) phenol in acetonitrile through a sulfamoylation process (Scheme 3) [9, 13].

Scheme 3

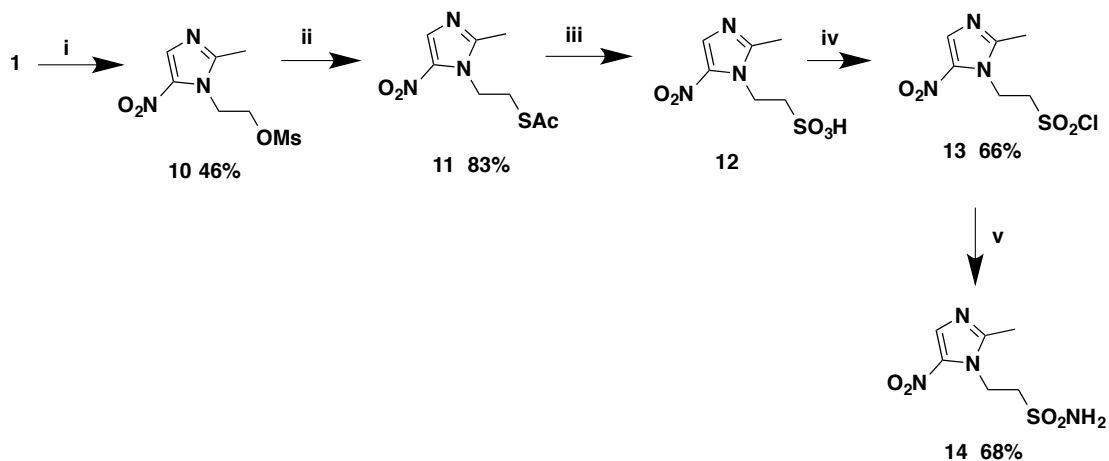


Reagents and conditions: (i) Thiophosgene, NaOH, CHCl₃, 0°C-rt; (ii) 4-(2-aminoethyl) aniline, CH₃CN, rt; (iii) NH₂SO₂Cl, DMA, rt; (iv) 4-(2-aminoethyl) phenol, CH₃CN, rt; (v) NH₂SO₂Cl, DMA, rt.

Compound **14** was synthesized using a series of reaction conditions starting from metronidazole **1** converted to **10** using methane sulfonyl chloride under basic conditions, then to compound **12** using potassium thioacetate and oxidizing conditions

followed by phosgene treatment to obtain **13**. Finally, compound **14** was obtained by treatment with ammonia in 1, 4-dioxane at room temperature (Scheme 4) [14].

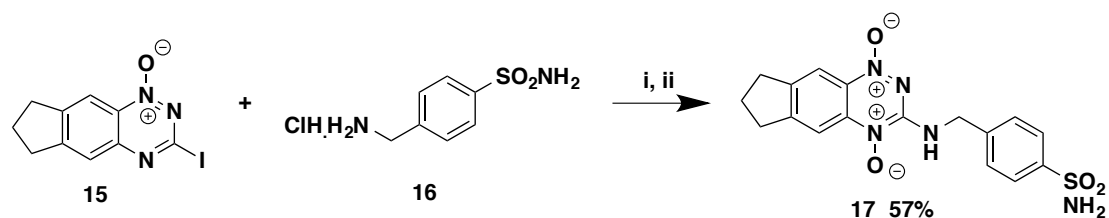
Scheme 4



Reagents and conditions: (i) $\text{CH}_3\text{SO}_2\text{Cl}$, NEt_3 , DMPA, DCM, 0°C - rt; (ii) KSAc, DMF, rt; (iii) 35% H_2O_2 - CH_3COOH , rt; (iv) Phosgene, cat. dry DMF, dry DCM, rt, (v) Liq. NH_3 in 1, 4 Dioxane, Benzene, rt.

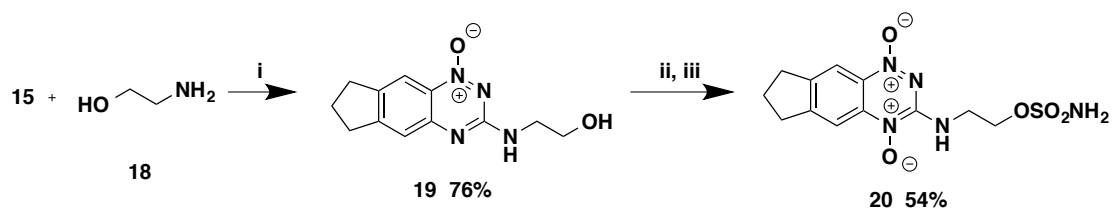
Tirapazamine derivatives **17** and **22** were obtained by reacting respectively **15** and **21** with **16** under reflux conditions followed by oxidation of the mono-oxides using hydrogen peroxide (Scheme 5 and 7). Derivatives **20** and **23** were synthesized starting from respectively **15** and **21** by reacting with ethanolamine **18** followed by sulfamoylation and oxidation of the mono-oxides using hydrogen peroxide (Schemes 6 and 8) [15, 16].

Scheme 5



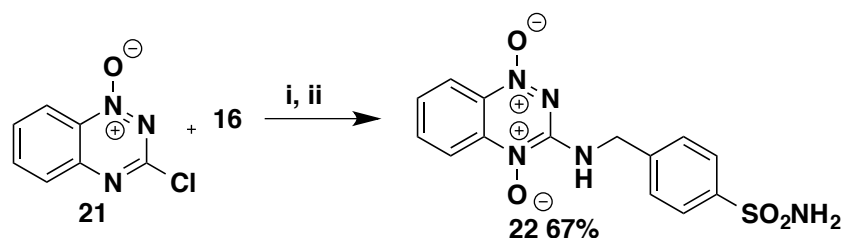
Reagents and conditions: (i) NEt_3 , EtOH, 60°C ; (ii) H_2O_2 (35%), $(\text{CF}_3\text{CO})_2\text{O}$, DCM, rt.

Scheme 6



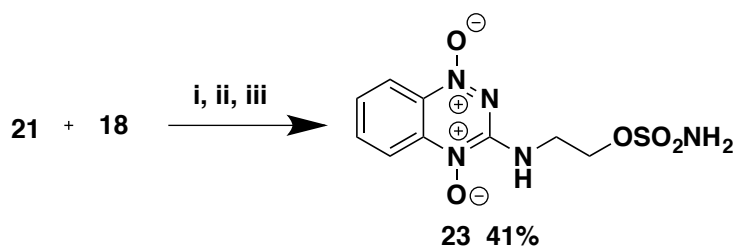
Reagents and conditions: (i) DME, reflux; (ii) $\text{NH}_2\text{SO}_2\text{Cl}$, DMA, rt; (iii) H_2O_2 (35%), $(\text{CF}_3\text{CO})_2\text{O}$, DCM, rt.

Scheme 7



Reagents and conditions: (i) NEt_3 , DCM, 45°C ; (ii) H_2O_2 (35%), $(\text{CF}_3\text{CO})_2\text{O}$, DCM, rt.

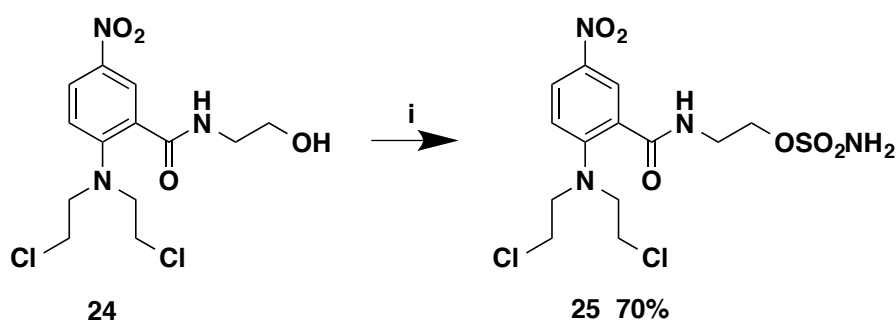
Scheme 8



Reagents and conditions: (i) DME, reflux; (ii) $\text{NH}_2\text{SO}_2\text{Cl}$, DMA, rt; (iii) H_2O_2 (35%), $(\text{CF}_3\text{CO})_2\text{O}$, DCM, rt.

Compound **25** was obtained via sulfamoylation of **24** similarly as used for compound **19** (Scheme 9) [9].

Scheme 9



Reagents and conditions: (i) $\text{NH}_2\text{SO}_2\text{Cl}$, DMA, rt.

The new compounds were characterized extensively by spectral and physico-chemical methods, which confirmed their structures (supplementary data).

CA Inhibition assay

All compounds reported here were assayed as inhibitors of three physiologically relevant CA isoforms, the cytosolic hCAI and II (h = human isoform) and the transmembrane, tumor-associated hCAIX using the CO_2 hydrase assay (Table 1) [17]. The clinically employed sulfonamide acetazolamide (AAZ, 5-acetamido-1, 3, 4-thiadiazole-2-sulfonamide) has been used as standard in these measurements.

All compounds, except **5** that was prepared as an analogue of compound **4** (inhibition data not shown), not showed any binding affinity towards hCAI, hCAII and hCAIX. Against the abundant, cytosolic isoform hCAI compounds **5**, **14** and **25** didn't show any inhibition potency, with K_I values of > 10000 , 6428 and 4155 nM respectively. The thiourea derivatives **8** and **9** demonstrated weak inhibition potency against all CA isoforms. However compound **9** binds significantly to hCAII ($K_I = 58.6$ nM) with a selectivity ratio for inhibiting hCAII over hCAIX of 0.09 explained by the influence of the substitution on the benzene ring. Compound **14**, the sulfonamide derivative of the sulfamide and sulfamate analogues previously reported and biologically evaluated by our group [9], shows moderate binding efficacy towards hCAII ($K_I = 199.2$ nM) and hCAIX ($K_I = 147.3$ nM) compared to the other analogues. This might be explained by stability under acidic conditions of these three analogues, i.e. sulfonamide $>$ sulfamide $>$ sulfamate. Compounds **17**, **20**, **22** and **23** showed significant binding efficiency towards all CA isoforms compared with the previously

reported analogues by our group [10]. Different linkers might influence the binding capacity of these compounds ranging from 186 nM to 7.1 nM (hCAII) and is supported by the selectivity ratios for inhibiting hCAII over hCAIX ranging between 0.07 and 1.54. The sulfamate derivative of the nitrogen mustard **25** shows no significant binding capacity towards any of the isoforms tested. Nevertheless, considering the difficulty to obtain small compounds with a better affinity for the tumor-associated isozymes over CAII, the selectivity obtained for these series is comparable with those of all the clinically used CA inhibitors, which have selectivity ratios for the inhibition of CAII over CAIX <1.

Table 1: Inhibition data of hCA I, hCA II, hCA IX for the reported compounds and the standard sulfonamide inhibitor acetazolamide (**AAZ**) using a stopped flow CO₂ hydrase assay.

Compound	K_i (nM)*			Selectivity ratios K_i hCAII/ K_i hCAIX
	hCA I	hCA II	hCA IX	
5	>10000	>10000	1285.5	
8	152.2	612.8	290.6	2.10
9	127.8	58.6	642.6	0.09
14	6428.4	199.2	147.3	1.35
17	169.1	7.1	93.3	0.07
20	79.9	33.5	212.8	0.15
22	88.9	52.2	156.1	0.33
23	59.6	186.1	120.7	1.54
25	4155.7	903.9	201.4	4.48
AAZ	250	12.0	25	0.48

*Average from 3 different assays, by a stopped flow technique (errors were in the range of \pm 5-10 % of the reported values).

Conclusion

We have designed and synthesized three different classes of CAIX inhibitors containing 1) 5-nitroimidazole moieties with different linkers, 2) Tirapazamine derivatives with different substitution on the benzene ring and 3) a sulfamate derivative of nitrogen mustard, a DNA alkylating agent. These molecules showed weak to moderate inhibition profiles towards all tested CA isoforms. Different substitutions and linkers in the same family compounds would influence the binding capacity of molecules to CAIX [17]. For example compounds **17** and **20** belongs to same family with different linkers and substitutions but showed different binding capacity. Alternative strategies to target hypoxic tumors and increasing understanding of the CAIX conformation upon hypoxia would help to design novel CAIX inhibitors.

Experimental Section

Chemistry

General: All reagents and solvents were of commercial quality and used without further purification unless otherwise specified. All reactions were carried out under an inert atmosphere of nitrogen. TLC analyses were performed on silica gel 60 F254 plates (Merck Art. no. 1.05554). Spots were visualized under 254 nm UV illumination or by ninhydrin solution spraying. Melting points were determined on a Büchi Melting Point 510 and are uncorrected. ^1H and ^{13}C NMR spectra were recorded on Bruker DRX-400 spectrometer using DMSO- d_6 as solvent and tetramethylsilane as internal standard. For ^1H NMR spectra, chemical shifts are expressed in δ (ppm) downfield from tetramethylsilane, and coupling constants (J) are expressed in hertz. Electron Ionization mass spectra were recorded in positive or negative mode on a Water MicroMass ZQ. All compounds that were tested against purified physiological isoforms of CAs were analyzed by high-resolution ESI mass spectra (HRMS) using on a Q-ToFI mass spectrometer fitted with an electrospray ion source in order to confirm the purity of >95%.

General procedure for Boc-protected sulfamoylation [A] (4, 5): A solution of chlorosulfonyl isocyanate (1.2 equiv.) and *tert*-butanol (1.2 equiv.) in 2 mL of methylene chloride (prepared *ab initio*) was added to a solution of concern amine (1 equiv.) and triethylamine (4 equiv.) in 10 mL of methylene chloride. The mixture was stirred at room temperature for one hour, then diluted with ethyl acetate and washed with water. The organic layer was dried over anhydrous sodium sulfate, filtered, and concentrated under vacuum. The residue was purified by chromatography on silica gel using methylene chloride-methanol 98:2 as eluent.

General procedure for Boc-deprotection: [B] (4, 5): Boc protected intermediate was diluted in a solution of trifluoroacetic acid in methylene chloride (20% volume) and stirred at room temperature for 6 h. The mixture was then concentrated under vacuum and co-evaporated several times with diethyl ether to give the expected sulfamide as a white powder.

General procedure for sulfamoylation: [C] (8, 9, 20, 23, 25): Sulfamoyl chloride (3 equiv.) was added to a solution of the concerned alcohol or amine (1 equiv.) in N,N-dimethylacetamide. The mixture was stirred at room temperature for one night, then diluted with ethyl acetate and washed three times with water. The organic layer was dried over anhydrous magnesium sulfate, filtered, and concentrated under vacuum. The residue was purified by chromatography on silica gel using methylene chloride–methanol 9:1 as eluent.

General procedure for amination of 3-Chlorobenzotriazine- 1,4-di-N-oxides [D] (19): Concerned amine (3.0 equiv.) was added to a stirring solution of 3-chlorobenzotriazine-1, 4-di-N-oxide (1.0 equiv.) in DME, DCM or EtOH (30 mL) and the mixture was stirred overnight at reflux temperature. The reaction mixture was cooled to room temperature and concentrated under vacuum. The residue was dissolved in ammonium hydroxide solution and extracted with ethyl acetate. The organic layer was dried over anhydrous sodium sulfate, filtered and concentrated under vacuum. The residue was purified by chromatography using a silica gel with methylene chloride-methanol 98:2 v-v as eluent to obtain the expected compound as a yellow powder with a 42-96% yield.

General procedure for oxidation [E] (17, 20, 22 and 23): Hydrogen peroxide (10 equiv.) was added dropwise to a stirred solution of trifluoroacetic anhydride (10 equiv.) in DCM at 0°C. This reaction mixture was stirred at 0°C for 5 min, warmed to room temperature for 10 min, and cooled to 5°C. Next, the mixture was added to a stirred solution of mono oxide (1.0 equiv.) in DCM at 0°C and stirred at room temperature for 2-3 days. The reaction mixture was carefully diluted with water and basified with aqueous NH₄OH and extracted with CHCl₃. The organic fraction was dried over anhydrous Na₂SO₄, filtered and evaporated to obtain the residue. This residue was purified by chromatography using a silica gel with methylene chloride-methanol 98:2 v-v as an eluent to obtain the expected compound as an orange red powder with a 41-67% yield.

1-(2-iodoethyl)-2-methyl-5-nitro-1H-imidazole (2): Metronidazole **1** (1equiv.), triphenylphosphine (1 equiv.), Imidazole (2.5 equiv.) and Iodine (1 equiv.) were dissolved in dry DCM allowed to stir at room temperature for 2 hours, then the

reaction mixture was washed with water and extracted with DCM. The organic layer was dried over sodium sulfate, filtered and concentrated under vacuum. The residue was dissolved in minimum amount of DCM and precipitated with diethyl ether to give iodometronidazole as powder. Yield: Quantitative. ^1H NMR (DMSO- d_6 , 400 MHz) δ 8.05 (s, 1H), 4.61 (t, $J = 7.3$, 2H), 3.51 (t, $J = 7.3$, 2H), 2.50 (s, 3H); ^{13}C NMR (DMSO- d_6 , 101 MHz) δ 151.08, 138.18, 133.14, 47.09 (s, 1H), 14.09, 2.28. MS (ESI $^+$ /ESI $^-$) m/z 281.97 [M+H] $^+$.

tert-butyl 4-(2-(2-methyl-5-nitro-1H-imidazol-1-yl)ethyl)piperazine-1-carboxylate (3): Iodometronidazole **2** (1equiv.) and Boc-Piperazine (2equiv.) were dissolved in THF and allowed to reflux for overnight. The reaction mixture was washed with water and extracted with Ethyl acetate. The organic layer was washed with brine and dried over anhydrous sodium sulfate, filtered and concentrated under vacuum to get residue and was The residue was purified by chromatography on silica gel using methylene chloride-methanol 9:1 as eluent. Yield: 21%, ^1H NMR (DMSO- d_6 , 400 MHz) δ 8.00 (s, 1H), 4.38 (t, $J = 6.0$, 2H), 3.23 (s, 3H), 2.61 (t, $J = 6.0$, 2H), 2.46 (s, 3H), 2.39 – 2.32 (m, 4H), 1.38 (s, 9H). ^{13}C NMR (DMSO- d_6 , 101 MHz) δ 153.59 , 151.10 , 138.42 , 132.54 , 78.62 , 56.84 , 52.54 , 43.06 , 27.83 , 13.71. MS (ESI $^+$ /ESI $^-$) m/z 341.20 [M+H] $^+$.

4-(2-(2-methyl-5-nitro-1H-imidazol-1-yl) ethyl) piperazine-1-sulfonamide (4): Synthesized using general procedures **A** and **B**. Yield: Quantitative, ^1H NMR (DMSO- d_6 , 400 MHz) δ 8.08 (s, 1H), 7.05 (s, 2H), 4.51 (t, $J = 6.7$, 2H), 3.51 – 2.93 (m, 14H). ^{13}C NMR (DMSO- d_6 , 101 MHz) δ 151.85, 138.87, 133.45, 65.33, 51.47, 44.36, 15.58, 14.22. MS (ESI $^+$ /ESI $^-$) m/z 319.12 [M+H] $^+$.

Piperazine-1-sulfonamide (5): Synthesized using general procedure **A** and **B**, Yield: 70%, ^1H NMR (400 MHz, DMSO- d_6) δ 9.50 (s, 1H), 7.07 (s, 2H), 3.17 (dd, $J = 17.4, 5.9$, 8H). ^{13}C NMR (101 MHz, DMSO- d_6) δ 42.83, 41.92. MS (ESI/ESI) m/z 166.07 [M+H].

1-(2-isothiocyanatoethyl)-2-methyl-5-nitro-1H-imidazole (7): Thiophosgene (1 equiv.) and sodium hydroxide (2 equiv.) were added to a solution of **6** (0.5 equiv.) in chloroform and water (4:1) at 0°C, and reaction mixture was warmed to room temperature. Thin layer Chromatography confirmed complete disappearance of the

starting material. Reaction mixture was washed with water and extracted with DCM. The organic layer was dried over anhydrous sodium sulfate, filtered and evaporated to get crude. This crude was purified by chromatography on silica gel using ethyl acetate and petroleum ether as a gradient from 5-5 to 9-1 as eluent. Yield: 64%, ¹H NMR (400 MHz, DMSO-*d*₆) δ 8.10 (s, 1H), 4.65 – 4.60 (m, 2H), 4.17 – 4.12 (m, 2H), 3.35 (s, 3H). ¹³C NMR (101 MHz, DMSO-*d*₆) δ 151.80, 138.80, 133.65, 129.62, 45.06, 14.28. MS (ESI⁺/ESI⁻) *m/z* 213.04 [M+H]⁺.

4-(2-(3-(2-(2-methyl-5-nitro-1*H*-imidazol-1-yl)ethyl)thioureido)ethyl)phenyl

sulfamate (8): 4-(2-aminoethyl) aniline (1 equiv.) was added to a solution of 7(1 equiv.) in acetonitrile and allowed to stir at room temperature for overnight. Reaction mixture was washed with water and extracted with Ethyl acetate. The organic layer was dried over anhydrous sodium sulfate, filtered and evaporated under vacuum to get crude. This crude was used for general procedure C further without purification. Yield: 43%, ¹H NMR (400 MHz, DMSO-*d*₆) δ 9.35 (s, 1H), 8.03 (s, 1H), 7.51 (s, 2H), 7.11 (d, *J* = 9.1, 4H), 7.01 (s, 2H), 4.41 (s, 2H), 3.81 (s, 2H), 2.68 (s, 2H), 2.36 (s, 3H). ¹³C NMR (101 MHz, DMSO-*d*₆) δ 151.98, 139.08, 138.13, 133.70, 133.45 – 133.11, 129.40, 118.95, 55.38, 45.93, 14.30. MS (ESI⁺/ESI⁻) *m/z* 428.12 [M+H]⁺.

4-(2-(3-(2-(2-methyl-5-nitro-1*H*-imidazol-1-yl)ethyl)thioureido)ethyl)phenyl

sulfamate (9): Same protocol as for the synthesis of compound 8 starting from 7. Yield: 60%, ¹H NMR (400 MHz, DMSO-*d*₆) δ 8.03 (s, 1H), 7.95 (s, 2H), 7.58 (d, *J* = 38.2, 2H), 7.29 (d, *J* = 8.5, 2H), 7.20 (d, *J* = 8.5, 2H), 4.42 (s, 2H), 3.82 (s, 2H), 2.77 (s, 2H), 2.36 (s, 3H). ¹³C NMR (101 MHz, DMSO-*d*₆) δ 151.44, 148.56, 138.56, 137.61, 133.16, 129.77, 121.97, 45.39, 30.63, 13.75. MS (ESI⁺/ESI⁻) *m/z* 429.10 [M+H]⁺.

2-(2-methyl-5-nitro-1*H*-imidazol-1-yl) ethyl methanesulfonate (10): Methane sulfonylchloride (1.1 equiv.) was added dropwise to a stirred solution of metronidazole (1 equiv.), triethylamine (2 equiv.) and DMAP (1.1 equiv.) in anhydrous DCM at 0°C. The reaction mixture was allowed warm to room temperature and stirred for overnight. The reaction mixture was diluted with DCM and washed with water and brine, extracted with DCM. The organic layer was dried over anhydrous sodium sulfate, filtered and evaporated to get crude. Crude was used

further without purification. Yield: Quantitative. ^1H NMR (DMSO- d_6 , 400 MHz) δ 8.05 (s, 1H), 4.61 (t, $J = 7.3$, 2H), 3.51 (t, $J = 7.3$, 2H), 2.50 (s, 3H); ^{13}C NMR (DMSO- d_6 , 101 MHz) δ 151.08, 138.18, 133.14, 47.09 (s, 1H), 14.09, 2.28. MS (ESI $^+$ /ESI $^-$) m/z 281.97 [M+H] $^+$.

S-(2-(2-methyl-5-nitro-1H-imidazol-1-yl)ethyl) ethanethioate (11): Potassium thioacetate (2 equiv.) was added to a solution of 10 (1 equiv.) in anhydrous DMF at room temperature for 16 hours. The reaction mixture was partitioned between ethyl acetate and water, the organic layer was washed with water and brine dried over anhydrous sodium sulfate, filtered and solvent evaporated under vacuum to give thioacetate. Yield: 83%, ^1H NMR (400 MHz, DMSO- d_6) δ 8.01 (s, 1H), 4.45 (t, $J = 6.6$, 2H), 3.27 (t, $J = 6.6$, 2H), 2.46 (s, 3H), 2.29 (s, 3H). ^{13}C NMR (101 MHz, DMSO) δ 194.59, 151.25, 138.42, 132.92, 44.68, 30.32, 27.87. MS (ESI $^+$ /ESI $^-$) m/z 230.06 [M+H] $^+$.

2-(2-methyl-5-nitro-1H-imidazol-1-yl)ethane-1-sulfonyl chloride (13): A solution of 11 (1 equiv.) was treated with hydrogen peroxide [35% w/w in water (6mL)] and acetic acid (7 mL). The reaction mixture was allowed to stir for 2 overnights at room temperature; the excess hydrogen peroxide was quenched by addition of 10% Pd/C (0.050 g). The mixture was filtered on celite, concentrated, and co-evaporated with toluene. The obtained sulfonic acid was used further without purification. To the crude 2-(2-methyl-5-nitro-1H-imidazol-1-yl) ethane-1-sulfonic acid 12 (1 equiv.) was suspended in anhydrous DCM and a solution of phosgene in toluene (20% m/m, 3.5 mL) and dry DMF (1mL) was added under argon atmosphere. After 1 hr. an additional 1 mL phosgene solution was added and the mixture was stirred for 2 hours under same conditions. The reaction mixture was filtered to get pure compound as solid. Yield: 66%, ^1H NMR (400 MHz, DMSO- d_6) δ 8.80 (s, 1H), 4.63 (t, $J = 6.3$, 2H), 2.92 (t, $J = 6.3$, 2H), 2.78 (s, 3H)., ^{13}C NMR (101 MHz, DMSO- d_6) δ 149.90, 138.05, 123.91, 48.67, 44.17, 12.13. MS (ESI $^+$ /ESI $^-$) m/z 236.00 [M+H] $^+$.

2-(2-methyl-5-nitro-1H-imidazol-1-yl)ethane-1-sulfonamide (14): Compound 13 (1 equiv.) was made as suspension in benzene and added 0.5M solution of liq. ammonia in 1,4-dioxane (2 ml) at room temperature. After 1 hour, the reaction mixture was filtered to afford pure compound as white solid. Yield: 68%, ^1H NMR (400 MHz,

DMSO-*d*₆) δ 8.03 (s, 1H), 7.39 (s, 2H), 4.63 (t, *J* = 7.0, 2H), 3.49 (t, *J* = 7.0, 2H), 2.49 (s, 3H). ¹³C NMR (101 MHz, DMSO-*d*₆) δ 151.43, 138.36, 133.04, 53.08, 40.85, 13.94. MS (ESI⁺/ESI⁻) *m/z* 235.05 [M+H]⁺.

3-((4-sulfamoylbenzyl)amino)-7,8-dihydro-6*H*-indeno[5,6-*e*][1,2,4]triazine 1,4-dioxide (17): Synthesized using general procedures **D** and **E**. Yield: 57%, mp 192-194 °C; ¹H NMR (400 MHz, DMSO-*d*₆) δ 8.86 (t, *J* = 6.6, 1H), 7.99 (d, 2H), 7.77 (d, *J* = 8.4, 2H), 7.54 (d, *J* = 8.4, 2H), 7.31 (s, 1H), 4.64 (t, *J* = 6.6, 2H), 3.10 – 2.95 (m, 4H), 2.12 – 2.06 (m, 2H). ¹³C NMR (101 MHz, DMSO-*d*₆) δ 154.6, 149.34, 145.26, 142.74, 137.92, 129.50, 127.42, 125.71, 115.15, 111.20, 43.60, 32.77, 31.83, 30.66 – 29.87, 25.27. MS (ESI⁺/ESI⁻) *m/z* 388.11 [M+H]⁺.

3-((2-(sulfamoyloxy)ethyl)amino)-7,8-dihydro-6*H*-indeno[5,6-*e*][1,2,4]triazine 1,4-dioxide (20): Synthesized using general procedures **C**, **D** and **E**. Yield: 54%, mp 152-154 °C; ¹H NMR (400 MHz, DMSO-*d*₆) δ 8.24 (t, *J* = 5.9, 1H), 8.00 (d, 2H), 7.52 (s, 2H), 4.24 (t, *J* = 5.9, 2H), 3.71 (d, *J* = 5.9, 2H), 3.04 (dt, 4H), 2.15 – 2.05 (m, 3H). ¹³C NMR (101 MHz, DMSO-*d*₆) δ 154.66, 149.26, 145.31, 137.78, 129.36, 115.12, 111.13, 66.61, 32.27, 25.21. MS (ESI⁺/ESI⁻) *m/z* 342.09 [M+H]⁺.

3-((4-sulfamoylbenzyl)amino)benzo[*e*][1,2,4]triazine 1,4-dioxide (22): Synthesized using general procedures **D** and **E**. Yield: 67%, ¹H NMR (400 MHz, DMSO-*d*₆) δ 8.97 (s, 1H), 8.17 (s, 2H), 7.95 (s, 1H), 7.77 (d, *J* = 5.8, 2H), 7.56 (s, 3H), 7.33 (s, 2H), 4.68 (s, 2H). ¹³C NMR (101 MHz, DMSO-*d*₆) δ 149.76, 142.66, 138.33, 135.50, 130.3, 127.30, 125.68, 121.08, 116.97, 43.58. MS (ESI⁺/ESI⁻) *m/z* 348.08 [M+H]⁺.

3-((2-(sulfamoyloxy)ethyl)amino)benzo[*e*][1,2,4]triazine 1,4-dioxide (23): Synthesized using general procedures **C**, **D** and **E**. Yield: 41%, ¹H NMR (400 MHz, DMSO-*d*₆) δ 8.37 (t, *J* = 5.8, 1H), 8.22 (d, *J* = 8.7, 1H), 8.15 (d, *J* = 8.5, 1H), 7.95 (ddd, 1H), 7.63 – 7.56 (m, 1H), 7.51 (s, 2H), 4.24 (t, *J* = 5.8, 2H), 3.73 (q, *J* = 5.8, 2H). ¹³C NMR (101 MHz, DMSO-*d*₆) δ 149.69, 138.22, 135.54, 130.19, 127.25, 121.08, 116.92, 66.57. MS (ESI⁺/ESI⁻) *m/z* 302.06 [M+H]⁺.

2-(2-(bis(2-chloroethyl)amino)-5-nitrobenzamido)ethyl sulfamate (25): Synthesized using general procedure **C**. Yield: 70%, ¹H NMR (400 MHz, DMSO-*d*₆)

δ 8.86 (t, $J = 5.6$, 1H), 8.14 (d, $J = 2.8$, 1H), 8.12 (d, $J = 2.8$, 1H), 8.10 (d, $J = 2.8$, 1H), 7.55 (s, 2H), 4.17 (t, $J = 5.6$, 2H), 4.03 (q, $J = 7.1$, 1H), 3.80 – 3.69 (m, 9H), 3.57 (q, $J = 5.6$, 2H). ^{13}C NMR (101 MHz, DMSO- d_6) δ 167.56, 151.69, 138.20, 127.28 – 124.02, 117.98, 66.87, 59.38, 52.42, 41.10, 20.49, 13.83.%, MS (ESI⁺/ESI⁻) m/z 429.04 [M]⁺.

CA Inhibition Assays

An Applied Photophysics stopped-flow instrument was used for assaying the CA-catalyzed CO₂ hydration activity [18]. Phenol red (at a concentration of 0.2 mM) was used as an indicator, working at the absorbance maximum of 557 nm, with 20 mM Hepes (pH 7.5) as buffer and 20 mM Na₂SO₄ (for maintaining the ionic strength constant), following the initial rates of the CA-catalyzed CO₂ hydration reaction for a period of 10–100 s. The CO₂ concentrations ranged from 1.7 to 17 mM for the determination of the kinetic parameters and inhibition constants. For each inhibitor, at least six traces of the initial 5–10% of the reaction were used for determining the initial velocity. The uncatalyzed rates were determined in the same manner and subtracted from the total observed rates. Stock solutions of inhibitor (0.1 mM) were prepared in distilled–deionized water, and dilutions up to 0.01 nM were done thereafter with distilled–deionized water. Inhibitor and enzyme solutions were pre-incubated together for 15 min at room temperature prior to assay to allow for the formation of the E–I complex. The inhibition constants were obtained by nonlinear least-squares methods using PRISM 3 and represent the average from at least three different determinations. CA isoforms were recombinant ones obtained in house as reported earlier.

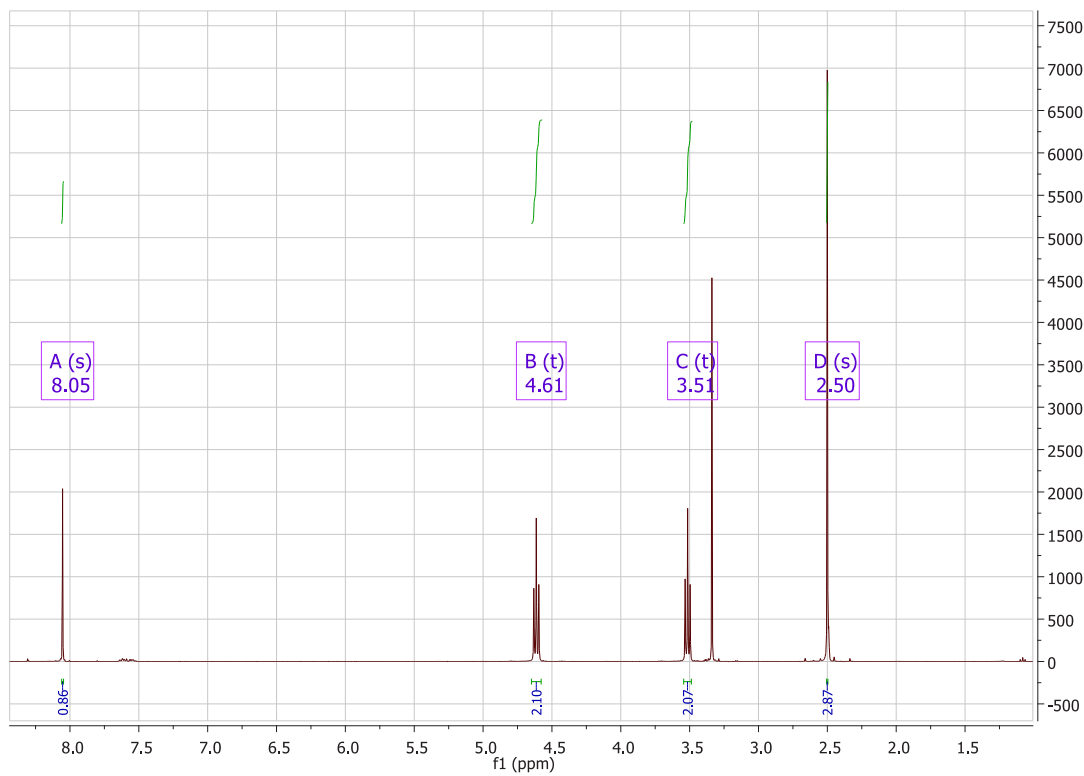
References

1. Vaupel, P. and A. Mayer, *Hypoxia in cancer: significance and impact on clinical outcome*. *Cancer Metastasis Rev*, 2007. **26**(2): p. 225-39.
2. Vaupel, P., M. Hockel, and A. Mayer, *Detection and characterization of tumor hypoxia using pO₂ histography*. *Antioxid Redox Signal*, 2007. **9**(8): p. 1221-35.
3. Nordmark, M., et al., *Prognostic value of tumor oxygenation in 397 head and neck tumors after primary radiation therapy. An international multi-center study*. *Radiother Oncol*, 2005. **77**(1): p. 18-24.
4. Jubb, A.M., F.M. Buffa, and A.L. Harris, *Assessment of tumour hypoxia for prediction of response to therapy and cancer prognosis*. *J Cell Mol Med*, 2010. **14**(1-2): p. 18-29.
5. McDonald, P.C., et al., *Recent developments in targeting carbonic anhydrase IX for cancer therapeutics*. *Oncotarget*, 2012. **3**(1): p. 84-97.
6. Supuran, C.T., *Carbonic anhydrases: novel therapeutic applications for inhibitors and activators*. *Nat Rev Drug Discov*, 2008. **7**(2): p. 168-81.
7. Neri, D. and C.T. Supuran, *Interfering with pH regulation in tumours as a therapeutic strategy*. *Nat Rev Drug Discov*, 2011. **10**(10): p. 767-77.
8. Rami, M., et al., *Hypoxia-targeting carbonic anhydrase IX inhibitors by a new series of nitroimidazole-sulfonamides/sulfamides/sulfamates*. *Journal of medicinal chemistry*, 2013. **56**(21): p. 8512-20.
9. Dubois, L., et al., *Targeting carbonic anhydrase IX by nitroimidazole based sulfamides enhances the therapeutic effect of tumor irradiation: a new concept of dual targeting drugs*. *Radiother Oncol*, 2013. **108**(3): p. 523-8.
10. van Kuijk, S.J., et al., *New approach of delivering cytotoxic drugs towards CAIX expressing cells: A concept of dual-target drugs*. *Eur J Med Chem*, 2017. **127**: p. 691-702.
11. Rami, M., et al., *Hypoxia-targeting carbonic anhydrase IX inhibitors by a new series of nitroimidazole-sulfonamides/sulfamides/sulfamates*. *J Med Chem*, 2013. **56**(21): p. 8512-20.

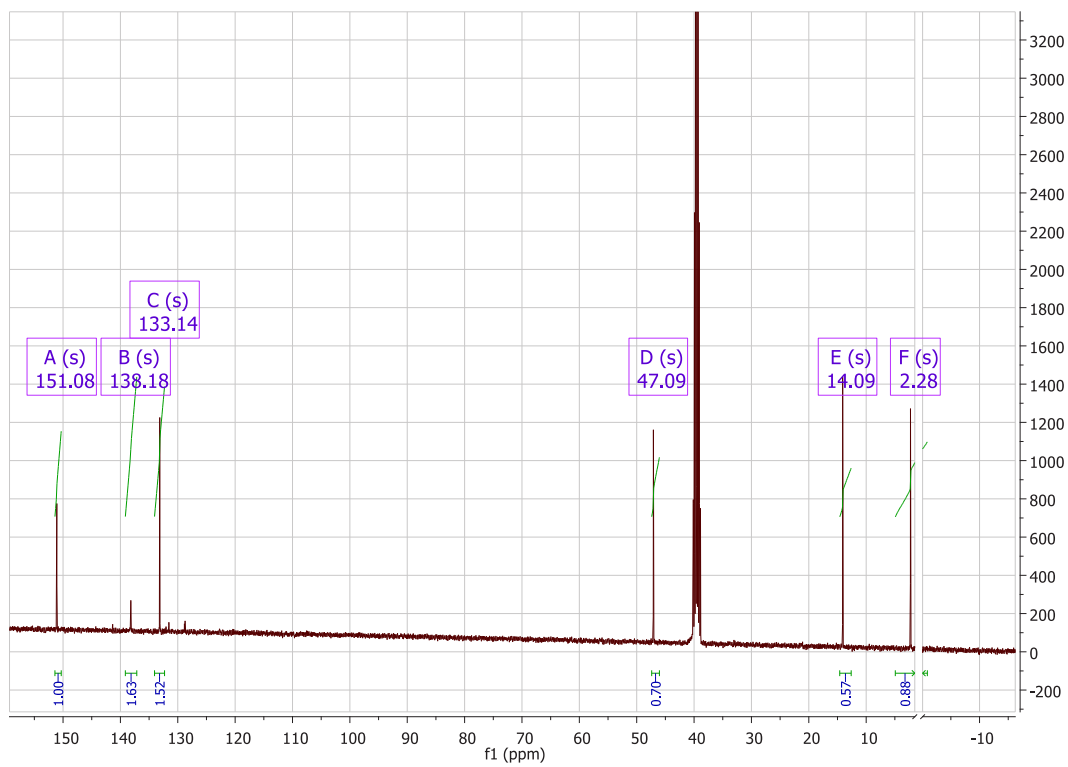
12. Giglio, J., et al., *Synthesis and biological characterisation of novel dithiocarbamate containing 5-nitroimidazole (99m)Tc-complexes as potential agents for targeting hypoxia*. *Bioorg Med Chem Lett*, 2011. **21**(1): p. 394-7.
13. Ernst, I.M., et al., *Synthesis and Nrf2-inducing activity of the isothiocyanates iberverin, iberin and cheirolin*. *Pharmacol Res*, 2013. **70**(1): p. 155-62.
14. Bonnet, M., et al., *Novel nitroimidazole alkylsulfonamides as hypoxic cell radiosensitisers*. *Bioorg Med Chem*, 2014. **22**(7): p. 2123-32.
15. Chopra, S., et al., *Discovery and optimization of benzotriazine di-N-oxides targeting replicating and nonreplicating Mycobacterium tuberculosis*. *J Med Chem*, 2012. **55**(13): p. 6047-60.
16. Hay, M.P., et al., *Tricyclic [1,2,4]triazine 1,4-dioxides as hypoxia selective cytotoxins*. *J Med Chem*, 2008. **51**(21): p. 6853-65.
17. Mboge, M.Y., et al., *Structure activity study of carbonic anhydrase IX: Selective inhibition with ureido-substituted benzenesulfonamides*. *Eur J Med Chem*, 2017. **132**: p. 184-191.
18. Khalifah, R.G., *The carbon dioxide hydration activity of carbonic anhydrase. I. Stop-flow kinetic studies on the native human isoenzymes B and C*. *J Biol Chem*, 1971. **246**(8): p. 2561-73.

Supplementary data:

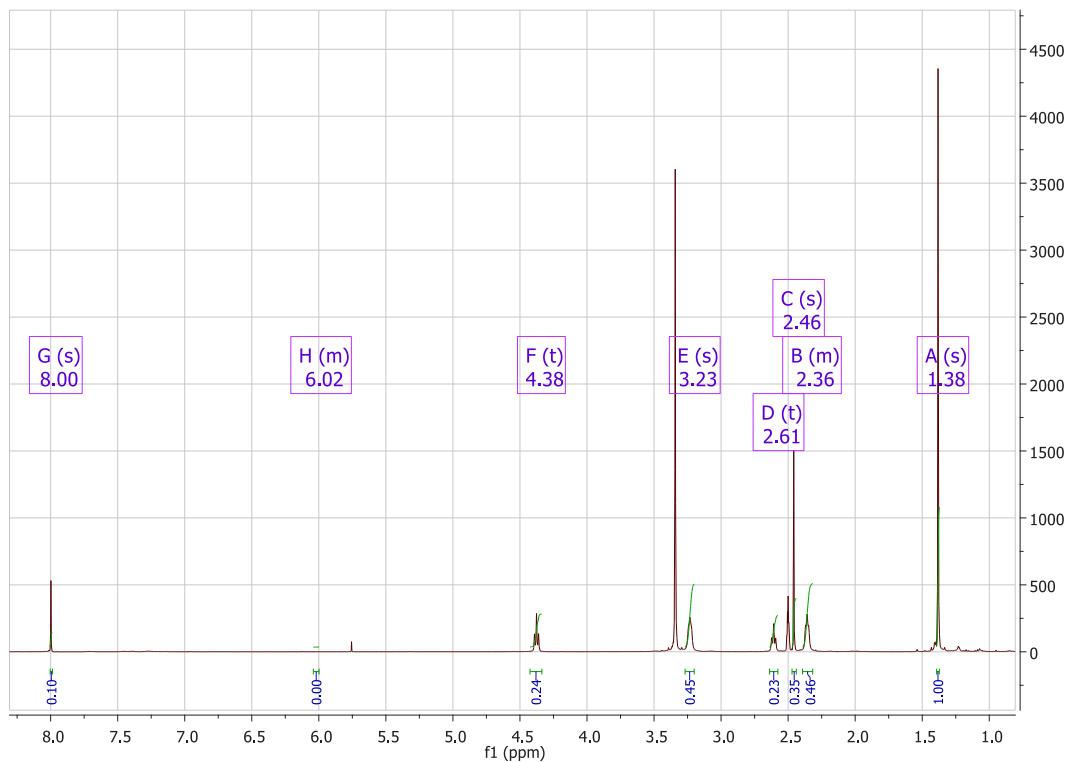
^1H NMR spectrum of compound **2**



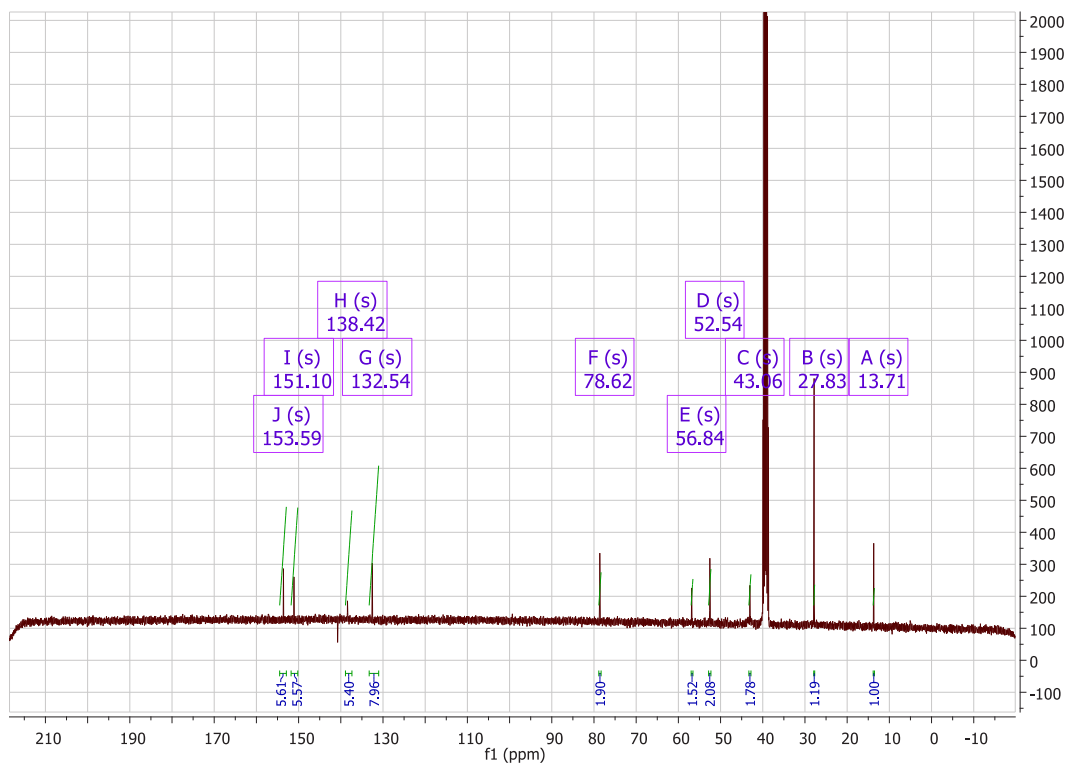
^{13}C NMR spectra of compound **2**



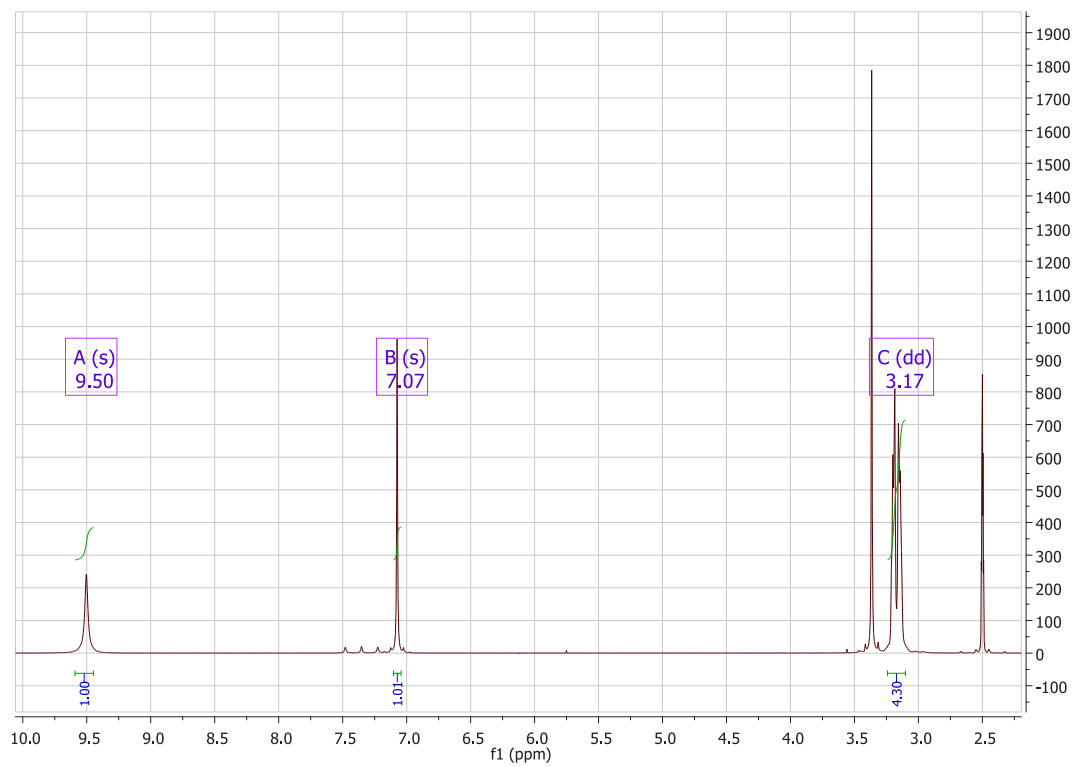
¹H NMR spectra of compound 3



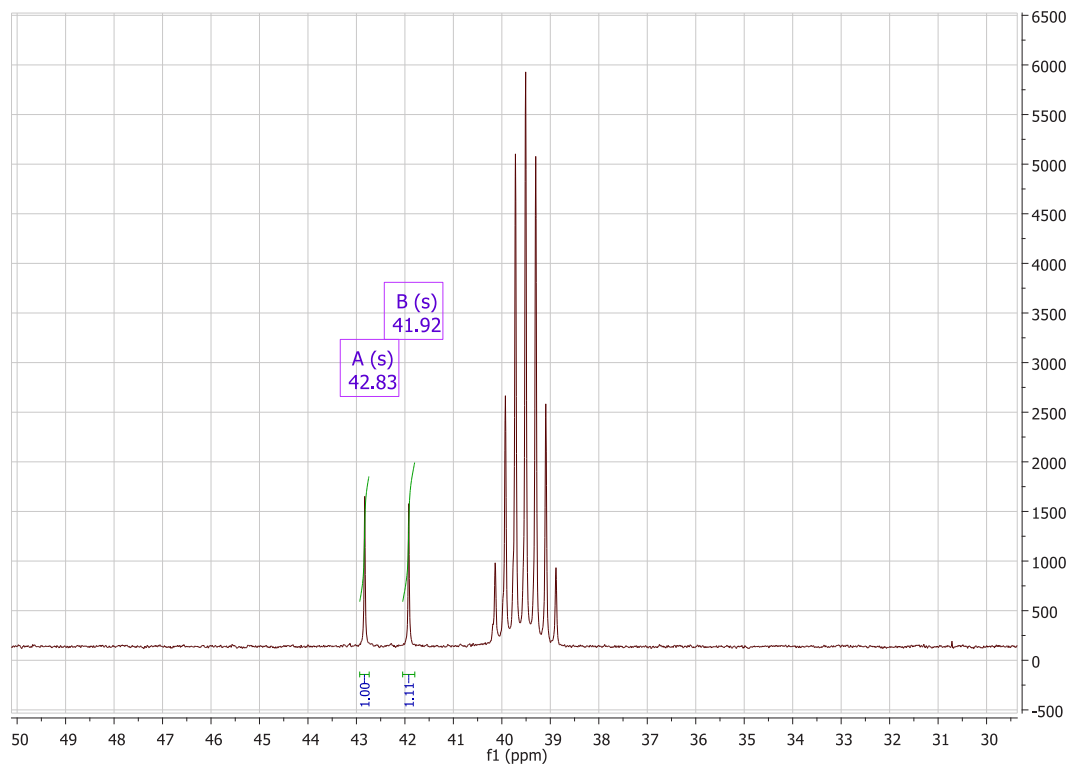
¹³C NMR spectra of compound 3



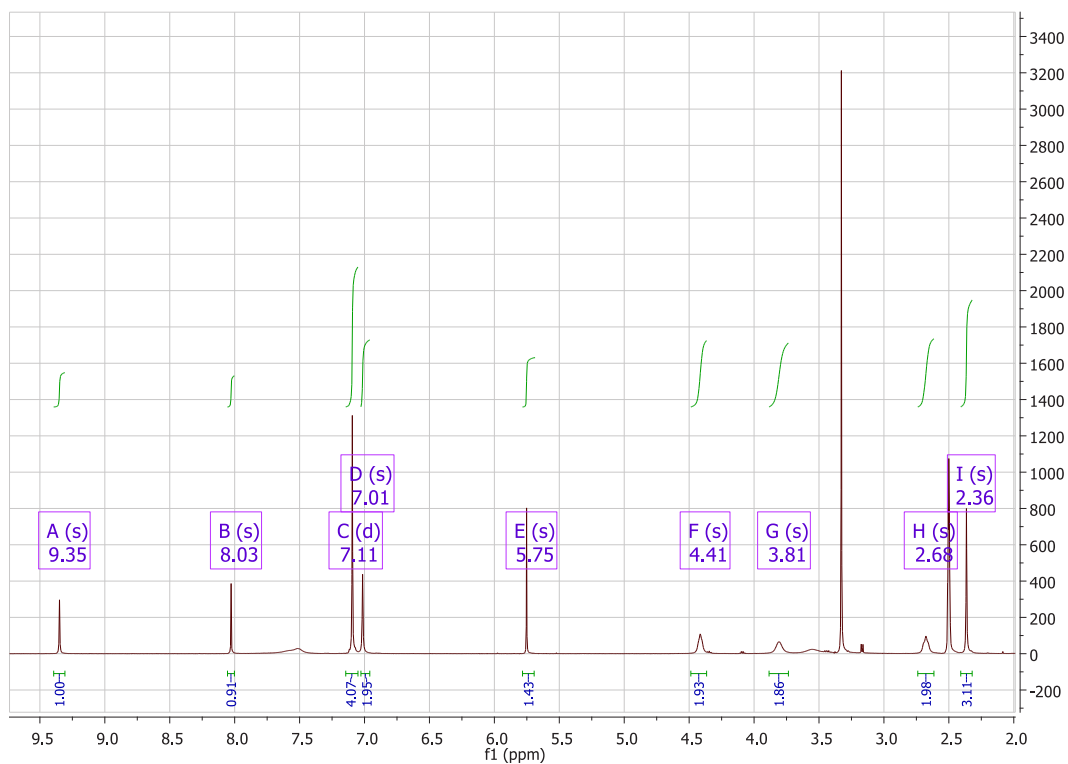
^1H NMR spectra of compound **5**



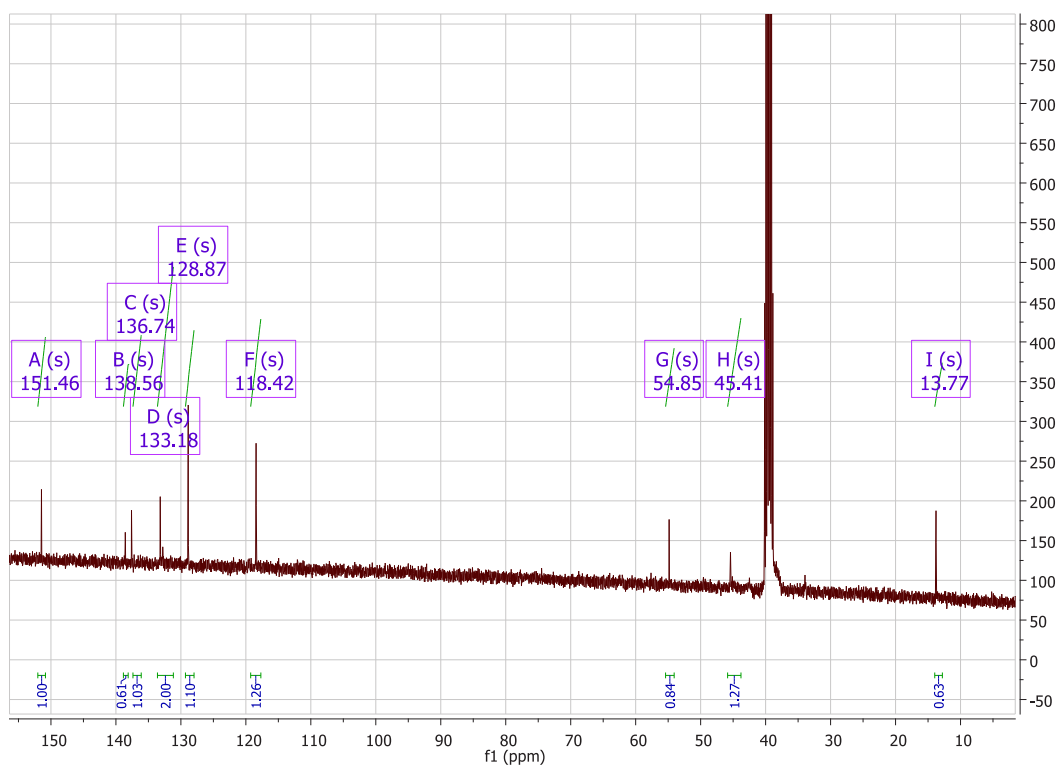
^{13}C NMR spectra of compound **5**



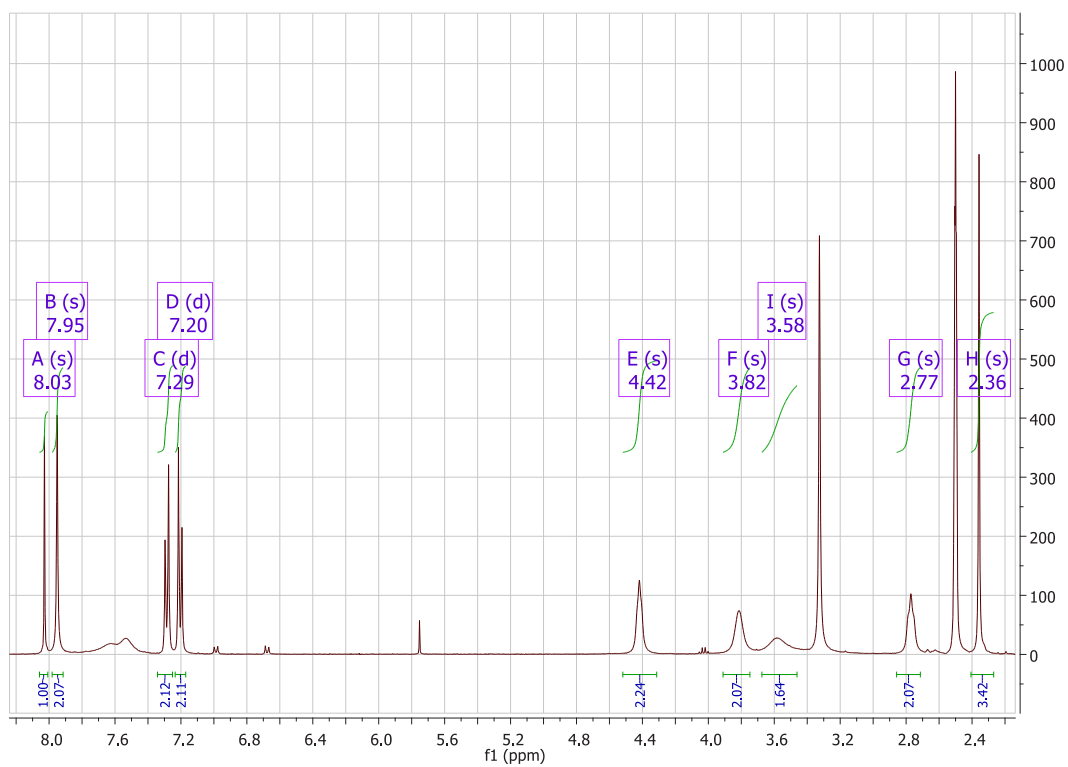
¹H NMR spectra of compound **8**



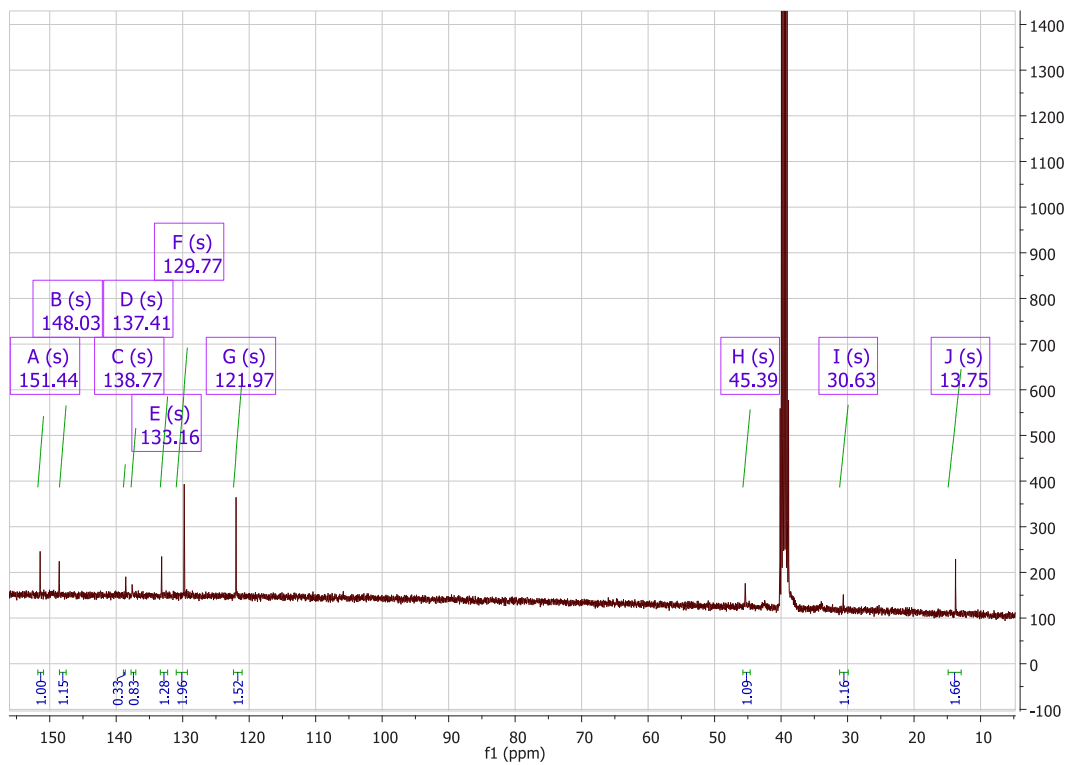
¹³C NMR spectra of compound **8**



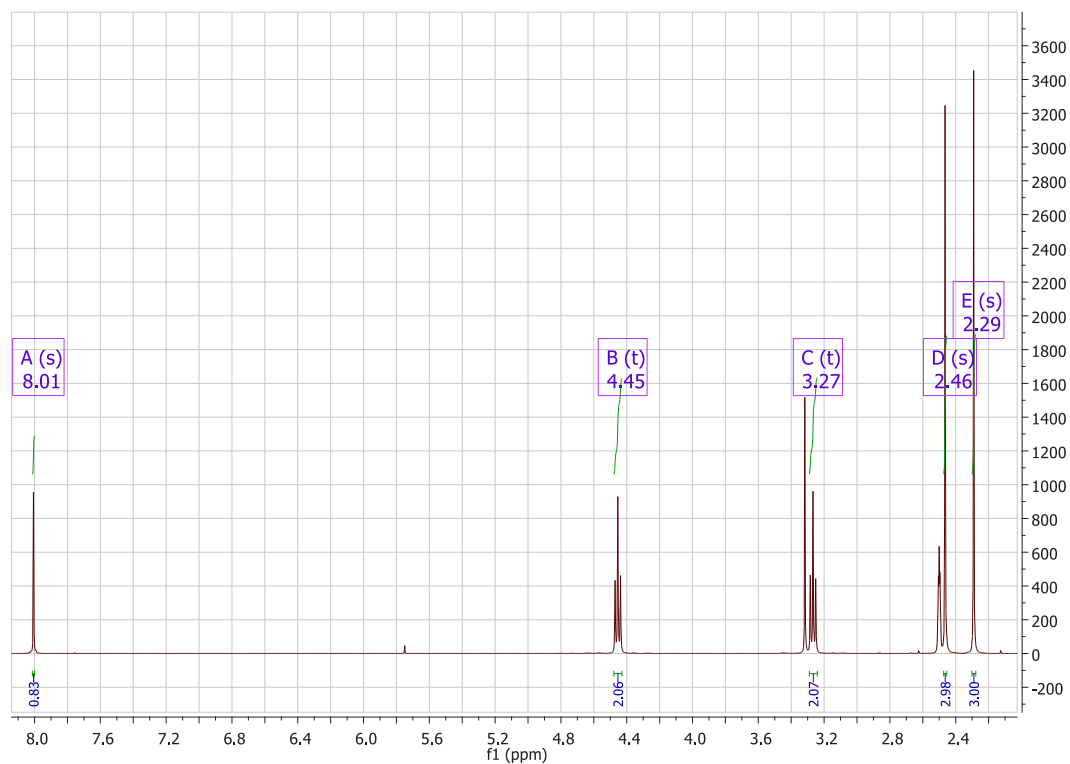
^1H NMR spectra of compound **9**



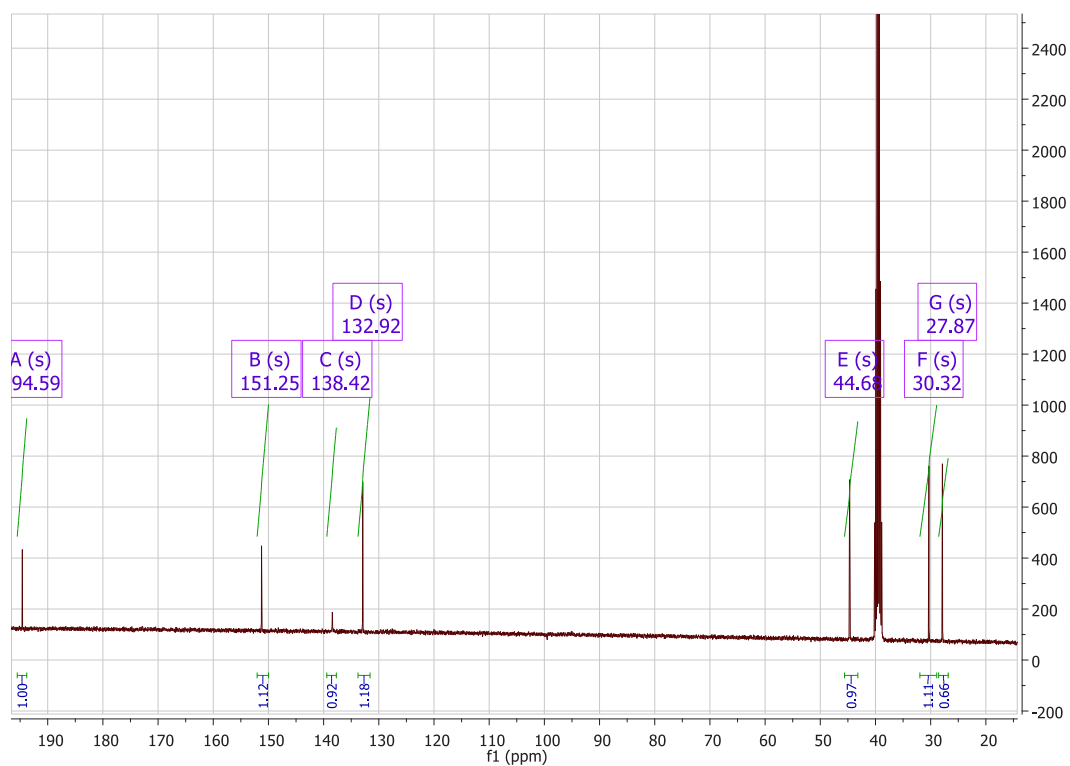
^{13}C NMR spectra of compound **9**



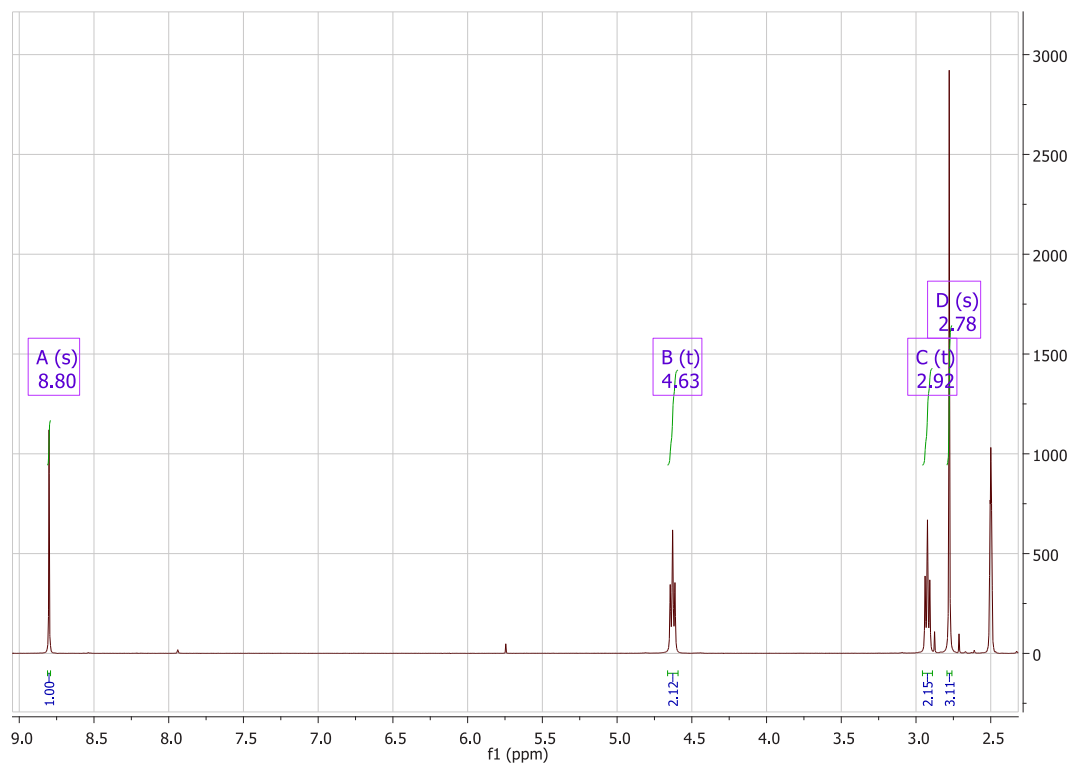
^1H NMR spectra of compound **11**



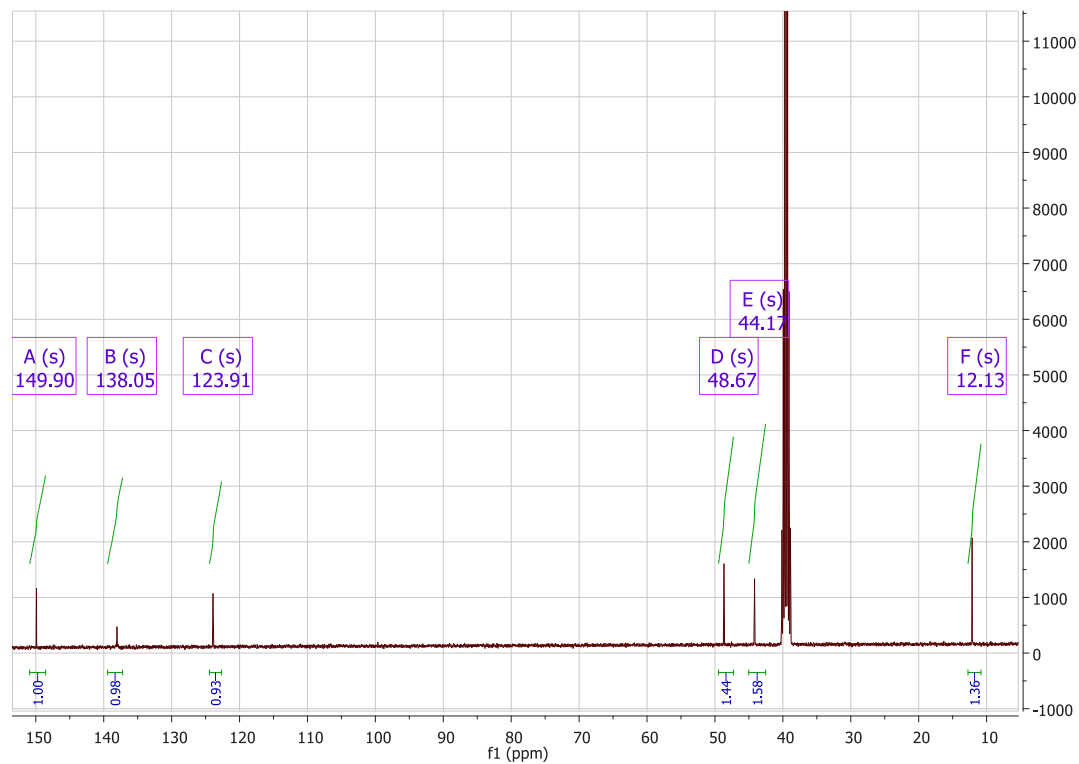
^{13}C NMR spectra of compound **11**



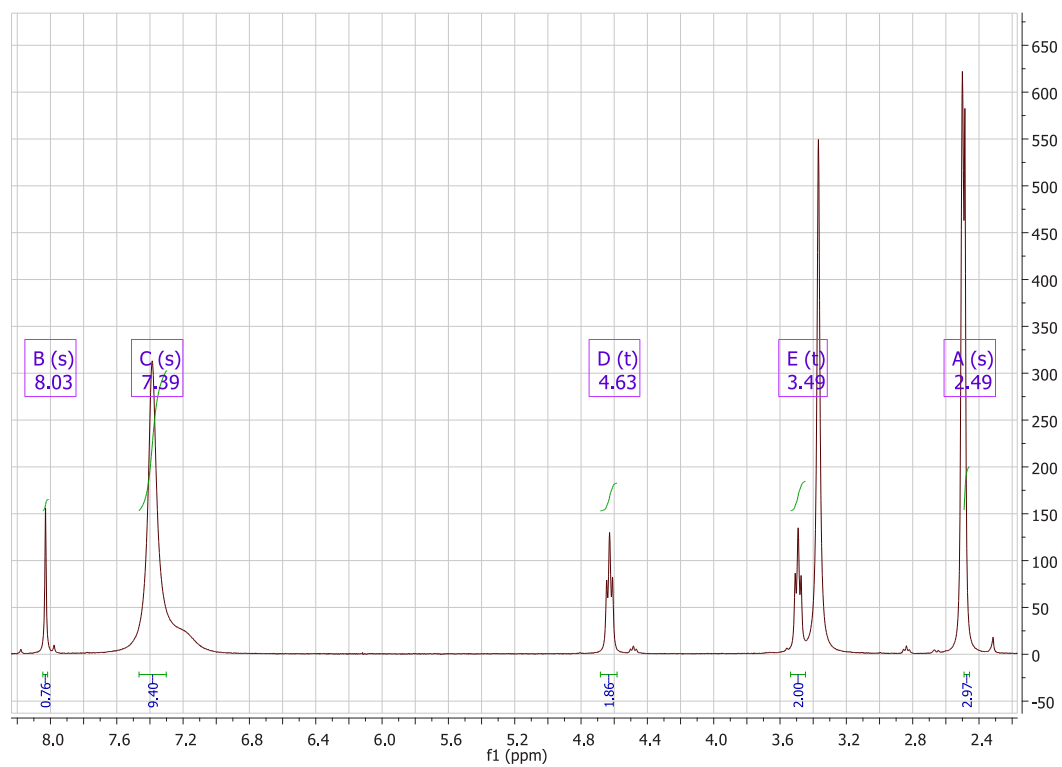
^1H NMR of spectra of compound **13**



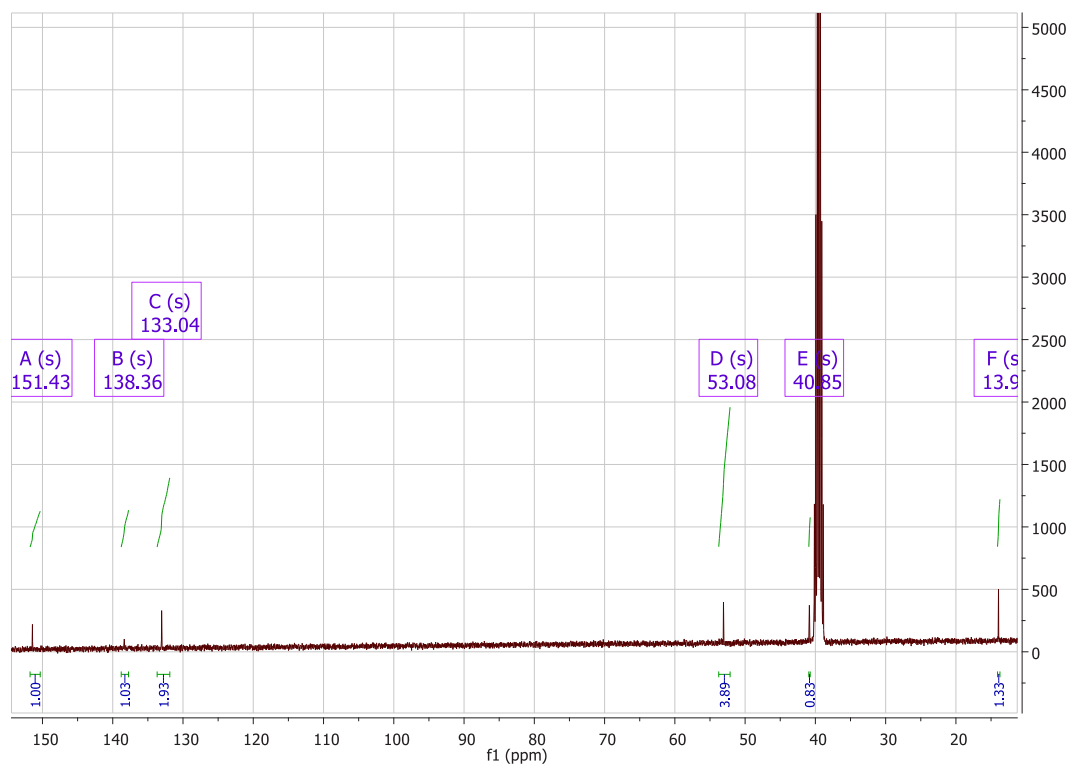
^{13}C NMR spectra of compound **13**



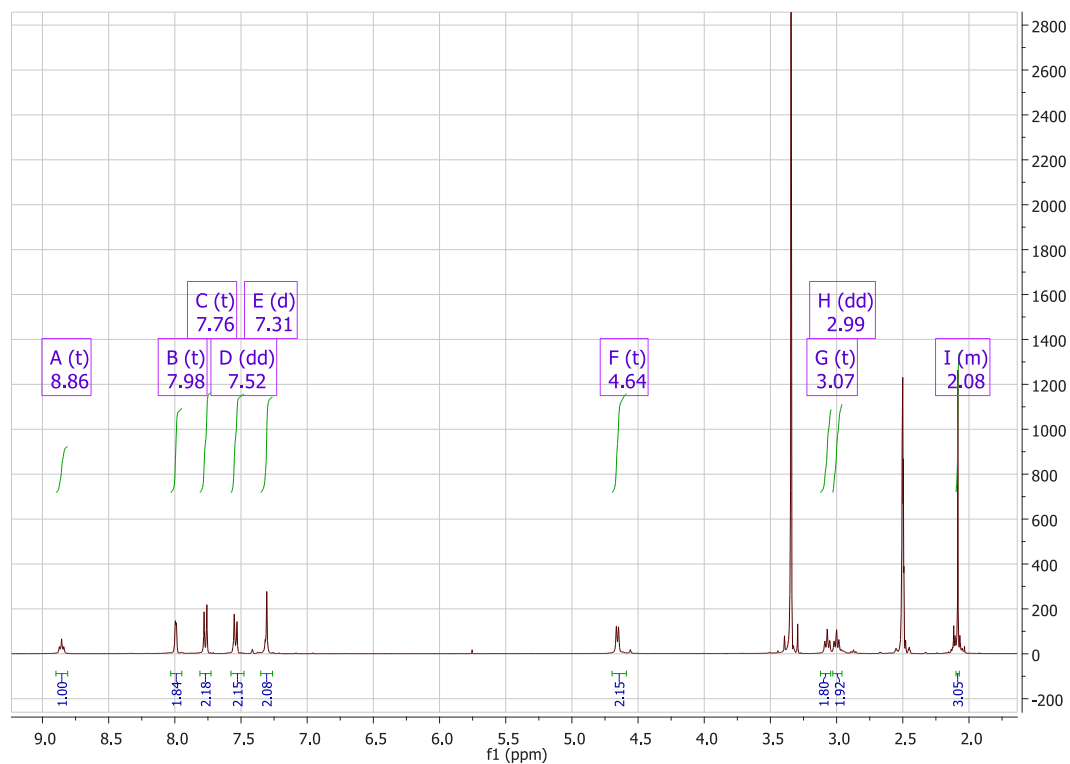
^1H NMR spectra of compound **14**



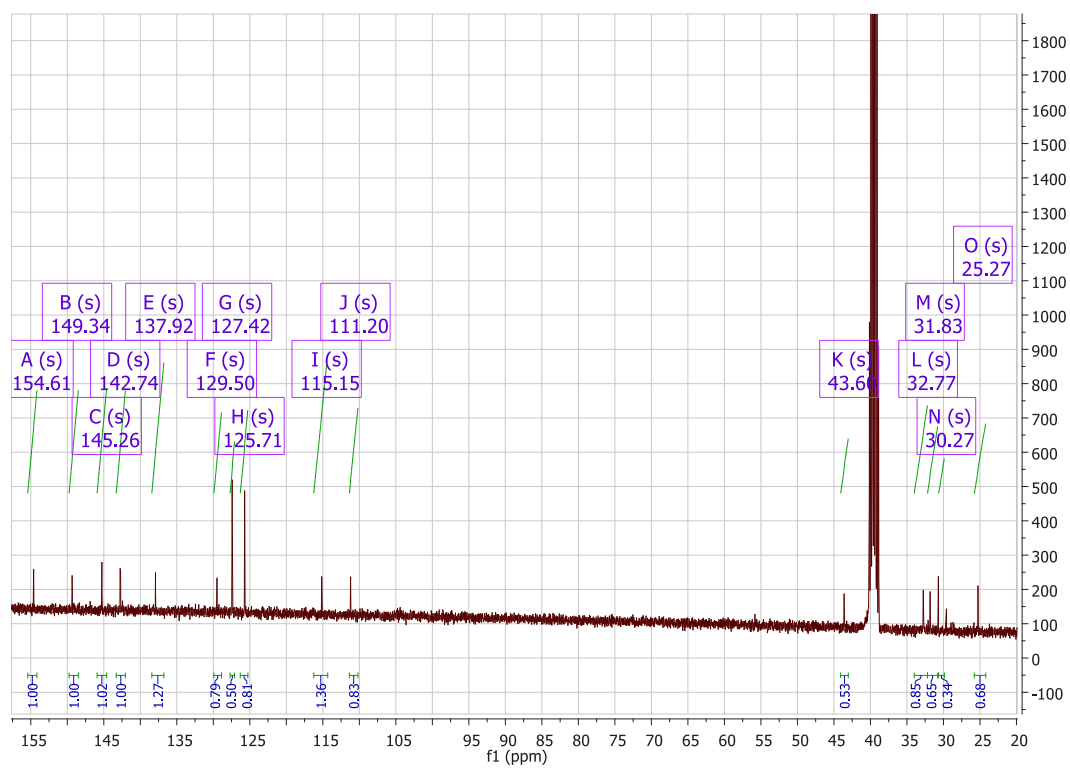
^{13}C NMR spectra of compound **14**



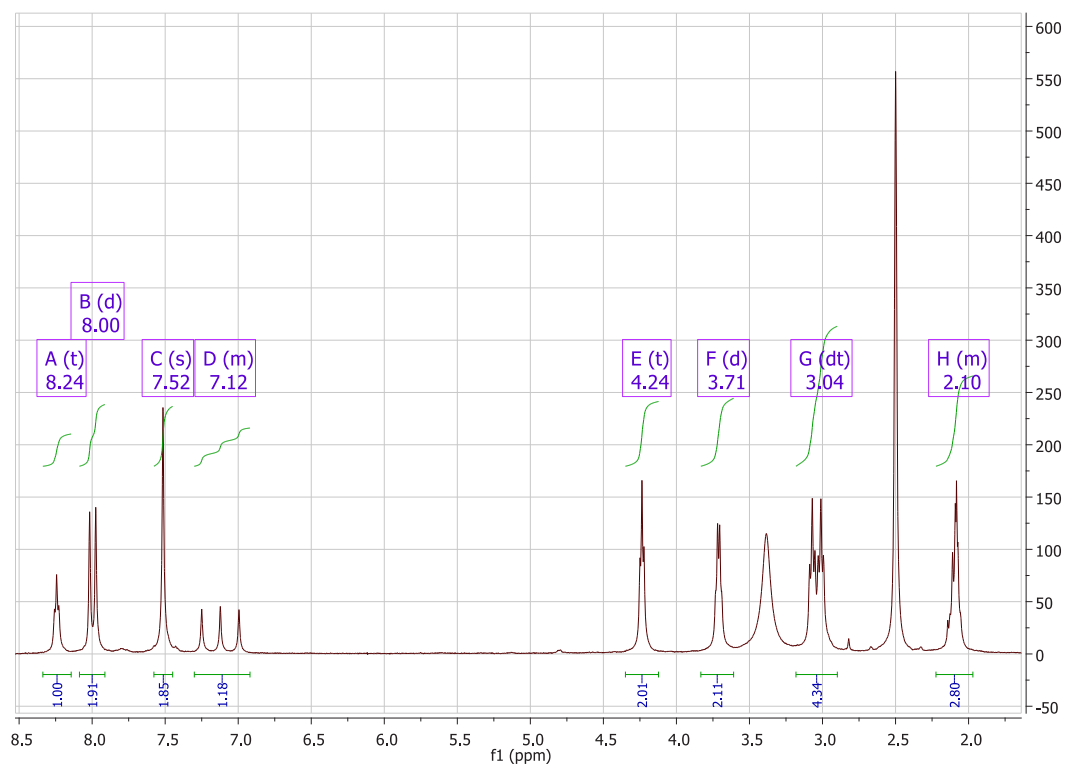
^1H NMR spectra of compound 17



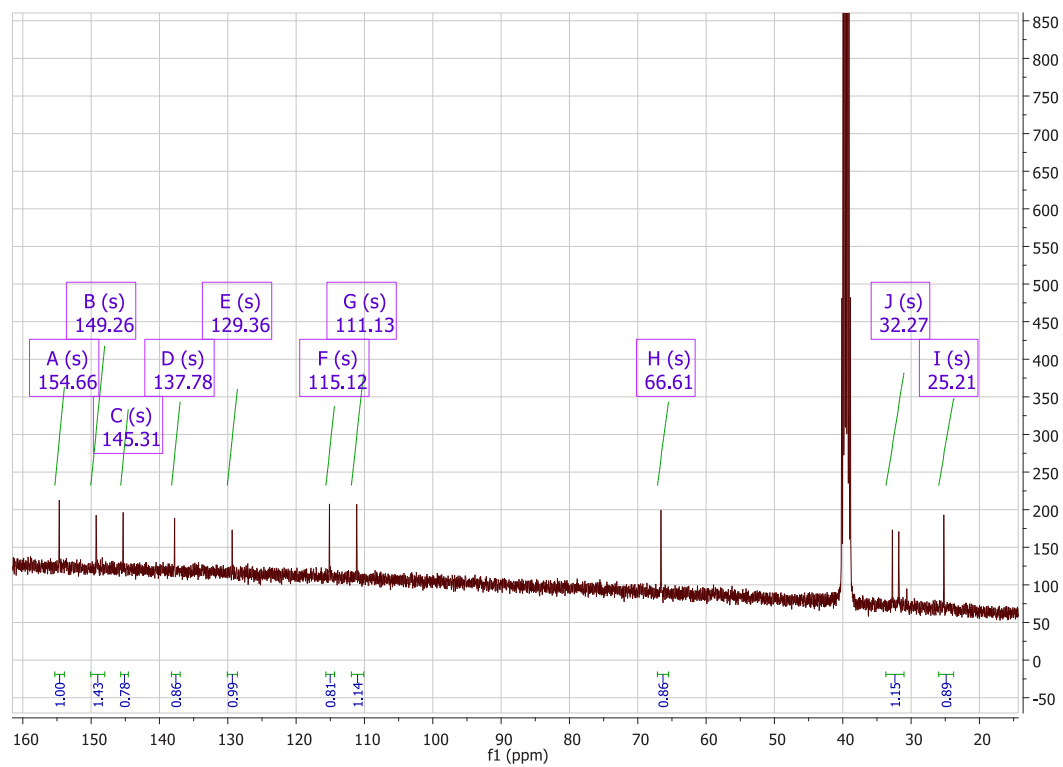
^{13}C NMR spectra of compound 17



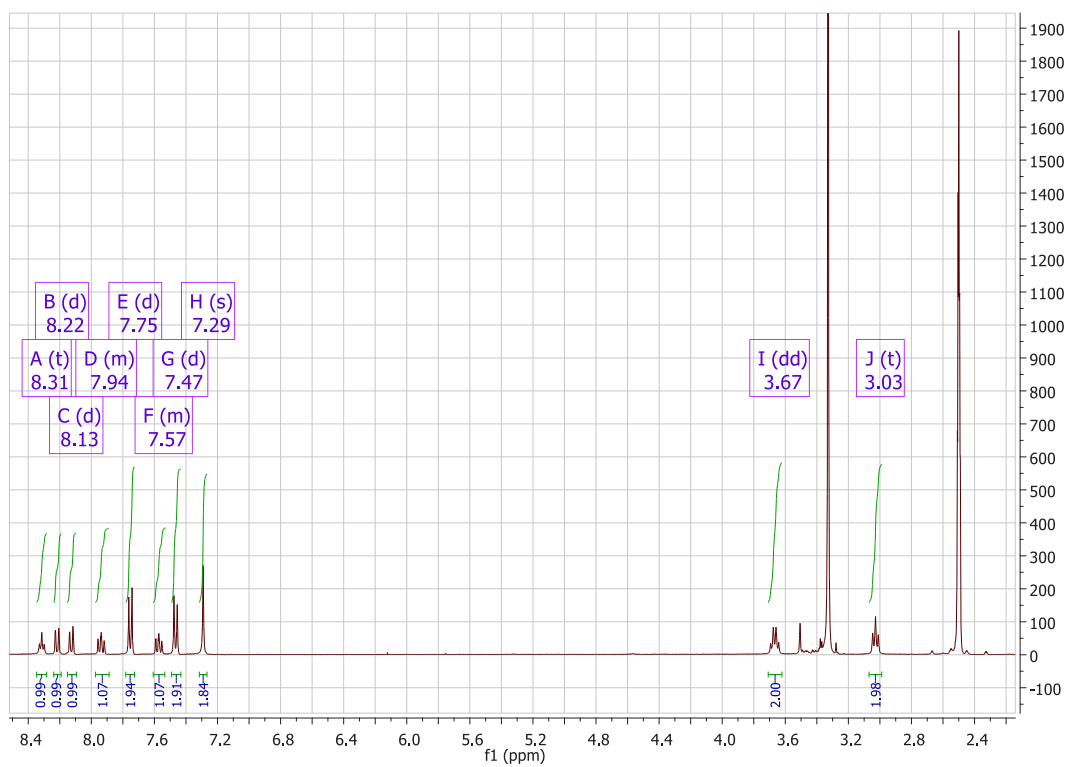
^1H NMR spectra of compound **20**



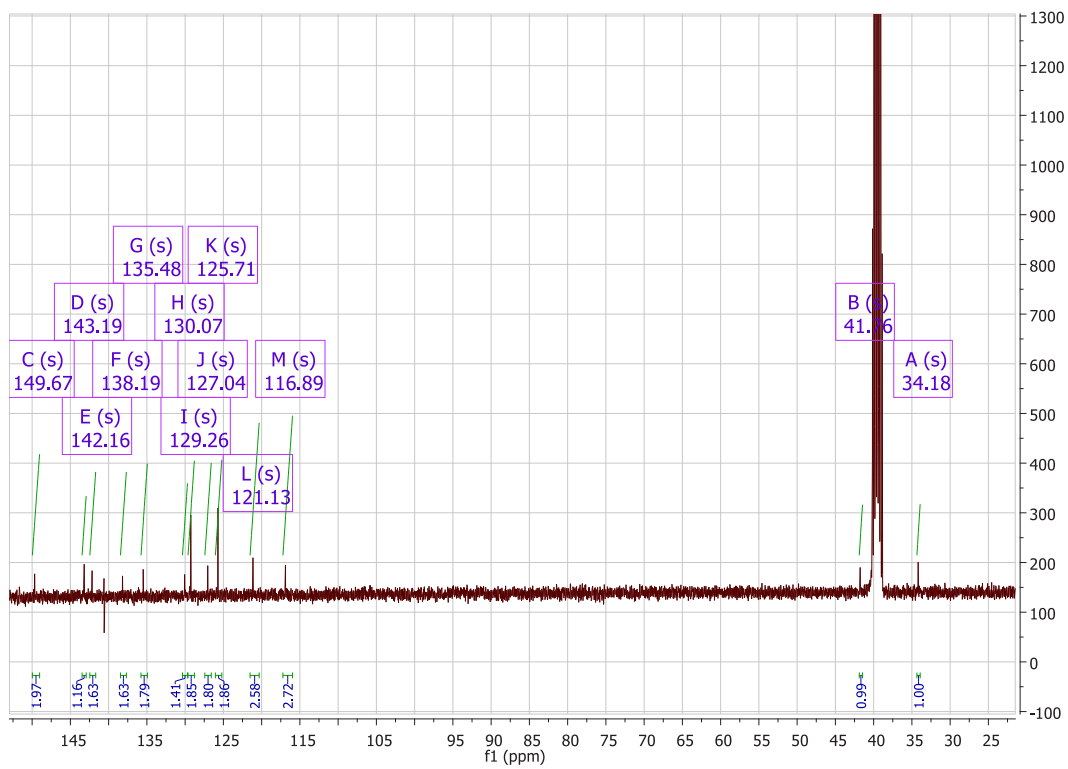
^{13}C NMR spectra of compound **20**



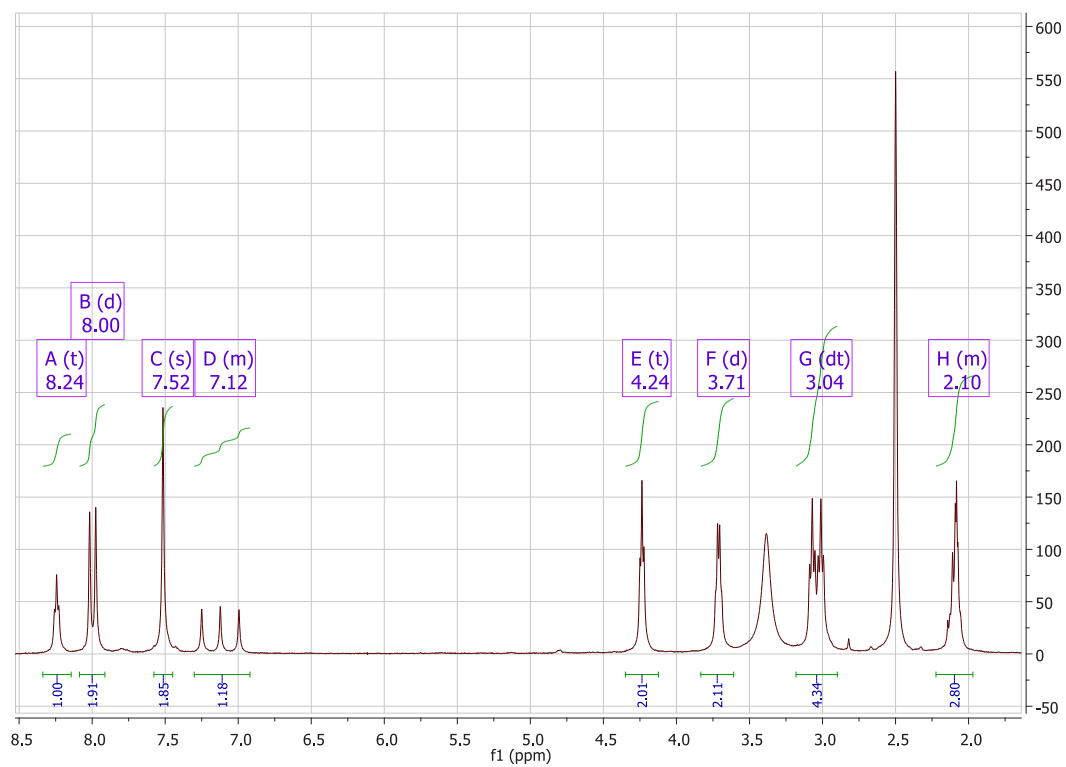
^1H NMR spectra of compound **22**



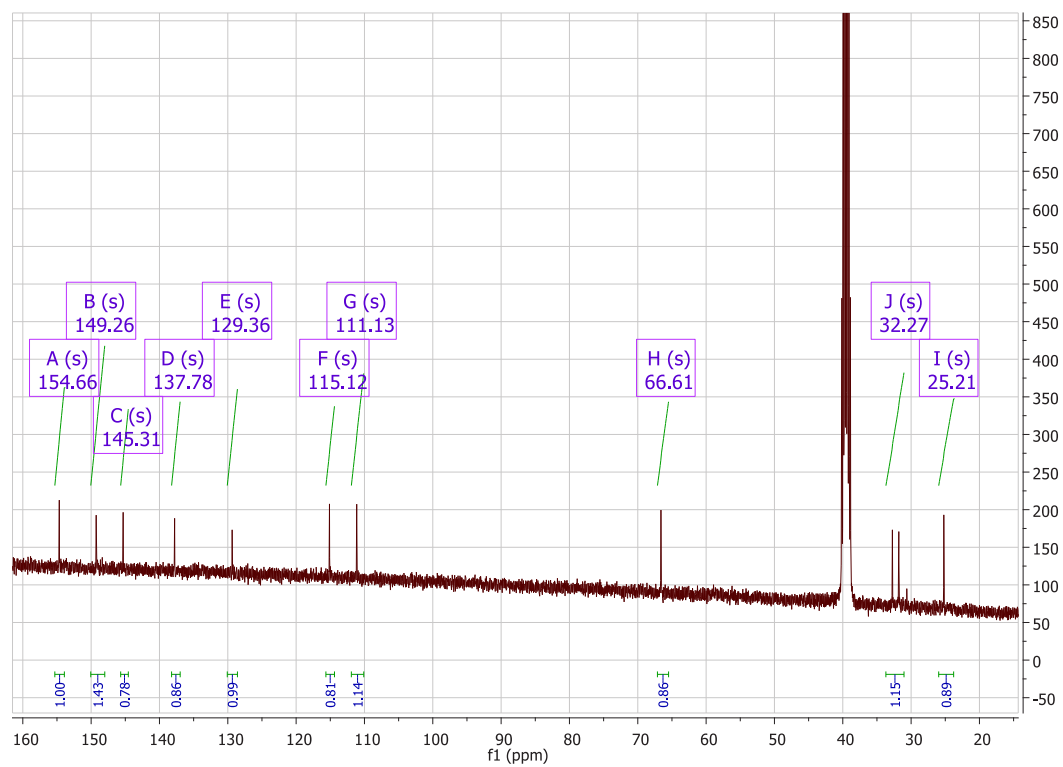
^{13}C NMR spectra of compound **22**



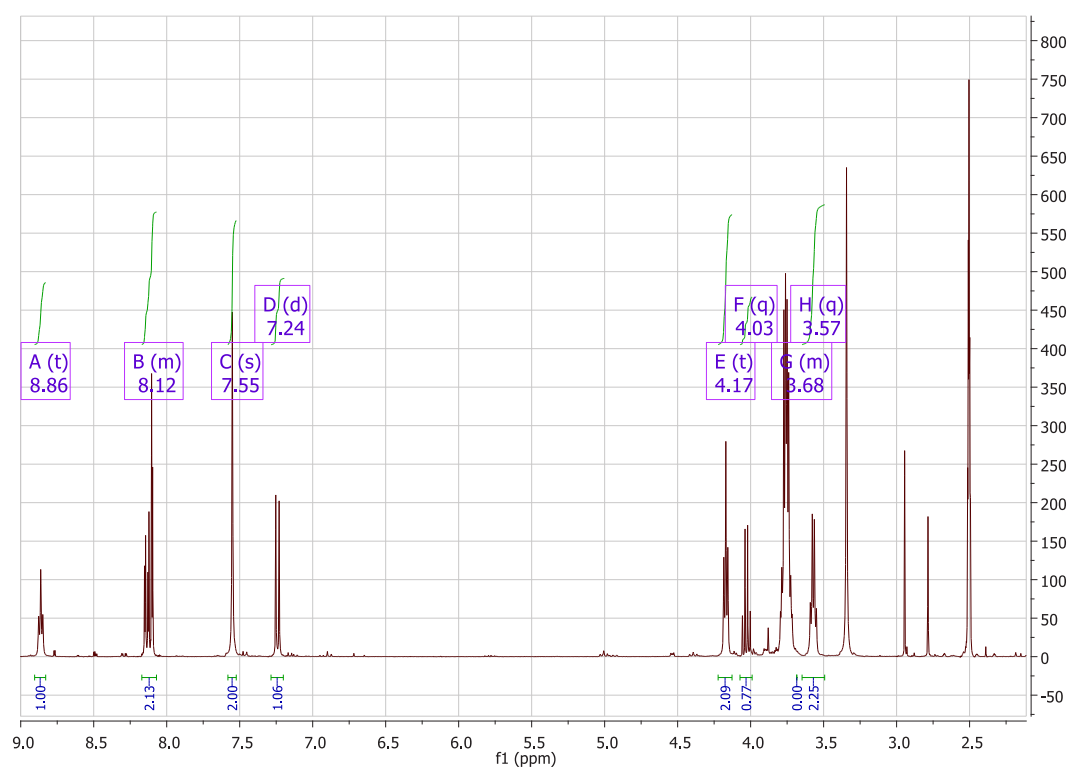
^1H NMR spectra of compound **23**



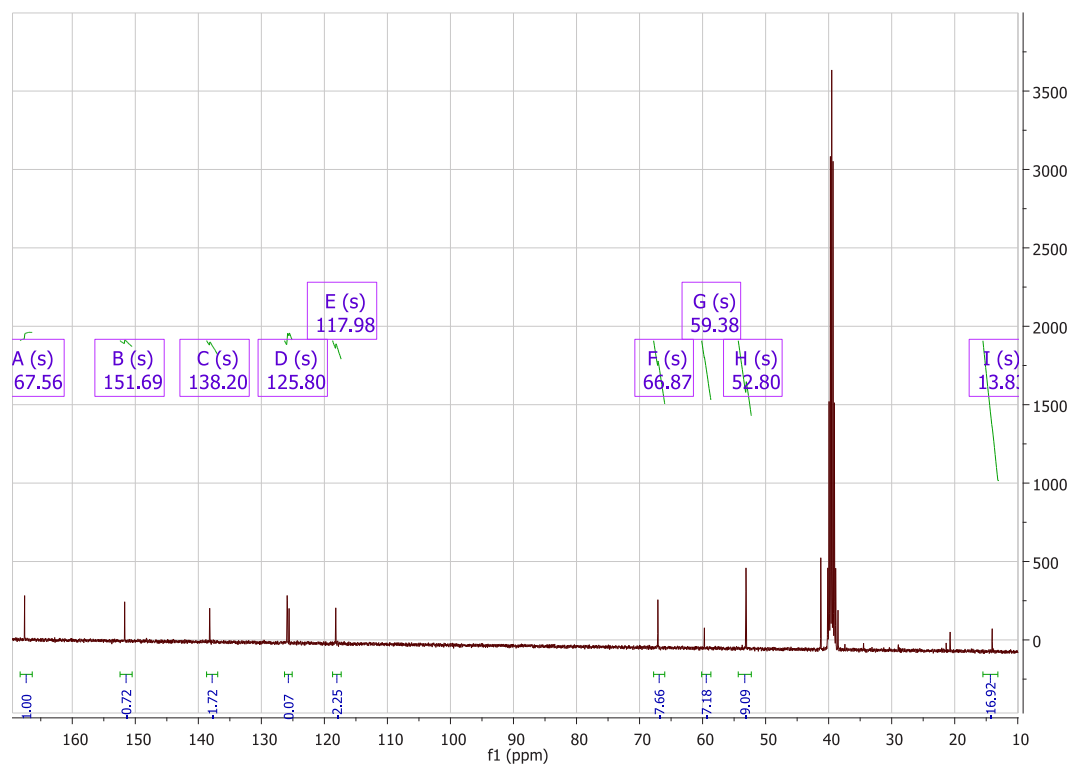
^{13}C NMR spectra of compound **23**



^1H NMR spectra of compound **25**



^{13}C NMR spectra of compound **25**



Chapter 6

Novel carbonic anhydrase IX targeting bio-reducible sulfonamides

In preparation

Nanda Kumar Parvathaneni, Raymon Niemans, Ala Yaromina, Silvia Bua, Dennis Suylen, Rianne Biemans, Natasja Lieuwes, Claudiu T. Supuran, Ludwig Dubois, Jean-Yves Winum, Philippe Lambin

Abstract

A novel class of 2-, 5-nitroimidazole and nitrogen mustard derivatives incorporating an aromatic sulfonamide with carbamate linker has been synthesized and evaluated, with the aim to design bio-reductive inhibitors targeting the hypoxia-regulated, tumor-associated carbonic anhydrase IX. Compounds showed nanomolar inhibitory activity against the physiologically relevant isoforms CAII ($K_i = 3.1$ to 83.7 nM) and CAIX ($K_i = 12.1$ to 88.7 nM). All the compounds, containing a carbamate linker, were stable to extreme acidic and basic conditions. Derivatives **1b** and **3b** displayed cytotoxicity in both HCT116 and HT29 cell lines with a respective hypoxia cytotoxicity ratio (HCR) of 2.50 and 2.74. Cell survival was not affected upon treatment with compound **1b** up to a concentration of $100 \mu\text{M}$. Compounds **2b** and **2c** were not cytotoxic but are likely to act solely as radiosensitizers. These novel bio-reducible carbamate linked aromatic sulfonamides will provide more information to the design of new classes of hypoxia selective cytotoxins and radiosensitizers in future.

Introduction

Hypoxia, i.e. low oxygen, and an acidic extracellular pH (pHe) constitute hallmarks of many solid tumors and cause resistance towards conventional treatments like chemo- and radiotherapy leading to poor patient prognosis [1]. Hypoxia inducible factor (HIF) activation is the most understood and characterized molecular response governing many of these altered metabolic pathways upon hypoxia [2, 3]. Under normoxic conditions HIF-1 α is hydroxylated by prolyl hydroxylases (PHDs) enabling subsequent binding and ubiquitylation by the von Hippel-Lindau protein (pVHL). This leads to the rapid proteasomal degradation of HIF-1 α [4-7]. Conversely, under hypoxic conditions, the PHD enzymes cannot hydrolyze HIF-1 α ; therefore stabilized HIF-1 α forms a complex with HIF-1 β and translocates into the nucleus together with the co-factor P300. In the nucleus the dimerized complex binds to the hypoxia responsive element (HRE) regions in the promoter of multiple genes, resulting in the transcription of e.g. Glucose Transporter 1 (GLUT1), Vascular Endothelial Growth Factor (VEGF) and Carbonic anhydrase IX (CAIX) to promote cellular survival during hypoxia [8, 9].

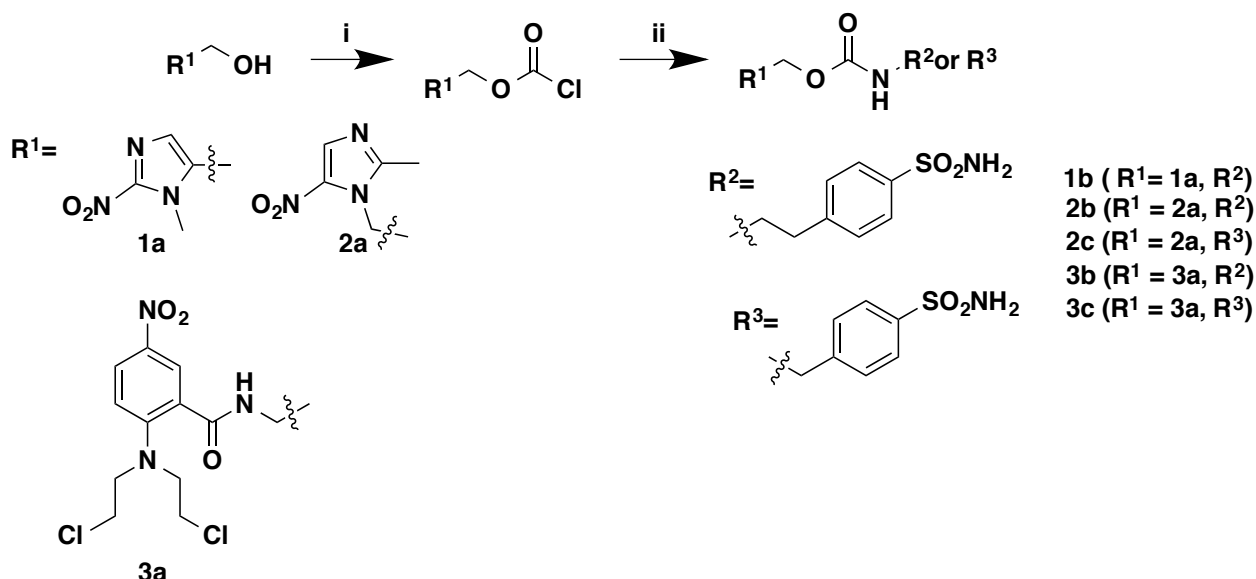
CAIX is a transmembrane isozyme amongst 16 isoforms identified so far and is involved in the cellular pH regulation by catalyzing the reversible hydration of carbon dioxide to bicarbonate and a proton. CAIX is involved in pH homeostasis, ion transport and biosynthetic processes [10, 11], as well as in tumor progression by increasing the extracellular pH [12, 13]. The predominant tumor-specific expression combined with its hypoxia-regulated transcription potentiated the use of CAIX as an endogenous hypoxia biomarker. Meta-analysis studies showed clearly that high CAIX expression is an adverse prognostic marker in solid tumors and it has been proven that CAIX is a druggable target, being inhibited by sulfonamides, sulfamides and sulfamates [14-17]. When potent and selective inhibitors block CAIX activity, pHe returns to a more physiological range and causes an increase in intracellular pH resulting in cell death. Previous reports have shown that some CA inhibitors do show anticancer activity *in vivo* [18-20]. One approach for improving the selectivity of tumor cell killing by anticancer drugs and sparing healthy cells consists of the use of bio-reducible produgs that can be selectively activated in the tumor tissue, by exploiting some of the unique aspects of tumor physiology such as hypoxia and hypoxia-associated overexpression of CAIX [21]. In fact, many examples have been

described in the literature using bio-reductive prodrugs, such as quinones, N-oxides and nitroaromatics, which are reduced by endogenous enzymes or radiation [21-25]. Until now, only a very low number of CA inhibitors have been designed for this type of application [26, 27]. Here, we report on a new class of 2-, 5-nitroimidazole and nitrogen mustards (alkylating agents) based bio-reducible drugs, harboring a CAIX inhibiting sulfonamides to target CAIX.

Results

Chemistry

Derivatives of 2-, 5- nitroimidazole and nitrogen mustard bearing aromatic sulfonamides with a carbamate linker were synthesized by converting the corresponding hydroxy group into chloroformate using phosgene, followed by reacting with amine under basic conditions (scheme 1) [28]. Synthesis yields were ranging from 46% to 83%. The new compounds were characterized extensively by spectral and physico-chemical methods, which confirmed their structures (supplementary data).



Scheme 1: Reagents and conditions: (i) Phosgene, THF, 0°C- rt; (ii) NEt₃, DMF, rt.

CA inhibition assay

All compounds reported here were assayed using the CO₂ hydrase assay as inhibitors of three physiologically relevant CA isoforms, the cytosolic hCAI and II (h = human isoform) and the transmembrane, tumor-associated hCAIX (Table 1) [29]. The clinically used sulfonamide acetazolamide (AAZ, 5-acetamido-1, 3, 4- thiadiazole-2-sulfonamide) has been taken along as standard in these measurements.

All compounds acted as inhibitors against the three isoforms hCAI, II and IX, although with varying potency (Table 1). Against the abundant, cytosolic isoform hCAI compound **3c** showed a weak inhibition potency (2180 nM). Compound **1b**

showed moderate inhibition activity towards all CA isoforms (K_I ranging from 188 to 30.5 nM), while compounds **2b** and **2c** strongly inhibited all CA isoforms (K_I ranging from 2.3 to 14.1 nM). Although compounds **2b** and **2c** are both 5-nitroimidazole derivatives, slight differences in the selectivity ratios hCAII over hCAIX (**2b**= 0.35, **2c**= 0.28) of these compounds might be explained by the substitution of different aromatic sulfonamides. Compounds **3b** and **3c** showed moderate inhibition towards hCAIX, compound **3b** binding with CAII was very tight (3.1 nM). The large difference in binding capacity or selectivity ratios (**3b**= 0.09, **3c**= 0.94) of compounds from the same family (nitrogen mustard) supports the substitution effect on the carbamate linker. Nevertheless, considering the difficulty to obtain small compounds with a better affinity for the tumor-associated isozymes (CAIX and CAXII) over CAII, the selectivity obtained for these series is comparable or better than those of the clinically used CA inhibitor acetazolamide.

Table 1: Inhibition data obtained using a stopped flow CO₂ hydrase assay for hCAI, hCAII, hCAIX with the synthesized compounds and the sulfonamide inhibitor acetazolamide (**AAZ**).

Compounds	K_I (nM) *			Selectivity ratio
	hCAI	hCAII	hCAIX	K_I hCAII/ K_I hCAIX
1b	188.3	36.5	30.5	1.19
2b	3.7	4.3	12.1	0.35
2c	2.3	4.0	14.1	0.28
3b	83.0	3.1	32.3	0.09
3c	2179.9	83.7	88.7	0.94
AAZ	250	12.0	25	0.48

* Mean from 3 different assays (errors in the range of \pm 5-10 % of the reported values).

Stability of carbamate linker under acidic conditions

Stability to chemical hydrolysis of compounds **1b–3c** was evaluated by measuring peak area or retention time of the compound after incubation at varying pH conditions up to 8 hours. No degradation was observed at any pH condition for all tested compounds, indicating significant stability (Figure 1). Additionally, all tested compounds were found to be stable for at least 8 h to harsh acid-catalyzed hydrolysis (pH = 2.0, 37 °C, data not shown). Literature studies have shown that the electron-

withdrawing nitro group conjugated with the carbamate linker resulted in a remarkable decrease in stability, which may explain the apparent low inhibitory potency of these compounds toward FAAH, due to decomposition under the assay conditions [30]. Of all compounds (**1b-3c**), the nitro group was not in direct conjugation with the carbamate linker, thereby showing no stability loss when incubated under various pH conditions.

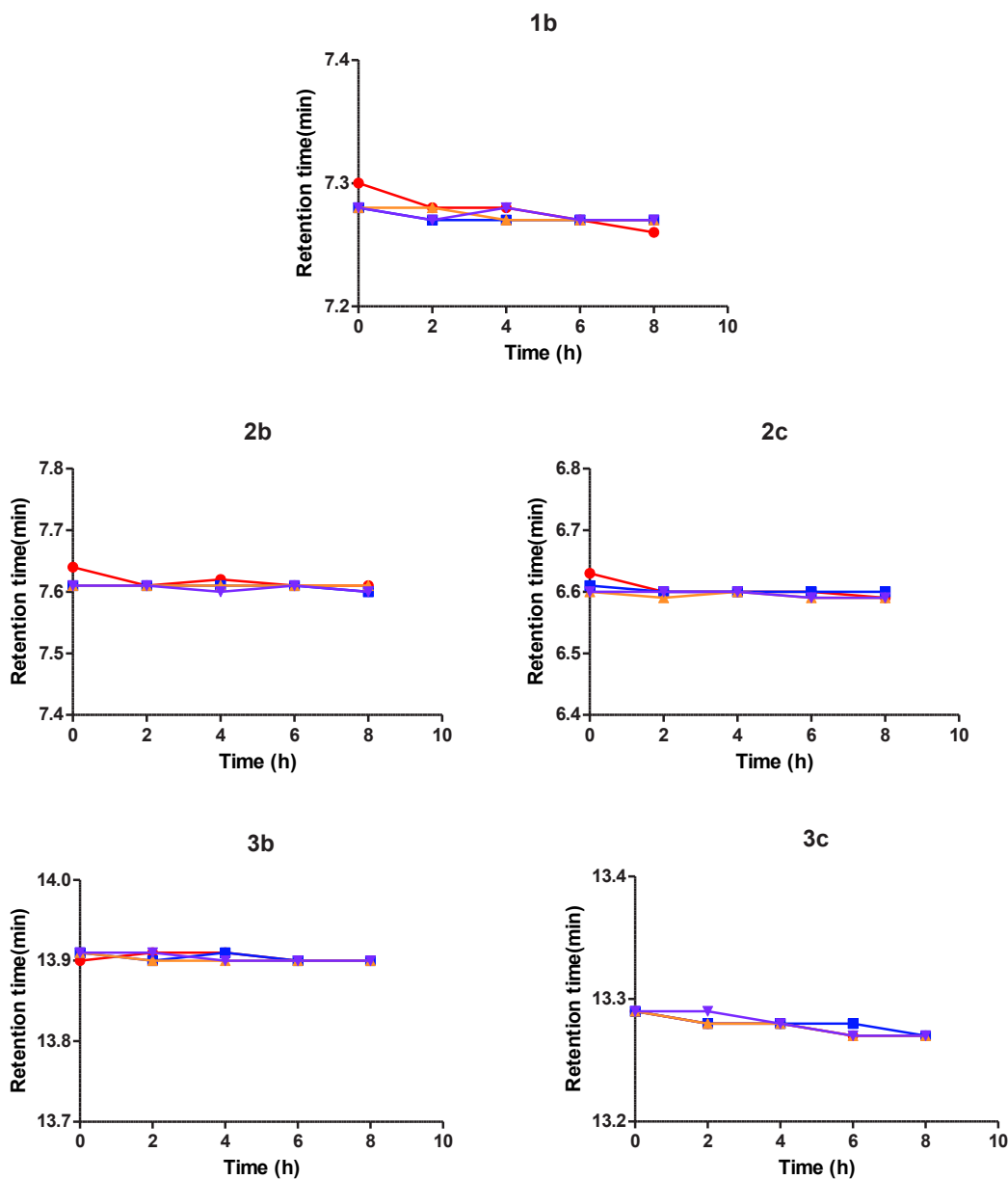


Figure. 1: Chemical stability over time of compounds (**1b**, **2b**, **2c**, **3b**, **3c**) under different pH. 6.2 (red), 6.6 (blue), 7.0 (orange) and 7.4 (violet). Peak areas were similar at different time points indicating no hydrolysis of the carbamate linker.

Biology

The cytotoxicity of all compounds (**1b-3c**) was determined in a panel of human tumor cell lines. Compound **1b** showed an IC_{50} of 204.5 μ M ($p < 0.0001$) in HT29 cells under anoxia (IC_{50A}) and no detectable cytotoxicity ($IC_{50} >$ highest tested concentration) was observed under normoxia (Figure 2). Furthermore, in HCT116 cells compound **1b** resulted in an IC_{50} of 148.6 μ M and 59.3 μ M under normoxic and anoxic

conditions respectively, resulting in a hypoxia selectivity cytotoxicity ratio (HCR) of 2.5 (Table 2). All other compounds, except compound 3b in HCT116 cells, did not show any cytotoxicity for the tested concentrations. Compound **3b** resulted in a cell dependent cytotoxicity with a HCR of 2.7 in HCT116 cells, while no cytotoxicity in HT29 cells was observed.

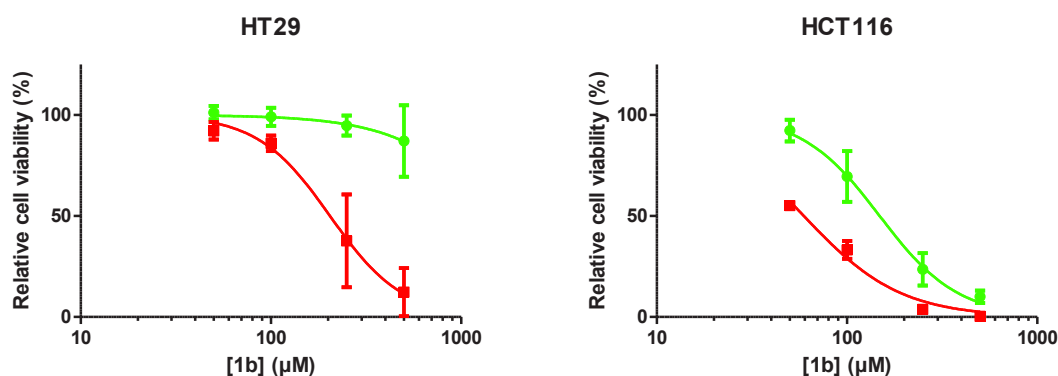


Figure 2: Relative cell viability (%) in HT29 and HCT116 cells exposed to increasing concentrations of the derivative **1b** under normoxic (green) and anoxic (red) conditions. Data represent the average \pm SEM of three independent biological repeats.

Table 2: HCR of all compounds IC_{50N} vs IC_{50A}

Compounds	HT29			HCT116		
	IC_{50N}	IC_{50A}	HCR (IC_{50N}/IC_{50A})	IC_{50N}	IC_{50A}	HCR (IC_{50N}/IC_{50A})
1b	> 500	204.5	>2.44	148.6	59.36	2.50
2b	>500	>500	-	>500	>500	-
2c	>500	>500	-	>500	>500	-
3b	>500	>500	-	267.1	97.27	2.74
3c	>500	>500	-	>500	>500	-

Abbreviations: IC_{50} : Concentration of an inhibitor where the response is reduced by half; Normoxia (N); Anoxia (A); Hypoxia selectivity cytotoxicity ratio (HCR).

Based on its selective cytotoxicity under anoxia in both cell lines, Compound **1b** was selected for further studies investigating its effects on cell survival. Compound **1b** did not reduce clonogenic cell survival under normoxia or anoxia for the tested concentrations (Figure 3). TH-302, a 2-nitroimidazole based hypoxia-activated prodrug-alkylating agent [31] was used as positive control (data not shown).

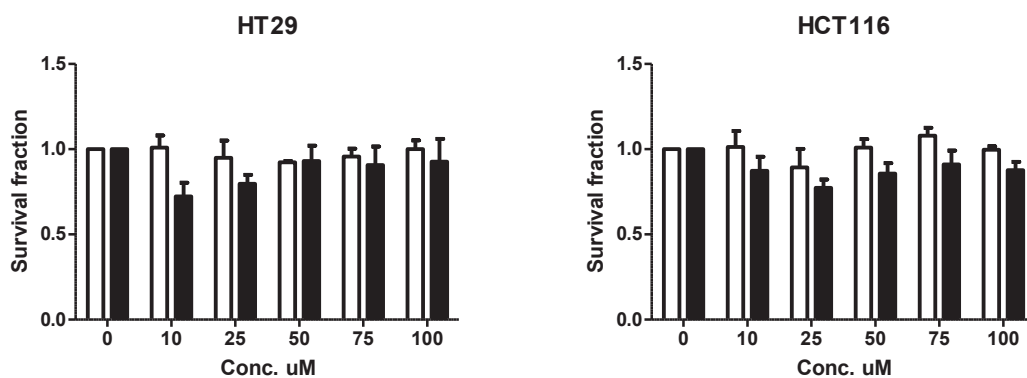


Figure 3: Clonogenic cell survival of HT29 and HCT116 cells during normoxia (white bars) and anoxia (black bars) when exposed to compound **1b**. Data represent the average \pm SEM of three independent biological repeats.

Discussion

In the present study we reported the design and synthesis of a series of novel bio-reducible 2-, 5-nitroimidazole and nitrogen mustards incorporating an aromatic sulfonamide to target the hypoxia-activatable CAIX. Such compounds may be reduced enzymatically (or chemically) under reducing conditions present in hypoxic tumors. 2- and 5-nitroimidazoles are known to be reduced under hypoxic conditions and serve as efficient radiosensitizers [32]. In our study, only the 2-nitroimidazole derivative **1b** was cytotoxic in both cell lines. This cytotoxicity might be explained by the higher reduction potential of 2-nitroimidazoles compared to those of the 5-nitroimidazoles. This raises the prospect of a “mixed mechanism” of radiosensitization and hypoxia selective cytotoxicity, which is also seen with the clinically tested misonidazole and etanidazole [32-34]. Whether **1b** also leads to normal tissue toxicity remains to be determined. The 5-nitroimidazole derivatives **2b** and **2c** were less cytotoxic and are therefore more likely to act solely as radiosensitizers [32]. Work is in progress to determine this radiosensitizing efficacy. The clonogenic survival efficacy of compound **1b** was evaluated in HT29 and HCT116 cell lines in a range of concentrations (10 to 100 μ M) acquired from IC₅₀ values of anoxia. Surprisingly derivative **1b** did not show any reduction in cell survival in both cell lines. This might be explained by the fact that a reduction in cell survival should happen at higher concentrations (for which experiments are under progress), or compound **1b** does not have significant effect on cell survival at all. In future experiments, combination of radiation and compound **1b** might show a reduction in cell survival [32]. Nitrogen mustards are well-known hypoxia-activated prodrugs and are reduced by nitroreductases or oxidoreductases present in hypoxic tumors [35]. The nitrogen mustard derivative **3b** was effective in a highly cell dependent manner, being effective under normoxia and anoxia only in the HCT116 cell line. This might be explained by the low concentration tested or by a differential expression of aromatic nitroreductases between both cell lines [36, 37]. Derivative **3c** did not show any cytotoxicity, which might be explained by the substitution of the aromatic sulfonamide on the nitrogen mustard [37].

We have identified a new 2-nitroimidazole-based sulfonamide with a carbamate linker with a high hypoxia cytotoxicity ratio in both cell lines tested, which is stable under hostile acidic and basic conditions. Our future studies aim to optimize the

radiosensitizing efficacy of **2b** and **2c** and further explore the cytotoxic properties of **1b**. Work is in progress to find out the reduction potentials and radiosensitizing efficacy of all compounds.

Experimental section

Chemistry

General. All reagents and solvents were of commercial quality and used without further purification unless otherwise specified. All reactions were carried out under an inert atmosphere of nitrogen. TLC analyses were performed on silica gel 60 F254 plates (Merck Art. no. 1.05554). Spots were visualized under 254 nm UV illumination or by ninhydrin solution spraying. Melting points were determined on a Büchi Melting Point 510 and are uncorrected. ^1H and ^{13}C NMR spectra were recorded on a Bruker DRX-400 spectrometer using $\text{DMSO-}d_6$ as solvent and tetramethylsilane as internal standard. For ^1H and ^{13}C NMR spectra, chemical shifts are expressed in δ (ppm) downfield from tetramethylsilane, and coupling constants (J) are expressed in hertz. Electron Ionization mass spectra were recorded in positive or negative mode on a Water MicroMass ZQ. All compounds that were tested in the biological assays were analyzed by high-resolution ESI mass spectra (HRMS) using a Q-ToFI mass spectrometer fitted with an electrospray ion source in order to confirm the purity of >95%.

General procedure for preparation of chloroformate: The corresponding hydroxy starting compound (**1a**, **2a** and **3a**) (2 mmol) in tetrahydro furan (10 mL) was added to phosgene (4mL, 8 mmol) and THF (15mL) at 0°C. The reaction was stirred for 16 h, then the solvent was removed *in vacuo*. The crude chloroformate was used without further purification.

General procedure for synthesis of 1b, 2b, 2c, 3b, and 3c: A suspension of chloroformate (23.4 mmol) in dry THF (100 ml) was treated with trimethylamine (50 mmol). The corresponding amine (23.4 mmol) was added afterwards and the reaction was stirred overnight at room temperature. The solvent was removed *in vacuo*. The residue was dissolved in chloroform and washed with 1.0 N sodium hydroxide (2X) and water. The organic phase was dried over sodium sulfate, filtered and concentrated under vacuum. The residue was purified by chromatography on silica gel using methylene chloride–methanol 98:2 as eluent.

(1-methyl-2-nitro-1H-imidazol-5-yl) methyl (4-sulfamoylphenethyl) carbamate (1b):

^1H NMR (400 MHz, $\text{DMSO-}d_6$) δ 7.73 (d, $J = 8.3$, 2H), 7.48 (t, $J = 5.6$, 1H), 7.38 (d, $J = 8.3$, 2H), 7.30 (s, 2H), 7.21 (s, 1H), 5.12 (s, 2H), 3.89 (s, 3H), 3.26 (dd, $J = 13.2, 6.7$, 2H), 2.79 (t, $J = 7.1$, 2H). ^{13}C

NMR (101 MHz, DMSO-*d*₆) δ 155.36, 145.99, 143.42, 142.09, 133.83, 129.17, 128.41, 125.68, 54.82, 48.62, 34.69, 34.16 – 33.11. MS (ESI⁺/ESI⁻) *m/z* 384.10 [M+H]⁺

2-(2-methyl-5-nitro-1*H*-imidazol-1-yl) ethyl (4-sulfamoylphenethyl) carbamate (2b):

¹H NMR (400 MHz, DMSO) δ 8.03 (s, 1H), 7.73 (d, *J* = 8.3, 2H), 7.38 – 7.32 (m, 3H), 7.31 (s, 2H), 4.48 (t, *J* = 4.9, 2H), 4.30 (t, *J* = 4.9, 2H), 3.17 (dd, *J* = 13.1, 6.7, 2H), 2.72 (t, *J* = 7.1, 2H), 2.39 (s, 3H). ¹³C NMR (101 MHz, DMSO) δ 155.69, 151.86, 143.61, 142.11, 138.56, 133.18, 129.26, 125.81, 61.93, 35.01, 14.02. MS (ESI⁺/ESI⁻) *m/z* 398.23 [M+H]⁺

2-(2-methyl-5-nitro-1*H*-imidazol-1-yl) ethyl (4-sulfamoylbenzyl) carbamate (2c):

¹H NMR (400 MHz, DMSO-*d*₆) δ 8.04 (s, 1H), 7.88 (t, *J* = 6.1, 1H), 7.76 (d, *J* = 8.4, 2H), 7.34 (d, *J* = 8.4, 2H), 7.32 (s, 2H), 4.54 (t, *J* = 5.0, 2H), 4.36 (t, *J* = 5.0, 2H), 4.19 (d, *J* = 6.1, 2H), 2.44 (s, 3H). ¹³C NMR (101 MHz, DMSO-*d*₆) δ 155.87, 151.72, 143.53, 142.68, 138.45, 133.07, 127.26, 125.65, 62.11, 45.52, 43.37, 13.98. MS (ESI⁺/ESI⁻) *m/z* 384.22 [M+H]⁺

2-(2-(bis(2-chloroethyl)amino)-5-nitrobenzamido)ethyl (4-sulfamoylphenethyl)carbamate (3b):

¹H NMR (400 MHz, DMSO-*d*₆) δ 8.72 (t, *J* = 5.3, 1H), 8.15 – 8.05 (m, 2H), 7.73 (d, *J* = 8.1, 2H), 7.39 (t, *J* = 6.9, 2H), 7.29 (s, 2H), 7.23 (s, 0H), 7.21 (s, 0H), 4.11 (t, *J* = 5.4, 2H), 3.74 (dt, *J* = 9.9, 4.9, 8H), 3.46 (d, *J* = 5.4, 3H), 3.25 (dd, *J* = 13.8, 6.5, 2H), 2.80 (t, *J* = 7.3, 2H). ¹³C NMR (101 MHz, DMSO-*d*₆) δ 167.45, 156.11, 151.59, 143.54, 142.05, 138.21, 129.11, 126.33 – 123.92, 118.08, 62.04, 59.78, 53.12, 41.38, 34.44, 31.23, 30.39. MS (ESI⁺/ESI⁻) *m/z* 577.3 [M+H]⁺

2-(2-(bis(2-chloroethyl)amino)-5-nitrobenzamido)ethyl (4-sulfamoylbenzyl)carbamate (3c):

¹H NMR (400 MHz, DMSO) δ 8.75 (t, *J* = 5.5, 1H), 8.17 – 8.08 (m, 2H), 7.80 (dd, *J* = 12.0, 5.9, 1H), 7.76 (d, *J* = 8.2, 2H), 7.43 (d, *J* = 8.1, 2H), 7.31 (s, 2H), 7.23 (d, *J* = 9.1, 1H), 4.26 (t, *J* = 8.1, 2H), 4.15 (t, *J* = 5.2, 2H), 3.80 – 3.69 (m, 8H), 3.17 (s, 2H). ¹³C NMR (101 MHz, DMSO) δ 167.56, 156.53, 151.68, 143.90, 142.68, 138.32, 127.41, 125.76, 117.97, 56.19, 53.22, 48.69, 41.33, 21.08. MS (ESI⁺/ESI⁻) *m/z* 563.13 [M+H]⁺

In vitro chemical stability and analytical method

The chemical stability of the compounds **1b**, **2b**, **2c**, **3b** and **3c** at various pH (6.2, 6.6, 7.0 and 7.4) was measured on a Waters XEVO QTOF G2 Mass Spectrometer, with an Acquity H-class solvent manager, FTN-sample manager and TUV-detector. The system was equipped with a reversed phase C18-column (Waters, acquity PST 130A, 1.7μm 2.1 x 50mm i.d.), column temperature 40 degrees. Mobile phases consisted of 0.1% formic acid in water and 90% acetonitrile. FTN-purge solvent was 5% acetonitrile in water. Mobile phase gradient was maintained starting with 5% acetonitrile to 50% acetonitrile for 15 minutes at 220nm wavelength. Stock solutions

of compounds were prepared in DMSO and each sample was incubated at a final concentration of 1–5 μM in pre-thermostated buffered solution. The final DMSO concentration in the samples was kept at 1%. The samples were maintained at 37 °C in a temperature-controlled shaking water bath (60 rpm). At various time points, 100 μL aliquots were removed and injected into the High Performance Liquid Chromatography (HPLC) system for analysis. Mass was measured in positive sensitivity mode; mass range between 100 and 1000 Da.

CA inhibition assays

The CA-catalyzed CO_2 hydration activity was measured using an Applied Photophysics stopped-flow instrument [29]. To maintain ionic strength, Na_2SO_4 (20 mM) was used with HEPES (20 mM, pH 7.5) as a buffer and Phenol red (0.2 mM) as an indicator working at the maximum absorbance of 557 nm, which was used to follow the initial rates of the CA-catalyzed CO_2 hydration for duration of 10–100 s. To determine the kinetic parameters and inhibition constants varying CO_2 concentrations were included (1.7–17 mM). Initial velocity was assayed with at least six traces of the initial 5–10% of the reaction for each compound. Compounds were dissolved in distilled-deionized water (0.01 nM). The combined enzyme solutions and compounds were incubated for 15 min at room temperature to allow for the E-I complex formation prior to measurements. The nonlinear least-squares method of PRISM 3 was used to estimate the inhibition constants and the mean of three independent estimations is reported. The CA isoforms included are recombinant proteins obtained in house.

Biological assays

Cells

Human colorectal HCT116 and HT29 carcinoma cells were cultured in DMEM (Lonza) supplemented with 10% fetal bovine serum and 1% PenStrep. Cells were exposed to anoxic conditions for 24 h in a hypoxic chamber (MACS VA500 microaerophilic workstation, Don Whitley Scientific, UK) with an atmosphere consisting of $\leq 0.02\%$ O_2 , 5% CO_2 and residual N_2 . Normoxic cells were grown in regular incubators with 21% O_2 , 5% CO_2 at 37 °C.

Cell viability assays

The cytotoxic efficacy of the bio-reducible derivatives was determined based on cell viability assays using alamarBlue® (Invitrogen). In short, HT29 and HCT116 were seeded in 96-well plates and allowed to attach overnight. The next day plates were exposed to normoxia or anoxia and medium was replaced with pre-incubated normoxic or anoxic DMEM. Compounds were dissolved in DMSO (0.5%, Sigma-Aldrich) and final concentrations were made with pre-incubated anoxic or normoxic DMEM and added to the wells after 24 h of exposure. Cells were exposed to compounds for a total of 2 h, after which medium was washed off and replaced with fresh medium. Cells were allowed to grow for an additional 72 h under normoxic conditions prior to measurement. Cells were incubated with alamarBlue® for 2 h during normoxic conditions, which corresponds with their metabolic function, a measure for cell viability. Fluorescence was measured using plate reader (FLUOstar Omega, BMG LABTECH) using a fluorescence excitation wavelength of 540- 580 nm.

Clonogenic assays

Clonogenic survival of HT29 and HCT116 cells were seeded with high density for CAIX-dependent extracellular acidification [38]. Compound **1b** doses were selected from corresponding IC_{50} (anoxic/normoxic) ranging from 10 to 100 μ M for preliminary experiments. These cells were exposed to 23:30 h normoxic or anoxic conditions and 30 min to drugs after which cells were trypsinized and reseeded in triplicate with known cell numbers. Cells were allowed to grow for 9 (HCT116) and 14 (HT29) days to form colonies that were quantified after staining and fixation with 0.4% methylene blue in 70% ethanol. Surviving fractions were calculated and compared to control survival curves produced in the same experiment without compound treatment.

Statistical analyses

GraphPad Prism (version 5.03) was used for all statistical analyses. For the cytotoxic compounds IC_{50} values were estimated with the curve of the log (inhibitor) vs. normalized response (Variable slope).

Reference

1. Patiar, S. and A.L. Harris, *Role of hypoxia-inducible factor-1alpha as a cancer therapy target*. *Endocr Relat Cancer*, 2006. **13 Suppl 1**: p. S61-75.
2. Schofield, C.J. and P.J. Ratcliffe, *Oxygen sensing by HIF hydroxylases*. *Nature reviews. Molecular cell biology*, 2004. **5**(5): p. 343-54.
3. Leochler, E., *Environmental carcinogens and Mutagens*. www.els.net (standard article), 2003.
4. Maxwell, P.H., et al., *The tumour suppressor protein VHL targets hypoxia-inducible factors for oxygen-dependent proteolysis*. *Nature*, 1999. **399**(6733): p. 271-5.
5. Berra, E., et al., *Hypoxia-inducible factor-1 alpha (HIF-1 alpha) escapes O(2)-driven proteasomal degradation irrespective of its subcellular localization: nucleus or cytoplasm*. *EMBO Rep*, 2001. **2**(7): p. 615-20.
6. Ivan, M., et al., *HIF1alpha targeted for VHL-mediated destruction by proline hydroxylation: implications for O2 sensing*. *Science*, 2001. **292**(5516): p. 464-8.
7. Kondo, K., et al., *Inhibition of HIF is necessary for tumor suppression by the von Hippel-Lindau protein*. *Cancer Cell*, 2002. **1**(3): p. 237-46.
8. Denko, N.C., *Hypoxia, HIF1 and glucose metabolism in the solid tumour*. *Nature reviews. Cancer*, 2008. **8**(9): p. 705-13.
9. Wouters, B.G. and M. Koritzinsky, *Hypoxia signalling through mTOR and the unfolded protein response in cancer*. *Nature reviews. Cancer*, 2008. **8**(11): p. 851-64.
10. Pastorekova, S.P., J., *Cancer-Related Carbonic Anhydrase Isozymes*. In *Carbonic Anhydrase. Its Inhibitors and Activators*; Supuran, C. T., Scozzafava, A., Conway, Eds.; CRC Press: Boca Raton, FL, 2004: p. 253-280.
11. Supuran, C.T., A. Scozzafava, and A. Casini, *Carbonic anhydrase inhibitors*. *Medicinal research reviews*, 2003. **23**(2): p. 146-89.
12. Kurtz, I., *Molecular mechanisms and regulation of urinary acidification*. *Compr Physiol*, 2014. **4**(4): p. 1737-74.
13. Kato, Y., et al., *Acidic extracellular microenvironment and cancer*. *Cancer Cell Int*, 2013. **13**(1): p. 89.
14. van Kuijk, S.J., et al., *Prognostic Significance of Carbonic Anhydrase IX Expression in Cancer Patients: A Meta-Analysis*. *Front Oncol*, 2016. **6**: p. 69.

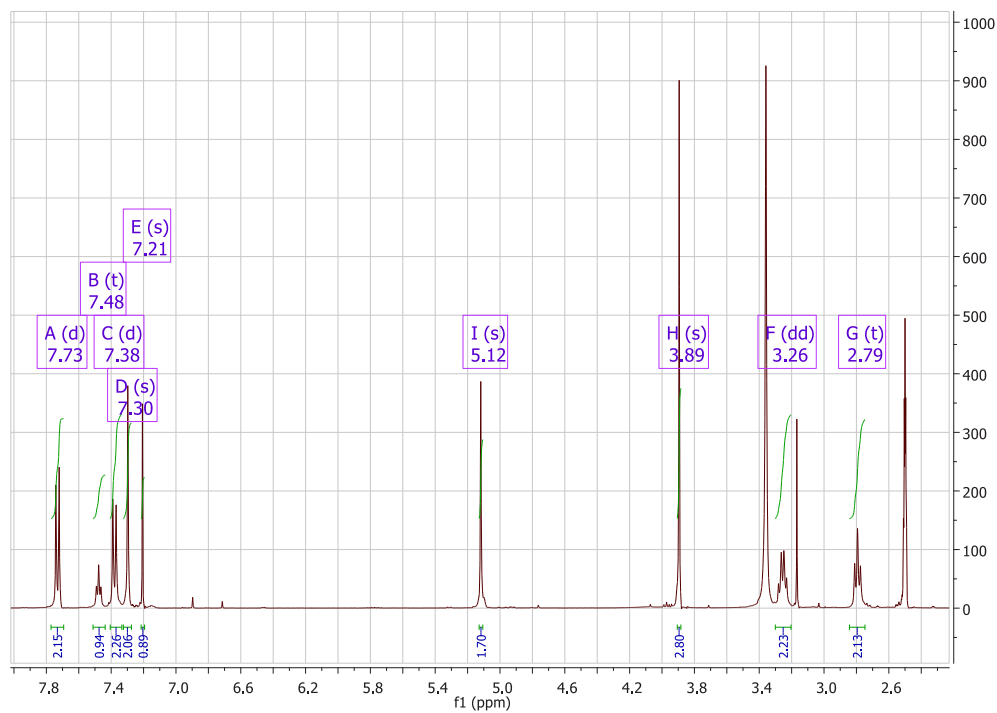
15. Svastova, E., et al., *Hypoxia activates the capacity of tumor-associated carbonic anhydrase IX to acidify extracellular pH*. FEBS Lett, 2004. **577**(3): p. 439-45.
16. Cecchi, A., et al., *Carbonic anhydrase inhibitors. Design of fluorescent sulfonamides as probes of tumor-associated carbonic anhydrase IX that inhibit isozyme IX-mediated acidification of hypoxic tumors*. J Med Chem, 2005. **48**(15): p. 4834-41.
17. Rami, M., et al., *Hypoxia-targeting carbonic anhydrase IX inhibitors by a new series of nitroimidazole-sulfonamides/sulfamides/sulfamates*. J Med Chem, 2013. **56**(21): p. 8512-20.
18. Supuran, C.T., et al., *Carbonic anhydrase inhibitors: sulfonamides as antitumor agents?* Bioorg Med Chem, 2001. **9**(3): p. 703-14.
19. Parkkila, S., et al., *Carbonic anhydrase inhibitor suppresses invasion of renal cancer cells in vitro*. Proc Natl Acad Sci U S A, 2000. **97**(5): p. 2220-4.
20. Pastorekova, S., et al., *Carbonic anhydrases: current state of the art, therapeutic applications and future prospects*. J Enzyme Inhib Med Chem, 2004. **19**(3): p. 199-229.
21. Denny, W.A., *Tumor-activated prodrugs--a new approach to cancer therapy*. Cancer Invest, 2004. **22**(4): p. 604-19.
22. Hay, M.P., et al., *DNA-targeted 1,2,4-benzotriazine 1,4-dioxides: potent analogues of the hypoxia-selective cytotoxin tirapazamine*. J Med Chem, 2004. **47**(2): p. 475-88.
23. Seow, H.A., et al., *1,2-Bis(methylsulfonyl)-1-(2-chloroethyl)-2-[[1-(4-nitrophenyl)ethoxy]carbonyl]hydrazine: an anticancer agent targeting hypoxic cells*. Proc Natl Acad Sci U S A, 2005. **102**(26): p. 9282-7.
24. Nomura, M., S. Shuto, and A. Matsuda, *Synthesis of the cyclic and acyclic acetal derivatives of 1-(3-C-ethynyl-beta-D-ribo-pentofuranosyl)cytosine, a potent antitumor nucleoside. Design of prodrugs to be selectively activated in tumor tissues via the bio-reduction-hydrolysis mechanism*. Bioorg Med Chem, 2003. **11**(11): p. 2453-61.
25. Phillips, R.M., et al., *Pharmacological and biological evaluation of a series of substituted 1,4-naphthoquinone bioreductive drugs*. Biochem Pharmacol, 2004. **68**(11): p. 2107-16.

26. De Simone, G., et al., *Carbonic anhydrase inhibitors: Hypoxia-activatable sulfonamides incorporating disulfide bonds that target the tumor-associated isoform IX*. J Med Chem, 2006. **49**(18): p. 5544-51.
27. D'Ambrosio, K., et al., *Carbonic anhydrase inhibitors: bioreductive nitro-containing sulfonamides with selectivity for targeting the tumor associated isoforms IX and XII*. J Med Chem, 2008. **51**(11): p. 3230-7.
28. Musser, J.H., et al., *Synthesis and antilipolytic activities of quinolyl carbanilates and related analogues*. Journal of medicinal chemistry, 1987. **30**(1): p. 62-7.
29. Khalifah, R.G., *The carbon dioxide hydration activity of carbonic anhydrase. I. Stop-flow kinetic studies on the native human isoenzymes B and C*. The Journal of biological chemistry, 1971. **246**(8): p. 2561-73.
30. Tarzia, G., et al., *Synthesis and structure-activity relationships of FAAH inhibitors: cyclohexylcarbamic acid biphenyl esters with chemical modulation at the proximal phenyl ring*. ChemMedChem, 2006. **1**(1): p. 130-9.
31. Meng, F., et al., *Molecular and cellular pharmacology of the hypoxia-activated prodrug TH-302*. Mol Cancer Ther, 2012. **11**(3): p. 740-51.
32. Bonnet, M., et al., *Novel nitroimidazole alkylsulfonamides as hypoxic cell radiosensitisers*. Bioorg Med Chem, 2014. **22**(7): p. 2123-32.
33. Adams, G.E. and I.J. Stratford, *Hypoxia-mediated nitro-heterocyclic drugs in the radio- and chemotherapy of cancer. An overview*. Biochem Pharmacol, 1986. **35**(1): p. 71-6.
34. Wong, T.W., G.F. Whitmore, and S. Gulyas, *Studies on the toxicity and radiosensitizing ability of misonidazole under conditions of prolonged incubation*. Radiat Res, 1978. **75**(3): p. 541-55.
35. Guise, C.P., et al., *Bioreductive prodrugs as cancer therapeutics: targeting tumor hypoxia*. Chin J Cancer, 2014. **33**(2): p. 80-6.
36. Lukashev, A.N., et al., *Late expression of nitroreductase in an oncolytic adenovirus sensitizes colon cancer cells to the prodrug CB1954*. Hum Gene Ther, 2005. **16**(12): p. 1473-83.
37. Johnson, K.M., et al., *Toward hypoxia-selective DNA-alkylating agents built by grafting nitrogen mustards onto the bioreductively activated, hypoxia-selective DNA-oxidizing agent 3-amino-1,2,4-benzotriazine 1,4-dioxide (tirapazamine)*. J Org Chem, 2014. **79**(16): p. 7520-31.

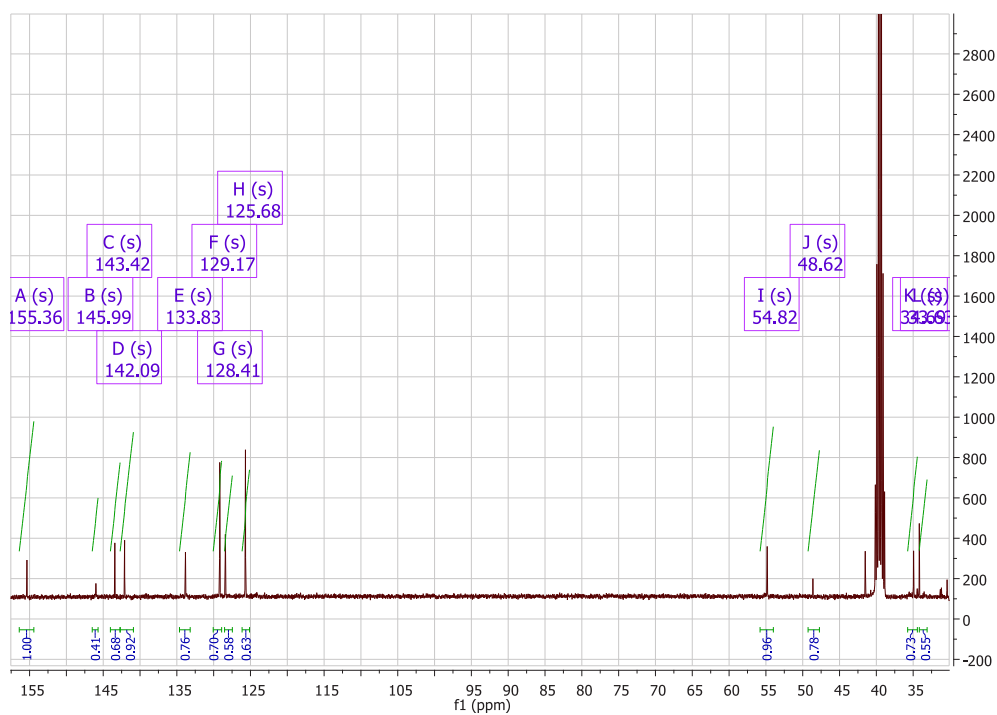
38. Ditte, P., et al., *Phosphorylation of carbonic anhydrase IX controls its ability to mediate extracellular acidification in hypoxic tumors*. *Cancer research*, 2011. **71**(24): p. 7558-67.

Supplementary data

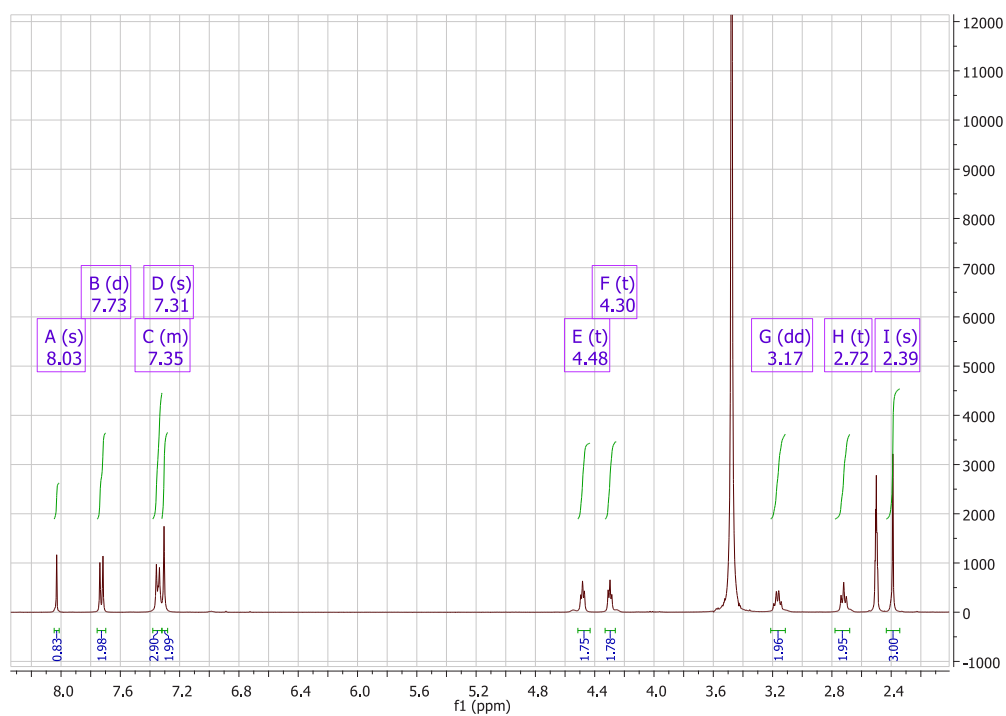
^1H NMR spectrum of compound **1b**



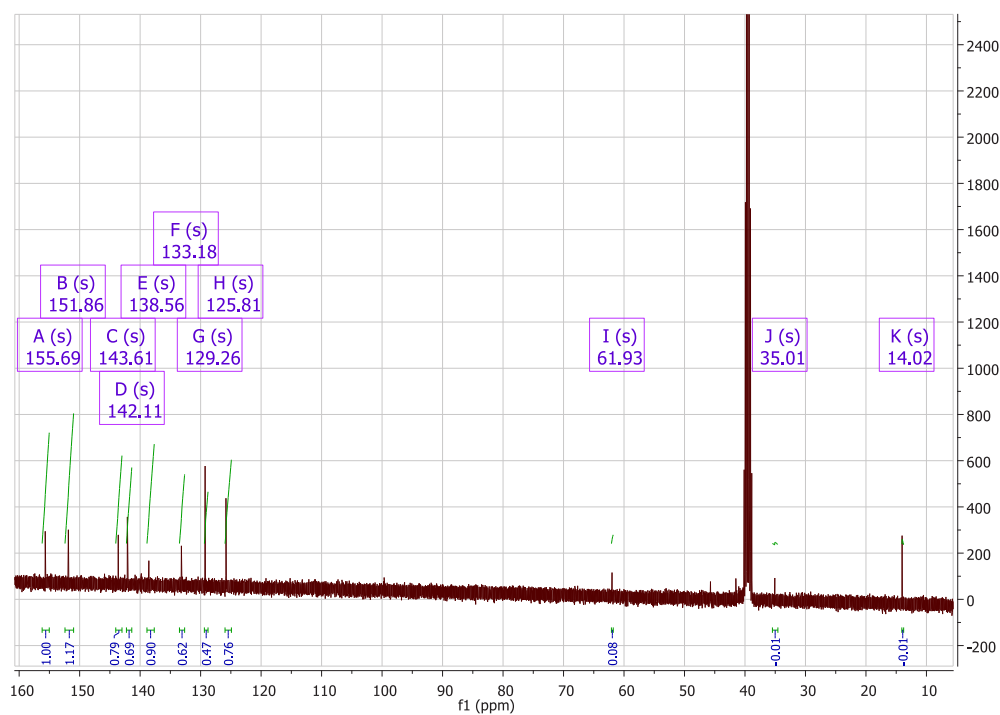
^{13}C NMR spectrum of compound **1b**



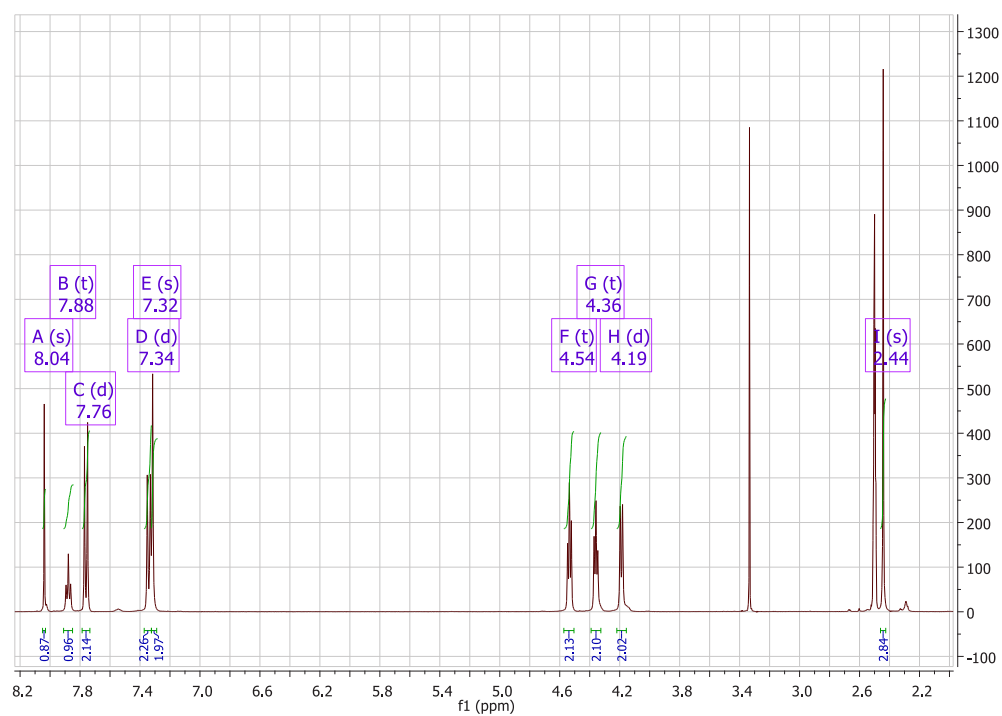
^1H NMR spectrum of compound **2b**



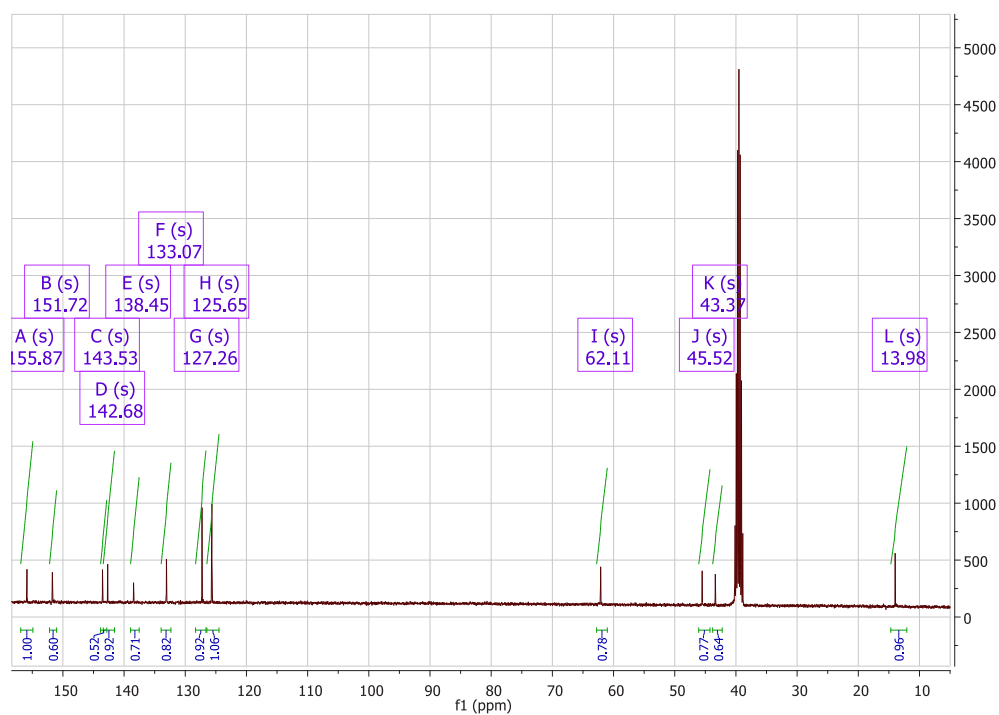
^{13}C NMR spectrum of compound **2b**



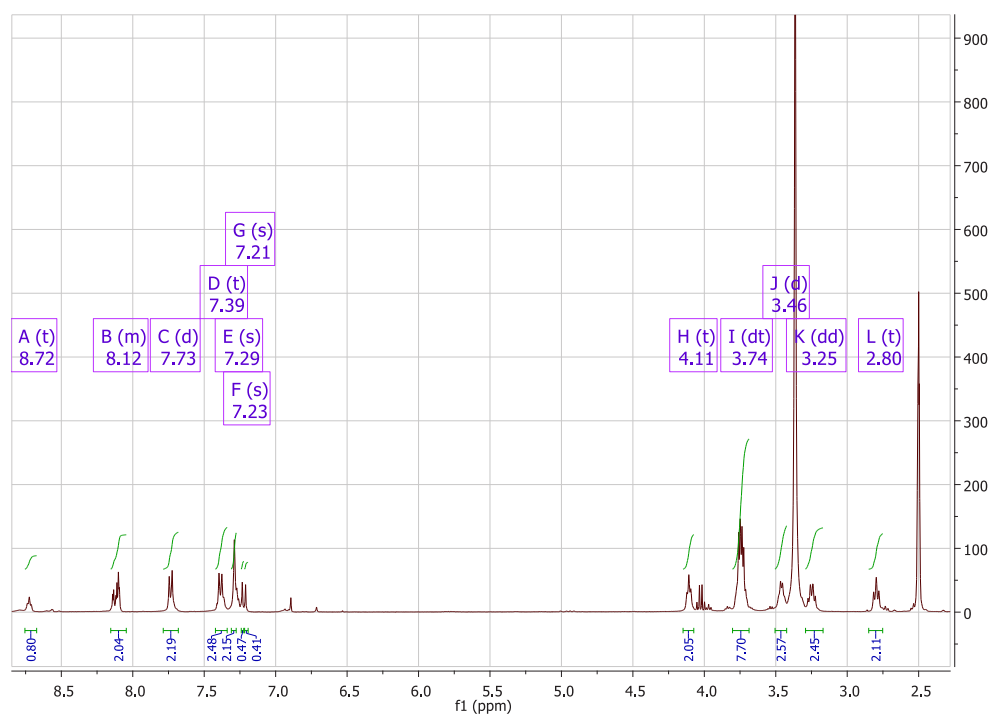
¹H NMR spectrum of compound **2c**



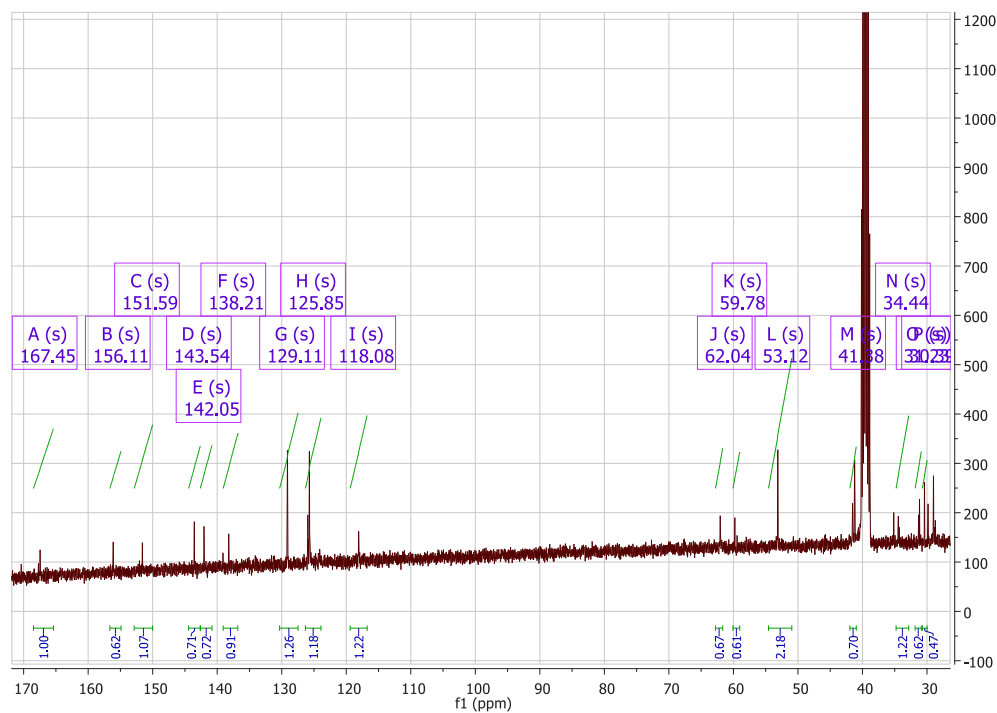
¹³C NMR spectrum of compound **2c**



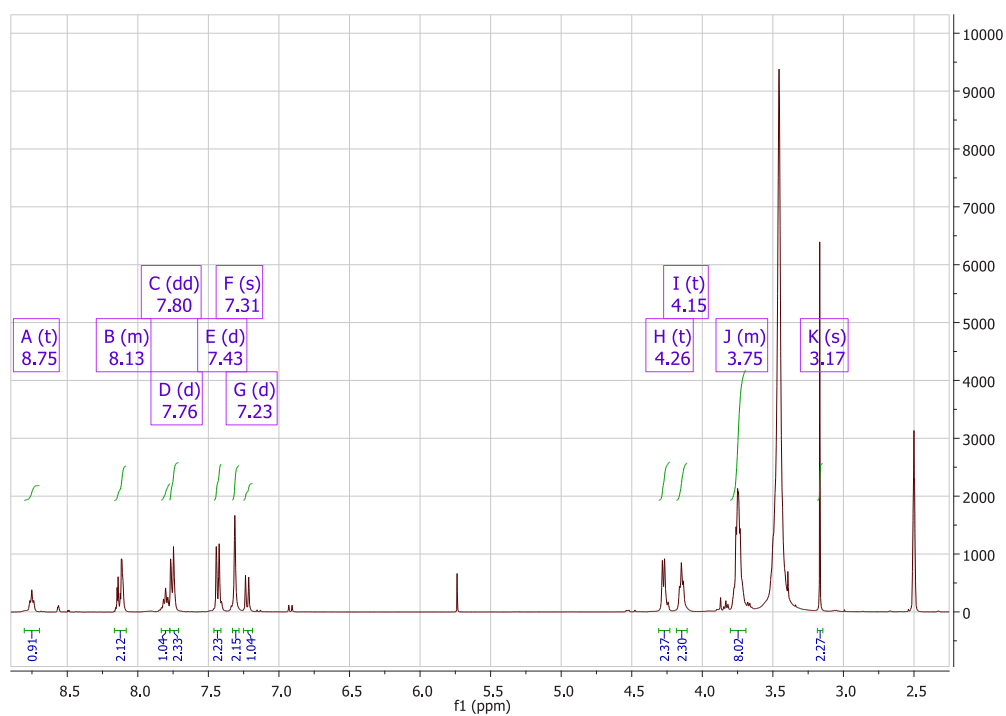
¹H NMR spectrum of compound **3b**



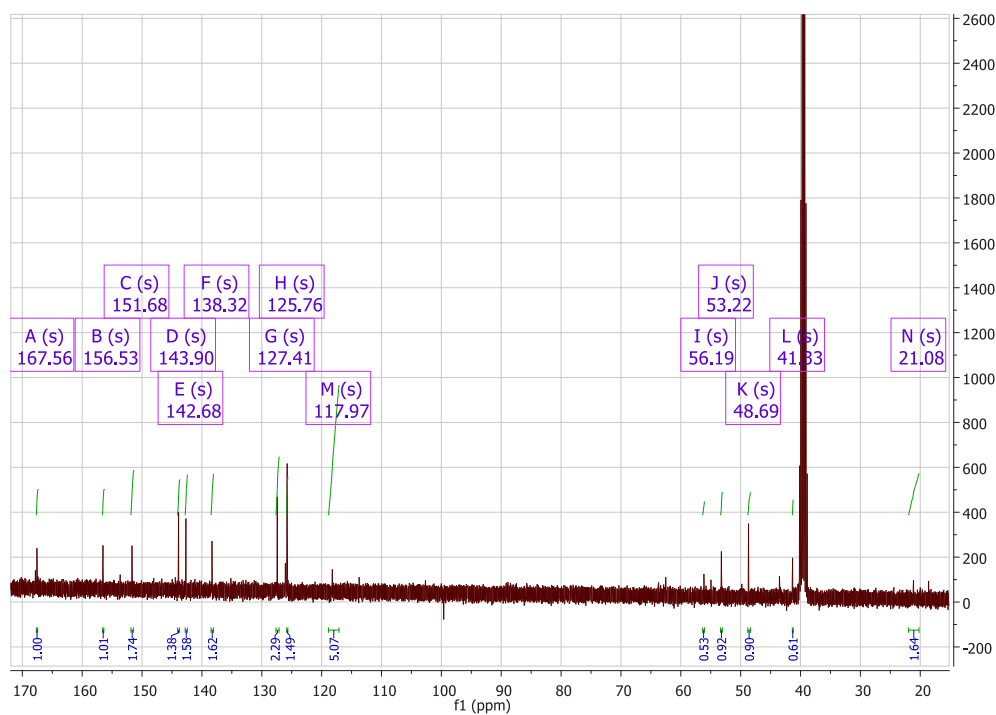
¹³C NMR spectrum of compound **3b**



¹H NMR spectrum of compound 3c



¹³C NMR spectrum of compound 3c



Chapter 7

Discussion and future perspectives

CAIX as therapeutic target

Hypoxia occurs within solid tumors and affects the tumor biology by modifying various cellular mechanisms such as tumor angiogenesis, vasculogenesis, invasiveness and metastasis, as well as glycolytic energy metabolism [1-5]. The glycolytic energy metabolism results in an increased production of acid, which requires compensatory mechanism to maintain the balance between intracellular and extracellular pH [6-8]. Several proteins are involved in this process such as anion exchangers (AE), glucose transporter 1 (GLUT1), monocarboxylate transporter (MCT), sodium-bicarbonate cotransporter (NBC) and carbonic anhydrase IX (CAIX) [7-10]. The extracellular location, identification of a hypoxia responsive element (HRE) in its promoter region and its predominant tumor-specific expression are the main reasons for considering CAIX as target for cancer therapy [11, 12]. The specific CAIX overexpression under hypoxia stimulated many studies to investigate the prognostic significance of CAIX in solid tumors [13-17]. Several meta-analysis studies showed clearly that high CAIX expression is associated with worse prognosis in wide variety of cancer types, thereby strengthening its clinical importance [18-20].

Different strategies to target CAIX

The transmembrane-located CAIX contains Zn^{2+} at its active site, which mainly catalyses of reversible hydration of carbon dioxide and water to bicarbonate and a proton [10], thereby acidifying the tumor microenvironment [21]. Low extracellular pH (pHe) has been associated with tumorigenic transformation, extracellular matrix breakdown, migration and invasion [12, 21]. CAIX plays a role in providing bicarbonate to maintain an alkaline intracellular environment promoting tumor cell survival [22, 23]. Recent years have brought forward the development of a large variety of different CAIX inhibitors [24-26] that binds within the Zn^{2+} active site to block the catalytic activity, thereby decreasing extracellular acidification, but more importantly, causing intracellular acidification to induce cell death [27, 28]. Hypoxic tumors show resistance towards chemotherapy because the uptake of weak-basic drug like doxorubicin is hampered because of extracellular acidity [29-32]. Following radiotherapy, lack of oxygen reduces the production of reactive and cytotoxic species, such as ROS, and ultimately prevents irreparable DNA damage from occurring in cancer cells, preventing cancer cell death. Hypoxia also upregulates HIF-1 α which independently promotes radioresistance [33]. The limited success of hypoxia

modification strategies in clinical trials, such as hyperbaric oxygen, hyperthermia, blood transfusions and erythropoietin stimulating agents [34], stimulated the search for alternative chemical sensitizers, such as nitroimidazoles [35]. To sensitize hypoxic tumors towards radiotherapy many nitroimidazole-based small molecules, mimicking the effect of oxygen during irradiation, have been identified based on their electron affinity [36, 37]. Chapter 2 provides an extensive study on nitroimidazoles as anti-anaerobic agents and hypoxic cell sensitizers. Structure Activity Relationship (SAR) studies on 2-, 4- and 5-nitroimidazole and their derivatives might provide an important tool in the development of new anti-anaerobic bacterial agents and radiosensitizers with minimal side effects. Combining these nitroimidazole moieties with sulfonamide/sulfamide/sulfamate to target CAIX results in a decrease in extracellular acidity and sensitizes hypoxic tumors to radiotherapy [38]. In this study, upon treatment with the CAIX-specific dual targeting sulfamide **7**, the therapeutic effect of irradiation was enhanced in a CAIX dependent manner with a Sensitization Enhancement Ratio (SER) of 1.50, without systemic toxicity as evaluated by body weight loss [38]. Chemosensitization efficacy of **7** was evaluated with combination of doxorubicin in HT29 tumor bearing mice (Chapter 3). The combination of **7** and doxorubicin treated mice showed a reduction in tumor growth [26]. The X-ray crystal structure of the hCA II/7 adduct showed that the binding of derivative **7** in the middle of the enzyme active site and proves that CA inhibition will reduce the extracellular acidification of tumor microenvironment resulting in sensitization towards radio- and chemotherapy [26, 38].

Over expression of tumor-associated CAIX in hypoxic areas of the tumor combined with a minimal expression in healthy tissues and its cell-surface location can be exploited to specifically deliver drugs to the tumor site thereby minimizing normal tissue toxicity. There are several possibilities to do so, such as specific delivery of cytotoxic anticancer drugs, bio-reductive drugs or hypoxia-activated prodrugs. Currently, cytotoxic anti-cancer drugs have frequently failed in clinical trials due to their unwanted adverse effects. Therefore, different families of dual-targeting cytotoxic compounds have been designed and synthesized to specifically exert their effect on CAIX expressing cells through binding with a CAIX targeting inhibitory moiety [39]. Here (Chapter 4) we tested some clinically approved cytotoxic anti-cancer drugs conjugated with CAIXi. The alkylating agent chlorambucil, the *N*-oxide hypoxia-activated prodrug tirapazamine, the pH-sensitive alkylating agent

temozolomide and ATR inhibitors (ATRi) were chosen and conjugated with CAIX specific sulfonamides and sulfamates. Only the ATRi derivative **12** proved to be more effective when combined with radiation in CAIX expressing cells as compared to cells that do not express CAIX. Poor binding affinity of the other dual-target compounds for recombinant CAIX and the absence of an increased efficacy during hypoxic conditions however suggested that the effect of these compounds was not solely depending on the binding to CAIX. Alternatively, the difference in response to ATRi when combined with radiation between cells overexpressing CAIX and cells not expressing CAIX might be the result of a lower number of cells in the resistant S-phase of cell cycle [40], or by a decrease in DNA repair capacity in cells with lower intracellular pH [41-43], i.e. those cells that do not express CAIX. These possibilities may explain the different response between cells overexpressing CAIX and those do not express CAIX, when exposed to cytotoxic dual-targeting drugs, although further investigations are required to prove this casual relationship [38].

The significance of hypoxia in resistance to cytotoxic therapy has regained interest in targeting these cells [44], thereby bio-reducible drugs and hypoxia-activated prodrugs proved their success to treat hypoxic tumors [45, 46]. Bio-reducible nitroimidazoles (Chapter 2), well-known radiosensitizers and recent studies indicate hypoxia selective cytotoxicity of 2-nitroimidazole alkylsulfonamides towards hypoxic tumor cells [47]. The sulfonamide (CAIXi) group lowers aqueous solubility and also has a strong influence on the electron affinity of the nitroimidazole ring and this raises the E(1) by up to 42 mV, leading to an increase in hypoxic cytotoxicity and hypoxic selectivity [47]. Although several hypoxia-selective prodrugs have progressed through clinical trials, none have yet been approved for clinical use. For example, TPZ, the most advanced clinical candidate, suffers from excessive metabolic consumption as it penetrates the extravascular space [48, 49]. Metabolic reduction by concerted two-electron oxidoreductases can unexpectedly corrupt the oxygen-inhibited activation as recently reported for PR-104 [50]. Indeed, early reports of anti-tumor efficacy of TH-302 (2-nitroimidazole based mustard) in clinical trials garner optimism, leads to phase III clinical trials (MAESTRO) [51]. Combining these bio-reducible drugs with CAIX inhibitors would facilitate the specific activation of cytotoxic drugs at the hypoxic tumor site and reduce the normal tissue toxicity [52]. Bio-reducible nitroimidazole and nitrogen mustard alkylating agents were designed and synthesized to target specifically hypoxia-associated CAIX (Chapter 5 and 6). Previous studies suggest that

linker and bulky substituted aromatic sulfonamides negatively influence the CA inhibition potency and selectivity [53], as observed for the newly synthesized derivatives (Chapter 5). To study the influence of the linker and substitutions, we designed and synthesized bio-reducible drugs with a carbamate linker and only a substitution of the aromatic sulfonamide (Chapter 6). All compounds showed tight binding efficacy towards all recombinant CA isoforms tested. Of all tested compounds, the 2-nitroimidazole derivative **1b** showed cytotoxicity under anoxia. Work is in progress to find out the radiosensitizing efficacy of all other compounds. Cytotoxicity of **1b** might be explained by the higher electron reduction potential of 2-nitroimidazoles compared to 5-nitroimidazoles (**2b and 2c**) (Chapter 6) [47]. Structure Activity and Relationship (SAR) studies might help to design and synthesize efficient bio-reducible or hypoxia activated prodrugs with specific cytotoxicity for hypoxic tumor cells by sparing normal cells.

Alternative therapeutic targets

The primary function of CAIX is the hydration of carbon dioxide to bicarbonate and a proton, thereby maintaining an alkaline intracellular pH and promoting an acidic extracellular space [6-8]. Studies suggest that increasing the tumor pH via inhibition of CAIX might potentiate the efficacy of mTOR inhibitors. Consequently, in addition to hypoxia, an acidic tumor pH might further downregulate mTORC1 activity, promoting a mTORC1-independent cancer cell proliferation [54, 55]. Therapeutic strategies targeting the hypoxic tumor compartment, such as the inhibition of CAIX, potentiates the efficacy of rapamycin (mTORC1 inhibitor) and warrants further clinical evaluation [56]. Bevacizumab, an anti-VEGFA antibody, inhibits the developing vasculature of tumors, induces hypoxia and increases expression of hypoxia-regulated genes, including CAIX [57]. CAIX expression correlates with poor prognosis in most tumor types and with worse outcome in Bevacizumab-treated metastatic colorectal cancer patients [58]. Therefore, the combination of the CAIXi acetazolamide with bevacizumab might be an interesting approach as has been shown by the enhanced treatment efficacy of this combination in HT29 xenografts [59]. This experimental evidence highlights the value of developing small molecules or antibodies, which inhibit CAIX for combination therapy. In addition, human anti-CAIX targeted chimeric antigen receptor (CAR) T cells have been engineered to secrete human anti-programmed death ligand 1 (PD-L1) antibodies at the tumor site.

Tumor growth was 5-fold reduced upon local antibody delivery of anti-CAIX anti-PD-L1 producing CAR T cells when compared with anti-CAIX CAR T cells alone in a humanized mice model of clear cell renal carcinoma (ccRCC) [60]. Furthermore, combination of the 4-(3'-(3'', 5''-dimethylphenyl) ureido) phenyl sulfamate, S4 with the proton pump inhibitor lansoprazole indeed showed synergism in their efficacy [61], but these combinations and strategies do require further investigation and validation. Another more molecular interesting therapeutic target is the intracellular pH sensor protein soluble adenylyl cyclase (sAC) [62-64], which has been shown a promising protein to target in combination with CAIXi.

Future directions

The hypoxic solid tumors show resistance to conventional treatment modalities, i.e. radio- and chemotherapies. Chemical sensitizers like nitroimidazoles and their derivatives mimic oxygen and sensitize hypoxic tumors to radiotherapy. Combining these nitroimidazole with CAIXi results in a reduced extracellular acidification and sensitizes hypoxic tumors to chemotherapy (Chapter 3). The results described in this thesis indicate that the mechanism of action of CAIXi might not yet be completely understood when combined with radio/chemotherapies (Chapter 3). Therefore, SAR studies on the role of nitroimidazoles as antibacterial agents and radiosensitizers, as been discussed in chapter 2, and altering parameters such as lipophilicity, aqueous solubility and reduction potentials might help in the future development of suitable and ideal radiosensitizers with minimal side effects. Although a wide variety of CAIXi is currently available and still being developed, more focus should be on developing multiple strategies to aim different targets at the same time. Several criteria should be followed to select a good CAIXi, based on the compounds binding affinity towards recombinant CA isoforms, pharmacokinetic characteristics, *in vitro* and *in vivo* results. Molecular modeling and docking studies on CAIX might help to design inhibitors having specific selectivity towards CAIX [65, 66]. A detailed SAR studies might help to find suitable CAIX inhibitors with high binding affinity profiles [67]. Unfortunately, there is no perfect biological model to test other oncogene processes such as proliferation, survival, migration and invasion, when characterizing CAIXi. CAXII is also a transmembrane isozyme, expresses in most of the hypoxic solid tumors [68, 69] and CAIX targeting compounds can bind to CAXII [70]. So, there is a need for new models in which both CAIX and CAXII have been silenced.

There is evidence that single knockdown of CAIX upregulates CAXII as compensatory mechanism [71], so we need to shut down both CAIX and CAXII expression. The CAIX inhibitors will involve in CAXII inhibition as well, therefore double knockout cell lines might provide to evaluate or to develop selective inhibitors of CAIX or CAXII. Currently in our lab, the CRISPR/Cas9 technology has been used to generate CAIX/CAXII knockout tumor cells. So far no cell line was developed with CAIX and CAXII knockout, therefore no clear differentiation in mechanism and ratio of expression was established between CAIX and CAXII in same cell line.

Overall, the idea of targeting hypoxic tumors cells remains an interesting approach to increase efficacy of conventional treatment modalities. The use of dual-targeting cytotoxic compounds to target CAIX expressing cells has been described in Chapter 4. The efficacy of these compounds however seems not solely depend on CAIX binding. To evaluate why these drugs fail to kill the hypoxic tumor cells, we should understand the drug metabolism and pharmacokinetics under the proper assay conditions. One approach for improving tumor specific killing and to reduce the normal tissue toxicity of conventional anticancer drugs consists of a bio-reducible or hypoxia activated prodrug that can be selectively activated under hypoxia. By exploiting this feature, bio-reducible drugs to target CAIX described in Chapter 5 and Chapter 6 might be a valuable approach to develop bio-reducible cytotoxic drugs combined with conventional therapies like chemo- and radiotherapy. For example, compound **1b** (2-nitroimidazole derivative) shows hypoxia selective cytotoxicity under anoxia in HT29 cells, when combined with radiation this derivative might enhance the cytotoxicity towards treatment resistant hypoxic tumors. SAR studies on these types of compounds might help to develop new classes of bio-reducible drugs with minimal side effects. Other approaches such as antibody targeting [8, 72] might be a valuable approach in future but requires further investigation, because clinical studies indicate that CAIX is overexpressed in some cancer cells but not under conditions of hypoxia [73]. An Immunomodulatory drug, which targets CAIX, might also be a viable approach in the future to stimulate T and NK cells [74]. Tumor specific expression of CAIX also promotes its use as an antigen for immunotherapy. The results of therapeutic vaccines against CAIX in renal cell carcinoma are promising [75], but further research and investigation is required for the use of CAIX targeted immunotherapy.

References

1. Hill, R.P., D.T. Marie-Egyptienne, and D.W. Hedley, *Cancer stem cells, hypoxia and metastasis*. Semin Radiat Oncol, 2009. **19**(2): p. 106-11.
2. Chang, Q., et al., *Hypoxia predicts aggressive growth and spontaneous metastasis formation from orthotopically grown primary xenografts of human pancreatic cancer*. Cancer Res, 2011. **71**(8): p. 3110-20.
3. Pennacchietti, S., et al., *Hypoxia promotes invasive growth by transcriptional activation of the met protooncogene*. Cancer Cell, 2003. **3**(4): p. 347-61.
4. Semenza, G.L., *Hypoxia, clonal selection, and the role of HIF-1 in tumor progression*. Crit Rev Biochem Mol Biol, 2000. **35**(2): p. 71-103.
5. Kioi, M., et al., *Inhibition of vasculogenesis, but not angiogenesis, prevents the recurrence of glioblastoma after irradiation in mice*. J Clin Invest, 2010. **120**(3): p. 694-705.
6. Warburg, O., *On the origin of cancer cells*. Science, 1956. **123**(3191): p. 309-14.
7. Neri, D. and C.T. Supuran, *Interfering with pH regulation in tumours as a therapeutic strategy*. Nat Rev Drug Discov, 2011. **10**(10): p. 767-77.
8. Dubois, L.J., et al., *New ways to image and target tumour hypoxia and its molecular responses*. Radiother Oncol, 2015. **116**(3): p. 352-7.
9. Pastorek, J. and S. Pastorekova, *Hypoxia-induced carbonic anhydrase IX as a target for cancer therapy: from biology to clinical use*. Semin Cancer Biol, 2015. **31**: p. 52-64.
10. Supuran, C.T., *Carbonic anhydrases: novel therapeutic applications for inhibitors and activators*. Nat Rev Drug Discov, 2008. **7**(2): p. 168-81.
11. Pastorekova, S., et al., *Carbonic anhydrase IX, MN/CA IX: analysis of stomach complementary DNA sequence and expression in human and rat alimentary tracts*. Gastroenterology, 1997. **112**(2): p. 398-408.
12. Wykoff, C.C., et al., *Hypoxia-inducible expression of tumor-associated carbonic anhydrases*. Cancer Res, 2000. **60**(24): p. 7075-83.
13. Douglas, C.M., et al., *Lack of prognostic effect of carbonic anhydrase-9, hypoxia inducible factor-1alpha and bcl-2 in 286 patients with early*

- squamous cell carcinoma of the glottic larynx treated with radiotherapy. Clin Oncol (R Coll Radiol)*, 2013. **25**(1): p. 59-65.
14. Kim, S.J., et al., *Prognostic value of carbonic anhydrase IX and Ki-67 expression in squamous cell carcinoma of the tongue. Jpn J Clin Oncol*, 2007. **37**(11): p. 812-9.
 15. Smeland, E., et al., *Prognostic impacts of hypoxic markers in soft tissue sarcoma. Sarcoma*, 2012. **2012**: p. 541650.
 16. Stewart, D.J., et al., *Membrane carbonic anhydrase IX expression and relapse risk in resected stage I-II non-small-cell lung cancer. J Thorac Oncol*, 2014. **9**(5): p. 675-84.
 17. Wykoff, C.C., et al., *Expression of the hypoxia-inducible and tumor-associated carbonic anhydrases in ductal carcinoma in situ of the breast. Am J Pathol*, 2001. **158**(3): p. 1011-9.
 18. van Kuijk, S.J., et al., *Prognostic Significance of Carbonic Anhydrase IX Expression in Cancer Patients: A Meta-Analysis. Front Oncol*, 2016. **6**: p. 69.
 19. Zhao, Z., et al., *Prognostic value of carbonic anhydrase IX immunohistochemical expression in renal cell carcinoma: a meta-analysis of the literature. PLoS One*, 2014. **9**(11): p. e114096.
 20. Peridis, S., et al., *Carbonic anhydrase-9 expression in head and neck cancer: a meta-analysis. Eur Arch Otorhinolaryngol*, 2011. **268**(5): p. 661-70.
 21. Svastova, E., et al., *Hypoxia activates the capacity of tumor-associated carbonic anhydrase IX to acidify extracellular pH. FEBS Lett*, 2004. **577**(3): p. 439-45.
 22. Bartosova, M., et al., *Expression of carbonic anhydrase IX in breast is associated with malignant tissues and is related to overexpression of c-erbB2. J Pathol*, 2002. **197**(3): p. 314-21.
 23. Ebbesen, P., et al., *Taking advantage of tumor cell adaptations to hypoxia for developing new tumor markers and treatment strategies. J Enzyme Inhib Med Chem*, 2009. **24 Suppl 1**: p. 1-39.
 24. Lomelino, C. and R. McKenna, *Carbonic anhydrase inhibitors: a review on the progress of patent literature (2011-2016). Expert Opin Ther Pat*, 2016. **26**(8): p. 947-56.

25. Monti, S.M., C.T. Supuran, and G. De Simone, *Anticancer carbonic anhydrase inhibitors: a patent review (2008 - 2013)*. *Expert Opin Ther Pat*, 2013. **23**(6): p. 737-49.
26. Rami, M., et al., *Hypoxia-targeting carbonic anhydrase IX inhibitors by a new series of nitroimidazole-sulfonamides/sulfamides/sulfamates*. *J Med Chem*, 2013. **56**(21): p. 8512-20.
27. Swietach, P., et al., *The role of carbonic anhydrase 9 in regulating extracellular and intracellular pH in three-dimensional tumor cell growths*. *J Biol Chem*, 2009. **284**(30): p. 20299-310.
28. Swietach, P., et al., *Tumor-associated carbonic anhydrase 9 spatially coordinates intracellular pH in three-dimensional multicellular growths*. *J Biol Chem*, 2008. **283**(29): p. 20473-83.
29. Gray, L.H., et al., *The concentration of oxygen dissolved in tissues at the time of irradiation as a factor in radiotherapy*. *Br J Radiol*, 1953. **26**(312): p. 638-48.
30. Alfarouk, K.O., et al., *Resistance to cancer chemotherapy: failure in drug response from ADME to P-gp*. *Cancer Cell Int*, 2015. **15**: p. 71.
31. Eales, K.L., K.E. Hollinshead, and D.A. Tennant, *Hypoxia and metabolic adaptation of cancer cells*. *Oncogenesis*, 2016. **5**: p. e190.
32. Primeau, A.J., et al., *The distribution of the anticancer drug Doxorubicin in relation to blood vessels in solid tumors*. *Clin Cancer Res*, 2005. **11**(24 Pt 1): p. 8782-8.
33. Semenza, G.L., *Intratumoral hypoxia, radiation resistance, and HIF-1*. *Cancer Cell*, 2004. **5**(5): p. 405-6.
34. Hirn, M., *Hyperbaric oxygen in the treatment of gas gangrene and perineal necrotizing fasciitis. A clinical and experimental study*. *Eur J Surg Suppl*, 1993(570): p. 1-36.
35. Hall, E.J., et al., *The nitroimidazoles as radiosensitizers and cytotoxic agents*. *Br J Cancer Suppl*, 1978. **3**: p. 120-3.
36. Adams, D.E.F., J. F.; Wardman, P., *HYPOXIC CELL SENSITIZERS IN RADIOBIOLOGY AND RADIOTHERAPY*. *The British journal of cancer. Supplement*, 1978. **37**: p. 1-132.

37. Asquith, J.C., et al., *Electron affinic sensitization. V. Radiosensitization of hypoxic bacteria and mammalian cells in vitro by some nitroimidazoles and nitropyrazoles*. Radiation research, 1974. **60**(1): p. 108-18.
38. Dubois, L., et al., *Targeting carbonic anhydrase IX by nitroimidazole based sulfamides enhances the therapeutic effect of tumor irradiation: a new concept of dual targeting drugs*. Radiother Oncol, 2013. **108**(3): p. 523-8.
39. van Kuijk, S.J., et al., *New approach of delivering cytotoxic drugs towards CAIX expressing cells: A concept of dual-target drugs*. Eur J Med Chem, 2017. **127**: p. 691-702.
40. Doyen, J., et al., *Knock-down of hypoxia-induced carbonic anhydrases IX and XII radiosensitizes tumor cells by increasing intracellular acidosis*. Front Oncol, 2012. **2**: p. 199.
41. Kulshrestha, A., et al., *Selective inhibition of tumor cell associated Vacuolar-ATPase 'a2' isoform overcomes cisplatin resistance in ovarian cancer cells*. Mol Oncol, 2016. **10**(6): p. 789-805.
42. De Milito, A. and S. Fais, *Tumor acidity, chemoresistance and proton pump inhibitors*. Future Oncol, 2005. **1**(6): p. 779-86.
43. Liao, C., et al., *Genomic screening in vivo reveals the role played by vacuolar H⁺ ATPase and cytosolic acidification in sensitivity to DNA-damaging agents such as cisplatin*. Mol Pharmacol, 2007. **71**(2): p. 416-25.
44. Wilson, W.R. and M.P. Hay, *Targeting hypoxia in cancer therapy*. Nat Rev Cancer, 2011. **11**(6): p. 393-410.
45. Thambi, T., et al., *Bioreducible carboxymethyl dextran nanoparticles for tumor-targeted drug delivery*. Adv Healthc Mater, 2014. **3**(11): p. 1829-38.
46. Baran, N. and M. Konopleva, *Molecular Pathways: Hypoxia-Activated Prodrugs in Cancer Therapy*. Clin Cancer Res, 2017. **23**(10): p. 2382-2390.
47. Bonnet, M., et al., *Novel nitroimidazole alkylsulfonamides as hypoxic cell radiosensitisers*. Bioorg Med Chem, 2014. **22**(7): p. 2123-32.
48. Denny, W.A. and W.R. Wilson, *Tirapazamine: a bioreductive anticancer drug that exploits tumour hypoxia*. Expert Opin Investig Drugs, 2000. **9**(12): p. 2889-901.
49. Hicks, K.O., et al., *Use of three-dimensional tissue cultures to model extravascular transport and predict in vivo activity of hypoxia-targeted anticancer drugs*. J Natl Cancer Inst, 2006. **98**(16): p. 1118-28.

50. Guise, C.P., et al., *The bioreductive prodrug PR-104A is activated under aerobic conditions by human aldo-keto reductase 1C3*. *Cancer Res*, 2010. **70**(4): p. 1573-84.
51. Van Cutsem, E., et al., *Evofofosamide (TH-302) in combination with gemcitabine in previously untreated patients with metastatic or locally advanced unresectable pancreatic ductal adenocarcinoma: Primary analysis of the randomized, double-blind phase III MAESTRO study*. *Journal of Clinical Oncology*, 2016. **34**(4).
52. De Simone, G., et al., *Carbonic anhydrase inhibitors: Hypoxia-activatable sulfonamides incorporating disulfide bonds that target the tumor-associated isoform IX*. *J Med Chem*, 2006. **49**(18): p. 5544-51.
53. Bozdag, M., et al., *Structural insights on carbonic anhydrase inhibitory action, isoform selectivity, and potency of sulfonamides and coumarins incorporating arylsulfonylureido groups*. *J Med Chem*, 2014. **57**(21): p. 9152-67.
54. Balgi, A.D., et al., *Regulation of mTORC1 signaling by pH*. *PLoS One*, 2011. **6**(6): p. e21549.
55. Pouyssegur, J., et al., *Growth factor activation of an amiloride-sensitive Na⁺/H⁺ exchange system in quiescent fibroblasts: coupling to ribosomal protein S6 phosphorylation*. *Proc Natl Acad Sci U S A*, 1982. **79**(13): p. 3935-9.
56. Faes, S., et al., *Targeting carbonic anhydrase IX improves the anti-cancer efficacy of mTOR inhibitors*. *Oncotarget*, 2016. **7**(24): p. 36666-36680.
57. Li, J.L., et al., *Delta-like 4 Notch ligand regulates tumor angiogenesis, improves tumor vascular function, and promotes tumor growth in vivo*. *Cancer Res*, 2007. **67**(23): p. 11244-53.
58. Hong, Y.S., et al., *Carbonic anhydrase 9 is a predictive marker of survival benefit from lower dose of bevacizumab in patients with previously treated metastatic colorectal cancer*. *BMC Cancer*, 2009. **9**: p. 246.
59. McIntyre, A., et al., *Carbonic anhydrase IX promotes tumor growth and necrosis in vivo and inhibition enhances anti-VEGF therapy*. *Clin Cancer Res*, 2012. **18**(11): p. 3100-11.

60. Suarez, E.R., et al., *Chimeric antigen receptor T cells secreting anti-PD-L1 antibodies more effectively regress renal cell carcinoma in a humanized mouse model*. *Oncotarget*, 2016. **7**(23): p. 34341-55.
61. Federici, C., et al., *Lansoprazole and carbonic anhydrase IX inhibitors synergize against human melanoma cells*. *J Enzyme Inhib Med Chem*, 2016. **31**(sup1): p. 119-125.
62. Tresguerres, M., L.R. Levin, and J. Buck, *Intracellular cAMP signaling by soluble adenylyl cyclase*. *Kidney Int*, 2011. **79**(12): p. 1277-88.
63. Wuttke, M.S., J. Buck, and L.R. Levin, *Bicarbonate-regulated soluble adenylyl cyclase*. *JOP*, 2001. **2**(4 Suppl): p. 154-8.
64. Rahman, N., J. Buck, and L.R. Levin, *pH sensing via bicarbonate-regulated "soluble" adenylyl cyclase (sAC)*. *Front Physiol*, 2013. **4**: p. 343.
65. Zengin Kurt, B., et al., *Synthesis, biological activity and multiscale molecular modeling studies for coumaryl-carboxamide derivatives as selective carbonic anhydrase IX inhibitors*. *J Enzyme Inhib Med Chem*, 2017. **32**(1): p. 1042-1052.
66. Chun-Lin Lu, L.Z., Zi-Cheng Li, Xiang Gao, Wei Zhang, *Pharmacophore modeling, virtual screening, and molecular docking studies for discovery of novel Carbonic anhydrase IX inhibitors*. *Med Chem Res*, 2012. **21**: p. 3417-3427.
67. Abdel-Hamid, M.K., et al., *Quantitative structure-activity relationship (QSAR) studies on a series of 1,3,4-thiadiazole-2-thione derivatives as tumor-associated carbonic anhydrase IX inhibitors*. *J Enzyme Inhib Med Chem*, 2009. **24**(3): p. 722-9.
68. Liao, S.Y., M.I. Lerman, and E.J. Stanbridge, *Expression of transmembrane carbonic anhydrases, CAIX and CAXII, in human development*. *BMC Dev Biol*, 2009. **9**: p. 22.
69. Ilie, M.I., et al., *Overexpression of carbonic anhydrase XII in tissues from resectable non-small cell lung cancers is a biomarker of good prognosis*. *Int J Cancer*, 2011. **128**(7): p. 1614-23.
70. Touisni, N., et al., *Glycosyl coumarin carbonic anhydrase IX and XII inhibitors strongly attenuate the growth of primary breast tumors*. *J Med Chem*, 2011. **54**(24): p. 8271-7.

71. Chiche, J., et al., *Hypoxia-inducible carbonic anhydrase IX and XII promote tumor cell growth by counteracting acidosis through the regulation of the intracellular pH*. *Cancer Res*, 2009. **69**(1): p. 358-68.
72. Zatovicova, M., et al., *Monoclonal antibody G250 targeting CA : Binding specificity, internalization and therapeutic effects in a non-renal cancer model*. *Int J Oncol*, 2014. **45**(6): p. 2455-67.
73. Li, J., et al., *Is carbonic anhydrase IX a validated target for molecular imaging of cancer and hypoxia?* *Future Oncol*, 2015. **11**(10): p. 1531-41.
74. Chang, X., et al., *Mechanism of immunomodulatory drugs' action in the treatment of multiple myeloma*. *Acta Biochim Biophys Sin (Shanghai)*, 2014. **46**(3): p. 240-53.
75. Combe, P., et al., *Trial Watch: Therapeutic vaccines in metastatic renal cell carcinoma*. *Oncoimmunology*, 2015. **4**(5): p. e1001236.

Summary

Hypoxia is a salient feature in many solid tumors and arises due to an inadequate and immature vascular supply resulting in a decreased delivery of oxygen and nutrients. These hypoxic regions show resistance towards conventional treatment modalities such as radio- and chemotherapy and are associated with poor survival. To survive these hostile microenvironmental stress tumor cells have to adapt, which can partly be mediated via stabilization of the hypoxia-inducible factor 1 alpha (HIF-1 α). Under hypoxic conditions HIF-1 α dimerizes with HIF-1 β and binds to the hypoxia responsive element (HRE) in the promoter regions to enhance the expression of many target genes, one of them being carbonic anhydrase IX (CAIX). CAIX is a transmembrane enzyme, which is involved in maintaining the pH balance between an acidic extracellular and an alkaline intracellular environment by reversible hydration of carbon dioxide to bicarbonate and a proton. The specific overexpression of CAIX in hypoxic solid tumors and minimal/no expression in normal tissues makes CAIX a good biomarker for endogenous hypoxia but also an attractive therapeutic target for cancer therapy. Therefore, the aim of this thesis was to target CAIX using various dual target drugs combined with radiosensitizers, cytotoxic drugs and bio-reducible drugs. In this thesis several CAIX targeting approaches have been investigated.

First we discussed Structure Activity Relationship (SAR) studies on nitroimidazoles and their derivatives known as anti-anaerobic agents and hypoxic cell sensitizers (Chapter 2). SAR studies demonstrated that nitroimidazole derivatives with higher reduction potentials might serve as good hypoxic cell sensitizers. Altering parameters such as aqueous solubility and electron affinity would also help in the development of an optimal radiosensitizer with minimal side effects.

Since nitroimidazoles are good hypoxic cell sensitizers, we have designed several dual target compounds existing out of a combination of a nitroimidazole and a carbonic anhydrase IX inhibitory moiety (Chapter 3). It has been shown that extracellular acidity limits the uptake of weak basic chemotherapeutic drugs, such as doxorubicin, and thereby decreases its efficacy. We hypothesized that combining these nitroimidazole moieties with a sulfonamide/sulfamide/sulfamate to target CAIX results in a decrease in extracellular acidosis and sensitizes hypoxic tumors to chemo- and radiotherapy. Previously, our group has shown that the sulfamide-based derivative **7** enhanced the therapeutic efficacy of irradiation in a CAIX dependent

manner with a sensitization enhancement ratio (SER) of 1.50, which is higher than several clinically tested radiosensitizers such as misonidazole and nimorazole. Chemosensitization efficacy was observed upon combination of **7** with doxorubicin in HT29 tumor-bearing mice (Chapter 3). X-ray crystal structure of hCAII/**7** shows the binding of derivative **7** to the active site of the enzyme and strengthens our data that CA inhibition reduces extracellular acidification, thereby sensitizing tumors towards chemo- and radiotherapy.

A similar dual target approach may be exploitable to deliver cytotoxic drugs towards CAIX expressing cells, resulting in a specific tumor targeted delivery and consequently reduced normal tissue toxicity. Chapter 4 describes the design and synthesis of new series of dual target compounds combining several anti-cancer drugs, including the chemotherapeutic agents chlorambucil, tirapazamine, temozolamide, two ataxia telangiectasia and Rad3-related protein inhibitors (ATRi), and the anti-diabetic biguanide agent phenformin. Only one compound, i.e. an ATRi derivative, showed a higher efficacy in combination with radiation in CAIX overexpressing cells as compared to cells lacking CAIX expression. Nevertheless, the efficacy of this compound for CAIX expressing cells might not solely depend on binding of the compound to CAIX, since all of the synthesized derivatives exhibit a low binding affinity to CAIX and other human carbonic anhydrase isoforms. The hypothesis that these dual target compounds specifically affect CAIX expressing tumor cells was not confirmed, but targeting CAIX with combination of cytotoxic drugs continues to be an interesting area for future drug development.

The significance of hypoxia in resistance to cytotoxic drugs has regained interest in targeting hypoxic tumors, since bio-reducible drugs and hypoxia-activated prodrugs proved their success to treat these tumors. Chapter 5 describes the design and synthesis of various bio-reducible nitroimidazole derivatives, nitrogen mustard alkylating agents and N-oxide derivatives combined with a carbonic anhydrase IX inhibiting moiety. All these compounds showed weak to moderate inhibition profiles towards several tested CA isoforms. We have observed that different substitutions and linkers within the same family of compounds influence the binding capacity to CAIX. For example derivatives **17** and **20** belong to same family, but have a different linker and substitution of the aromatic ring, leading to a different binding capacity towards

CAIX. This suggests that there is an urgent need for better understanding the interaction of CAIX inhibitors with the active site of the protein.

To expand our study on bio-reducible drugs, Chapter 6 describes the design and synthesis of 2-, 5-nitroimidazole and nitrogen mustards combined with carbonic anhydrase IX inhibitors by a carbamate linker. The 2-nitroimidazole derivative **1b** revealed cytotoxicity in HT29 and HCT116 cell lines and might be explain by the higher reduction potential of 2-nitroimidazoles compared to 5-nitroimidazoles, since our results did show no cytotoxicity of the 5-nitroimidazole derivatives. The nitrogen mustard derivatives was effective, but in a highly cell dependent manner, being effective under normoxia and anoxia only in the HCT116 cell line (derivative **3b**), whereas derivative **3c** did not show any cytotoxicity, which might be explained by substitution of the aromatic sulfonamide on the nitrogen mustard. Our future studies aim to optimize the radiosensitizing efficacy of **2b** and **2c** and further explore the cytotoxic properties of **1b**. Our results however stress the need for SAR studies on bio-reducible drugs combined with carbonic anhydrase IX moieties to guide the development of new cytotoxic anti-cancer drugs.

In conclusion, this thesis showed that the dual target nitroimidazole combined with CAIXi increases the efficacy of standard treatment modalities such as chemo- and radiotherapy. Targeting CAIX with combination of cytotoxic drugs continues to be an interesting approach to target hypoxic tumors in future. Bio-reducible drugs with higher reduction potentials would serve as potential cytotoxic agents to hypoxic tumors thereby decreasing the normal tissue toxicity. However SAR studies, docking and molecular modeling studies are needed for the design of CAIX inhibitors with higher selectivity.

Valorization addendum

This thesis describes different dual target approaches to target hypoxic tumor-associated carbonic anhydrase IX (CAIX). Firstly, the design, synthesis and biological evaluation of nitroimidazoles combined with carbonic anhydrase IX inhibitors (CAIXi), which showed the potential of increasing the efficacy of conventional treatment modalities such as chemo- and radiotherapy, has been described. Secondly, the development, synthesis and evaluation of anti-cancer drugs in combination with CAIXi derivatives, targeting the hypoxic tumor microenvironment to decrease normal tissue toxicity, have been demonstrated. Lastly, the design, synthesis and evaluation of biological efficacy of bio-reducible drugs, which undergo a reduction under hypoxic conditions, incorporating a CAIXi moiety have been described. However, developing new anti-cancer drugs remains challenging, since cancer is an extremely heterogeneous disease consisting of distorted versions of a person's own cells. Moreover increasing cancer incidence has a severe socio-economic impact and the development of new anti-cancer drugs remains essential. This valorization addendum discusses CAIX targeting using different approaches, its value for the gain for general society and future of cancer treatment.

Clinical Relevance

Since the treatment of cancer patients is progressing into a personalized treatment, the knowledge about the hypoxic tumor microenvironment and heterogeneity plays an important role. Conventional therapies such as chemo- and radiotherapy are less effective towards hypoxic tumors and therefore patient prognosis is worse. Many biomarkers have been already identified to stratify patients for a personalized treatment. CAIX is a transmembrane enzyme, its overexpression is highly tumor-specific especially under hypoxic conditions and generally associated with worse prognosis for cancer patients. Therefore, CAIX might be considered as a valuable biomarker for stratification of cancer patients, although the specific treatment based on this type of stratification remains to be identified. Since CAIX expression under hypoxic conditions is highly cell line dependent, targeted CAIX imaging may not be a universal hypoxia imaging strategy, and therefore, would be of limited use for clinical practice. CAIX catalyzes the reversible hydration of carbon dioxide to bicarbonate and a proton, a chemical reaction implicated in several carcinogenic processes such as invasion and migration. The clinical benefits of using CAIX inhibitors in patients

however remain to be investigated. The dual target compounds to target CAIX with different approaches described in this thesis (Chapter 3, 4, 5, 6) will unlikely be implemented in clinical practice due to limited efficacy. So far, there is only one CAIX inhibitor (i.e. SLC-0111) in clinical trials. The phase I clinical trial (NCT02215850) has been successfully finished end 2016. Currently the compound is scheduled to enter phase II trials this year.

Gain for Society

The Transmembrane location and the tumor-specific overexpression of CAIX can facilitate multiple targeting strategies. Firstly, since hypoxic tumors show resistance to conventional therapies such as chemo- and radiotherapy, a dual targeting approach with radiosensitizers targeting CAIX can increase the efficacy of standard treatment modalities. Secondly, treatment costs will decrease when healthy tissue side effects caused by anti-cancer therapy can be reduced, e.g. specific delivery of cytotoxic drugs to tumor site via targeting CAIX. Lastly, hypoxia activated prodrugs or bio-reducible drugs, which are activated and become cytotoxic under hypoxia, can also decrease side effects by killing specifically the hypoxic tumor cells. In general, any of these advancement in treatment of cancer has a potential gain for society.

Improvement in Health Care

CAIX expression in normal human tissues is rare, except in GI tract and this expression either decreased or lost during carcinogenesis. This atypical expression helps as biomarker for theragnostic purposes, inhibiting CAIX alone with inhibitors may not be enough to improve the health care. During the last decade, a large variety of CAIX inhibitors, several reported in this thesis, have been developed, but definitive conclusions regarding the efficacy of a single CAIX inhibitor treatment can only be drawn after completing clinical trials. Dual drug targeting approaches to increase the efficacy of conventional treatment modalities, sparing normal tissues by specific drug delivery to the tumor site and bio-reducible drugs that become cytotoxic only under hypoxic conditions are expected to improve health care as patients will experience less toxic side effects but required additional interventions (Chapter 3, 4, 5, 6). These approaches can potentially increase the therapeutic window of anti-cancer therapy and thereby result in an improvement in health care.

In addition, CAIX expression is tumor-specific and has prognostic value in a wide variety of cancers types. The expression levels of CAIX could therefore serves as excellent biomarker for patient selection, although the relevant therapies remain to be identified. CAIX might also be a diagnostic tool for early detection of malignant lesions, e.g. implementing CAIX imaging can lead to a great improvement in health care, since early detection of cancer can increase the patient's chance of survival.

Novelty of the Concept

Targeting CAIX with different inhibitors is not novel, but recently different approaches of dual drug targeting, as discussed in this thesis, gained a lot of interest by researchers. CAIX is a potential therapeutic target due to its tumor-specific expression and its involvement in maintaining a pH balance between the acidic extracellular and the alkaline intracellular environment of tumor cell. The acidic extracellular tumor microenvironment promotes several carcinogenic processes such as migration and invasion. By reducing this extracellular acidification via inhibiting CAIX activity using nitroimidazoles incorporated with CAIXi, the efficacy of conventional treatment modalities might increase (Chapter 3). The interaction between CAIXi and conventional treatment modalities needs to be understood very well before entering into clinical trials.

Although cytotoxic drugs targeting CAIX have been described previously, these approaches were studied predominantly in renal cell carcinoma where CAIX expression is upregulated due to a mutation in the VHL protein preventing HIF-1 α degradation. This thesis described a novel method of delivering anti-cancer drugs towards CAIX expressing cells via dual target compounds (Chapter 4), which conjugated with CAIXi. However, these dual target compounds showed little preference for CAIX expressing cells, which minimized their practical applicability. Further exploration on pharmacokinetic studies on these dual target drugs may help to design more potent approaches to deliver cytotoxic drugs towards CAIX expressing cells. This thesis describes a novel approach of bio-reducible cytotoxic warheads conjugated with CAIXi. Most of the bio-reducible drugs described in Chapter 5 did not show strong binding affinity towards physiologically relevant CA isoforms, this might be explained by the influence of the linker and substitution on aromatic ring. Chapter 6 described 2-, 5-nitroimidazole and nitrogen mustard sulfonamides based

derivatives. Interestingly, a cell dependent cytotoxicity has been observed for the 2-nitroimidazole-based compounds, an effect explained by the higher reduction potential of 2-nitroimidazoles compared to 5-nitroimidazoles. 2-nitroimidazole bio-reducible drugs may serve as less toxic drugs towards normal tissues surrounding the tumor and further combination with radiation might increase therapeutic efficacy. Structure Activity Relationship studies on bio-reducible drugs conjugated with CAIXi might help to develop new anti-cancer drugs.

Road to the Market

CAIX is an interesting anti-cancer therapeutic target and the tumoral expression of CAIX may be promising for the future market. The research described in this thesis does have potential clinical relevance that could eventually lead to an improved health care. However, additional *in vivo* preclinical and clinical experiments remain essential. The prognostic value, tumor-specific expression and surface location of CAIX facilitate it to be a potential biomarker. For this purpose, investigations on the outcome and progression of CAIX-positive hypoxic cancer versus CAIX-negative hypoxic cancer should be conducted. Immunohistochemical evaluation of CAIX expression requires a specific antibody to detect CAIX, currently the M75 antibody available in the market. However, the development of a fast and easy to use kit to evaluate CAIX expression might therefore more promising, which is currently unavailable. Many CAIX directed antibody-drug conjugated candidates were reported, but there is not yet an approved therapeutic drug targeting this antigen.

The CAIX inhibitors described in Chapter 3 however will not be pursued further as they were either ineffective as single agents, or unable to increase the efficacy of conventional treatment modalities. However, the single agent CAIX inhibitor i.e. SLC-0111 entered into phase II clinical trials and future clinical trials should also investigate the effect of SLC-0111 on the efficacy of conventional treatment modalities.

Monitoring of CAIX expression levels can be used to stratify patients for a specific therapy that has been proven to be effective for e.g. specific cytotoxic drug delivery to tumor site by targeting CAIX. Another approach is the use of bio-reductive drugs conjugated with CAIXi that might improve the drug uptake by tumors expressing

CAIX with minimal side effects. In future, this approach might help the development of new anti-cancer drugs targeting CAIX with a potentially clinical relevance.

Overall this thesis described several dual target approaches to target CAIX, but the most promising approach to utilize CAIX as target are the targeted drug delivery of cytotoxic compounds and bio-reductive cytotoxic drugs conjugated with CAIXi. In addition, the identification of alternative approaches to target CAIX remain essential, but requires further preclinical and clinical research in order to assess CAIX as a therapeutic target and its influence on healthcare and gain for society.

Acknowledgments

In the process to finish my PhD, many people, from different countries generously contributed personally and professionally to the work presented in this thesis. I will use this opportunity to extend my sincere thanks to all of them.

Firstly, family is my backbone in every success, without my elder sister's sacrifices and hard work I wouldn't reach the place where I am now. I am thankful for her constant encouragement and financial support which helped me to reach my goal. Akkaiah, a big thanks is not enough for what you did to me. I will be there for you through out my life.

Secondly, my teachers, I am very thankful to all of them whoever were involved since my childhood. Thanks for the guidance, knowledge and values you taught.

Finally, my wife Gayathri, though we married in the final year of my PhD, you are my life changer. Love you for your support, understanding during my hard times. Life is so beautiful with you and I am so happy to be with you and that happiness is going to be doubled with the arrival of our child.

This PhD would not have been possible without the contribution of many professional people. I would like to extend my thanks to the all of them who so generously contributed to the work presented in this thesis and who have helped me by giving moral support.

Philippe, I am very thankful to you for giving me the opportunity to do my master thesis and PhD in a collaboration project between Montpellier University and Maastricht University. Thank you for the conversations and your encouraging words which helped me build my confidence.

Jean-Yves, I am very thankful to you for your guidance and timely help and suggestions to solve my research problems. Many thanks for accepting me and for the friendly work environment in the lab. I had fun traveling with you for many conferences and I always wondered at some of your tricks. Thanks for the trust you placed in me.

Ludwig, full of energy with lot of patience and positivity that's how I will remember you always. Since I spent more than one year in Maastricht lab, I learned ample things from you especially planning my experiments, analysis of the results etc. Though I am new to a biology lab, you constantly helped me to cope up and to understand the protocols. Thank you for your encouragement and support you have given through out the final year of my PhD.

Special thanks to my thesis assessment committee: Prof. dr. F.C.S. Ramaekers (Chairman), Prof. dr. Guido R.M.M. Haenen, Prof. Daumantus Matulis (Vilnius University, Lithuania), Dr. Kasper M.A. Rouschop and Dr. Raivis Žalubovskis (Riga Technical University, Latvia) for their time, consideration and valuable remarks.

Thanks to all my co-authors. Thank you for all your contribution and scientific input.

To the people in IBMM Montpellier:

Thanks to all the people who were part of Glycochemistry and Molecular recognition during my PhD: Joanna, Simona, Karine, April, Camille, Delphin, Nasser, Alberto, Sebastian, and Mary. Thank you Joanna and Simona for all your help in translations from French to English. Karine, my Majesty....very big thank you for helping me in French administration during my PhD. Nasser, thank you for coffee breaks, nice weekends, travelling in summer and barbeques. You made my Montpellier life so joyful.

To the people in MAASTRO Lab:

Thanks to all the people from mCAT group: Ala, thank you for weekly discussions, inputs and help in all my projects. Simon, I spent very less time with you in Maastricht, thank you for your biological work to finish our dual drug project. Raymon, cool guy, thank you so much for your help to understand protocols and cell culture techniques, thank you for everything. All the best for winding up your PhD. Linda, thank you for your help in irradiating my dishes. Veronica and Damiënne, thank you for funny conversations and moments in the office, still long way to finish your PhD and good luck during your PhD. Marike, thank you for your help in the mito ROS project though it was dropped. Justina, my friend from Lithuania, thank you for being so nice to me, I never forgot those moments and drinks we had in conferences, since you are also

finishing your PhD soon, wish you the very. Alex, you just started enjoying your PhD and I wish you all the best. Rianne and Natasja, you have been very helpful with my experiments, Rianne you are master at clonogenics, thanks a lot for helping me out with those experiments. Carla, thank you for taking care of the administrative things.

Thanks to all the people from Notch and Autophagy groups: Marc, Arjan, Jan, Kasper, Carolien, Kim P, Hanneke, Lydie, Eloy, Lorena, Vinus, Judith, Jon, Tom and Marijke thank you all for being friendly and making me feel comfortable.

To the People in Germany:

Venkat, Shashank, Harsha, Kiran, Hari, Shashi and Rakesh thank you all for the wonderful time during my masters. Those weekends were crazy and thank you all for those late night discussions, Europe trips and Biryani.

To the People in Montpellier:

Bhupathi anna, Sridhar, Daya, Aasha, Rishi, Subbu, Sankari, Deethu, Parvathy and Srujana thank you all for weekend barbeques, nice holiday trips. Thanks for making me feel home in Montpellier.

To the people in Sweden:

Rajesh, Vino, Rathika, Pooja, Ganapathi, Sugandhi and Ramesh thank you all for your encouragement and help. I never forgot my first vacation with Gayathri and you people to Kiruna, it was an awesome experience for both of us. Let us keep travelling together.

To the People in India:

Sree, Reddy, Sivakrishna, Shesha Reddy, Vijay, Madhu, Rajesh, Sathish, Raju, John, Radha, Subbu, Siva, Hari, Purna, Vijay (fromIITK) and Raghav, thank you all for being with me in odd times and for your financial helps when in need.

Curriculum Vitae



Nanda Kumar Parvathaneni was born on June 10th 1983 in Nellimanda, Chittoor (Dist.), Andhra Pradesh, India, where he spent his childhood and finished primary school. He successfully obtained his bachelor and master degree in Organic Chemistry during 2000- 2006 at the Sri Venkateswara University in Tirupathi, India. After his masters he joined Laurus Pharmaceutical Labs Ltd. (Hyderabad) as a trainee chemist gaining experience in Process R&D. He moved to the Indian Institute of Technology, Kanpur, India, to work as a project associate under the supervision of Prof. V.K. Yadav and got acquainted with total synthesis and methodology of organic compounds. Having interest in biomedical sciences, he joined the Master program “Engineering in Biomedical engineering” as a joint degree at Anhalt University, Koethen and Martin Luther University, Halle-Wittenberg, Germany in 2011. During his Masters he did an internship in a collaborative project between the University of Montpellier, France and the Maastricht University, The Netherlands to develop and synthesize carbonic anhydrase IX inhibitors under the supervision of Prof. J.Y. Winum, Prof. P. Lambin and Dr. L. Dubois, which resulted in two research articles in 2013. He joined as a Cotutelle” PhD student at the University of Maastricht and the University of Montpellier under supervision of Prof. P. Lambin, Prof. J.Y. Winum and Dr. L. Dubois to continue this project and to develop a pipeline of carbonic anhydrase IX inhibitors. His research focused on the design, synthesis and biological efficacy evaluation of various dual-target approach drugs, targeting hypoxia associated carbonic anhydrase IX inhibitors. The results of his research are presented in this thesis.

List of Publications

Nanda Kumar Parvathaneni*, Raymon Niemons, Silvia Bua, Dennis Suylen, Rianne Biemans, Natasja Lieuwes, Ala Yaromina, Claudiu T. Supuran, Ludwig Dubois, Jean-Yves Winum, Philippe Lambin.
Novel carbonic anhydrase IX targeting bio-reducible sulfonamides.
In Preparation.

Nanda Kumar Parvathaneni*, Raymon Niemons, Ala Yaromina, Philippe Lambin, Ludwig J. Dubois, Jean-Yves Winum.
Overview of Structure-Activity Relationship studies on nitroimidazoles as antimicrobial and radiosensitizing agents.
Submitted to *Curr. Pharm.Design.* (Review).

Nanda Kumar Parvathaneni*, Ludwig Dubois, Ala Yaromina, Silvia Bua, Claudiu T. Supuran, Philippe Lambin, Jean-Yves Winum.
Design and synthesis of Carbonic anhydrase IX inhibitors with different bio-reducible warheads.
Submitted to *J. Enzym. Inhb.Med.Chem.*

Simon J.A. van Kuijk, **Nanda Kumar Parvathaneni***, Raymon Niemons, Marike W. van Gisbergen, Fabrizio Carta, Daniela Vullo, Silvia Pastorekova, Ala Yaromina, Claudiu T. Supuran, Ludwig J. Dubois, Jean-Yves Winum, Philippe Lambin.
New approach of delivering cytotoxic drugs towards CAIX expressing cells: A concept of dual-target drugs.
Eur. J. Med. Chem. **2017**, *127*, 691-702.

Ludwig Dubois, Raymon Niemons, Simon J.A. van Kuijk, Kranthi M. Panth, **Nanda Kumar Parvathaneni**, Sarah G.J.A. Peeters, Catharina M.L. Zegers, Nicole H. Rekers, Marike W. van Gisbergen, Rianne Biemans, Natasja G. Lieuwes, Linda Spiegelberg, Ala Yaromina, Jean-Yves Winum, Marc Vooijs, Philippe Lambin.
New ways to image and target tumour hypoxia and its molecular responses.
Radiother. Oncol. **2015**, *116*, 352-357.

Carol Ward, James Meehan, Peter Mullen, Claudiu Supuran, J. Michael Dixon, Jeremy S. Thomas, Jean-Yves Winum, Philippe Lambin, Ludwig Dubois, **Nanda Kumar Pavathaneni**, Edward J. Jarman, Lorna Renshaw, InHwa Um, Charlene Kay, David J. Harrison, Ian H. Kunkler, Simon P. Langdon.
Evaluation of carbonic anhydrase IX as a therapeutic target for inhibition of breast cancer invasion and metastasis using a series of *in vitro* breast cancer models.
Oncotarget, **2015**, *6*, 24856-24870.

Ludwig Dubois, Sarah G.J.A. Peeters, Simon J.A. van Kuijk, Ala Yaromina, Natasja. Lieuwes, Ruchi Saraya, Rianne Biemans, Marouan Rami, **Nanda Kumar Parvathaneni**, Daniela Vullo, Marc Vooijs, Claudiu T. Supuran, Jean-Yves Winum, Philippe Lambin.

Targeting carbonic anhydrase IX by nitroimidazole based sulfamides enhances the therapeutic effect of tumor irradiation: a new concept of dual targeting drugs.

Radiother. Oncol **2013**, *108*, 523–528.

Marouan Rami, Ludwig Dubois, **Nanda Kumar Parvathaneni**, Vincenzo Alterio, Simon van Kuijk, Simona Maria Monti, Philippe Lambin, Giuseppina De Simone, Claudiu T. Supuran, Jean-Yves Winum.

Hypoxia-targeting Carbonic anhydrase IX inhibitors by a new series of nitroimidazole-sulfonamide /sulfamide/sulfamte.

J. Med. Chem. **2013**, *56*, 8512–8520.

